TECHNICAL MANUSCRIPT S-2R
February 1971

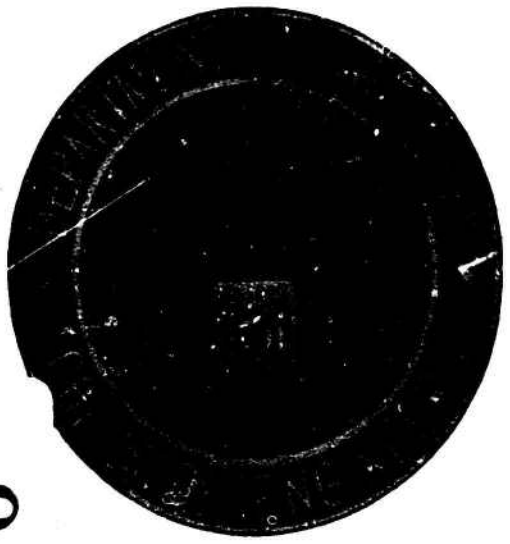

AD 729426

NUCLEAR WEAPONS EFFECTS: DUST AND AIR TEMPERATURE ENVIRONMENT

extracted from a
Final Technical Report

prepared by

IIT Research Institute
for the
Office of the Chief of Engineers

under
Contract No. DACA 73-67-C-0018

DDC
RELEASABLE
SEP
DISTRIBUTED
A

CONSTRUCTION ENGINEERING RESEARCH LABORATORY
Champaign, Illinois 61820

This document has been approved for public release and sale; its distribution is unlimited.

AD
E
R
L

282

DISCLAIMER NOTICE

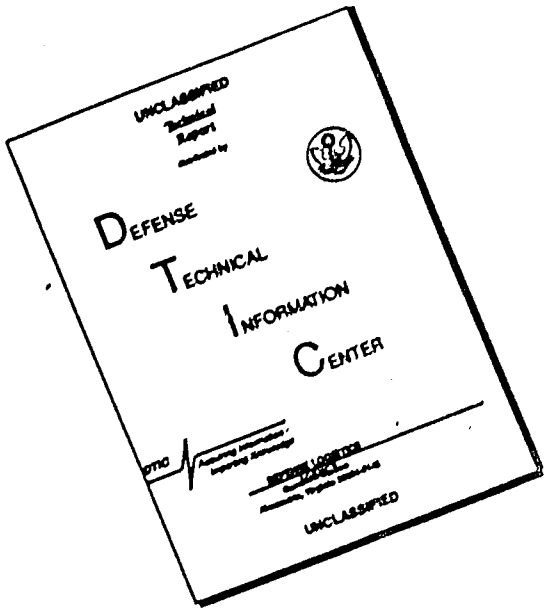

THIS DOCUMENT IS BEST QUALITY AVAILABLE. THE COPY FURNISHED TO DTIC CONTAINED A SIGNIFICANT NUMBER OF PAGES WHICH DO NOT REPRODUCE LEGIBLY.

UNCLASSIFIED

Security Classification

DOCUMENT CONTROL DATA - R & D

(Security classification of title, body of abstract and indexing annotation must be entered when the overall report is classified)

1. ORIGINATING ACTIVITY (Corporate author)
U. S. Army Construction Engineering Research Lab
P. O. Box 4005
Champaign, Illinois 61820

2a. REPORT SECURITY CLASSIFICATION
Unclassified

2b. GROUP
NA

3. REPORT TITLE

NUCLEAR WEAPONS EFFECTS: DUST AND AIR TEMPERATURE ENVIRONMENT

4. DESCRIPTIVE NOTES (Type of report and inclusive dates) Computer program documentation from a final technical report for the period May 66 - Sep 69.

5. AUTHOR(S) (First name, middle initial, last name)

James J. Swatosh, Jr. and Arne H. Wiedermann

6. REPORT DATE
February 1971

7a. TOTAL NO. OF PAGES
272

7b. NO. OF REFS
22

8a. CONTRACT OR GRANT NO.
Contract No. DACA DACA-73-67-C-0018

b. PROJECT NO.
NA

c.

d.

9a. ORIGINATOR'S REPORT NUMBER(S)
Technical Manuscript S-2 (Revised)

9b. OTHER REPORT NO(S) (Any other numbers that may be assigned this report)
The AD# for this report is obtainable from address block 1 above, ATTN: CERL-RL. Copies of this report are obtainable from:
National Technical Information Service
Springfield, Virginia 22151

10. DISTRIBUTION STATEMENT
This document has been approved for public release and sale; its distribution is unlimited.

11. SUPPLEMENTARY NOTES
This computer program documentation is extracted from a report by the IIT Research Institute Chicago, Illinois. The report

12. SPONSORING MILITARY ACTIVITY
Office of the Chief of Engineers
ATTN: ENGMC-ED
Department of the Army
Washington, D. C. 20314

13. ABSTRACT
This manual presents a computer program for calculating the dust and air temperature environment resulting from nuclear weapons detonations. The program can accommodate a wide variety of weapons detonations and ground surfaces. A weapons effects subroutine limits battle environment input data to the bare minimum.

Dust concentrations can be calculated at any significant range from ground zero and at any height to which dust is raised by blast wind erosion of soil and subsequent air transport. The soil may be considered either uniform or variable in the path of the blast wave. Soils are specified by particle size and terminal velocity, size distribution, and erodable depth. Land use is accounted for. The topography is assumed to be flat or gently rolling. Multiple burst dust concentrations can be computed for variously timed detonations. The effect of prevailing winds is introduced after cessation of blast winds.

Air temperature is treated as a dust-related phenomenon. The ground, heated by thermal radiation prior to arrival of the air blast, is eroded and transported by the blast wind. Its heat is transferred to air, primarily by convection, until thermal equilibrium is attained. The dust present from preceding bursts acts as a heat shield, transmitting only a portion of thermal radiation from succeeding bursts.

14. KEY WORDS

Nuclear Weapons Effects
Nuclear Weapons Environment
Atmospheric Weapons Effects
Dust and Air Temperature
Dust
Air Temperature
Hardened Air Intake and Exhaust Gas Systems
Hardened Power Systems

DD FORM 1 NOV 68 1473 REPLACES DD FORM 1473, 1 JAN 64, WHICH IS OBSOLETE FOR ARMY USE.

UNCLASSIFIED

Security Classification

R

The contents of this report are not to be used for advertising, publication, or promotional purposes. Citation of trade names does not constitute an official indorsement or approval of the use of such commercial products. The findings of this report are not to be construed as an official Department of the Army position, unless so designated by other authorized documents.

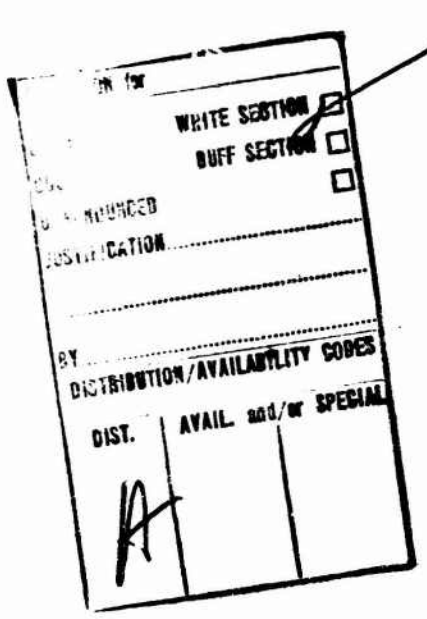

DESTROY THIS REPORT WHEN IT IS NO LONGER NEEDED
DO NOT RETURN IT TO THE ORIGINATOR

TECHNICAL MANUSCRIPT S-2
(Revised)

NUCLEAR WEAPONS EFFECTS: DUST AND AIR TEMPERATURE ENVIRONMENT

extracted from a
Final Technical Report
prepared by

IIT Research Institute

for the

Office of the Chief of Engineers
under
Contract No. DACA 73-67-C-0018

February 1971

Department of the Army
CONSTRUCTION ENGINEERING RESEARCH LABORATORY
P. O. Box 4005
Champaign, Illinois 61820

This document has been approved for public release and sale;
its distribution is unlimited.

ABSTRACT

This manual presents a computer program for calculating the dust and air temperature environment resulting from nuclear weapons detonations. The program can accommodate a wide variety of weapons detonations and ground surfaces. A weapons effects subroutine limits battle environment input data to the bare minimum.

Dust concentrations can be calculated at any significant range from ground zero and at any height to which dust is raised by blast wind erosion of soil and subsequent air transport. The soil may be considered either uniform or variable in the path of the blast wave. Soils are specified by particle size and terminal velocity, size distribution, and erodable depth. Land use is accounted for. The topography is assumed to be flat or gently rolling. Multiple burst dust concentrations can be computed for variously timed detonations. The effect of prevailing winds is introduced after cessation of blast winds.

Air temperature is treated as a dust-related phenomenon. The ground, heated by thermal radiation prior to arrival of the air blast, is eroded and transported by the blast wind. Its heat is transferred to air, primarily by convection, until thermal equilibrium is attained. The dust present from preceding bursts acts as a heat shield, transmitting only a portion of thermal radiation from succeeding bursts.

Originally intended for the NIKE-X Power Systems design studies, the program represents the culmination of four years' work and a $365,000 theoretical and experimental study. Although maximum benefit can be obtained

by using this manual with companion documents cited in the Foreword, enough theory is included with a user's guide so that this manual is virtually self-contained. The computer program output has also been designed as input to a hardened air intake and exhaust gas systems computer program.

FOREWORD

An investigation of the dust and air temperature environment resulting from atmospheric nuclear weapons detonations was performed under Contract No. DACA 73-67-C-0018 for the Office of the Chief of Engineers, Department of the Army, Directorate of Military Construction, Advanced Technology Branch, Washington, D.C. 20314. Technical direction was provided by Mr. John J. Healy and Mr. Roger L. Lapp, now with the U.S. Army Construction Engineering Research Laboratory, Champaign, Illinois 61820.

The work was done by the IIT Research Institute, 10 West 35th Street, Chicago, Illinois 60616. The project engineer was Mr. James J. Swatosh, Jr. Other personnel who contributed materially to the study were: A. Anderson, Thomas V. Eichler, and Arne H. Wiedermann.

This manual, while quite adequate for most uses, is extracted from a lengthier report, recourse to which will be of occasional benefit during initial trial runs and in case of question on details. Access to the complete report can be obtained by contacting the U.S. Army Construction Engineering Research Laboratory (CERL). Environmental output of the program can be used separately or as input to another computer program described in Air Blast Attenuation, Technical Manuscript S-1 (Revised), CERL, February 1971.

This page is left blank intentionally.

CONTENTS*

*Each appendix has its own Table of Contents and List of Figures and Tables.

LIST OF FIGURES AND TABLES

LIST OF FIGURES AND TABLES (CONTINUED)

LIST OF FIGURES AND TABLES (CONTINUED)

Chapter 1 (U)

GENERAL INTRODUCTION

DUST AND AIR-TEMPERATURE ENVIRONMENTAL STUDIES

The dust and air temperature environment generated by nuclear weapons detonations results in particle and thermal loads which may be detrimental to the operating characteristics of hardened power systems. This is especially so when the combustion air intake and exhaust gas systems operate continuously, open to the atmosphere both during and after a nuclear attack.

The purpose of the reported studies was to: develop the theory for predicting dust concentrations and air temperature, experimentally investigate empirical factors which theoretically describe and control the process (soil erosion, dust transport, and dust-to-air heat transfer rate coefficients), write a computer program to embody the developed theory and test data, evaluate potential NIKE-X Ballistic Missile Defense System power plant sites, and formulate power plant design instructions and criteria.

The lengthier final technical report mentioned in the Foreword presents a complete documentation of the studies and results. Its Chapter 2 summarizes the results of the studies. It is intended that the chapter will facilitate the designer by giving quick answers to the many design questions that arise concerning dust and air-temperature environments. Chapter 3 summarizes the studies performed under this contract. It is an information source for those who require only a general knowledge or summary of the studies. Chapters 4, 5, and 6 document the details of

R

the studies performed to date. The appendices of this report present the tools and necessary input information whereby a designer may compute detailed dust and air-temperature environments.

This manual contains: Chapters 5 and 6, the dust and air temperature theory; Appendix A, the dust and air temperature computer program, input-output descriptions, and sample problems; and Appendix C, the weapons effects theory. The theoretical material is presented as necessary background to the computer program for the engineer and is an integral part of what is usually called a computer program writeup. Program capabilities and limitations become apparent upon consulting the developed theory.

One limitation which was not thoroughly probed at the time of developing the theory concerns surface and near surface bursts and deserves mention here. A recent dust study* indicates that the dust and air temperature computer program should be modified to include the effect of upsweep, the lifting of the hot fireball gases near ground zero. In connection with this, the effect of the blast wave shape, the particle size distribution, and the erosion depth limit need to be examined, along with the interrelation of these variables. There appear to be surface burst cases where the present dust model may overstate the peak dust concentration in the low overpressure region by as much as a factor of two.

*Arne H. Wiedermann, Study of Dust Environment in the Access Tunnels of the NORAD Facility, by IIT Research Institute, Chicago, Illinois, for the U. S. Army Engineer District, Omaha, Nebraska, Contract No. DADC 45-71-C-0005, November 1970.

The dust portion of the computer program is subroutined to evaluate four different variable conditions. The first subroutine treats a single nuclear weapon attack and averages the soil characteristics in the vicinity of the hardened power system. The second subroutine of the program treats a multiple nuclear weapon attack and also treats a uniform soil distribution in the vicinity of the site. These two subroutines are useful in determining the dust environment at a site when particular details of the local terrain are unknown or the exact location of the site is unknown. The third subroutine of the program treats a single nuclear weapon attack and accounts for the variability of local soil characteristics such as residential area, grassland, woodland, and cultivated areas. A fourth subroutine of the program treats late-time dust environments, dust which has been transported to the site because of ambient surface winds after the blast winds have subsided.

The air temperature portion of the computer program developed herein is subroutined to evaluate two variable conditions. The first subroutine treats a uniform ground condition and the second treats a biuniform ground condition. The subroutines include erosion cutoff factors, single- or multiple-burst attacks, and computation of air temperature as a function of both height and time.

The changes made to the original IBM 7094 FORTRAN IV program to convert to CDC 6000 series FORTRAN are listed below:

CHANGES TO ORIGINAL IBM 7094 FORTRAN IV PROGRAM

1. Page A-49: Statement 2, formerly for IBM 7094 read -

```
2     FORMAT (18A4,2I2,L2)
```

This has been changed for CDC 6600 to read -

```
2     FORMAT (18A1,2I2,L2)
```

2. Page A-88: Lines 27-31, formerly for IBM 7094 read -

```
      TS(N) = TS(N)+((C5+A(I)*T(I))*C6/EXP(E2)-(C5+A(I)*T(I1))*C7/
     1EXP(E3))/1.5+C1*(A(I)*(3.*T(21)+C2)+B3(I))*(ERF(C4/C6)-ERF(C4/C7))
      GO to 106
105   TS(N) = TS(N)+CONS3*(C5+A(I)*T(I))/EXP(E1)+C1*(A(I)*(3.*T(21)+C2)+
     1B3(I))*(ERF(EF1)-1.)
```

This has been changed for CDC 6600 to read -

```
      ERX = ABS(C4/C6)
      CALL ERF(ERX,0.,ERX1,ERXA,ERXB)
      ERX = ABS(C4/C7)
      CALL ERF(ERX,0.,ERX2,ERXA,ERXB)
      TS(N) = TS(N)+((C5+A(I)*T(I))*C6/EXP(E2)-(C5+A(I)*T(I1))*C7/
     1EXP(E3))/1.5+C1*(A(I)*(3.*T(21)+C2)+B3(I))*(ERX1-ERX2)
      GO to 106
105   ERX = EF1
      CALL ERF(ERX,0.,ERX3,ERXA,ERXB)
      TS(N) = TS(N)+CONS3*(C5+A(I)*T(I))/EXP(E1)+C1*(A(I)*(3.*T(21)+C2)+
     1B3(I))*(ERX3-1.)
```

EXTRACTED

Chapter 5 (U)

DUST STUDIES

5.1 Introduction

The adequate design of hardened air breathing facilities requires that the local ambient air environment be established during a nuclear attack so that suitable compensatory action can be taken, thus ensuring proper functioning of the power system. The air in the vicinity of the facility may become dust ladened, and will experience a temperature and pressure transient.

The majority of the energy released by the detonation of a nuclear weapon in the atmosphere will appear in two primary forms. A blast wave will propagate outward from the burst point at supersonic speeds and will induce a motion to the air as well as change the air pressure and temperature. The hot fireball will radiate thermal energy which will raise the temperature of the ground and other surrounding surfaces. The soil may respond mechanically to this thermal disturbance and portions of it may be thrown upward into the surrounding quiescent air. Furthermore, the air blast-induced winds may scour the soil surface and transport heated particulate matter upward, thereby forming a dust cloud. The rising motion of the fireball may also generate surface winds, sometimes called "afterwinds", of considerable magnitude. These winds will also contribute to the generation or continued growth of the dust cloud. The soil particulate matter sucked up by the fireball motion will rise to great heights and then fall out, forming another type of dust cloud--one which exists over great distances. Finally, for sufficiently low heights of bursts, crater ejecta consisting of both large and small particles will be

deposited over a considerable surface region surrounding the burst point.

The coarse particulate matter will settle out of the air rapidly due to gravitational effects; however the very fine soil particles will remain airborne for a considerable period of time compared with the duration of the blast winds. These fine particles will be transported horizontally large distances due to the ambient surface winds.

Preliminary studies[5.1] have indicated that the major source of dust at the potential sites of interest will be that due to the blast-induced winds. Thus, a theoretical model of the dust cloud generated by the blast-induced winds has been developed and is discussed in this chapter. The influence of the thermal effects has been neglected in this dust model. However, the influence of the heated dust and other thermal effects is treated in a more complex model used to predict both the air temperature and dust density at the point of interest. The simplified or cold dust model is useful for generating data for intermediate, as well as late, times when the thermal effects become insignificant. This model also enables one to evaluate the relative influence of certain assumptions, variables, and coefficients associated with the dust cloud.

The cold dust problem as well as the overall dust and thermal problem is extremely complex. It is clear that if engineering type estimates are to be made of the local environment, a number of simplifying assumptions must be made. These assumptions, hopefully, must be such that the essential of predominant features of the process are retained as well as introducing a reasonable, but not excessive, degree of conservatism to the predictions or estimates.

The air blast environment in the absence of the dust and thermal effects is in itself a relatively complex problem, involving the nonlinear behavior of air in a transient-multi-dimensional space. A description of the air pressure, air temperature, and particle velocity, in some relatively simple burst conditions and associated geometric configurations, has been established, using theoretical considerations as well as experimental observations made during field tests of nominal size nuclear weapons. The inclusion of the dust and thermal aspects into the nonlinear gas dynamic problem would render the problem unsolvable within the allowable effort. However, reasonable estimates of the dust environment can be made, provided it can be assumed that the gas dynamic fields are essentially the same as those existing in the absence of the dust. Such an uncoupling assumption is made herein and is valid whenever the kinetic energy of the dust is small compared with the total energy locally. Thus, the particle velocity field and pressure field are assumed locally and are those established from the usual weapons effects data. The vertical transport of the dust is assumed to be due to the turbulent action of the air; therefore, it is assumed herein that, at least locally, the motion of the air is relatively uniform both in its gross motion and in its turbulent intensity. This assumption implies that we are dealing with flows near relatively flat surfaces. The model will tend to break down in the neighborhood of large surface perturbations which would give rise to strong local effects. Since we are concerned primarily with local effects, we can neglect the small horizontal and vertical gradients which exist in the gas dynamic fields.

Section 5.2 presents the details of the IITRI dust model and a similarity solution for a uniform soil condition.

Another section (Section 5.3) presents an evaluation of the coefficients used in the dust model, together with a comparison of some limited field data. This is followed by Section 5.4 which presents a series of typical results illustrating the influence of the many variables which contribute to the characteristics of the dust cloud. A list of symbols used in the dust model is given in Section 5.5 and Section 5.6 is a brief estimate of the dust cloud generated by crater ejecta.

5.2 IITRI Dust Cloud Model

5.2.1 General

The horizontal flow of air over the soil surface will result in aerodynamic forces acting upon portions of the soil mass or upon individual soil particles. If the forces are of sufficient magnitude, the soil particle or soil mass will move from its original position and bounce, roll, or otherwise be transported in the direction of the flow. During this erosion process the soil particles may obtain a vertical component of motion and thus become, at least momentarily, airborne. The cloud will, in addition to its grossly horizontal motion, be characterized by some degree of local turbulent motion. The soil particles, once airborne, can then be transported horizontally by the gross motion of the air and vertically by the inherent turbulent motion. Thus, one can expect that the blast-induced winds will erode some soil surfaces and transport the soil particles into the air, forming a dust cloud. As the intensity of the wind and the turbulence decay, gravitational forces will then permit the particulate matter to settle out of the cloud.

The very fine soil particles will remain airborne for periods of time which are much greater than the durations of the blast-induced winds. These particles will be transported great distances by the ambient surface winds which will

generally exist, hence the dust environment at a particular location may be influenced by the dust clouds generated at some distant locations.

"Soil" is a term used to describe a large variety of complex and varied substances. The soil can be characterized by its physical appearance, physical properties, chemical composition, geological origin, etc. and by the mass distribution of these quantities. Also, certain time-dependent characteristics such as moisture content and compaction may be exibited. Furthermore, the soil characteristics may change drastically with depth near the soil surface. Since the soil is such a complex entity, we must describe it in a few simple terms and adjust the dust cloud predictions for some of the other soil characteristics in a gross manner. We will therefore describe the soil as a particulate matter with a certain discrete particle-size distribution, particle density, and bulk or in situ soil density.

The following two basic assumptions are made in the IITRI dust cloud model. First, it is assumed that the horizontal motion of the dust, once ejected into the air, is identical to the gross horizontal motion of the air. This assumption is valid for a wide range of particle sizes provided that the time and space resolutions (required to obtain equilibrium with the air motion) are small. A particle at rest, but in the airstream, will be subjected initially to a large drag force. The particle will accelerate rapidly until it reaches (asymptotically) the air velocity. The response time will be of the order of milliseconds and will result in a lag of approximately several feet. The second basic assumption is that the motion of any particle or group of particles is independent of the existence or motion of any other particle or groups of particles. This assumption

will be valid provided the number of particles per unit volume is not excessive as is anticipated. This assumption permits one to treat each group of particles separately and to obtain the total effect by summing all of the groups.

5.2.2 The Erosion Process

The first phase of the dust cloud problem is the dust pickup of erosion phase. It is postulated that those soil particles which are at the surface will be subjected to an aerodynamic force acting primarily in the horizontal direction. These particles will move horizontally and be lifted into the airstream. It is clear that successive layers of particles cannot move into the airstream until the preceding particles have moved some finite distance away from their original resting place.

The force which acts on the particles will be equal to or be some fraction of the aerodynamic drag caused by the high wind velocity. This force will be proportional to $V^2 \times D^2$ where D is the diameter of the particle. The acceleration will be proportional to V^2/D due to the mass of the particle, and the time for the particle to move a given distance (in terms of its size D) will be proportional to D/V. The number of available particles per layer will be proportional to $1/D^2$. Therefore, this is the number of particles that can be stripped away or eroded in the above time interval; hence

$$\frac{dn}{dt} \approx \frac{V}{D^3} \approx V\nu_g \quad . \tag{5.1}$$

where

ν_g = number of particles available per unit volume,
V = air velocity,
n = number of particles in a given size class, and
t = time.

This relationship can be rewritten as

$$\frac{dw}{dt} = a\rho_s f p \, |V| \tag{5.2}$$

and

$$f = \left(1 - \frac{5V_t}{|V|}\right) H\left[1 - \frac{5V_t}{|V|}\right], \tag{5.3}$$

where

f = erosion cutoff criteria,
a = erosion constant,
w = weight of particle per unit area,
ρ_s = specific weight of soil,
t = time,
p = weight fraction of particles,
V = air velocity,
V_t = terminal velocity of particle, and
$H[\,]$ = unit step function.

The factor f (used in Equation 5.2) represents a cutoff mechanism which states that the air velocity must be some multiple of the terminal velocity (5, in this case) before a particle can leave the surface. Some experimental evidence[5.2] exists to support such a concept, at least for loose-sand surfaces. The cutoff function is arbitrarily made smooth by multiplying the unit function by the factor $(1 - 5V_t/|V|)$.

The factor a is the erosion constant and has been evaluated for some soils during the current program. These experiments are described in Appendix A. A value of 6×10^{-5} has been selected as being applicable to the current problem.

5.2.3 The Transport Process

The transport of the dust particles is postulated to be due to gross horizontal motion of the air, as well as

being due to local turbulent motion. It is possible now to consider the motion of a small group of particles (of the same size) which are ejected into the air at a range of $R = R_1$ and a time of $t = t_1$ (see Figure 5.1). The weight of this group of particles is dw. According to the first basic assumption, the horizontal motion of this group of particles is identical to the horizontal motion of the air (identified in Figure 5.1 as air column A). The air velocity is assumed uniform in the vertical direction, and no boundary layer effects are included. This assumption implies that the heights of interest are generally much greater than any boundary layer thickness. The individual particles of this group or dust packet will also move in the vertical direction due to the action of air turbulence and gravitational forces. However, the vertical motion will be bounded by some cloud height H. This is illustrated in Figure 5.1 at $t = t_2$ and $t = t_3$. The rate at which the cloud height grows (in the absence of gravity) will be approximately proportional to the absolute magnitude of the gross (horizontal) air velocity. The cloud, and therefore its extremity H, will also settle due to the action of gravity. This decreasing rate will be equal to the terminal velocity V_t of the particle. Thus, we conclude that the time history of the cloud height associated with the particular dust packet is given by

$$\frac{dH}{dt} = K|V| - V_t \ , \tag{5.4}$$

where V is the instantaneous horizontal wind velocity of air column A and K is a factor yet to be evaluated. The value of K will be some small fraction of unity since the turbulent velocity component will be some small fraction of the mean air velocity V. One can also postulate that the factor 5 used in Equation 5.3 is related to the factor K, as $K = 1/2$. This implies that the erosion cutoff depends upon the turbulent intensity of the air.

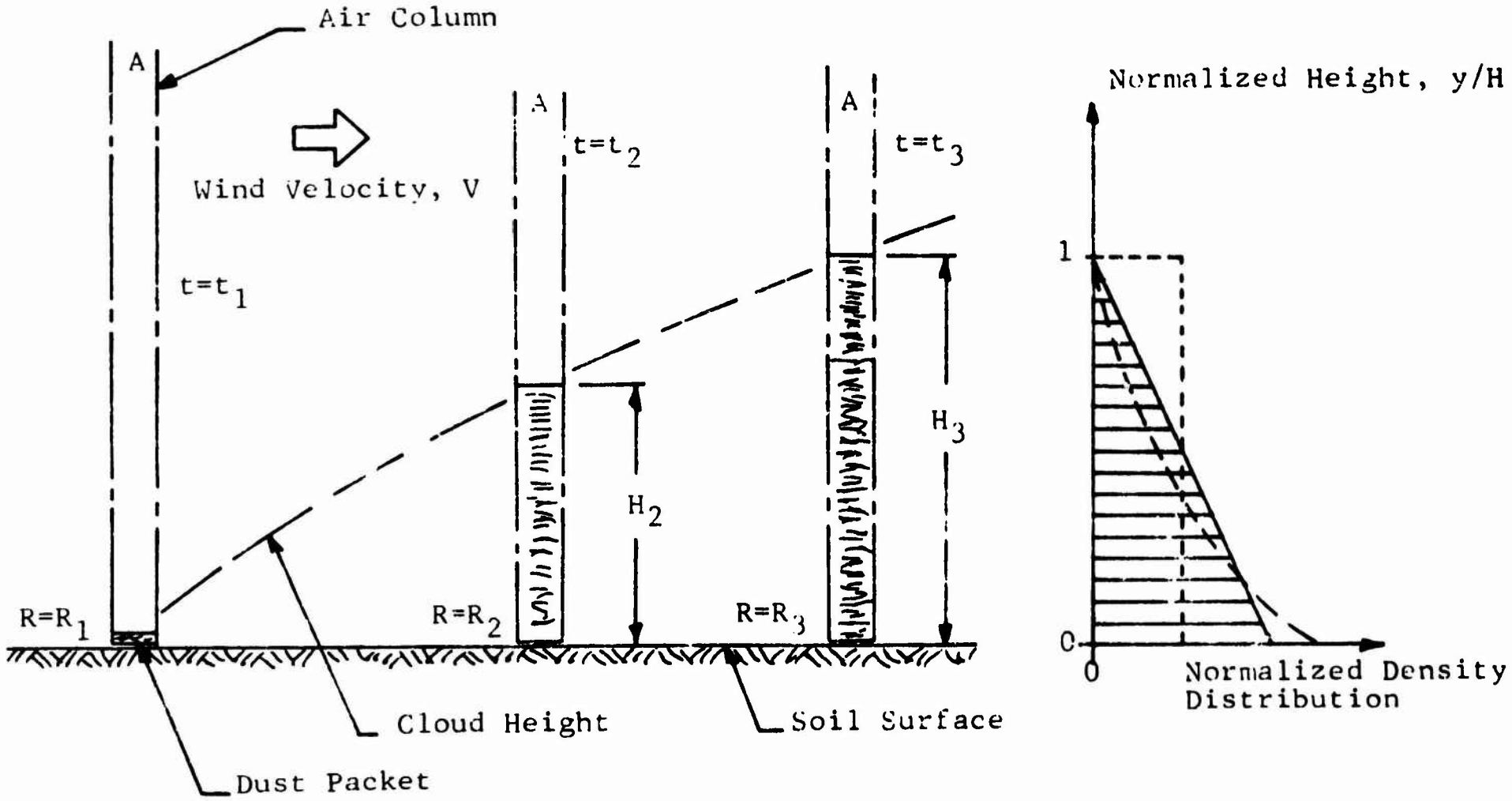

Figure 5.1 Basic Elements of Two-Dimensional Dust Model

The distribution of the particles within the cloud is needed to determine the number of particles per unit volume (i.e., the density) at any height y. It is assumed that the normalized distribution (or probability function) is similar at all times and for all particle sizes. At the present time there is little evidence to support the selection of any particular distribution function; however, one can make an intuitive selection and then evaluate the sensitivity of the results to this selection. The simplest distribution function that one might choose is a uniform (rectangular) density variation. Such a distribution is unlikely, and it is probable that most of the dust particles will concentrate at the lower end of the cloud. It is expected that the distribution will not be irregular, nor that the density will be vanishingly low near the upper portions of the cloud. If the latter were the case, then one could re-evaluate the constant K and select a new effective height.

The next simplest distribution selected was the triangular distribution in which the density decreases linearly with increasing height, assuming a value of zero at the top of the cloud. Thus, the density $d\rho$ is given by

$$d\rho = d\rho(0)\left[1 - \frac{y}{H}\right] \qquad 0 \le y \le H, \qquad (5.5a)$$

and

$$d\rho = 0 \qquad H \le y, \qquad (5.5b)$$

where $d\rho(0)$ is the value of $d\rho$ at y=0. Since the total weight dw of the dust packet is known, $d\rho(0)$ can then be evaluated. This yields

$$d\rho = \frac{2dw}{H}\left[1 - \frac{y}{H}\right] \qquad 0 \le y \le H. \qquad (5.6)$$

The distribution can be generalized somewhat by assuming that

$$d_0 = d_0(0)\left[1 - \frac{y}{H}\right] \exp\left(- \frac{cy}{H}\right)$$

$$0 \leq y < H. \qquad (5.7)$$

However, this introduces another unknown parameter c, which must be evaluated. Until some experimental evidence is developed, the triangular form (c=0) will be used. In a later part of this section a series of idealized problems for each of the above distribution functions is evaluated showing that the results are not significantly influenced by the selection of the distribution function. This is particularly true between the triangular form (c=0) and the concave triangle (c=1), the more realistic distribution functions.

The terminal velocity plays an important role in these dust studies. For particle sizes greater than 0.1 mm (100 microns) in diameter, Stokes' equation is inadequate. Stokes' equation is valid for Reynolds number N of unity or less. The drag coefficient C_d for spheres is presented in Figure 5.2. The drag coefficient decreases rapidly with increasing Reynolds number and reaches a constant value in the turbulent flow region. We have approximated the experimental results[5.3] by an equation of the form

$$C_d = \frac{24}{R_e} + \frac{1}{2} \; . \qquad (5.8)$$

This simple form appears adequate over the large Reynolds number range of concern (i.e., corresponding to particles up to the size of medium gravel). The terminal velocity V_t is given by

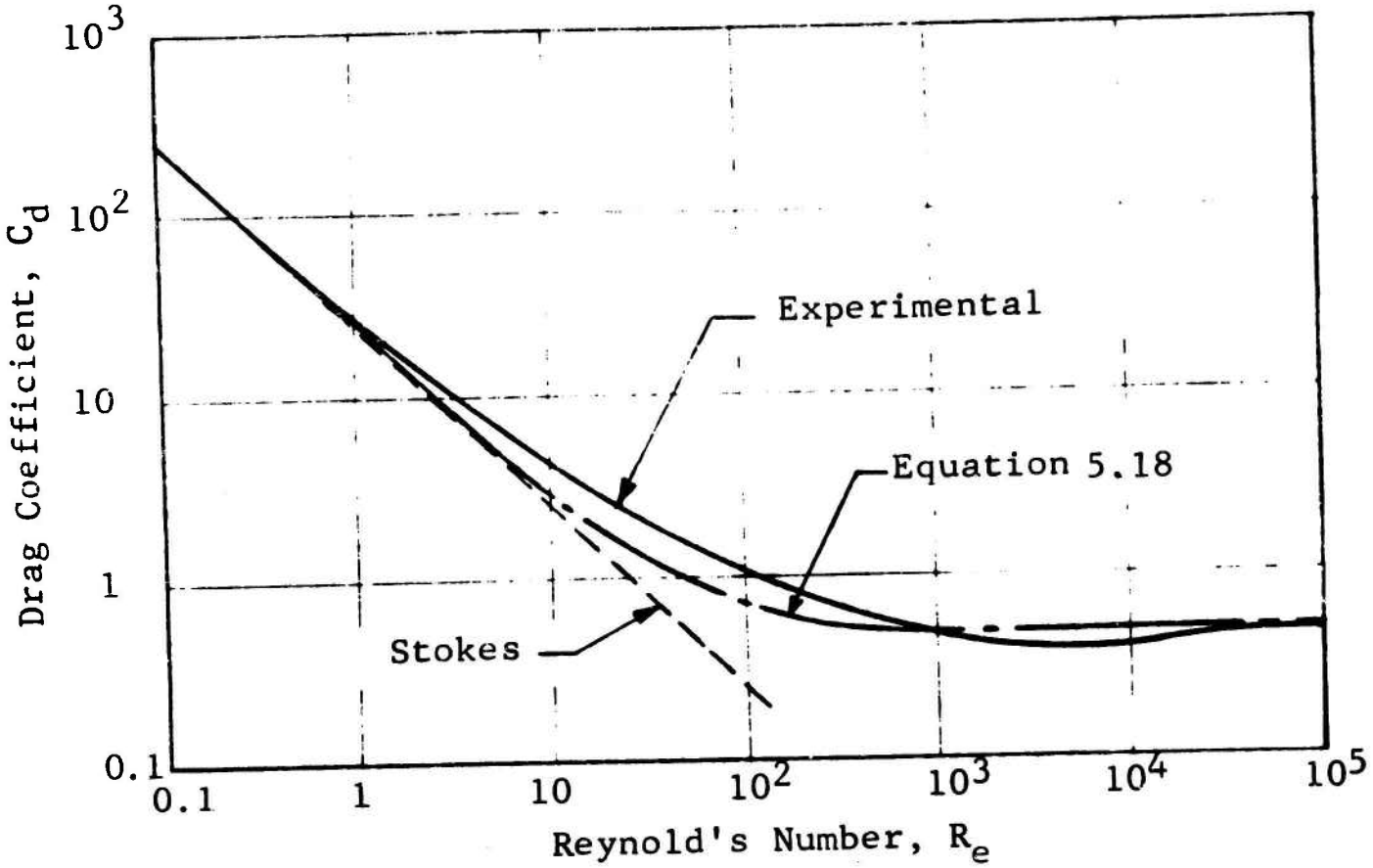

Figure 5.2 Drag Coefficient for Spheres

$$V_t = \sqrt{\left(\frac{24\mu}{\rho_a D}\right)^2 + \frac{8}{3}\left(\frac{\rho_c}{\rho_a}\right)gD} - \frac{24\mu}{\rho_a D}\ , \qquad (5.9)$$

where

D = diameter of particle,
μ = viscosity of air,
ρ_a = density of air, and
ρ_c = density of particle.

5.2.4 Blast-Induced Wind

The blast-induced winds are a function of the many weapons effects variables. The local wind variation or velocity field can be expressed in terms of a number of coefficients, which in turn must be evaluated from the specific nuclear attack situation. For a simple case, the velocity variation V_r of the air at a fixed range is generally assumed to be of the form

$$V_r = V_o \left[1 - \frac{t}{t_o}\right] \exp\left(-\frac{kt}{t_o}\right), \qquad (5.10)$$

where

V_o = peak air velocity,
t_o = positive phase duration, and
k = exponential coefficient.

Generally, this equation is valid well into the negative phase. Furthermore, it can be demonstrated that the maximum horizontal displacement of the air at the low overpressure range will be of the order of one-sixth of the slant range; and that over such an increment of range, the velocity field will not vary appreciably in the horizontal direction. Therefore, one can construct an expression for the velocity in terms of range and time from Equation 5.10 and from an assumption that the field is composed of simple waves. For the

current calculations, however, we need to know the velocity-time variation along an air particle path. Its derivation from the above indicated velocity field would be somewhat cumbersome. To avoid this complication, it is assumed that along an air particle path the velocity is of the form

$$V = V_o \left(1 - \frac{t}{t_o^*}\right) \exp\left(- \frac{kt}{t_o^*}\right) , \qquad (5.11)$$

where t_o^* is a modified positive phase duration and is equal to

$$t_o^* = t_o + \frac{R_o}{U} , \qquad (5.12)$$

where

R_o = maximum displacement of air, and
U = air shock velocity.

The positive phase duration has been increased, to account for the additional time that the particle is in motion. Figure 5.3 illustrates the air particle path and shows that the air particle originally at R_1 is displaced a maximum distance R_o and reaches this position after moving for a time equal to the sum $t_1 + t_o$. The time t_1 is the transit time of the shock front over the range increment R_o. The range $R=R_o$ is the range of interest. The problem is to determine the dust history at this particular position. The dust that exists at the location of interest is that dust which is picked up along the particular air particle path which intersects R_o. A simple integration of all of the elemental contributions along these paths yields

$$\rho = \int_{t_a}^{t} \frac{2}{H} \left(1 - \frac{Y}{H}\right) a\rho_s f_p |V| \, dt \qquad 0 \le Y \le H, \quad (5.13)$$

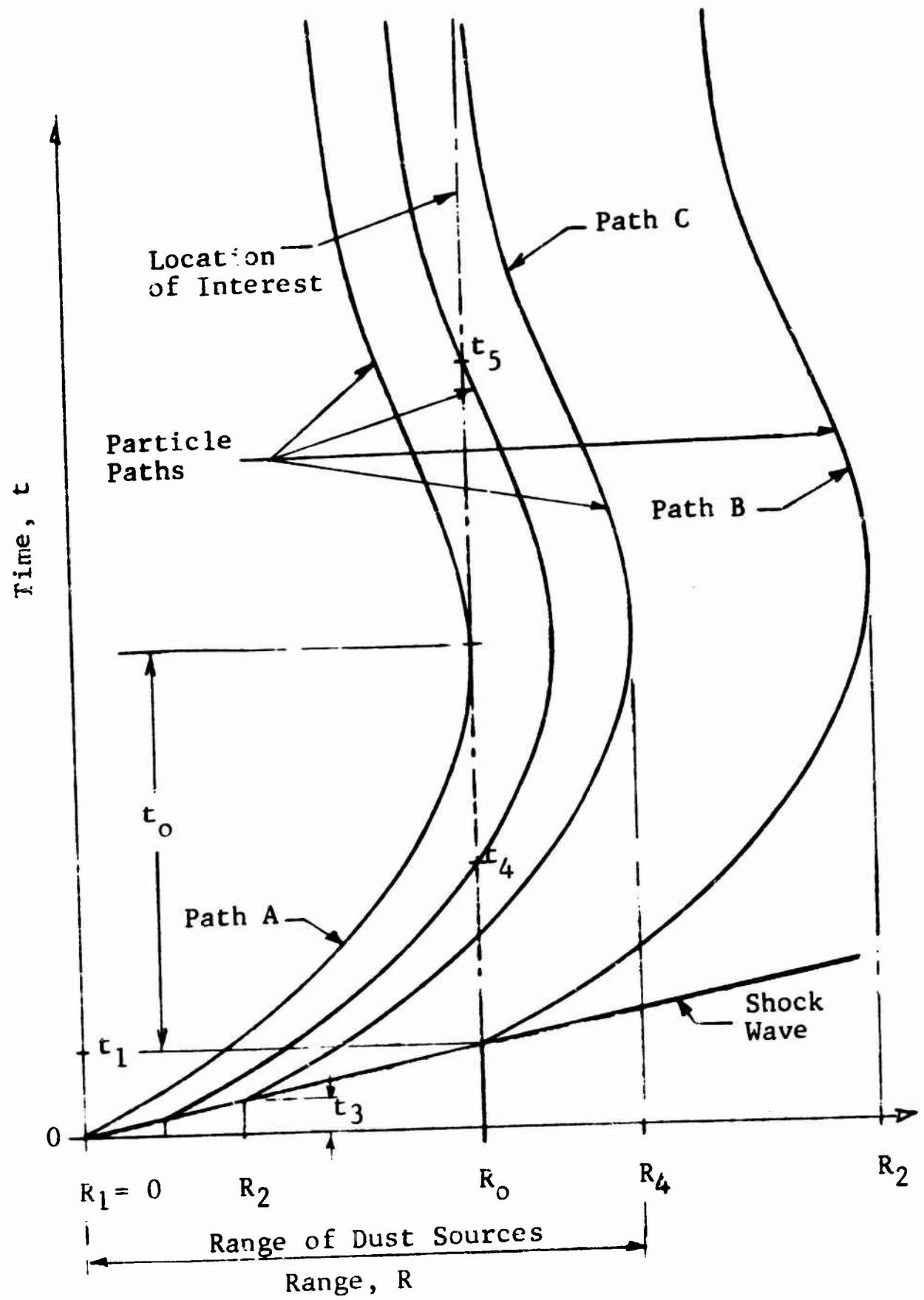

Figure 5.3 Wave Diagram for Dust Sources

and

$$\rho = 0 \qquad H \leq Y, \qquad (5.14)$$

where

Y = height of interest, and

t_a = time of arrival of air shock at R_1.

This integration is carried out for each particle size group. It should be noted (Figure 5.3) that some air particle paths (between Path A and Path C) cross the plant location twice, whereas others only cross the plant location once. The late-time dust conditions at the plant are those accumulated along Path C. Finally, one can place limits on the range increments from which the dust source may exist and still influence the dust cloud at $R=R_o$. The range increment R_o is given by

$$R_o = \frac{V_o t_o^*}{k^2} \left| k - 1 + e^{-k} \right| , \qquad (5.15)$$

and the range R_4 is given by

$$R_4 = 2R_o - \frac{V_o t_o^*}{k^2} (k - 1) . \qquad (5.16)$$

The range increment R_4 for a wide range of weapon conditions is of the order of 3000 ft or less.

Once the air velocity has been established we can integrate Equation 5.4 and determine the cloud height of any particular packet of dust; namely,

$$H(t_1,t,V_t) = H_1^*(t) - H_1^*(t_1) - V_t(t - t_1) \qquad (5.17)$$

where

$$H_1^*(t) = \frac{KV_o t_o^*}{k^2} \left\{(k - 1) + \left[\frac{kt}{t_o^*} - k + 1\right] \exp\left(- \frac{kt}{t_o^*}\right)\right\}, \quad (5.18)$$

when $t \leq t_o^*$; and

$$H_1^*(t) = 2KR_o - \frac{KV_o t_o^*}{k^2} \left\{(k - 1) + \left[\frac{kt}{t_o^*} - k + 1\right] \exp\left(- \frac{kt}{t_o^*}\right)\right\}, \quad (5.19)$$

when $t_o^* \leq t$. A typical example is presented in Figure 5.4 which illustrates the effect of particle size on the height of the cloud. It should be noted that the cloud height decreases and vanishes quite rapidly for the heavier particles.

5.2.5 Analytical Solutions

A series of analytical solutions can be readily obtained for the case of uniform ground conditions where the soil properties do not vary in the horizontal direction. These solutions are useful in examining the influence of some of the many variables, and in some instances will be useful for site evaluations. In particular, the sensitivity of the dust density to the form of the distribution can be examined.

The assumption of uniform ground conditions eliminates the need of knowing the position of the air column at any stage of the flow, and indicates that all of the air columns behave identically. We can obtain solutions for each particle class separately (let p=1) and combine the individual solutions for any particle size distribution of interest.

A general solution can be obtained by recalling that

$$dw = \frac{a\rho_s p}{K}(K|V| - V_t)\, dt, \quad (5.20)$$

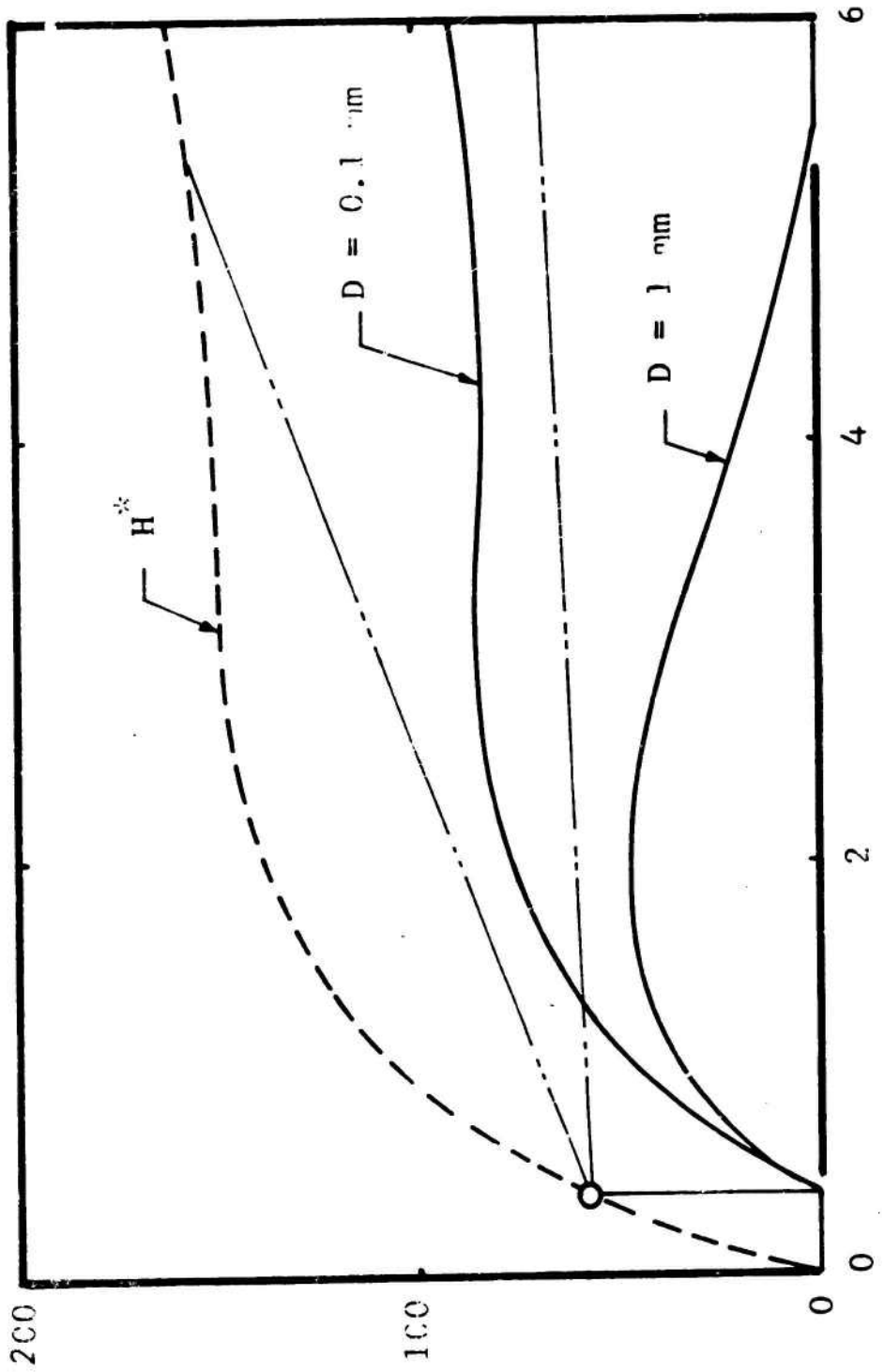

Figure 5.4 Cloud Height Variation with Time

and using

$$dt = \frac{dH}{(K|V| - V_t)} \tag{5.21}$$

to obtain

$$dw = \frac{a\rho_s p}{K} dH \ . \tag{5.22}$$

The elimination of the specific function defining the air velocity is the key to this simplification and can be accomplished by equating the factor 5 (Equation 5.3) to 1/K as discussed in the previous subsection. Thus, Equation 5.22 can be integrated over all dust packets to obtain the density of a given size class.

$$d\rho = \frac{2dw}{H}\left(1 - \frac{Y}{H}\right),$$

or

$$\rho = \frac{a\rho_s 2p}{K}\int_Y^{H^*}\left(1 - \frac{Y}{H}\right)\frac{dH}{H}\ , \tag{5.23}$$

where the limits of integration for H are from the top of the cloud H* to the elevation Y of interest. These integration limits are illustrated in Figure 5.5. The integration can be carried out over the variable t, or over the variable H. The integration of Equation 5.23 yields a similarity solution in the variable

$$\zeta = \frac{Y}{H^*}\ ; \tag{5.24}$$

that is,

$$\rho(\zeta) = \frac{2a\rho_s p}{K}(\zeta - 1 - \ln \zeta)\ . \tag{5.25}$$

H^* is a function of the time measured along a particle path. To convert to an observation time t' at a fixed position, one must use the relation

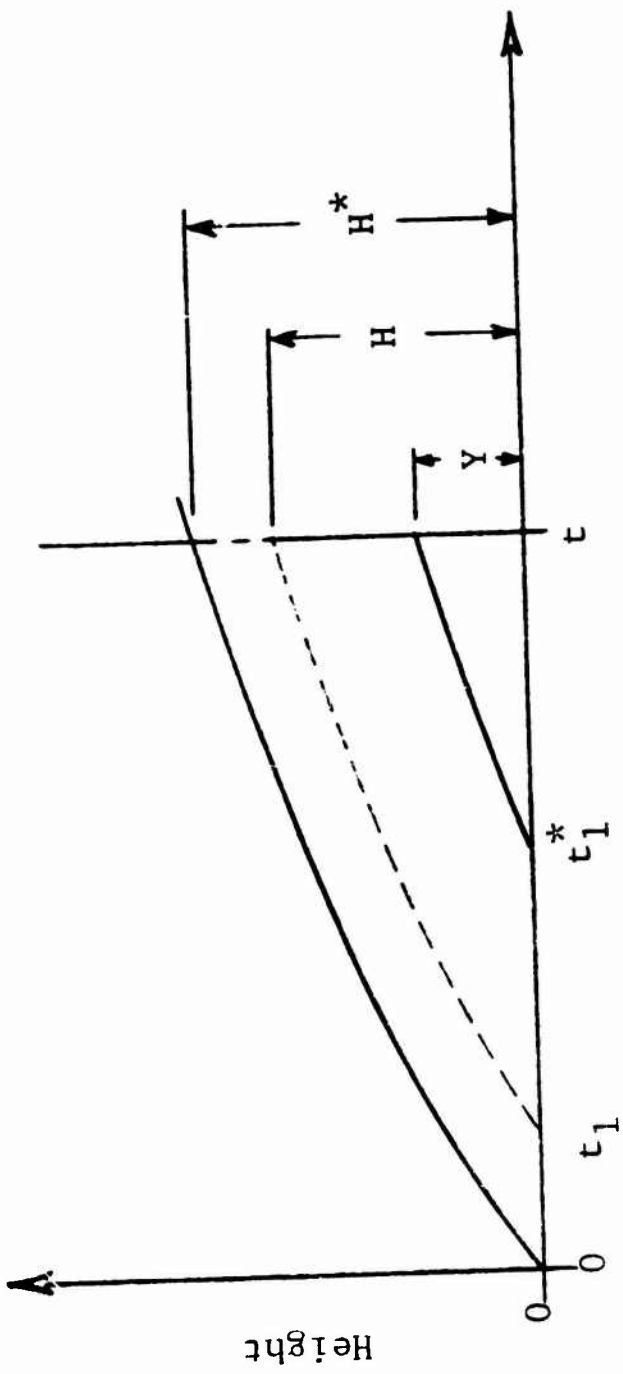

Figure 5.5 Integration Limits

$$t' = t - \frac{1}{U}\int_0^t V(t)\,dt \ . \tag{5.26}$$

H^* is obtained by integrating Equation 5.2 as

$$H^* = \int_0^t (K|V| - V_t)\,dt \ . \tag{5.27}$$

For the assumed velocity field discussed previously, these become

$$H^*(t) = H_1^*(t) - tV_t \ , \tag{5.28}$$

where $H_1^*(t)$ is defined by Equations 5.16 and 5.17. The above similarity solution is based on the triangular distribution function. Corresponding solutions have been obtained for both the rectangular and concave triangle distribution functions, respectively, as

$$\rho(Y,t) = \frac{a\rho_s p}{K} \ln \zeta \tag{5.29}$$

and

$$\rho(Y,t) = B\left[e^{-1} - e^{-\zeta} - \ln \zeta + \sum_{n=i}^{\alpha} \frac{(\zeta^n - 1)(-1)^{n-1}}{n.n!}\right], \tag{5.30}$$

where

$$B = \frac{ac^2\rho_s p}{K}\left[c - (1 - e^{-c})\right]^{-1} \ . \tag{5.31}$$

The dust density variation with height (actually the similarity variable ζ) is presented in Figure 5.6 for each of the assumed distribution functions. This variation clearly indicates that the density does not differ appreciably between the triangular and the concave triangle (c=1) distribution functions except at extremely low heights. These low heights are of no interest to the current problem and represent the

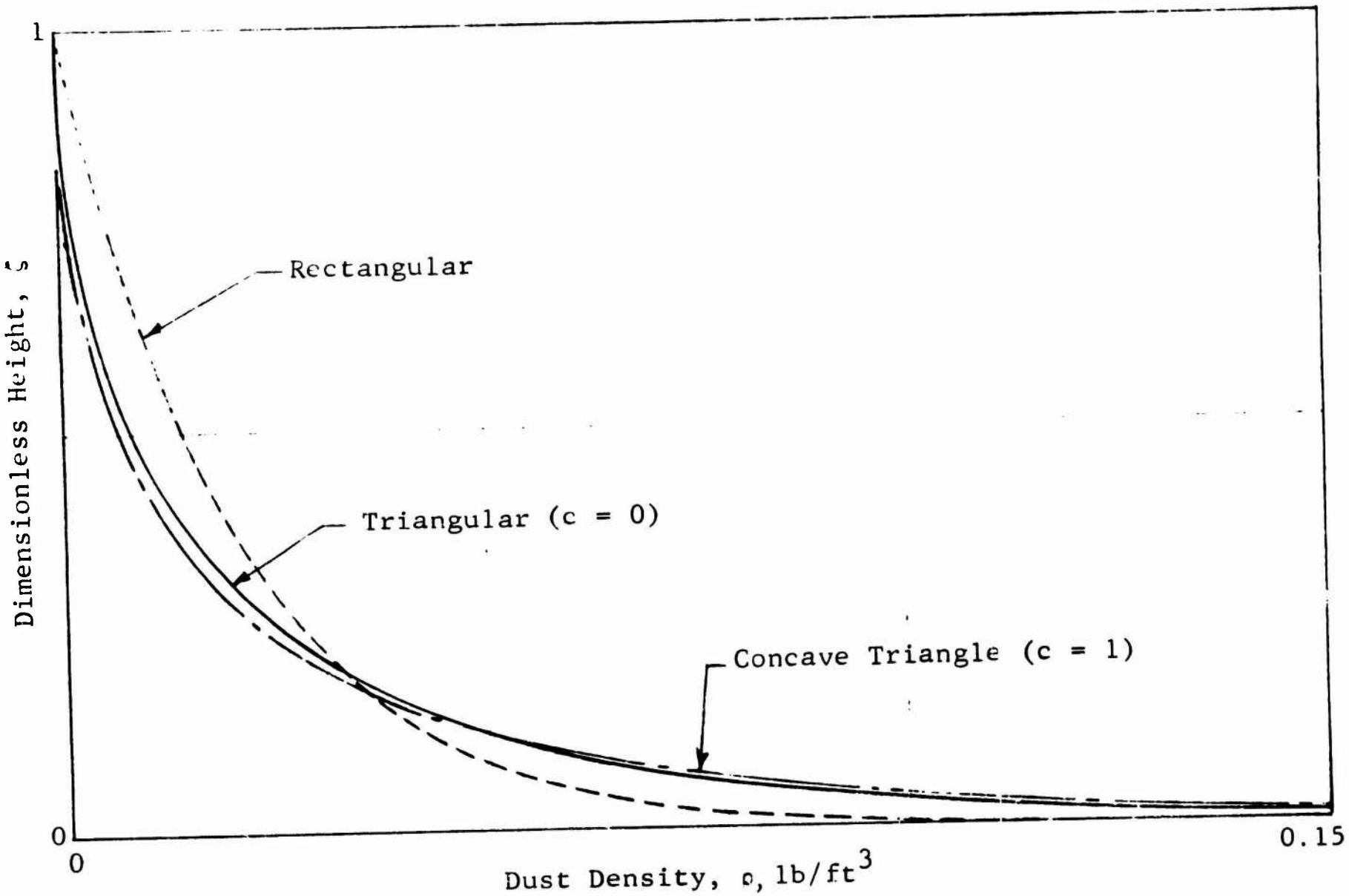

Figure 5.6 Density Distribution with Elevation above Ground

dust boundary layer immediately adjacent to the ground surface. The influence of the distribution function on the time details of the density is presented in Figure 5.7 for a representative set of parameter values. The results indicate that for multisecond time intervals, the triangular distribution is more than adequate.

5.2.6 Late Time Dust Cloud Model

The blast winds which accompany the detonation of a nuclear weapon in the atmosphere will generate wind induced dust clouds which cover a very large area and which will remain airborne for a substantial period of time. The properties of the dust cloud will vary throughout the cloud formation due to the local variations of the surface soil conditions and the variation in the magnitude and duration of the blast winds. The entire cloud formation will also be transported over the terrain due to the ambient surface winds. The larger soil particles which are initially raised by the strong blast winds will settle out of the cloud at the latter stages when the blast winds subside. However, the very fine soil particles will remain airborne and will be further dispersed due to the ambient winds. All of the airborne soil particles will be transported in a gross manner by the surface wind and will be accompanied by simultaneous turbulent diffusion in all directions. Other mechanisms will also contribute to the further local transport and/or mixing of the dust particles. These other mechanisms would include the influence of local thermal effects, the blast after winds when they occur, and other local meteorological phenomenon such as overturning.

The late-time dust effects are important since much of the mechanical and thermal air breathing equipment used

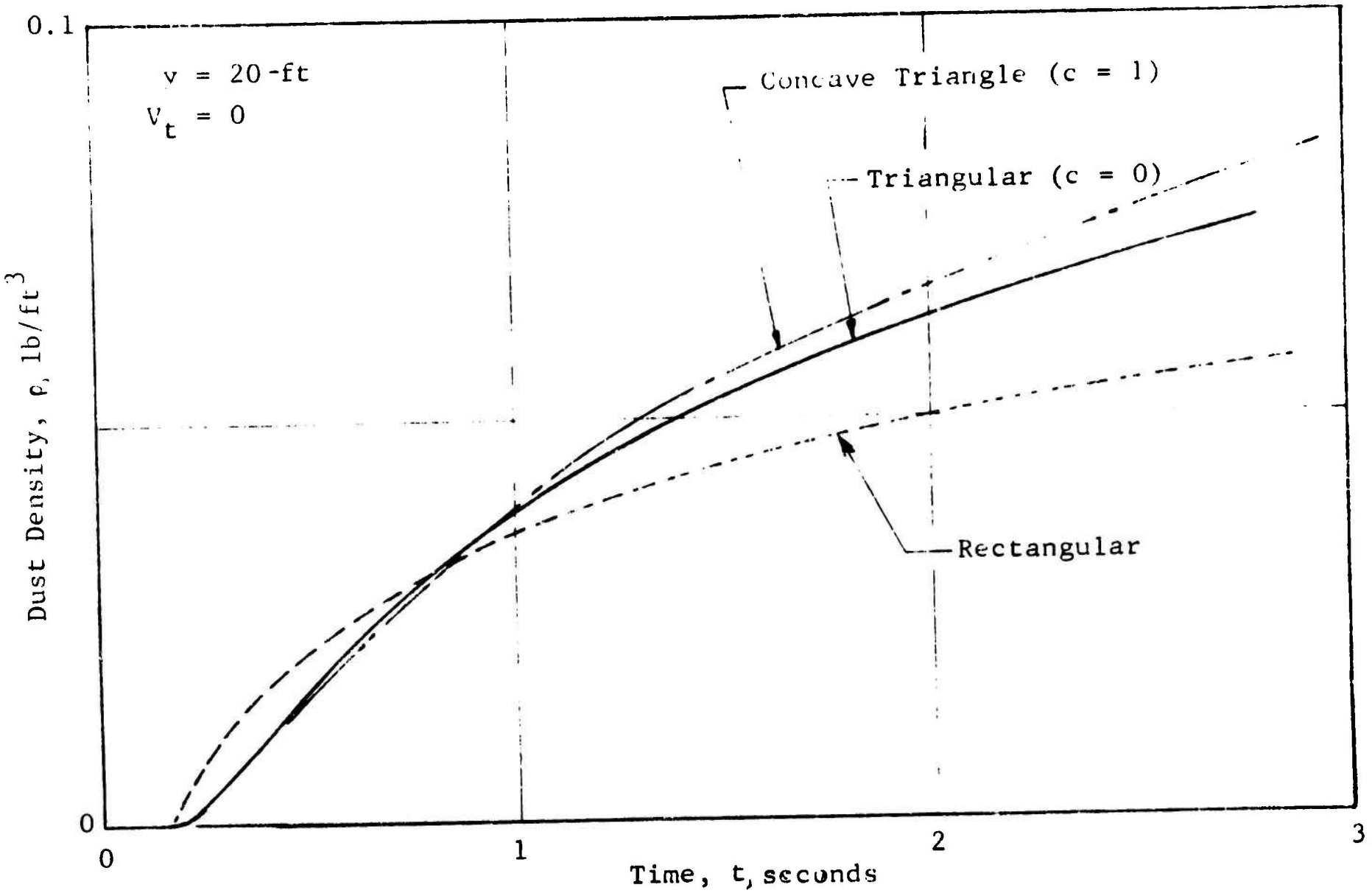

Figure 5.7 Influence of Distribution Function on Time Details

in hardened facilities must operate during the post-attack period. The fine details of the dust cloud are probably not important for long time performance of this type of equipment. Rather, average values of the dust density variations should be sufficient. Thus, this complex problem can be simplified considerably. A late-time dust model has been written and used to examine a variety of typical attacks and meterological conditions. This late-time dust cloud model utilizes an average or uniform ground condition for the area covered by the entire cloud formation. The ambient surface winds are assumed to be uniform in both magnitude and direction for the period of interest. Horizontal dispersion, as well as other transport and mixing mechanisms, have been excluded in this model. The neglect of the horizontal dispersion is reasonable on the basis that for uniform ground conditions, the horizontal gradients of the dust concentrations throughout the entire cloud formation will not be large. The vertical gradients are at least an order of magnitude greater than the horizontal gradients. The neglect of other transport and mixing mechanisms will result in a conservative estimate of the dust environment that is in an upper bound value. For low altitude burst conditions, crater ejecta, fireball dust, and dust raised by afterwinds will influence the dust environment, the latter two being late-time effects. The soil trapped in the fireball will be carried off and most likely be transported a great distance from the burst area before the soil particles settle out. All of these effects have been excluded from the present model.

The early phase of the growth and the settling of the dust cloud at any arbitrary position, such as at the site, has been determined. Typically the shock front emanating from the detonation will arrive at the site at times of the order of tens of seconds. The positive phase duration of the

blast wind will be of the order of many seconds such that the primary growth or establishment of the entire dust cloud formation will be completed in a very short time period. Thus, dust densities at a site typically reach their maximum values prior to 50-100 seconds after detonation. Thus, for late-time information, one can assume that the entire dust cloud formation is established instantaneously and at the time of detonation. Figure 5.8 illustrates the dust cloud formation and identifies the position of the site relative to the burst point or "ground zero" (the origin). The dust cloud formation will be symmetrical about the vertical axis through the burst point.

The ambient surface winds are assumed to be uniform in both magnitude and direction such that the cloud formation will drift past the site and create an effective path of the site relative to the cloud formation. This straight line path is illustrated in Figure 5.8(a) and is defined by the angle θ measured between the negative wind vector and a line generated by the site location and ground zero. The distance R_t measured along this path is given by

$$R_t = W \cdot t \tag{5.32}$$

where

W = wind velocity and

t = time.

The range R or distance from the origin of the cloud formation of a point along this path is given by

$$R = \sqrt{R_t^2 + R_s^2 - 2R_s R_t \cos \theta} \tag{5.33}$$

where

R_s = initial range of the site ($t = 0$).

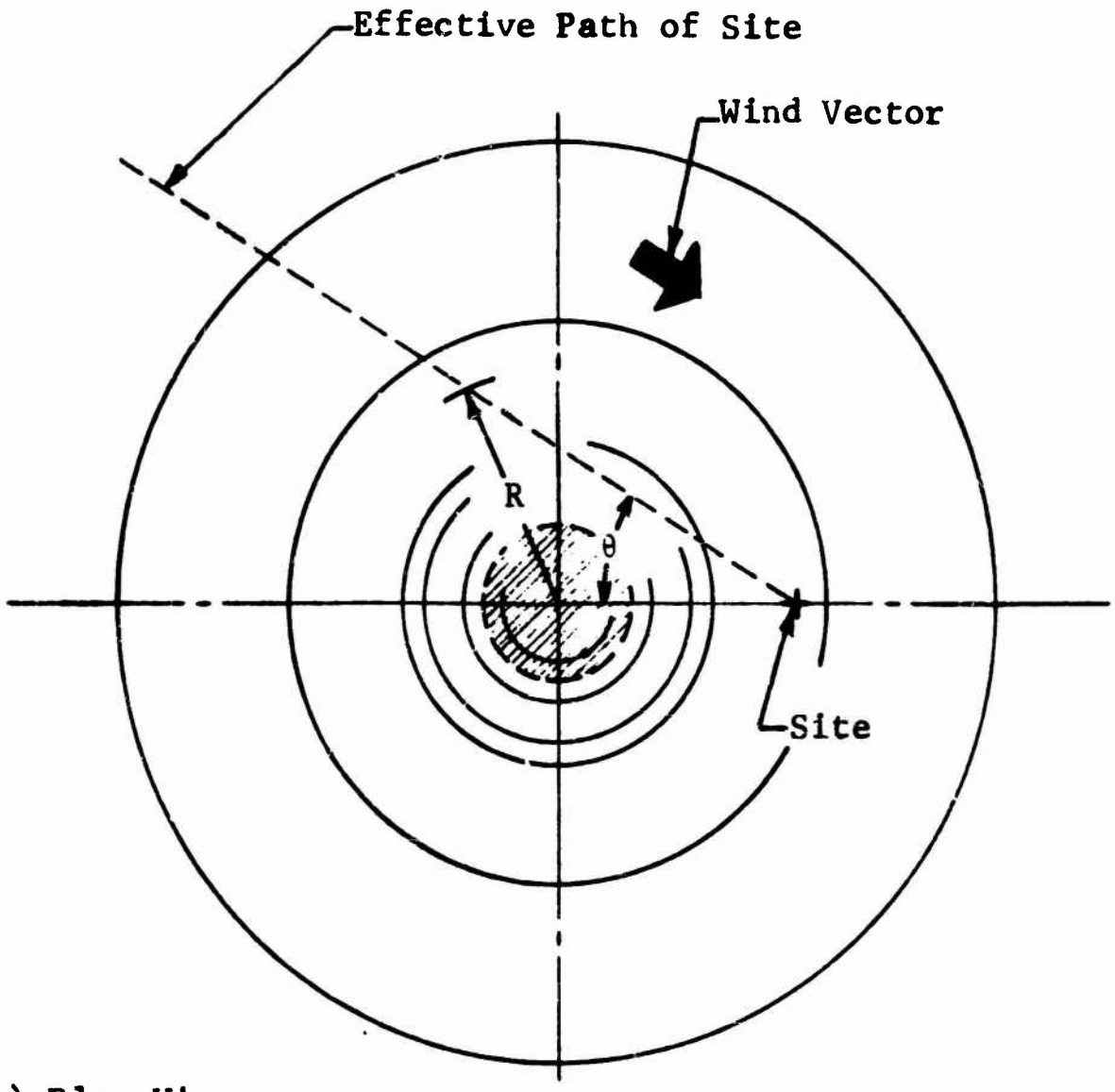

(a) Plan View

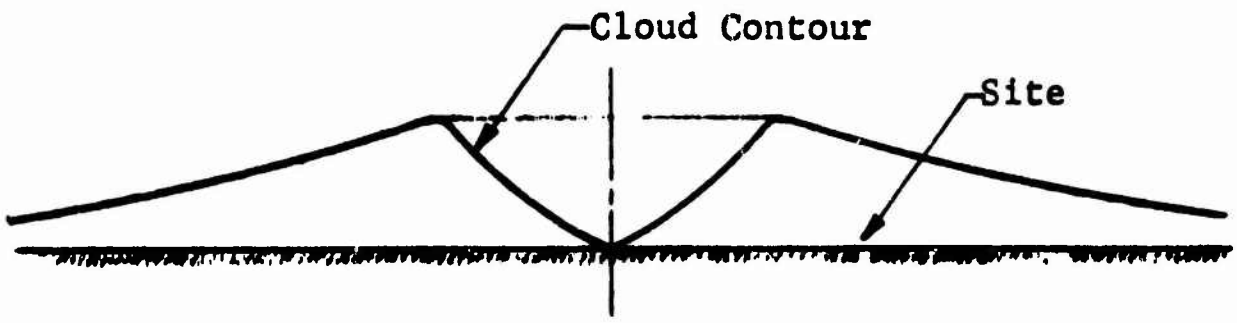

(b) Elevation

Figure 5.8 Dust Cloud Formation

The characteristics of the dust cloud are dependent upon both the location R within the dust cloud and the total elapsed time t. The location defines the overpressure and hence, the local blast wind parameters which generate the dust cloud; the total elapsed time defines the degree of cloud growth or settling which occurs at late times.

The previous subsections described a dust model for the early phases of the dust cloud formation. The similarity solution for a uniform ground condition will be used in this late-time dust model; however, some modifications will be introduced in order to better describe the late-time dust environment. The late-time model is restricted to a single burst situation and to a uniform ground condition. Neither of these restrictions is absolute; however, their adoption greatly simplifies the model and the subsequent computational effort involved in evaluating a particular problem. The similarity solution and its subsequent modifications apply to each specific particle-size class of interest or those available in the soil. The total dust density is equal to the sum of the dust density contributions from each of the individual particle size classes used.

The magnitude of the ambient surface winds will generally be sufficiently low such that additional surface soil erosion or soil "pickup" will not occur. It is therefore assumed that no soil particulate matter enters the cloud after the actual blast wind phase of the cloud development. The initial conditions or state of the dust cloud is therefore defined by the blast wind parameters. The total amount of dust for each size class and the initial height of the cloud formation, together with the distribution of the particulate matter, are sufficient to define the initial state of the dust environment.

The initial height of the dust cloud, neglecting settling, is given by the limiting value of $H_1^*(t)$ as $t \to \infty$. Equation 5.19 yields

$$\lim_{t\to\infty} H_1^*(t) = 2K_1R_o - \frac{K_1V_ot_o^*}{k^2}(k - 1) = H_o^* . \qquad (5.34)$$

The initial dust density for each particle size class is given by

$$o(\zeta) = \frac{2ao_sp}{K}(\zeta - 1 - \ell n\zeta) \qquad (5.35)$$

where

$$\zeta = Y/H_o^* . \qquad (5.36)$$

The rate of change of the cloud height as given by Equation 5.4 is still applicable; however, the ambient surface wind W is now the driving force. We therefore obtain

$$\frac{dH}{dt} = KW - V_t . \qquad (5.37)$$

If dH/dt is positive, then further growth of the cloud (i.e., for the specific particle size class associated with the value of V_t) will occur. Since no further erosion has occurred since the initial cloud was formed, the similarity solution does not apply directly. At some time, t, the cloud will reach a new height, H, given by

$$H = H_o^* - Ct \qquad (5.38)$$

where

$$C = V_t - KW . \qquad (5.39)$$

It is assumed that the particulate matter is distributed over the height H in the way that it was distributed originally over the height H_o^*, but conserving the overall mass of

the cloud. The dust density for the growth phase ($C < 0$) is given by

$$\sigma = \sigma^* \frac{H_o^*}{H} [\zeta - 1 - \ell n\, \zeta] \tag{5.40}$$

where

$$\sigma^* = (2a\rho_s p)/K \text{ and}$$
$$\zeta = Y/H.$$

For comparison purposes it will be convenient to recast this equation in terms of a dimensionless time parameter, τ. Therefore,

$$\sigma = \frac{\sigma^*}{(1 - \tau)} \left\{ \frac{\zeta_o}{(1 + \tau)^2} - 1 - \ell n \left[\frac{\zeta_o}{(1 + \tau)} \right] \right\}, \tag{5.41}$$

where

$$\zeta_o = \frac{Y}{H_o^*}, \quad 0 \le \zeta_o \le 1 \tag{5.42}$$

and

$$\tau = - \frac{Ct}{H_o^*}, \quad 0 \le \tau . \tag{5.43}$$

The density distribution for the growth phase is illustrated in Figure 5.9(a) and indicates that the density in the lower portion of the cloud decreases with time as the particulate matter migrates upward. The dust density in the upper portion of the cloud will, on the other hand, increase with time. The dust density at some height which is greater than the initial height of the cloud will be zero until the cloud height grows sufficiently to reach this elevation. Generally, interest will be limited to the lower portions of the initial cloud. The dust density variation with time for the growth phase is illustrated in Figure 5.10 for several values of ζ_c. The dust density varies quite slowly with time. The cloud height has doubled for a value of $\tau = 1$.

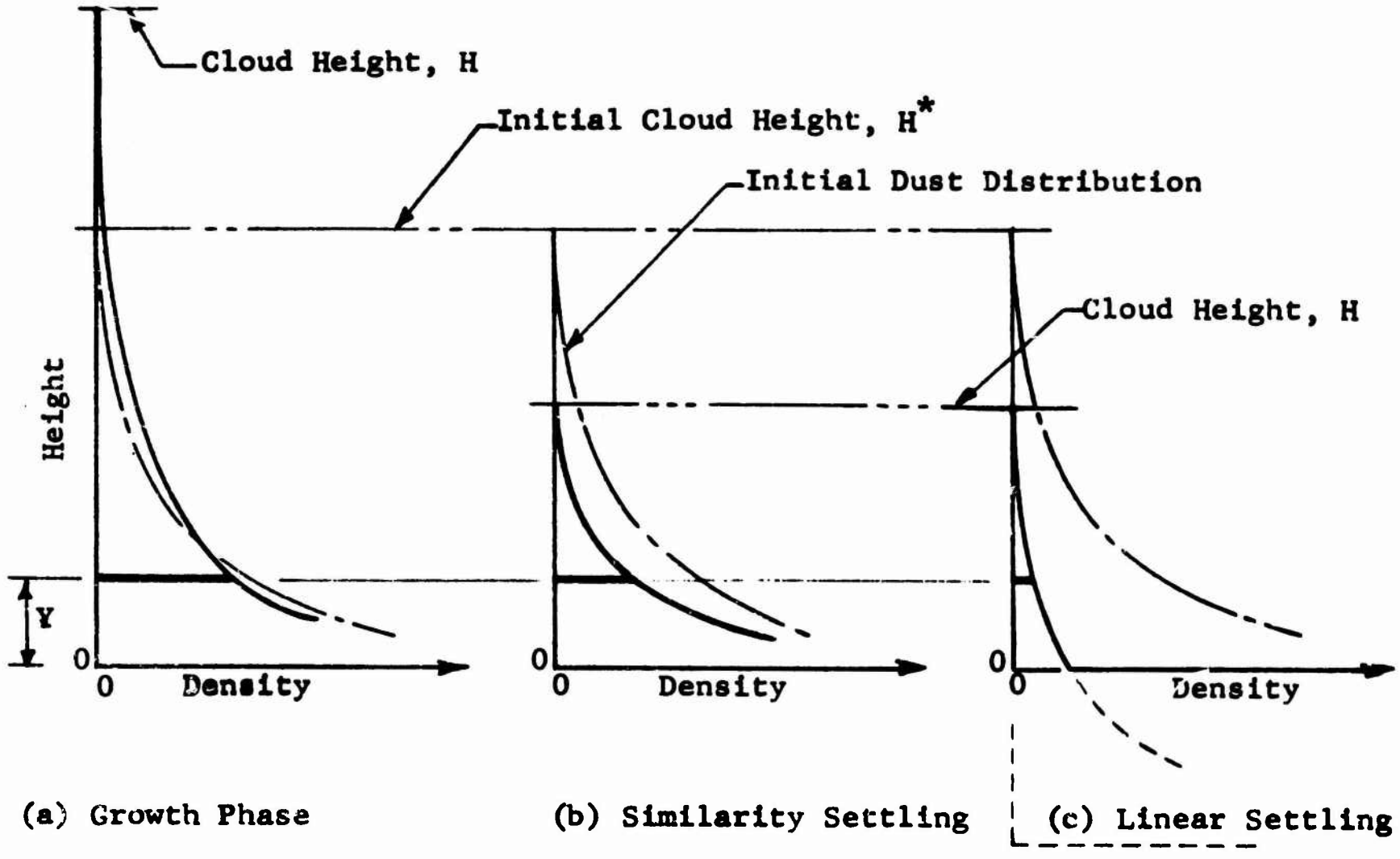

Figure 5.9 Late Time Dust Cloud Models

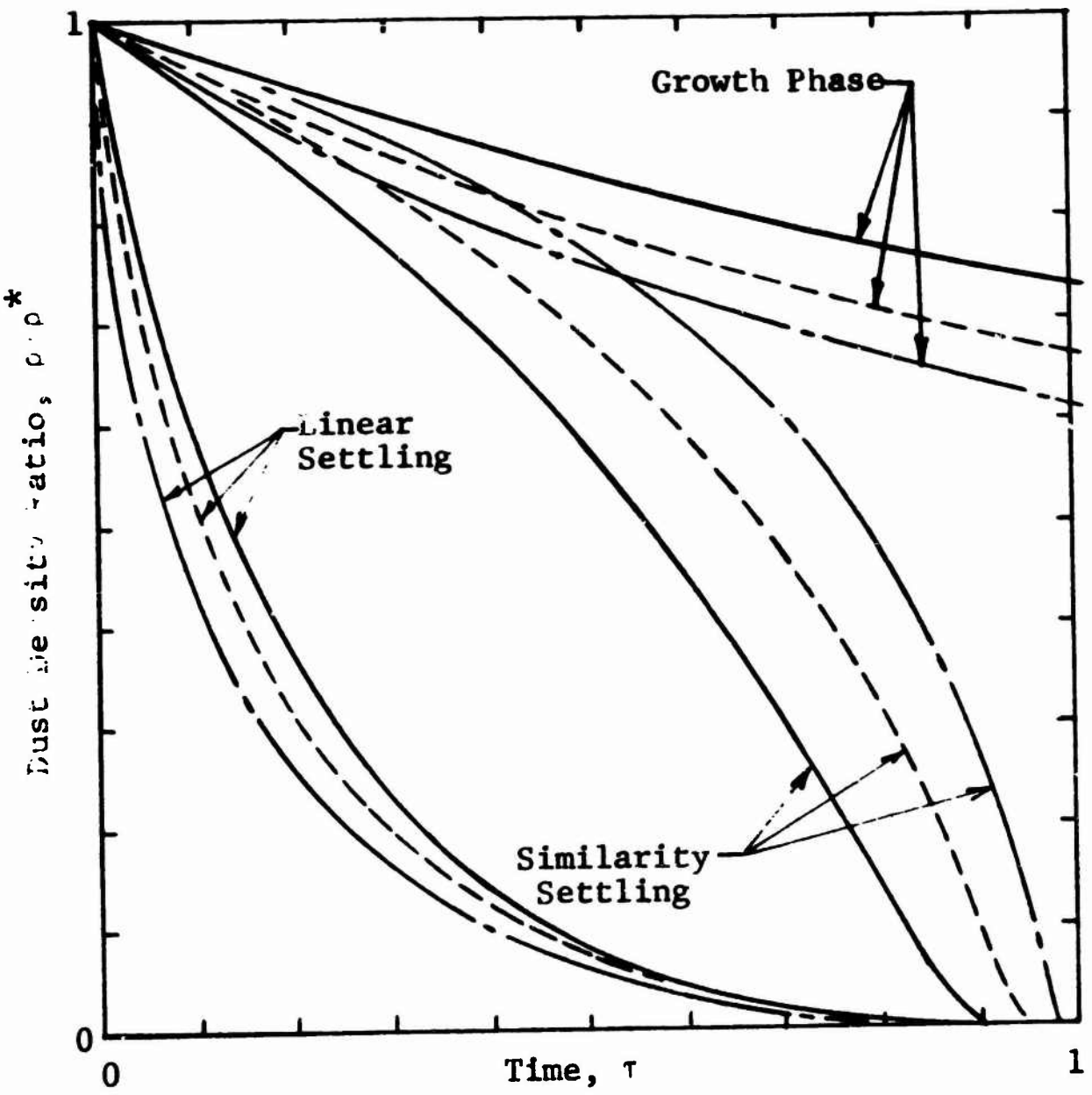

Figure 5.10 Late Time Dust Cloud Density Models

If dH/dt is negative (C > 0), then the cloud height will decrease and settling of the particulate material will occur. In this case, the similarity solution can be used, viz.

$$\rho = \rho_s \left[\zeta - 1 - \ell n\ \zeta\right] \tag{5.44}$$

where

$$\zeta = \frac{Y}{H} \ . \tag{5.45}$$

In terms of the dimensionless time, τ, Equation (5.44) becomes

$$\rho = \rho^* \left\{ \frac{\zeta_o}{1-\tau} - 1 - \ell n \left(\frac{\zeta_o}{1-\tau} \right) \right\} \tag{5.46}$$

where

$$\zeta_o = \frac{Y}{H_o^*} \quad , \quad 0 \leq \zeta_o \leq 1 \ ; \tag{5.47}$$

and

$$\tau = \frac{Ct}{H_o^*} \quad , \quad 0 \leq \tau \ . \tag{5.48}$$

Note that Equations (5.43) and (5.48) differ in sign. This difference is due to desire to make τ increase with increasing t while the sign of C differs between the growth and settling phase.

The above similarity settling equation describes the fact that the dust particles at the upper portions of the cloud fall faster than those near the bottom of the cloud. Thus the dust begins to concentrate near the bottom of the cloud. The dust density decreases with time since some particles do settle out on the ground surface. It would appear, however, that another, perhaps more realistic model could be adopted, namely one in which all of the dust particles settle at the same rate. This type of behavior is referred to as linear settling and the dust density is given by the relationship

$$\rho = \rho_s \left[\frac{(Y-Ct)}{H_o^*} - 1 - \ell n \left(\frac{Y-Ct}{H_o^*} \right) \right] \qquad (5.49)$$

or in terms of τ and τ_o, as

$$\rho = \rho_s \left[\tau_o + \tau - 1 - \ell n \left(\tau_o + \tau \right) \right] . \qquad (5.50)$$

Figure 5.9(b) and (c) illustrates the difference between similarity and linear settling. Figure 5.10 presents the dust history for several values of τ_o for each of the settling models. The linear settling model results in a much more rapid decrease in dust density with time. In both cases the dust density vanishes when $\tau = 1 - \tau_o$.

Figure 5.11 presents that value of the surface wind velocity for which a particular size particle will just settle out. This value of the wind velocity has been defined as the critical wind velocity W_c. It should be noted that particles which are greater than 100 to 200 microns in size will generally settle out of the cloud. Thus, the late time dust environment will consist of only the smaller particles. Figure 5.12 presents a comparison between the results of linear and similarity settling for a typical problem. The discontinuities in the curves are due to the discrete particle size classes used in the calculation and their settling out at specific times ($\tau = 1 - \tau_o$) for these size classes.

The linear settling model described above is the settling model which has been selected and used in all subsequent calculations.

5.3 Evaluation of Dust Model Coefficients

The dust environment model is based on a series of assumptions utilizing several coefficients to define the magnitude of some of the effects. It is essential to examine the validity of all of the details of the model in order to establish the overall reliability of the prediction.

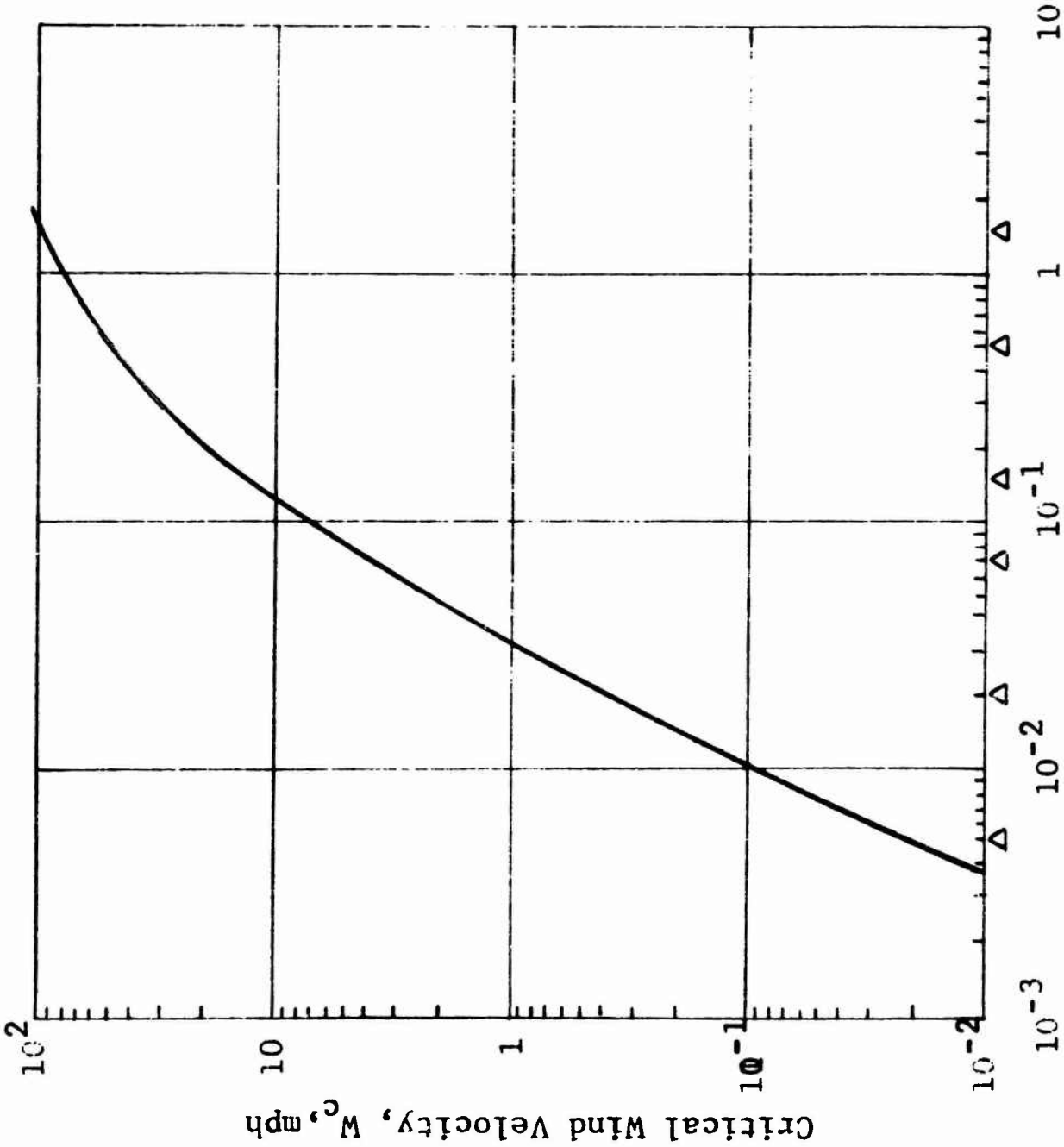

Figure 5.11 Critical Wind Velocity

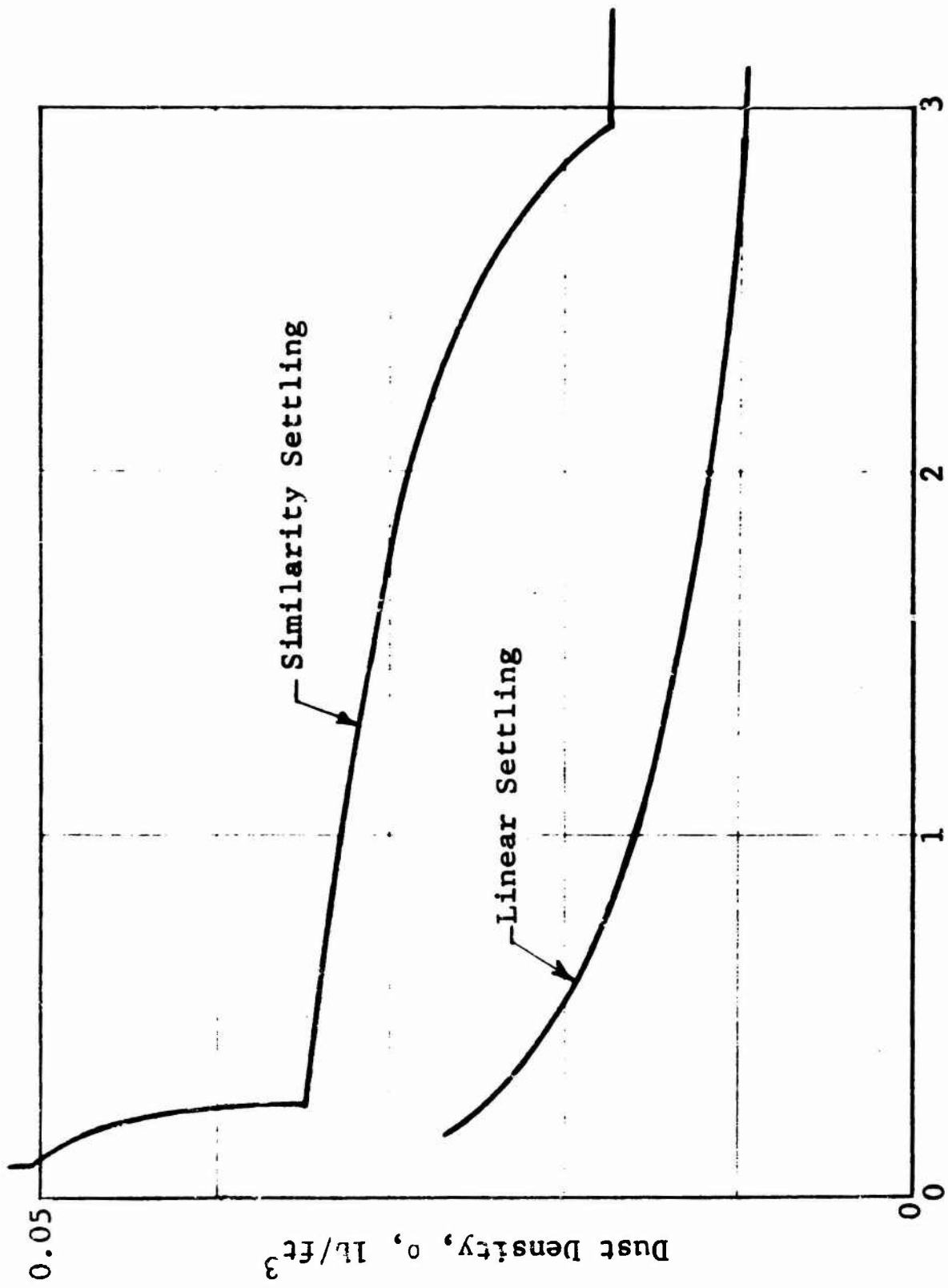

Figure 5.12 Comparison of Settling Models

Since the state of the art of generation and transport of dust clouds is not sufficiently advanced, a series of two experiments has been performed as part of the current program. One experiment deals with the erosion of the soil subjected to a transient surface wind and the results will assist in establishing the magnitude of the erosion constant a used in Equation 5.2. The second experiment deals with the transport of the dust cloud, once established. This experiment will determine the relationship between the transport constant K and the turbulent level of the air stream, and will also yield some information on the dust distribution within the cloud. Both experiments were rather limited in scope; however, they are sufficient to substantially increase the reliability of the prediction method. A description of these experiments is presented in Appendix D. In addition to these experiments, dust data have been obtained from both nuclear and high-explosive field tests. These data, however, are sparse and perhaps somewhat unreliable.

The erosion coefficient a was the most uncertain coefficient of the current model, and the predicted dust densities are directly proportional to its magnitude. The probable range of its value, however, was determined. The model considers the magnitude of the aerodynamic forces available to remove layers of particles, and then postulates the average distance the particles must move before the subsequent layers begin to move. The estimate of the time required to remove each layer and the number of particles (or the weight of) in each layer is sufficient to define the magnitude of the erosion constant. The following result is obtained for the case where the aerodynamic force is constant; that is, the particle velocity is small compared to the air velocity.

$$a = \sqrt{\frac{3}{16}\left(\frac{\rho_a}{\rho_c}\right)\frac{1}{N}}\,, \qquad (5.51)$$

where

ρ_a = density of the air,

ρ_c = density of the particle, and

N = the number of particle diameters traveled in horizontal direction.

The ratio of the air to particle densities is well known and will not vary significantly. The relatively insensitive square-root dependence of a on N indicates that a reasonable estimate of N will be sufficient. The value of the erosion constant is presented in Figure 5.13 as a function of N. The results of Equation 5.51 are indicated as Curve 1 in this figure. Curve 2 is the result of a more refined analysis in which the relative velocity between the dust particle and the air is taken into consideration when reducing the eroding force.

A dust boundary layer will exist in which the actual erosion process takes place. This boundary layer will be rather dense and the air velocity therein, which represents the driving force, will be substantially reduced from the free-field velocity. Therefore, the erosion factor must be reduced by the corresponding reduction factor in velocity. The dashed line in Figure 5.13 represents such a reduction corresponding to a factor of approximately 0.1.

The results of the erosion experiments indicated that the value of the erosion coefficient was considerably higher (approximately 10^{-3}) for very loose soils. However, whenever a small amount of compaction was applied, the value of the erosion coefficient was reduced considerably. The results of the erosion experiments are summarized in Figure 5.14. A value of 6×10^{-4} has been selected as a reasonable value for the erosion coefficient for the current problem, since the surface soils will be somwhat compacted.

The results of the transport experiments indicate that the value of the transport coefficients is not strongly

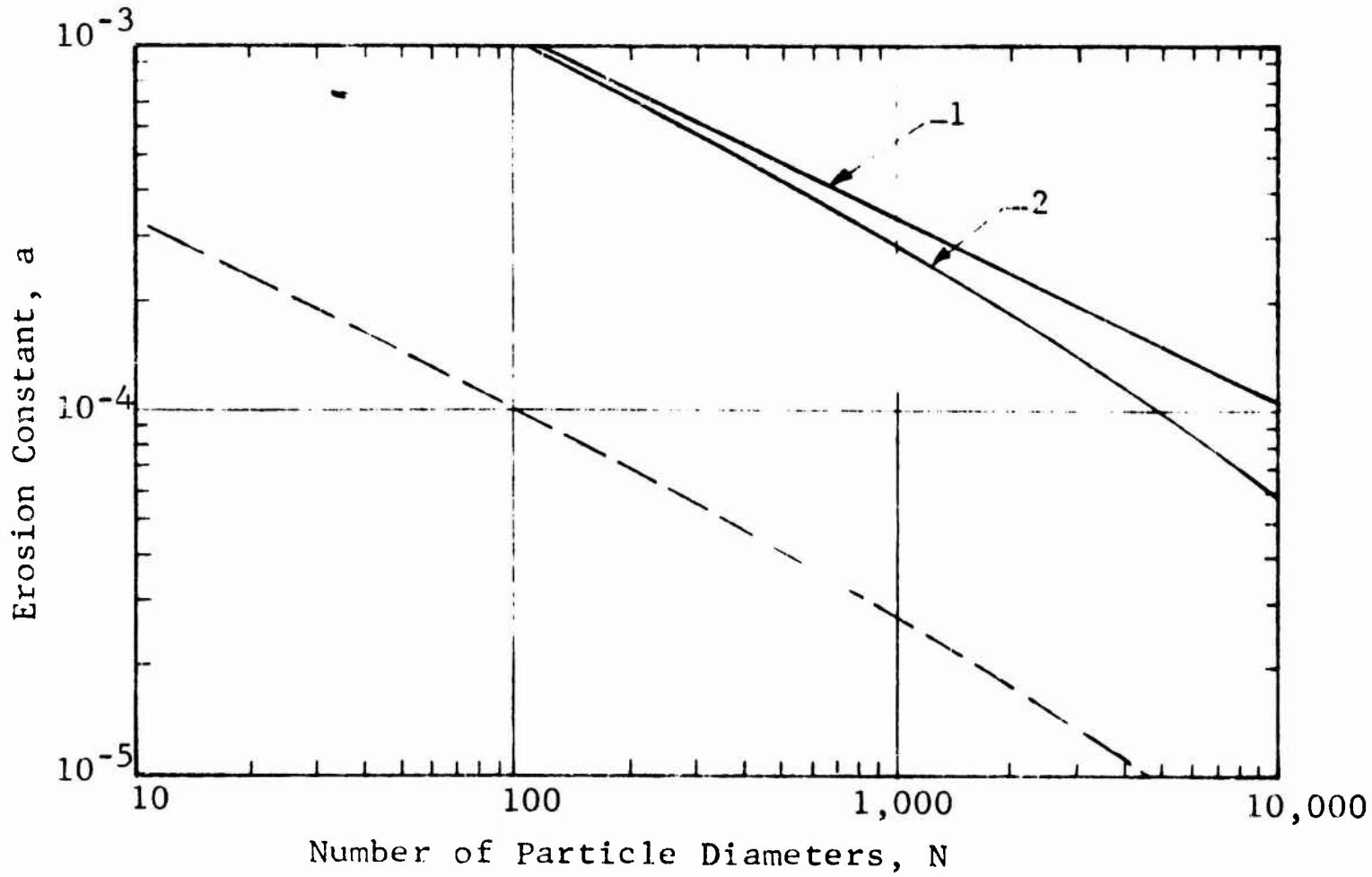

Figure 5.13 Probable Range of Erosion Constant

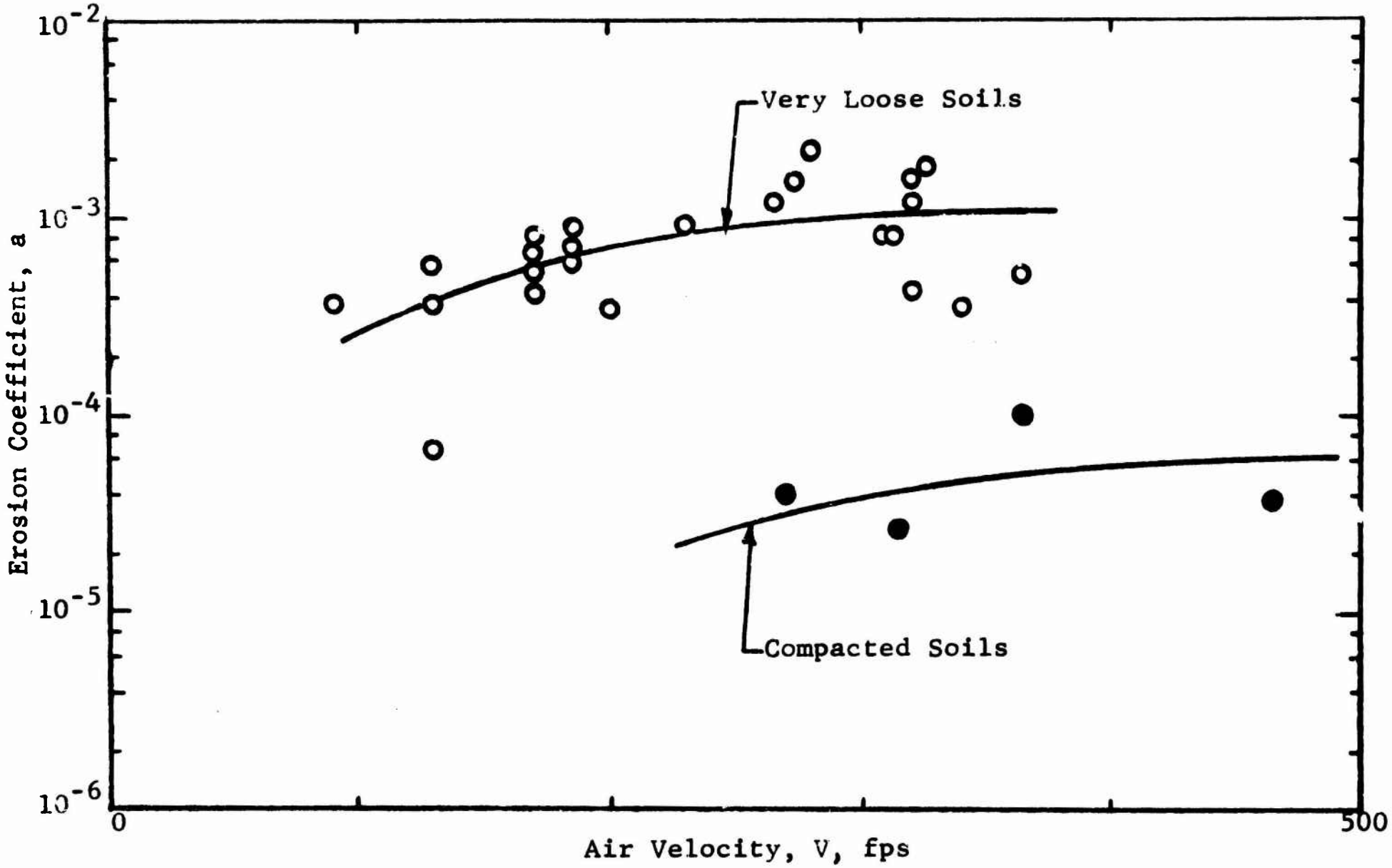

Figure 5.14 Erosion Coefficient Measurements

dependent upon either the turbulence level or the air velocity. These experimental results are presented in Figure 5.15. A value of 0.2 appears to be a reasonable value for the range of variables and soil types investigated.

Another estimate of the value of the transport coefficient can be obtained from a field experiment. The height of a dust cloud is one of the few characteristics which can be observed easily and with reasonable accuracy. Observation made during Shot 7 of Operation Greasystake[5.4] is presented in Figure 5.16, together with a prediction based on Equation 5.4. The velocity history was estimated based on the yield, the height of burst, and the overpressure level. A value for K of approximately 1/4 yields a good comparison with the experimental observations. It is significant that the comparison is good both initially where the peak velocity is well known and at the latter stages of the cloud growth (approximately one-half of the positive phase duration of the velocity). This particular observation was for a high-explosive test and may not be fully representative of a nuclear detonation.

Several dust density measurements have been made of dust clouds raised by the blast winds induced by low-yield nuclear detonations. The reliability of these observations is poor; however, these data represent the only opportunity with which to make a comparison at this time (these comparisons are presented in Figure 5.17). These predictions were based on a uniform soil assumption, and a single particle size (100 microns) was used. It should be noted that the observations were made during the first half of the positive phase duration and no late-time effects were observed.

The experimental observations exhibit rather large local fluctuation which may be due to either the variability of the soil in front of the dust probe or to the interaction of relatively large clumps of soil with the probe. These

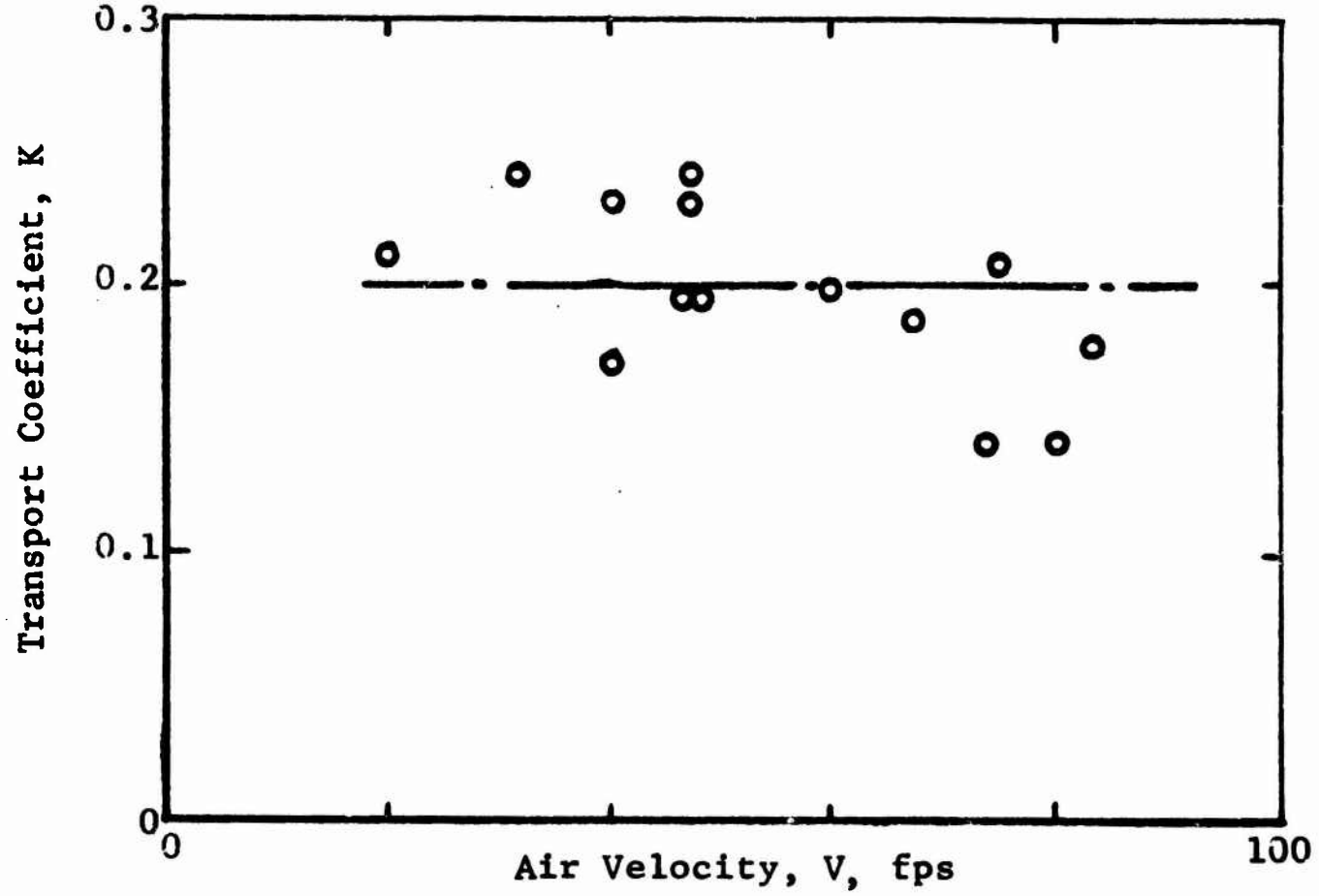

Figure 5.15 Transport Coefficient Measurements

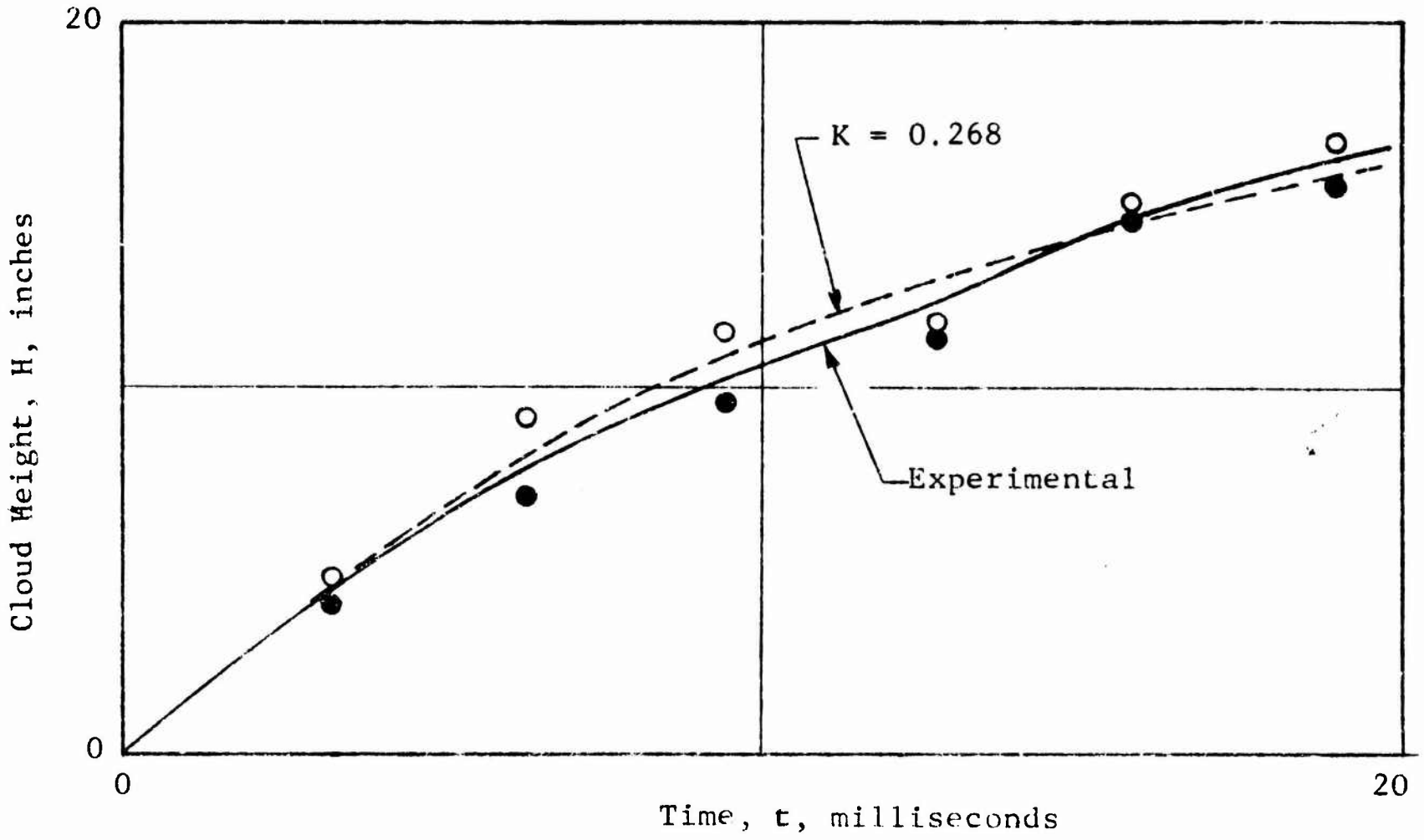

Figure 5.16 Comparison of Dispersion Factor with Experimental Data

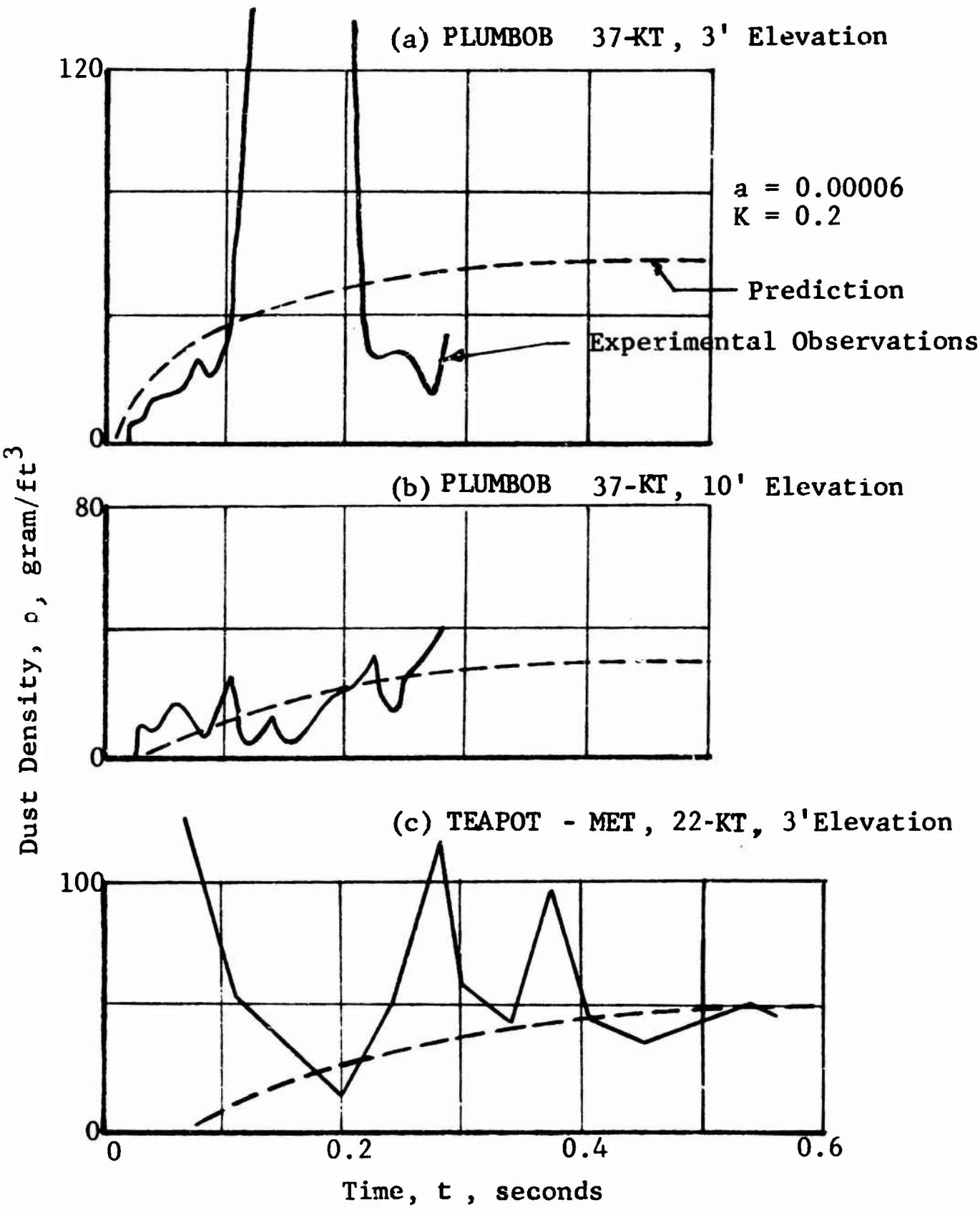

Figure 5.17 Comparison of Prediction with Experimental Observations

clumps are expected to exist close to the ground. The measurement made at the 3-ft elevation for PLUMBBOB closely agrees in form and magnitude with the predicted results except for a brief interval. The measurement made at the 10-ft elevation is uniformly erratic and slightly more dense than the corresponding predicted value. The comparison for MET shot is similar to this latter comparison. The overall agreement is qualitatively good. These experimental data are considered to be too unreliable to justify any change in the selected values of the erosion constant.

The value of 0.00006 for the erosion coefficient was used in the computations made for the current effort. A value of 0.20 was used for the transport constant K. These values should be sufficient for the current effort.

5.4 Typical Results

Four computer programs were written in FORTRAN IV for the purpose of predicting the dust environment at the elevations of interest. These programs are all based upon the previously developed cold dust models and will also treat the following specific cases:

(a) uniform ground conditions--single burst,

(b) uniform ground conditions--two or three bursts,

(c) variable ground conditions--single burst,

(d) late-time dust - uniform ground conditions -- single burst.

These programs are discussed in detail in Appendix A. This section presents the results of specific calculations and illustrates the influence of some of the pertinent variables.

5.4.1. Blast Wind Induced Dust Environment

It has been previously mentioned that the dust density is directly proportional to the value of the erosion coefficient. Furthermore it can be established that some surfaces are somewhat nonuniform and that erosion cannot be expected to occur locally over the entire surface. Therefore,

a land-use factor has been introduced which attempts to account in a gross manner for this characteristic of a particular surface or region of the surface. The numerical value of this factor lies between unity and zero and must be estimated on a highly subjective basis. As an example, an area of well sodded grass has been assigned a land-use factor of 0.1 which implies that only 10 percent of the soil surface contributes to the dust cloud. In the following results a variety of factors has been used.

Eight discrete particle sizes are incorporated into the computer programs, ranging in size from 5 microns to 5 mm. The dust density variation at a site surrounded by a uniform soil of a single particle size was computed for each of the eight particle size classes. The results are presented in Figure 5.18. These results apply at the 15-ft level and for a relatively large-yield weapon. Figure 5.19 presents the influence of the height above the ground for a typical site in which the soil distributed around the site is not uniform.

The dust density will persist at the site for an appreciable period of time after the passage of the shock wave. Figure 5.20 illustrates a typical result for a large-yield weapon. The positive phase duration of the wind is approximately 10 sec. The peak dust density occurs at approximately 50 sec. The dashed curve represents the dust density variation for discrete particle size groups and indicates when a particular size class drops below the height of interest. The solid line is merely a smooth curve illustrating the continuous decay that a continuous particle size distribution would yield. The dust density does not decay below one-half the peak dust density until approximately 3 hours after the burst. It is quite clear that the influence of ambient winds will modify these late-time results, in that dust raised at other nearby regions will have drifted

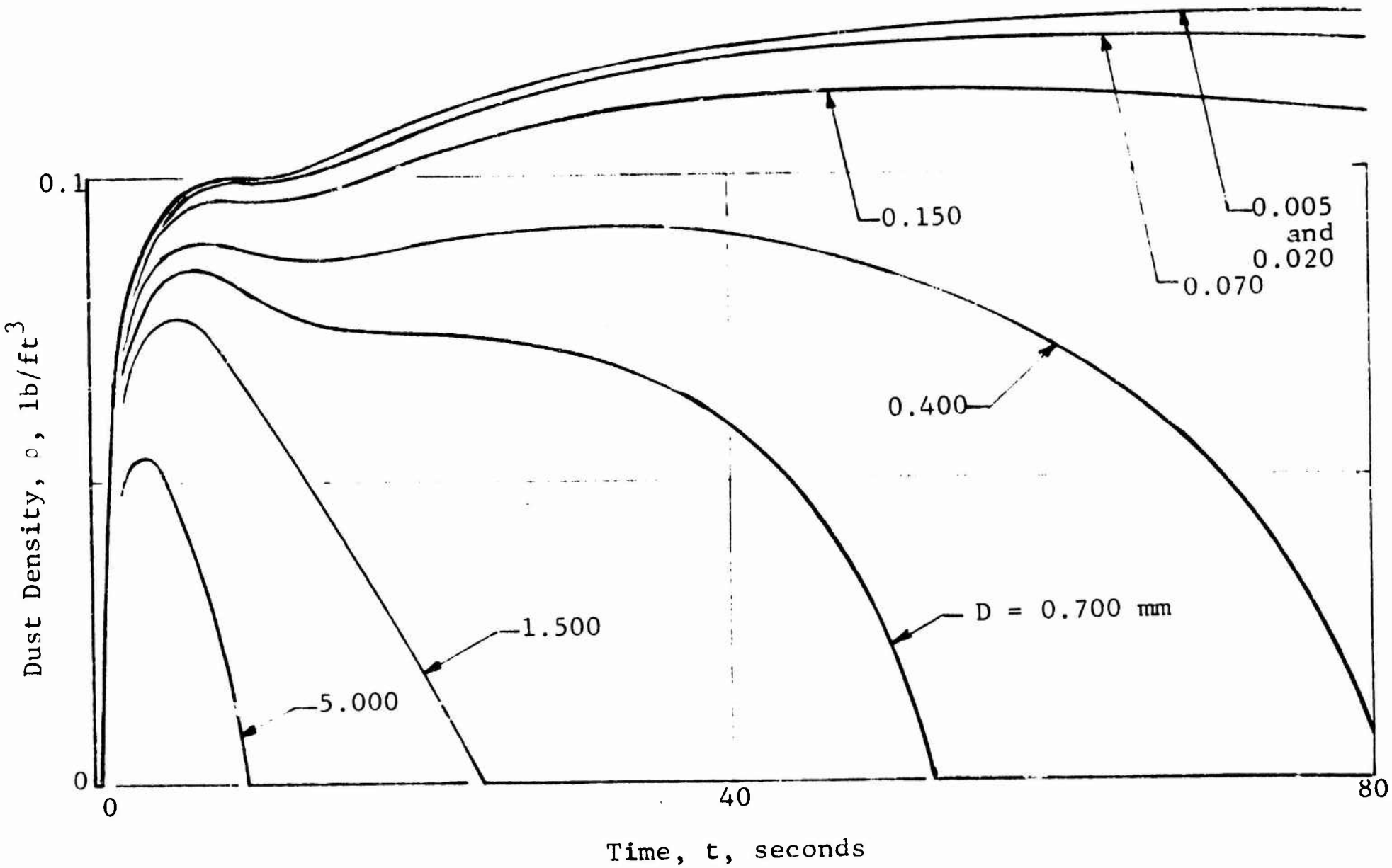

Figure 5.18 Effect of Particle Size

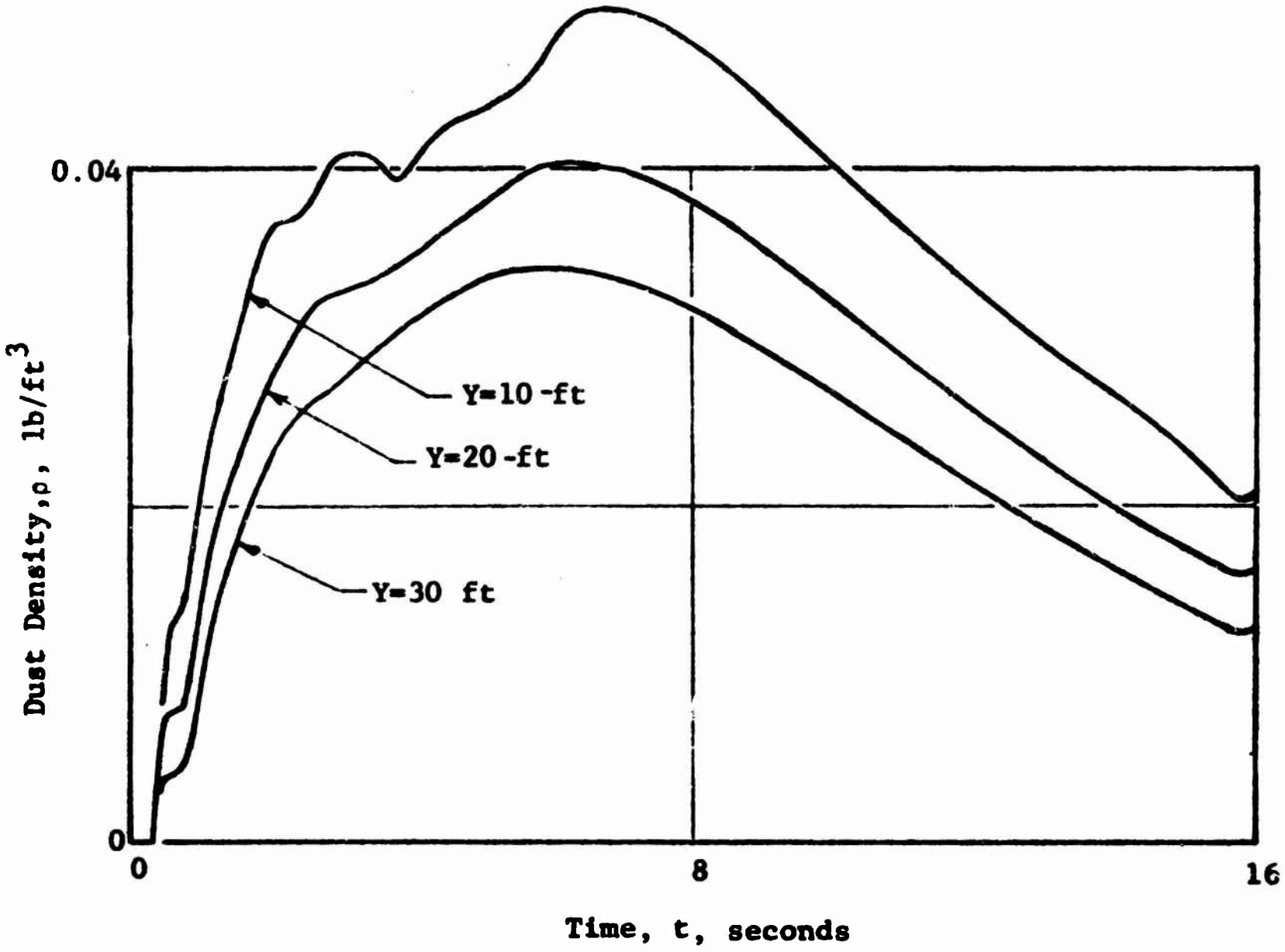

Figure 5.19 Dust Density Variation with Height

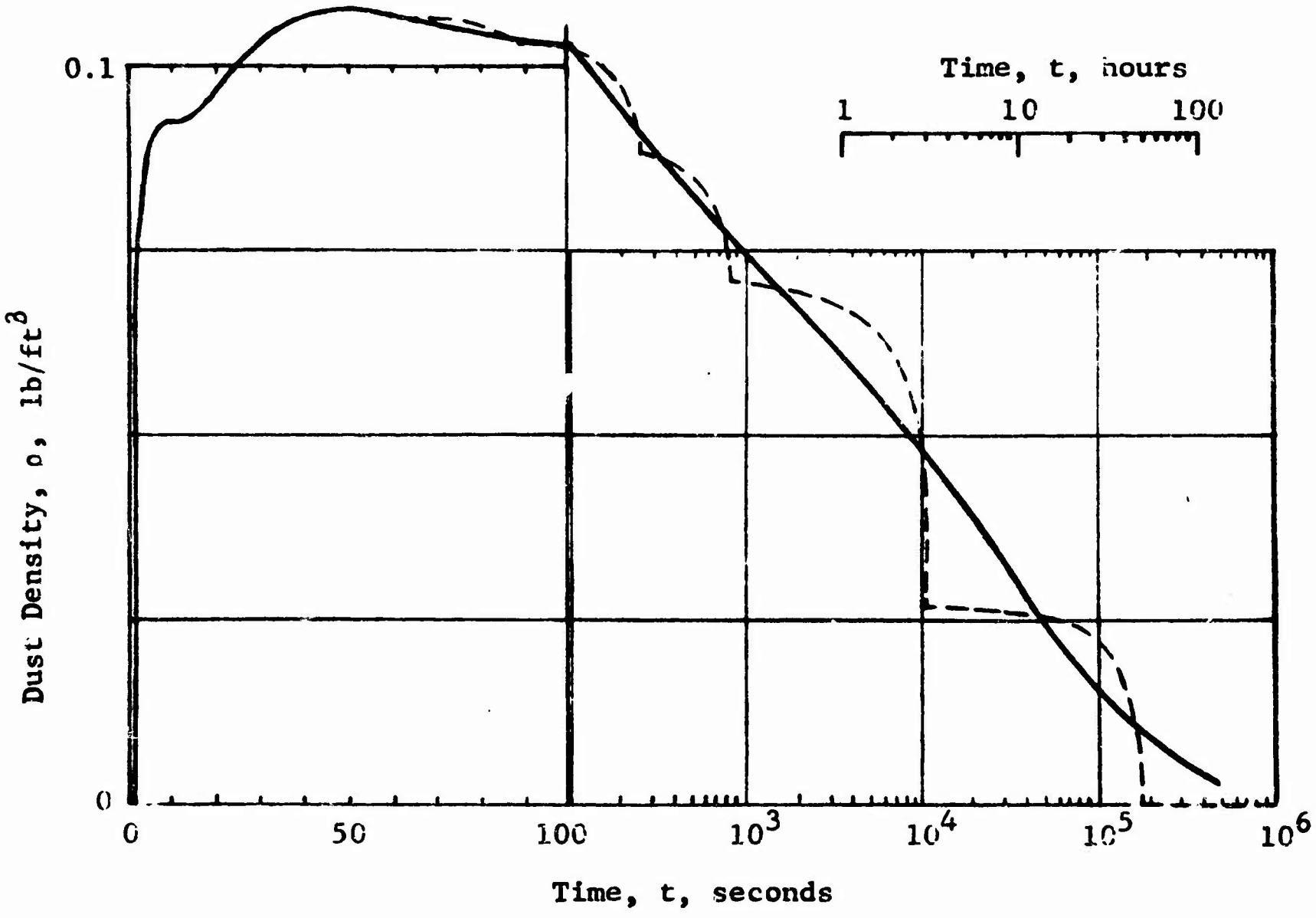

Figure 5.20 Late Time Effects

past the site. For this reason the late-time dust model was developed and typical results for late times are presented in the following subsection.

The variable ground dust code (single burst) permits one to calculate the dust density variation at the site for the case where the soil characteristics (e.g., weight factions and land use factors) vary with ground range in front of and behind the site. A series of calculations was made in which a circular region R, around the site, had a stabilized soil condition, such that no dust could be raised from this region. The region outside this circle, however, will contribute soil to the dust cloud. The results of these calculations are presented in Figure 5.21. The maximum range from the site, which still contributes to the dust cloud at the site, is approximately 2500 ft.

The third computer program permits one to compute the dust densities resulting from two or three bursts. These bursts must come from the same general direction, relative to the site, and apply to the uniform ground condition case. The results for a typical large yield case (for identical size weapons) are illustrated in Figure 5.22. The additional dust raised by the second and third bursts contributes relatively little to the dust density when compared with the first burst. This is due to the fact that although the overall cloud height may be nearly doubled for two bursts, the value of the similarity variable is reduced by a factor of approximately two. Such a reduction results in a small increase in the dust density for heights less than one-tenth the cloud height (see Figure 5.6).

5.4.2. Late-Time Dust Environment

The overall dust cloud formation must first be defined in general terms, and then the apparent location of the site within the cloud at any given time must be established. At this point the blast wave parameters can be evaluated and

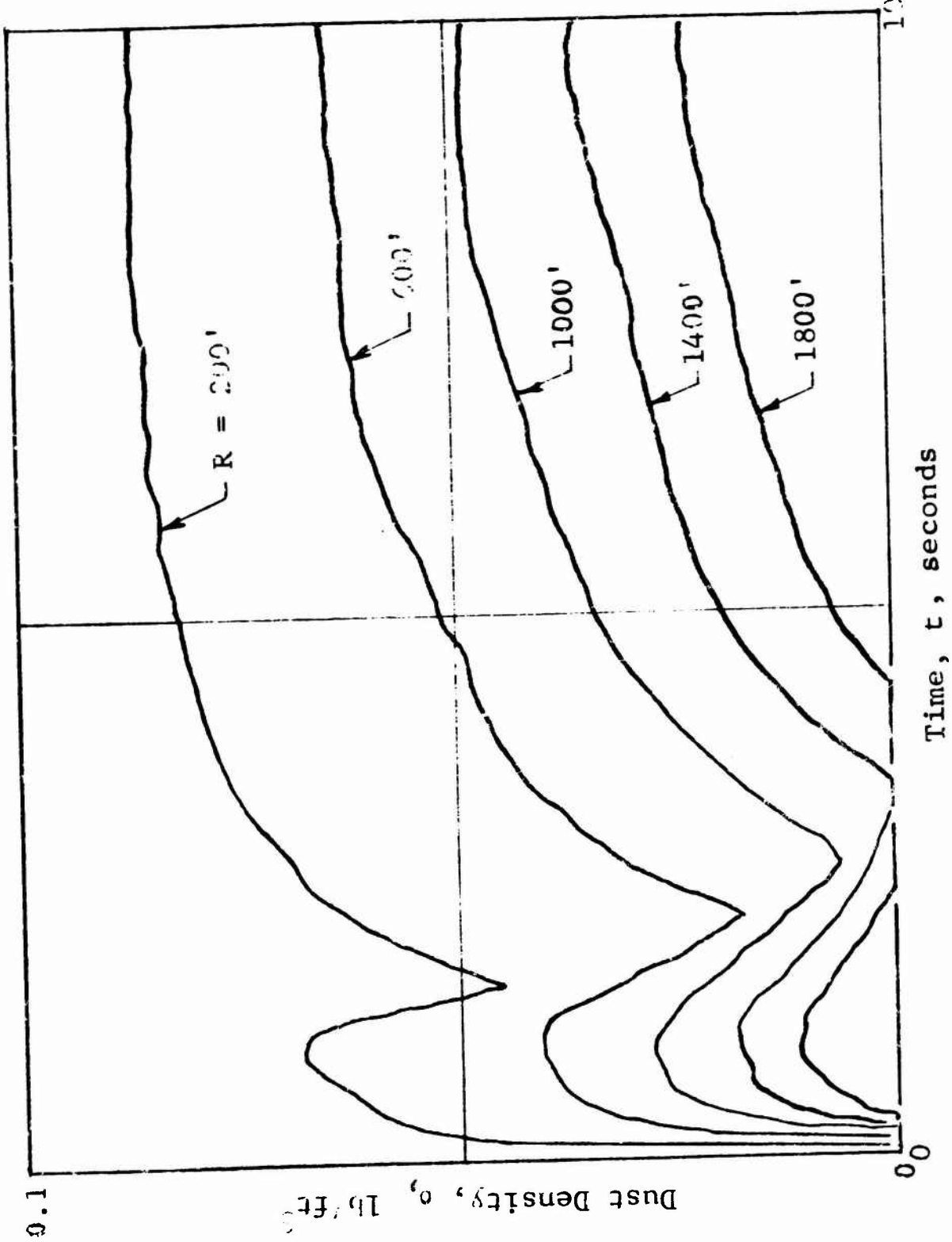

Figure 5.21 Influence of Soil Stabilization Around Site

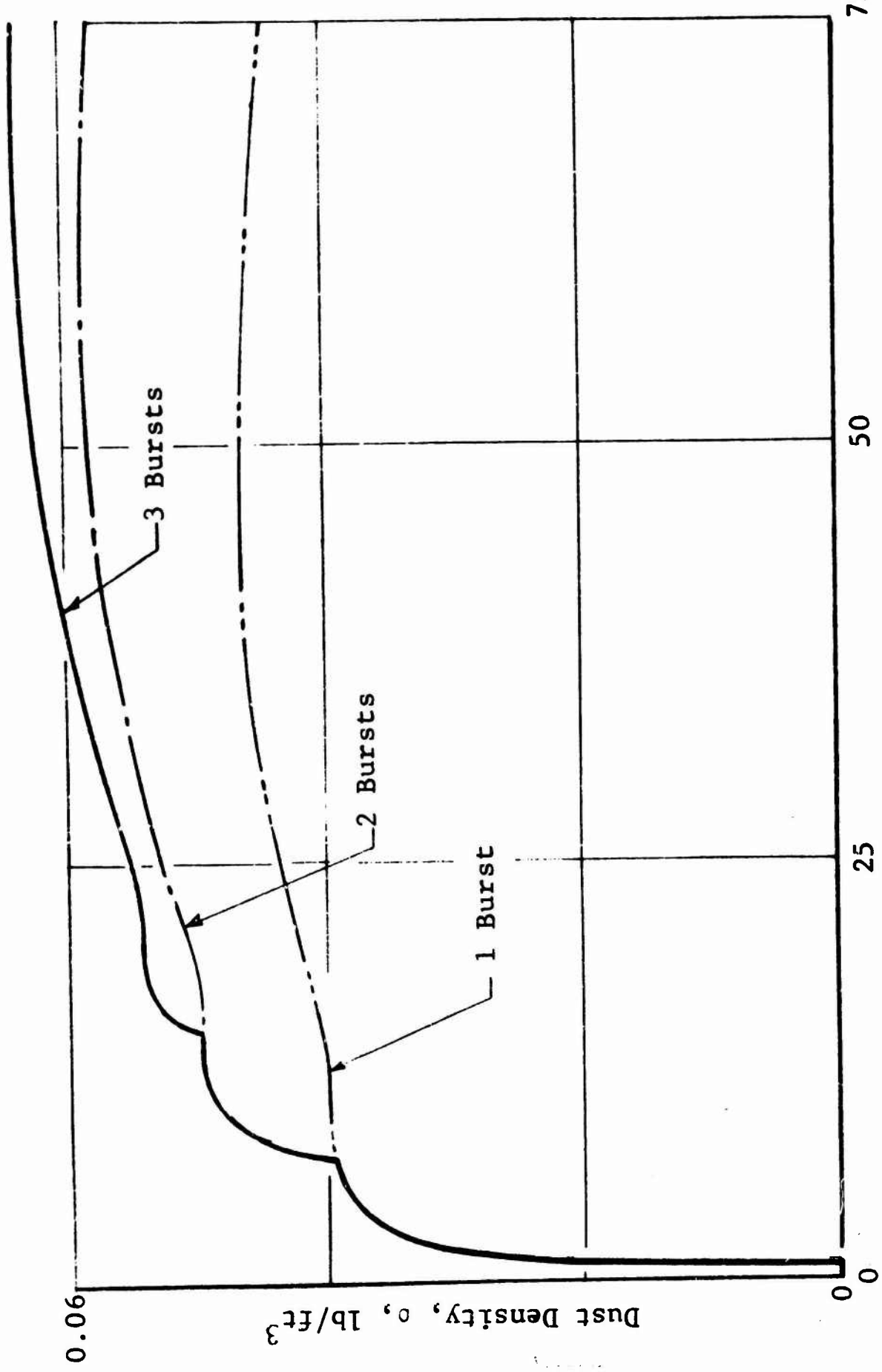

Figure 5.22 Multiburst Dust Cloud

the initial dust environment established at each point of interest in the cloud formation. It should be noted that for all nonsurface burst conditions the blast region will be divided in two shock reflection regions; regular and Mach reflection regions. The overpressure variation with range from the origin for a representative large yield burst condition is illustrated in Figure 5.23. The dividing point between the two reflection regions is defined as R_c. Figure 5.24 presents the initial height of the cloud H_o^* as a function of range for the same burst and yield conditions. The cloud height at the origin vanishes because the horizontal air motion is zero. The overpressure is a maximum at the origin as indicated in Figure 5.24. The dust model and the associated blast wave idealizations are valid for low to moderate overpressure levels. At the present time the weapons effects subroutines are valid to overpressures of approximately 60 psi. For a surface or near-surface burst the pressure at the origin will far exceed this maximum value and create a dust cloud environment which is not well established. This local region cannot be handled properly at the present time and must therefore be excluded from the present analysis and calculations. When this region exists it will be centered about the origin as indicated by the shaded area in Figure 5.8. The late-time dust computer code bypasses this region automatically. It should be noted that this exclusion will occur only in a very small number of problems of interest.

Typical results are presented in Figures 5.25, 5.26 and 5.27 for three different surface wind magnitudes and four different directions ranging from directly towards the origin to directly away from the origin. The site is initially located at the range where the maximum cloud height exists for these sets of calculations, hence the $\theta = 0°$ and $\theta = 45°$ results are characterized by cusps. This is due to the passage of the apparent path of the site through this cloud

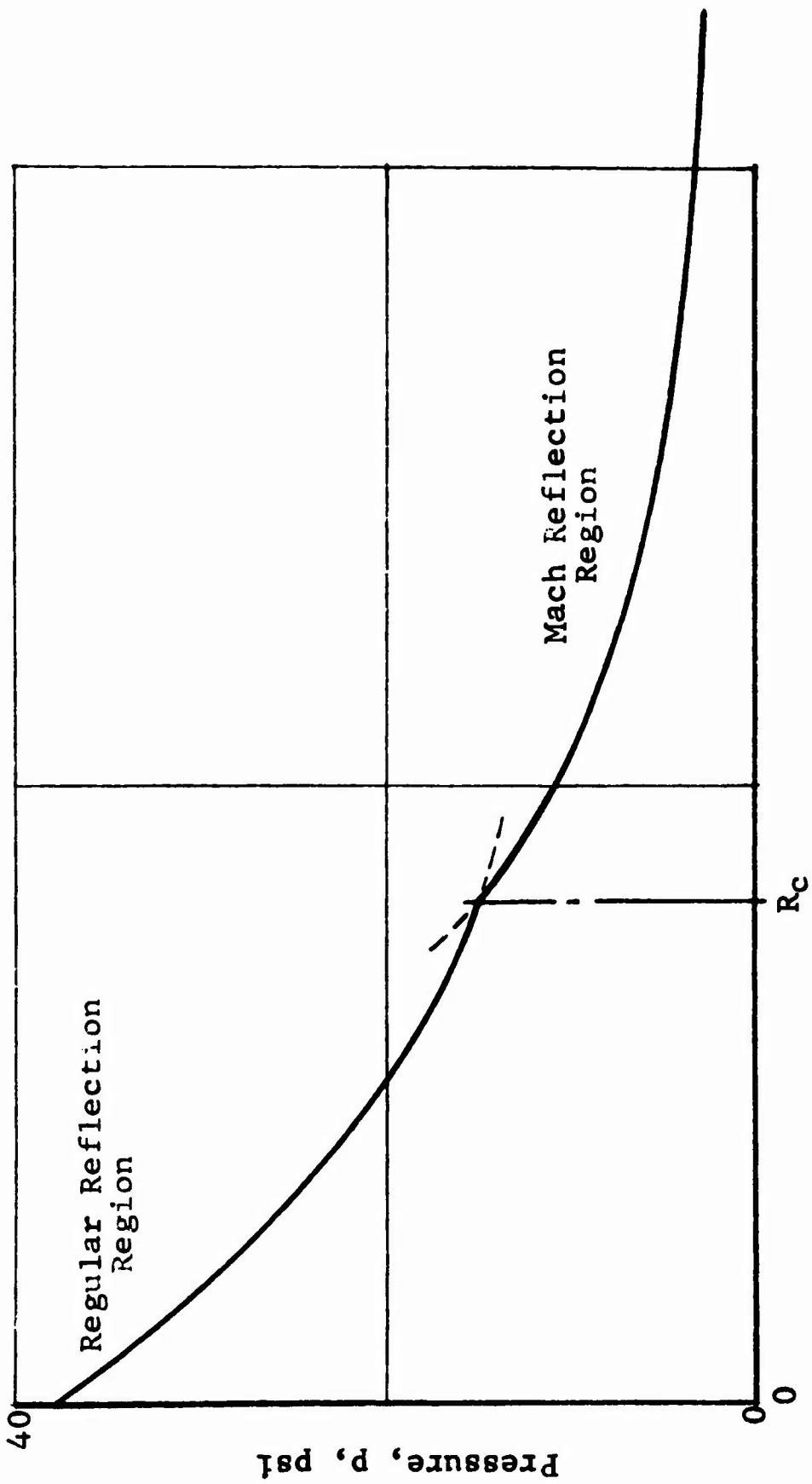

Figure 5.23 Overpressure Variation with Range

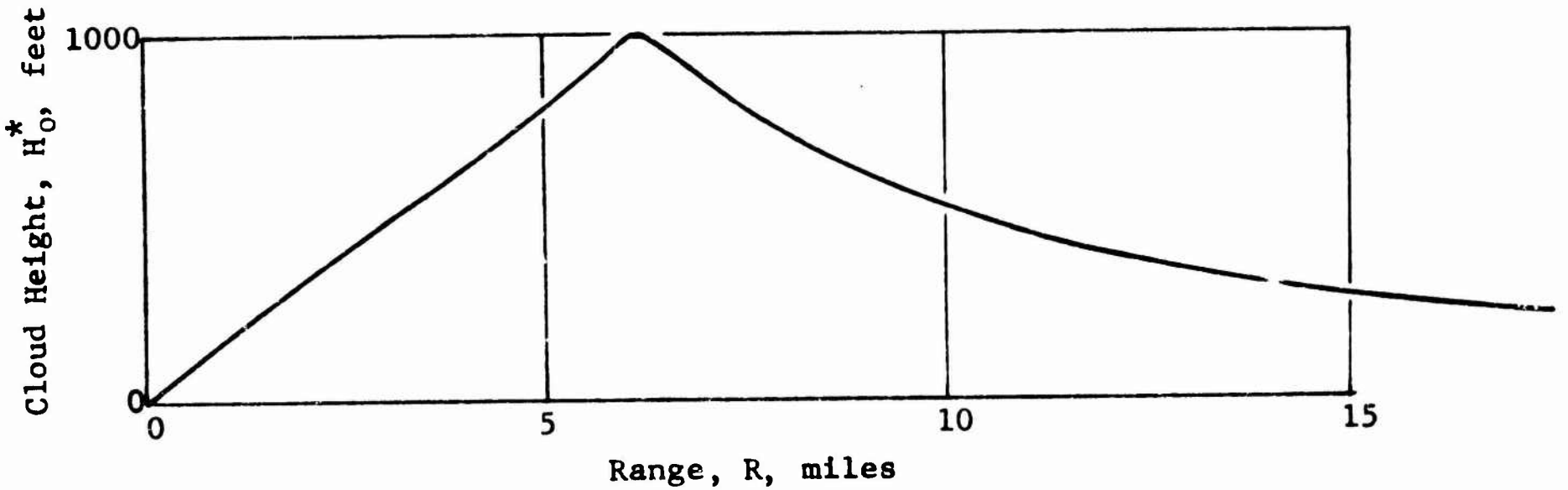

Figure 5.24 Typical Cloud Contour

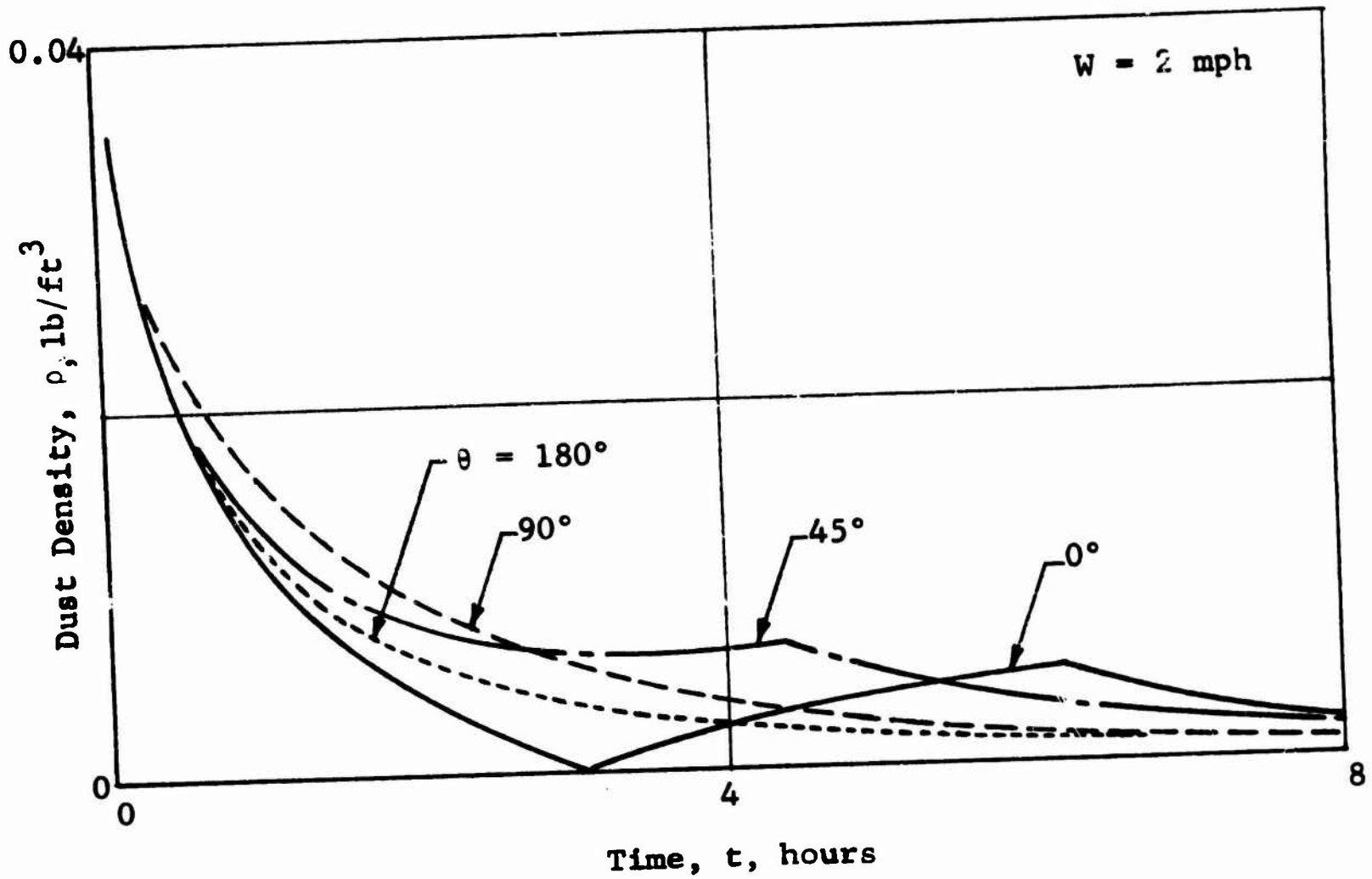

Figure 5.25 Influence of Wind Direction, W = 2 mph

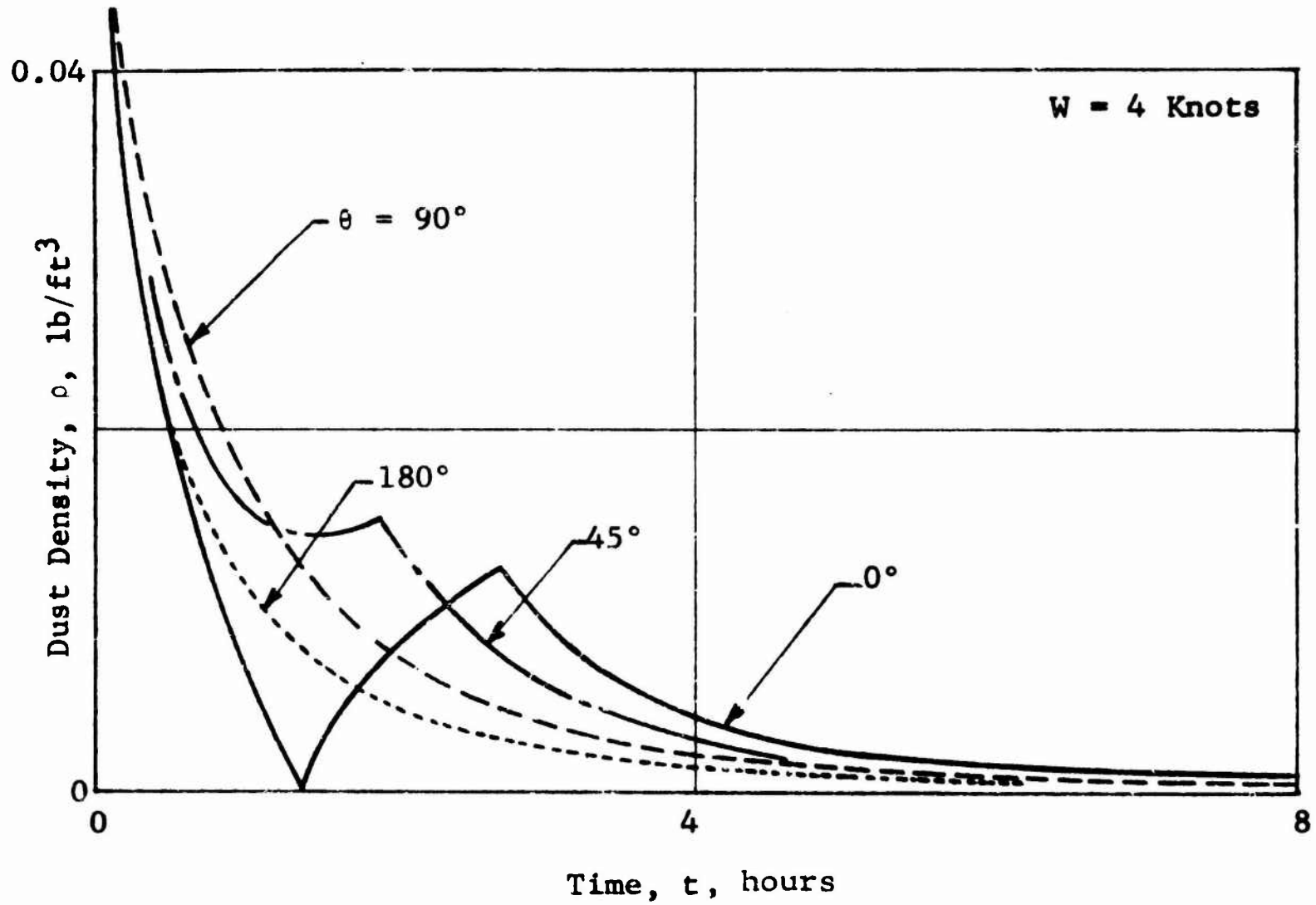

Figure 5.26 Influence of Wind Direction, W = 4 Knots

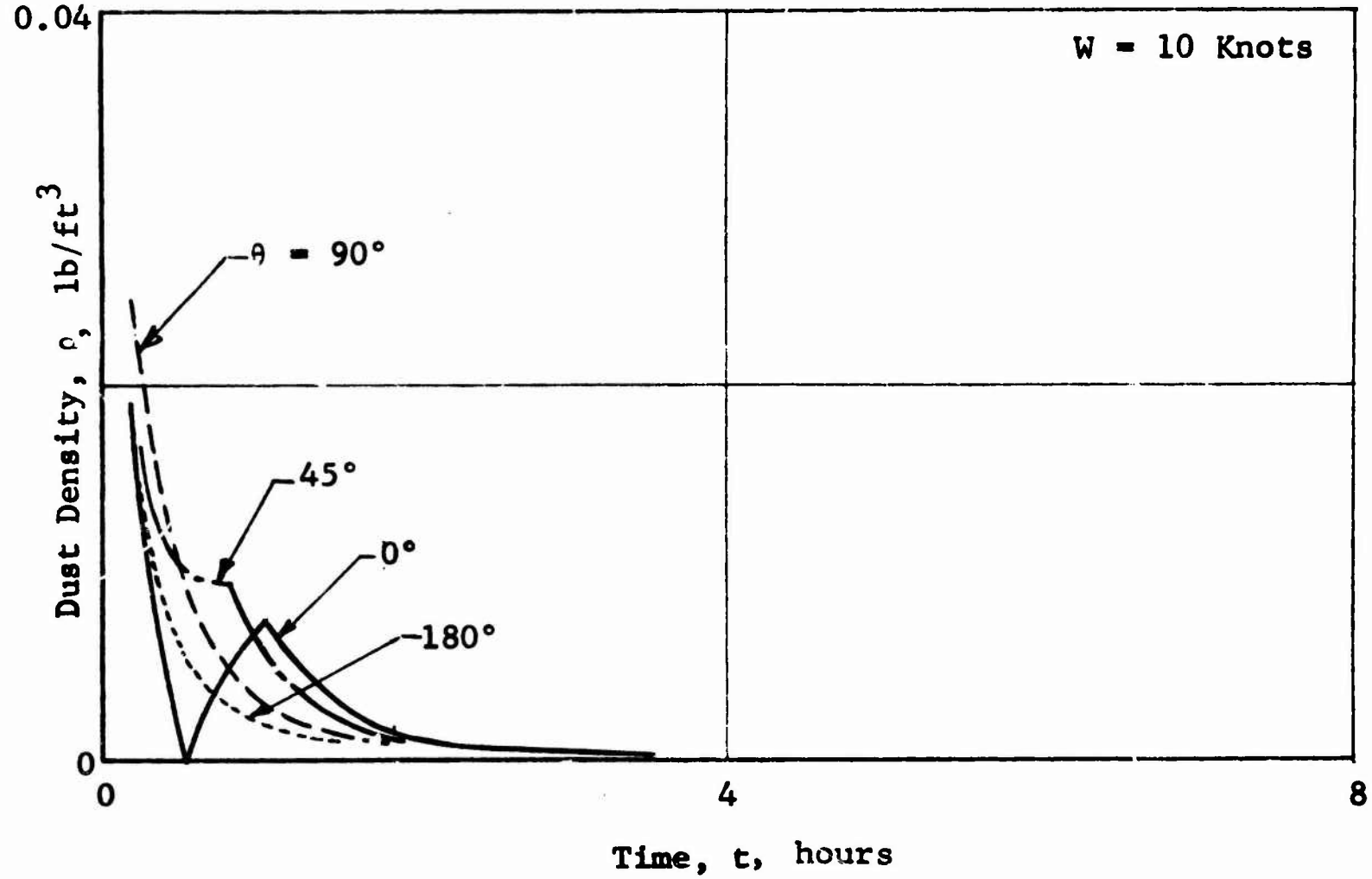

Figure 5.27 Influence of Wind Direction, W = 10 Knots

height maximum and therefore a local dust density maximum. The zero dust density result for $\theta = 0°$ is due to the passage of the apparent site path through the origin. The intermediate wind velocity case (W = 4 knots) appears to yield the largest dust densities during the time interval around 2 to 3 hours after burst. The influence of location within the cloud formation and elapsed time for settling combine to yield this approximate "worst" case situation.

The influence of the wind velocity is demonstrated in Figure 5.28 for a typical burst situation and wind direction. The worst case during the first four hours is clearly given by a wind velocity of 0.5 mph. The larger surface winds clearly blow the dust away. At latter times the worst case corresponds to a wind velocity of 0.02 mph. This case yields greater dust densities than for zero wind velocity because the wind magnitude is just great enough to keep airborne ($C < 0$) the smallest particle size class used (5 microns). Thus there is a real, although somewhat subtle influence, of particle size.

The influence of weapon size or yield is presented in Figure 5.29. Here, the effect is rather clearcut and significant. Figure 5.30 illustrates the influence of height of burst on the dust density. The only large difference is for the near overhead case of a height of burst of 30,000 ft, and the difference occurs only during the first four hour period. Figure 5.31 presents the influence of elevation above the ground surface. Clearly very little difference in dust density exists in the region of from 10 to 30 feet above the ground surface. Figure 5.32 presents the results of varying the blast overpressure at the site. The late-time dust environment is not very sensitive to this blast variable.

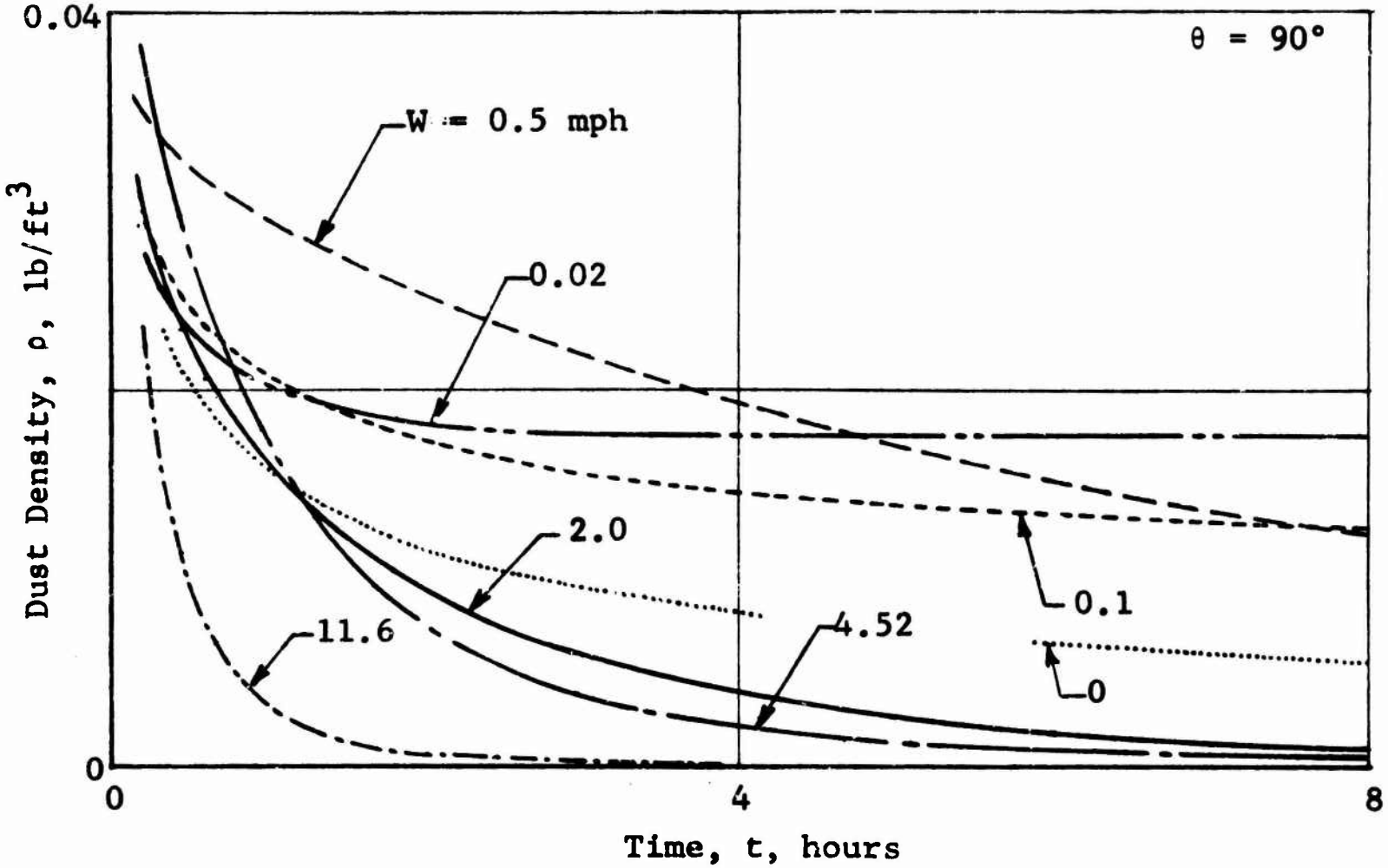

Figure 5.28 Influence of Wind Velocity

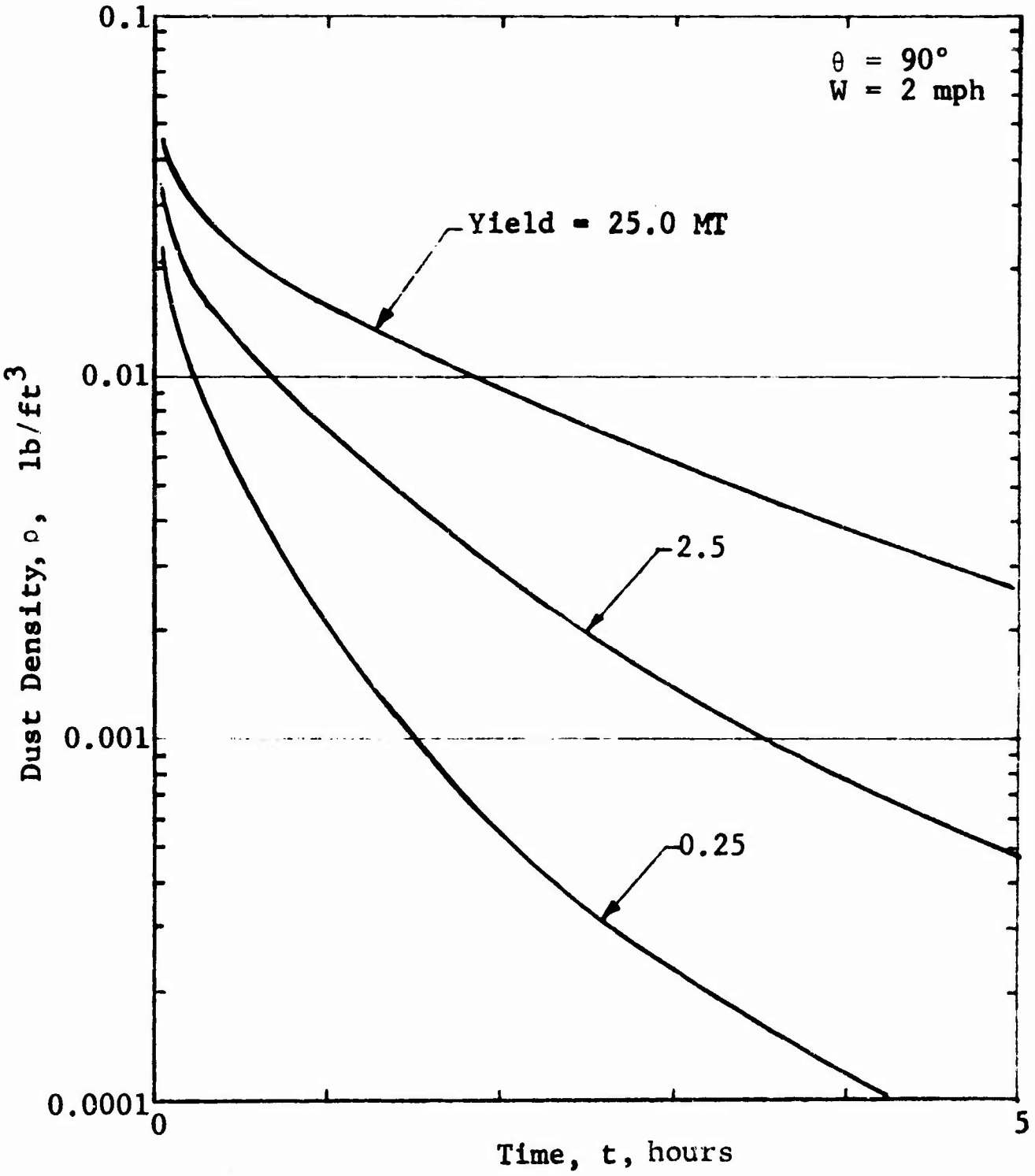

Figure 5.29 Influence of Yield

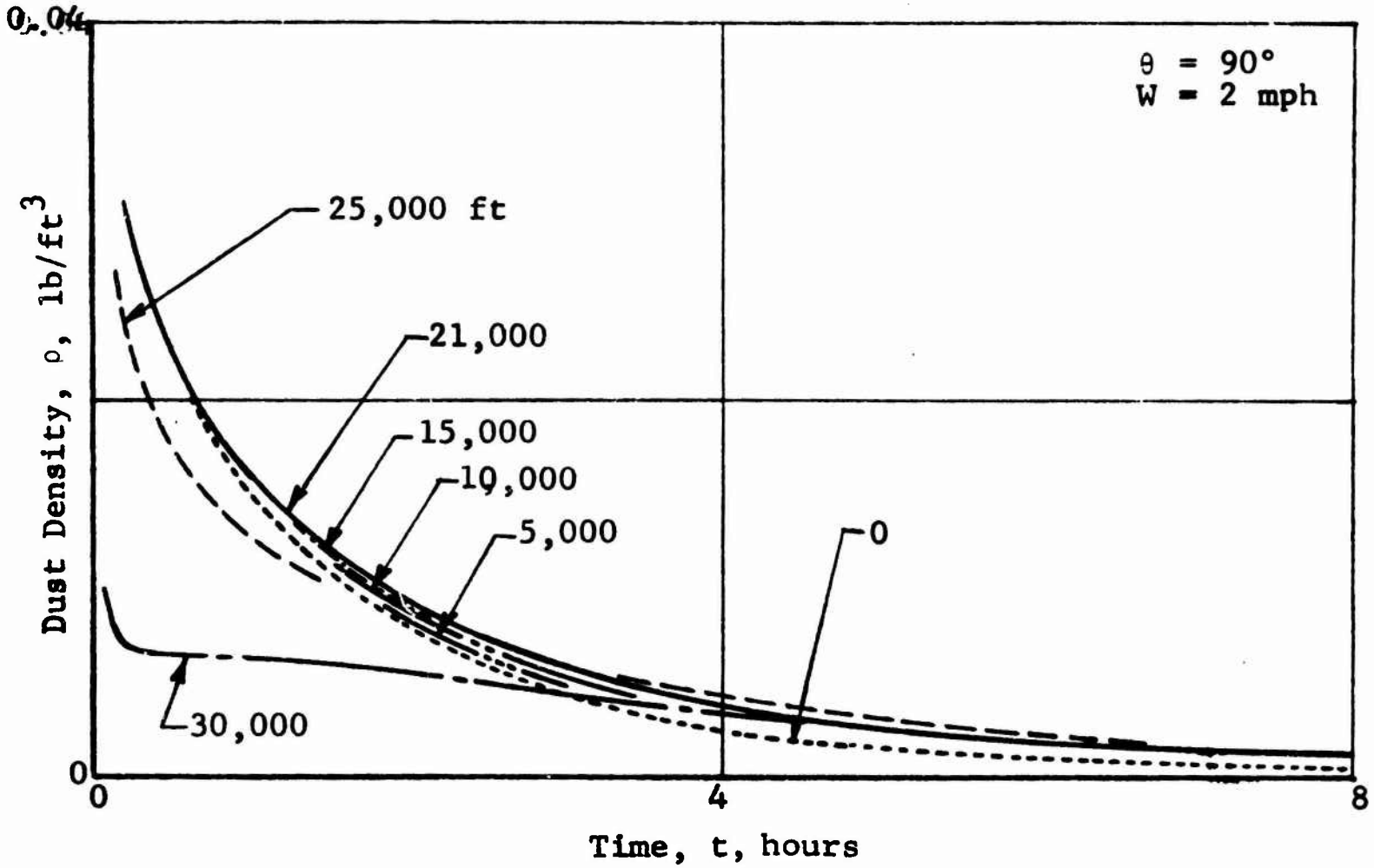

Figure 5.30 Influence of Height of Burst

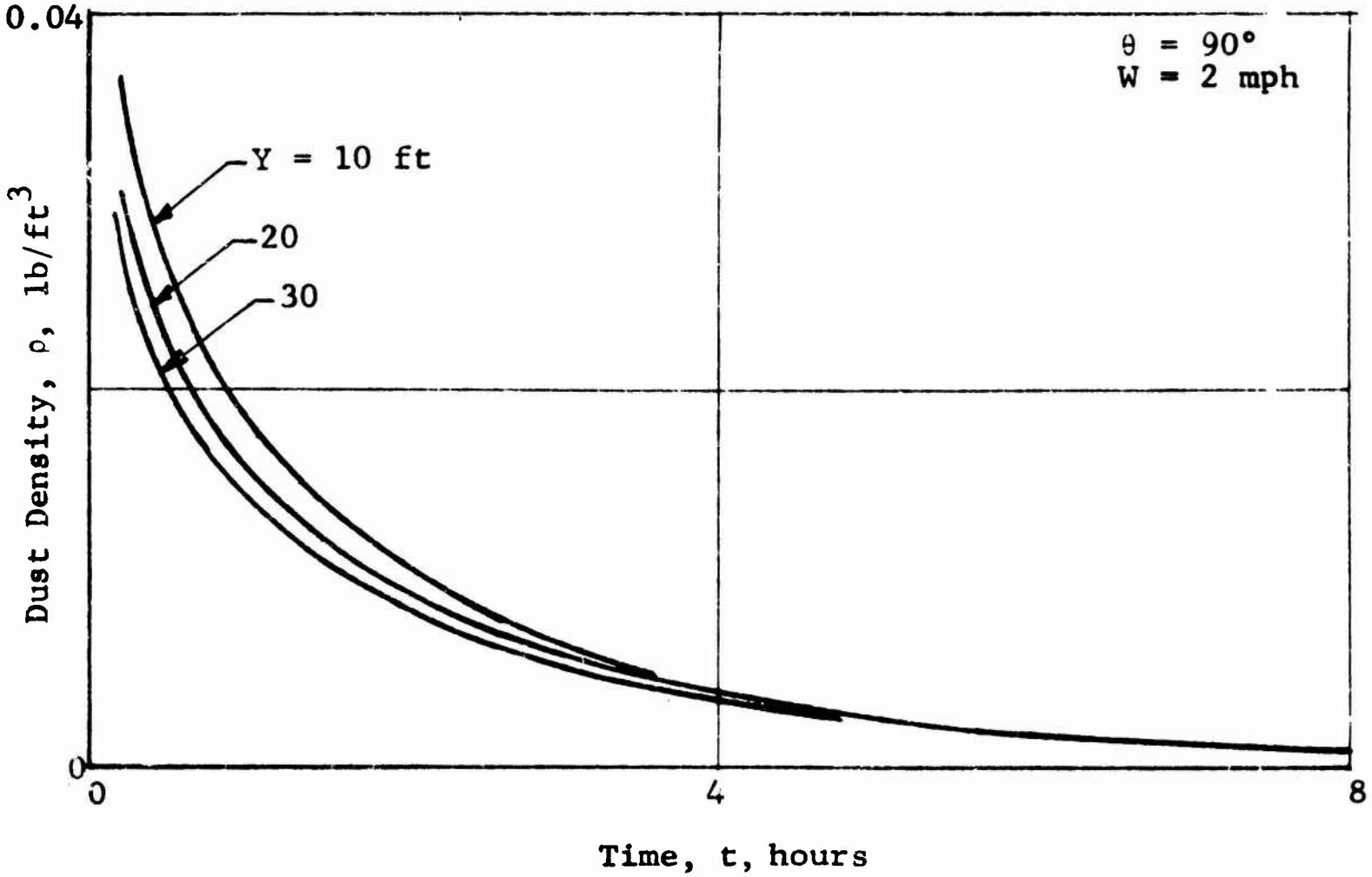

Figure 5.31 Influence of Elevation

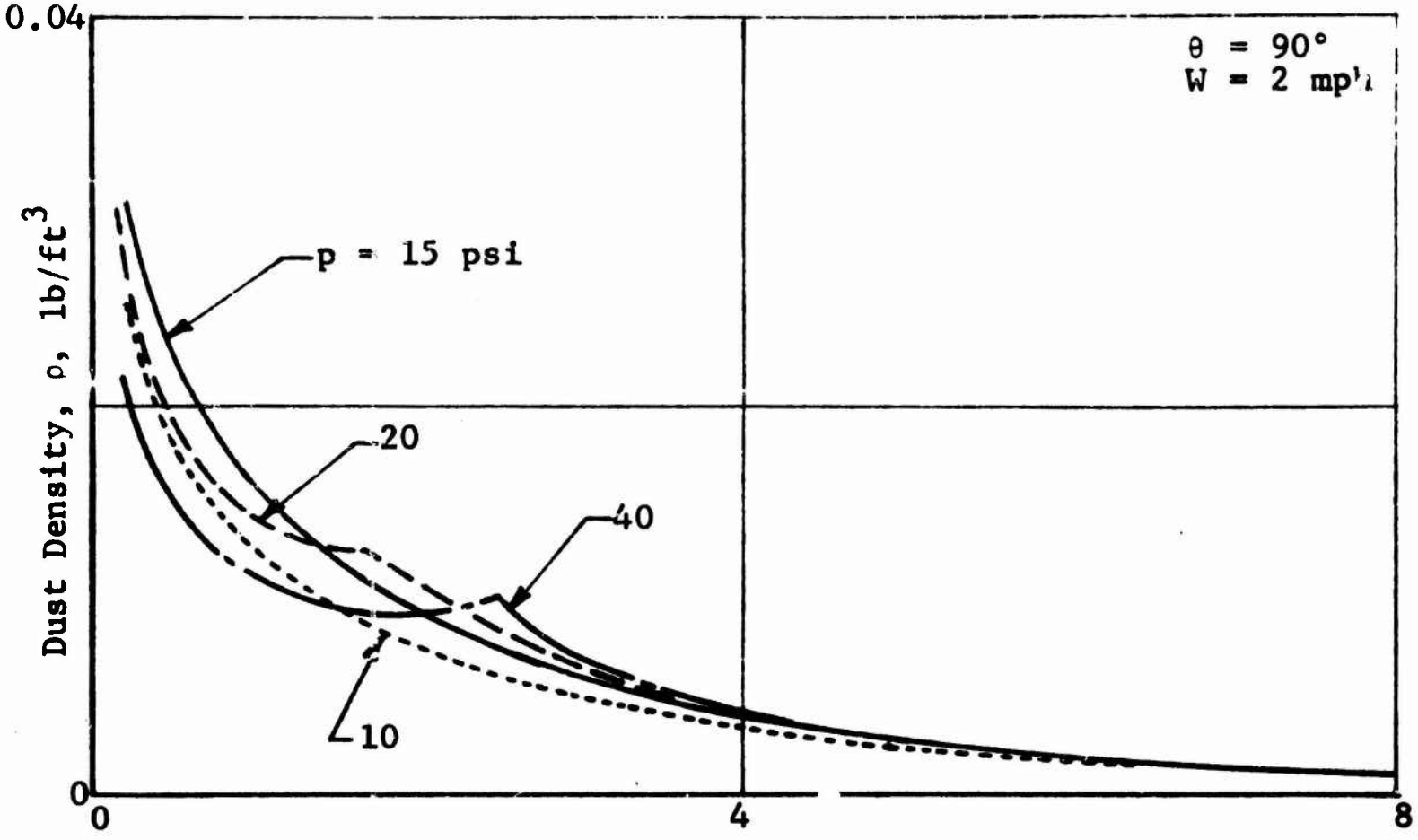

Figure 5.32 Influence of Overpressure

5.5 List of Symbols

a	Erosion coefficient
A	Constant
B	Constant
c	Constant
C	Constant
C_d	Drag coefficient
D	Particle diameter
f	Factor
$H, H_1, H_2, .. H_1^*, H_o^*$	Cloud height
k	Exponential coefficient
K	Transport coefficient
M	Weight of dust
N	Number of particle diameters
n	Number of particles
p	Weight Fraction
R_e	Reynolds number
$R, R_o, R_1, R_2, .. R_4, R_s, R_t$	Range
R_c	Critical Range
$t, t_1, ... t_5$	Time
t_a	Time of arrival
t_1^*	Constant
t_o	Positive phase duration
t_o^*	Modified positive phase duration
T, T', T*	Time
U	Air shock velocity
V	Air velocity
V_o	Peak air velocity
V_r	Air velocity at fixed range
V_t	Terminal velocity
w	Weight of dust
W	Wind velocity
W_c	Critical wind velocity

y, Y	Height
$)\!-\!(\,[\,]$	Heaviside unit function
ρ	Dust cloud density
$\rho(0)$, ρ^*	a constant
ρ_a	Density of air
ρ_c	Density of particles
ρ_s	Specific density of soil
μ	Viscosity of air
ν_g	Number of particles per unit volume
τ	Dimensionless time
ζ, ζ_o	Similarity variable
θ	Wind direction

5.6 Dust Cloud Generated by Crater Ejecta

Several sources contribute to the generation of a dust cloud after the detonation of a nuclear weapon. One such source is crater ejecta. An estimate of the quantity of dust generated via crater ejecta must be made and compared to the contribution of other sources. A previous attempt[5.5] to estimate crater ejecta dust assumed that all the dust was distributed over a cloud height of 25 ft. This assumption is arbitrary and indicated that the resulting dust cloud density was very high. The procedure used to make these estimates did not allow the crater ejecta to reach the location of interest over a finite period of time.

The characteristics of a dust cloud generated by crater ejecta are very complex. However, a simple model that characterizes the phenomenon should be adequate to predict the dust cloud density provided the predictions are conservative and are small in comparison to the other dust cloud sources.

It has been established[5.6] that the crater ejecta, which are thrown distances greater than several crater

diameters, originate at or near the soil surface. It is transported ballistically as a result of its initial velocity. The air is also being accelerated at this time. However, at late times the high velocity winds outrun the crater ejecta particles. A model which would adequately describe this phenomenon is one in which (1) the quantity and initial flight conditions of the ballistic ejecta are given, and (2) the time history of the ejecta particles are followed through the blast-accelerated air until they settle at the point of interest. The evaluation of such a model would require considerable effort if the influences of the blast winds and drag forces are included. It would be impossible to determine which particles reach a given range without examining the trajectories of all of the particles of the crater ejecta. Therefore, for the purpose of making an initial estimate of the dust density, the influence of both air motion and the drag forces acting on the crater ejecta has been neglected. The time of flight t_f for a specified quantity of debris to reach the range distance R is given by

$$t_f = \frac{2V_o}{g} \sin\left[\frac{1}{2} \text{ arc sin } \left(\frac{Rg}{V_o^2}\right)\right], \qquad (5.52)$$

where

t_f = time of particle flight,
R = range,
V_o = initial particle velocity, and
g = gravitational constant.

The initial angle of flight is uniquely related to the range and initial velocity of the particles, such that one pair of velocity-initial angle values will carry the particle to the range of interest. This angle θ is given as

$$\theta = \frac{1}{2} \arcsin \left(\frac{Rg}{V_o^2} \right) . \qquad (5.53)$$

It should be noted that θ can be measured either from the horizontal or vertical axis since the relationship is symmetric about $\theta = \pi/4$. Furthermore, since the value of the arc sin is bounded, there exists a minimum value of the initial velocity which will result in a flight of range R. This value occurs at $\theta = \pi/4$. Experimental evidence from crater ejecta studies[5.6] indicates that the maximum initial velocity of the crater ejecta is approximately 1400 fps. Thus, it is possible to place limits upon the value of the initial velocity of flight. The trajectories of the crater ejecta are illustrated in Figure 5.33.

The quantity of crater ejecta that reaches a given range is subject to some uncertainty. The results of Carlson[5.7] have been used for these calculations. The weight of ejecta w, per unit area, that reaches a specified range is given by

$$w = \frac{1}{2} \rho_s D_a \left(\frac{R_a}{R} \right)^{3.86} , \qquad (5.54)$$

where

w = weight of crater ejecta per unit area,
D_a = apparent crater depth,
R_a = apparent crater radius, and
ρ_s = particle density.

The manner in which the crater dimensions scale with weapon yield W is questionable. The weight of crater ejecta scales as $W^{-0.07}$ or $W^{-1/3}$. The estimates made herein use the latter scaling law.

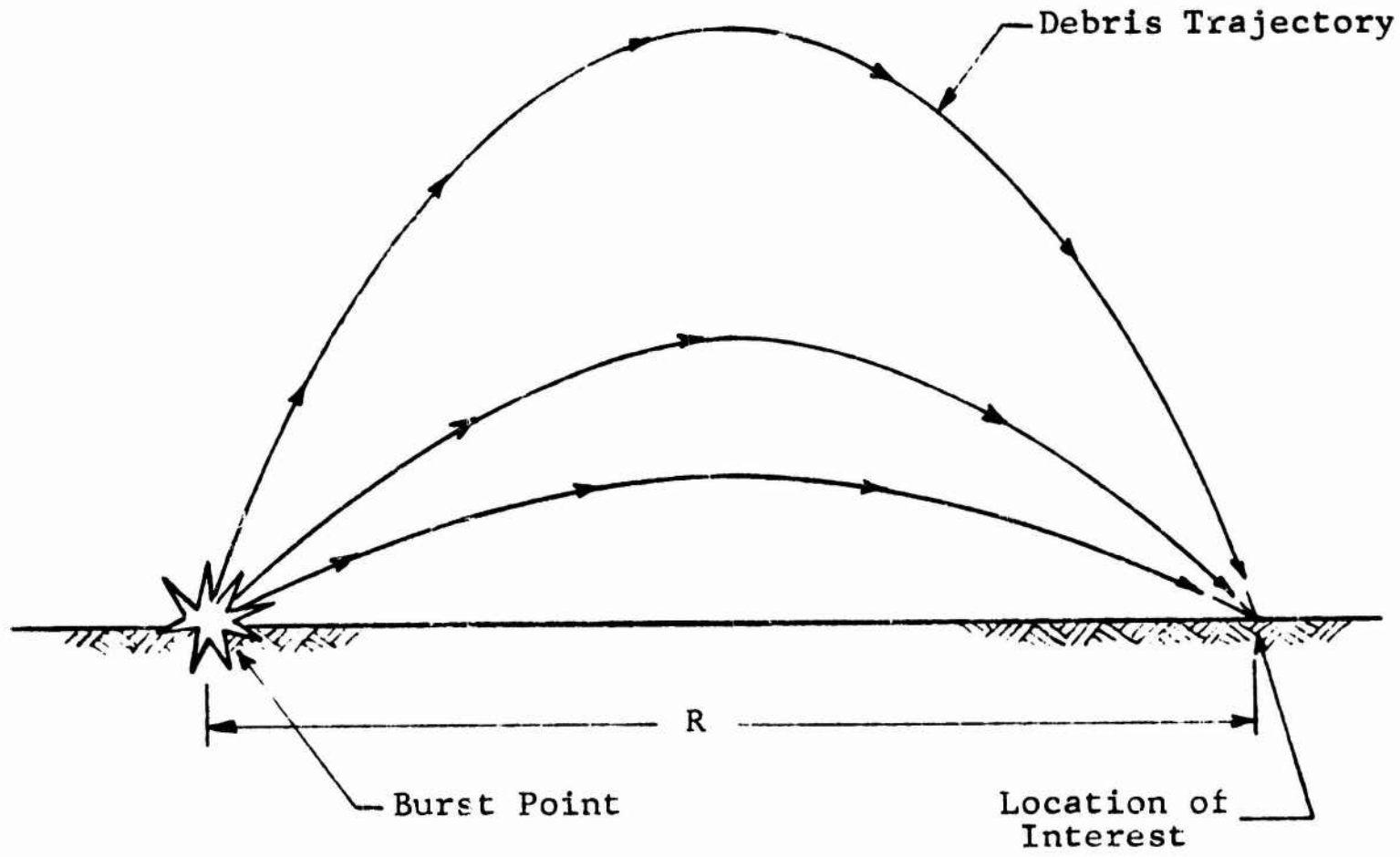

Figure 5.33 Crater Ejecta Trajectories

The distribution of ejecta mass with initial velocity is by no means clear. It would appear reasonable to assume that the majority of the mass leaves the crater with a low velocity and that very little ejecta mass has an initial velocity of 1400 fps. This computation assumes a linear relationship between mass and initial velocity, the peak occurring at the minimum velocity, and a value of zero occurring at V_o = 1400 fps. This mass is distributed symmetrically about $\theta = \pi/4$. The corresponding polar diagram is illustrated in Figure 5.34 for a large weapon yield. Based on the above, it is possible to compute the weight of ejecta (per unit area) that reaches the range of interest in a particular time interval.

The density of the dust due to the crater ejecta can be obtained by dividing the time rate of mass (weight) deposition by the vertical velocity of the ejecta. This velocity is $V_o \cos \theta$. It should be noted that the ejecta is impacting on the ground at its initial velocity, since no drag effects were incorporated into the model. One would expect the ejecta to fall at a lower velocity, such as its associated terminal velocity. The results of calculations based upon the above model are presented in Figure 5.35. They are given as a function of time for a small and large weapon yield. The peak dust-cloud density for the smaller yield is approximately 0.66 gr/ft^3 and is considerably less than the dust-cloud densities predicted for the blast-induced dust clouds. The peak dust-cloud density for the large yield weapon was less than 0.2 gr/ft^3.

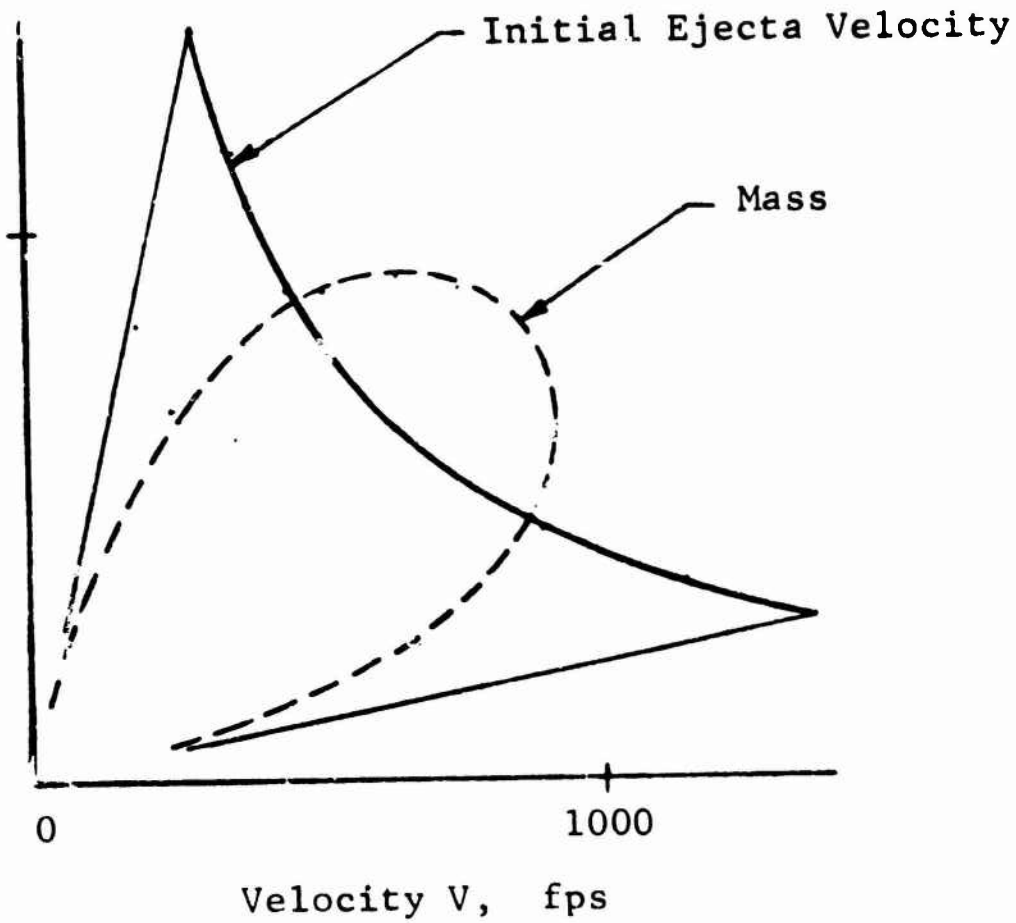

Figure 5.34 Polar Distribution of Ejecta Velocity and Mass Distribution

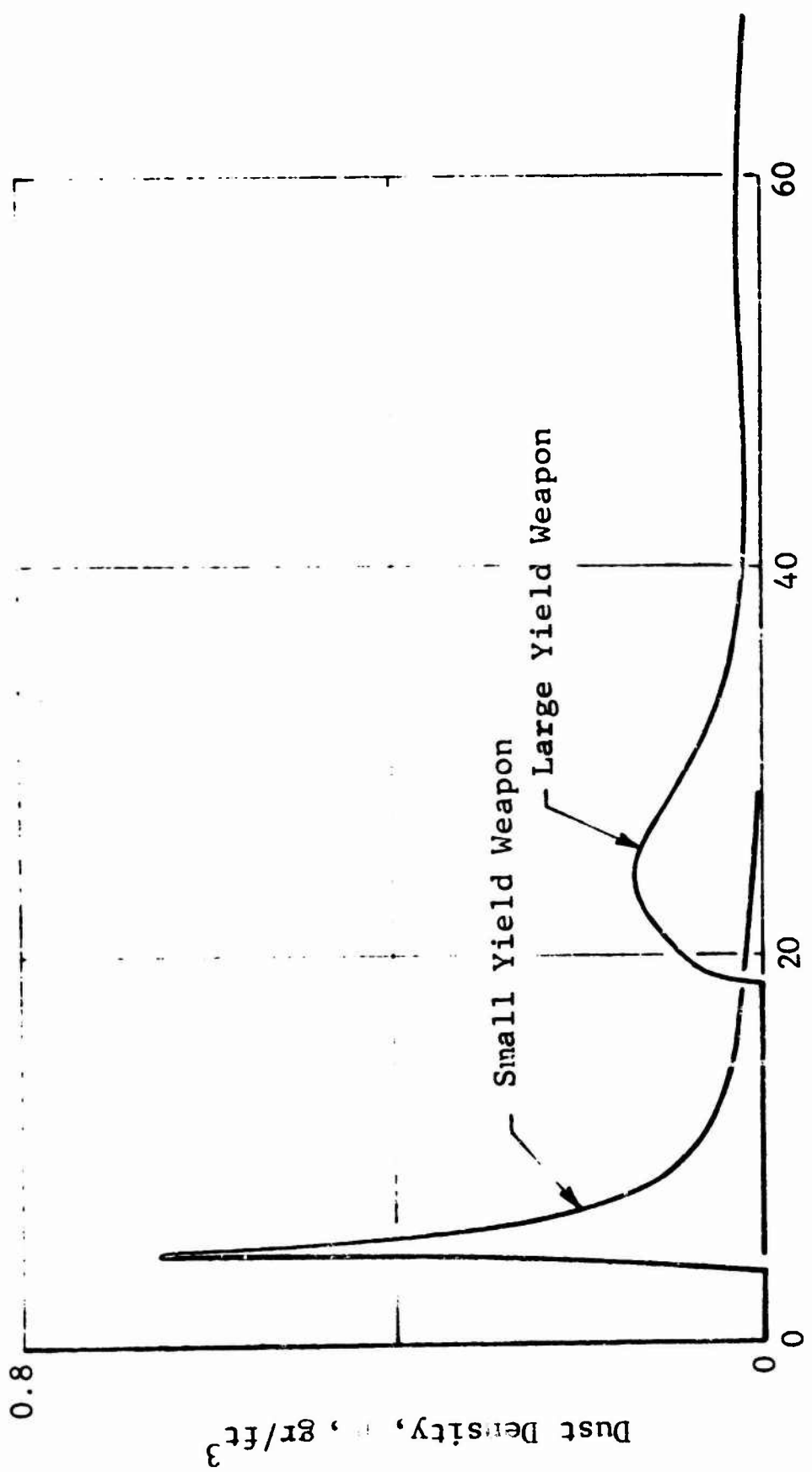

Figure 5.35 Dust Density due to Crater Ejecta

It is difficult to ascertain that the above calculations are indeed conservative, although it is obvious that the actual times of flight will be considerably greater than those computed by the previous model. The above model indicates that the debris arrives at the site between 19 and 85 seconds after the weapon detonates.

(This page is left blank intentionally)

EXTRACTED

Chapter 6 (U)

AIR-TEMPERATURE STUDIES

6.1 Introduction

The thermal radiation emitted by the fireball of an atmospheric burst will be transmitted through the surrounding air with relatively little absorption until it reaches some relatively opaque substance such as the ground, or perhaps a dust cloud. The deposition of the thermal energy in the opaque material will raise its temperature locally.

In the absence of a dust cloud, some of the thermal energy will heat the ground surface (and some portion immediately below the surface) to relatively high temperatures. The soil may respond mechanically to this thermal pulse, depending upon the temperature and thermal gradients which are generated. The soil may also melt or vaporize in some instances.

The passage of the shock wave at a particular position on the ground (say the site location) will result in the start of the blast-induced winds at that position. If the soil is such that it can be eroded by the blast winds, a dust cloud will begin to form. This phenomenon was described in the preceding chapter for the case of cold dust (i.e., no thermal effects were considered). As a result of the deposition of the thermal energy in the soil, some of the particulate matter which forms the dust cloud will be quite hot (relative to the air). The air will be heated by the shock compression and then cooled as the gas begins to expand. The passage of the hot dust through the air will result in the exchange of thermal energy between the dust and the air. Furthermore, additional energy will be deposited in the dust

cloud by the process of absorption of the fireball thermal radiation. This energy will also be transmitted to the air, thus further altering the air temperature at the heights of interest.

The overall air-temperature problem is quite complex and considerable simplification must be resorted to in order to achieve an engineering estimate of the air-temperature variation at the potential site locations. The air-temperature model which is described in this chapter is based upon the dust model described in the preceding chapter. All of the assumptions and simplifications made for the dust model are used herein, and the basic assumption relating to the uncoupling of the gas dynamic field from the local dust and air temperature variations is retained.

The following section presents a description of the thermal source as it relates to the current problem. Section 6.3 deals with the deposition of the thermal radiation in the soil and the resulting transient soil temperature. Section 6.4 treats the deposition of the thermal energy in a dust cloud. The basic IITRI air-temperature model which incorporates all of the preceding effects together with the dust cloud characteristics is then presented in Section 6.5. The next two sections (Sections 6.6 and 6.7) present typical results for single-and multiple-burst situations, respectively, and illustrate the influence of certain variables. The last section presents a list of symbols used in this chapter.

6.2 Thermal Radiation from the Fireball

The thermal energy emitted by the fireball is reasonably well known.[6.1] For the purpose of this study, a simple representation of the thermal emission will be used. The fireball will be treated as a point source rather than the finite source it actually is. This approximation is

reasonable for distances much greater than the fireball diameter. This is generally the case for the current problem.

The fireball emission is treated as black-body radiation at an effective temperature T_e. The thermal flux F_s is

$$F_s = \sigma T_e^4 \tag{6.1}$$

where σ is the Stefan's constant. The total radiant power emitted from a fireball of radius R is

$$P = 4\pi R^2 \sigma T_e^4 \ . \tag{6.2}$$

The flux at a slant-range distance D from the fireball ($R \ll D$) is

$$F = \tau_a P / 4\pi D^2 \tag{6.3}$$

where τ_a is the atmospheric transmittance. The radiant flux intensity πB_λ, as a function of the fireball surface temperature T, is shown in Figure 6.1.

For a weapon yield of W kilotons, the approximate maximum thermal emission[6.1] (calories per sec) is

$$P_{max} \sim 4(10^{12}) \sqrt{W} \ . \tag{6.4}$$

The approximate time (sec) after explosion for the temperature maximum is

$$t_{max} \approx 0.032 \sqrt{W} \ . \tag{6.5}$$

An alternate expression involving the height of burst is

$$t_{max} = 0.82 \ W^{.42} \exp(-.09 \ H_B) \ . \tag{6.6}$$

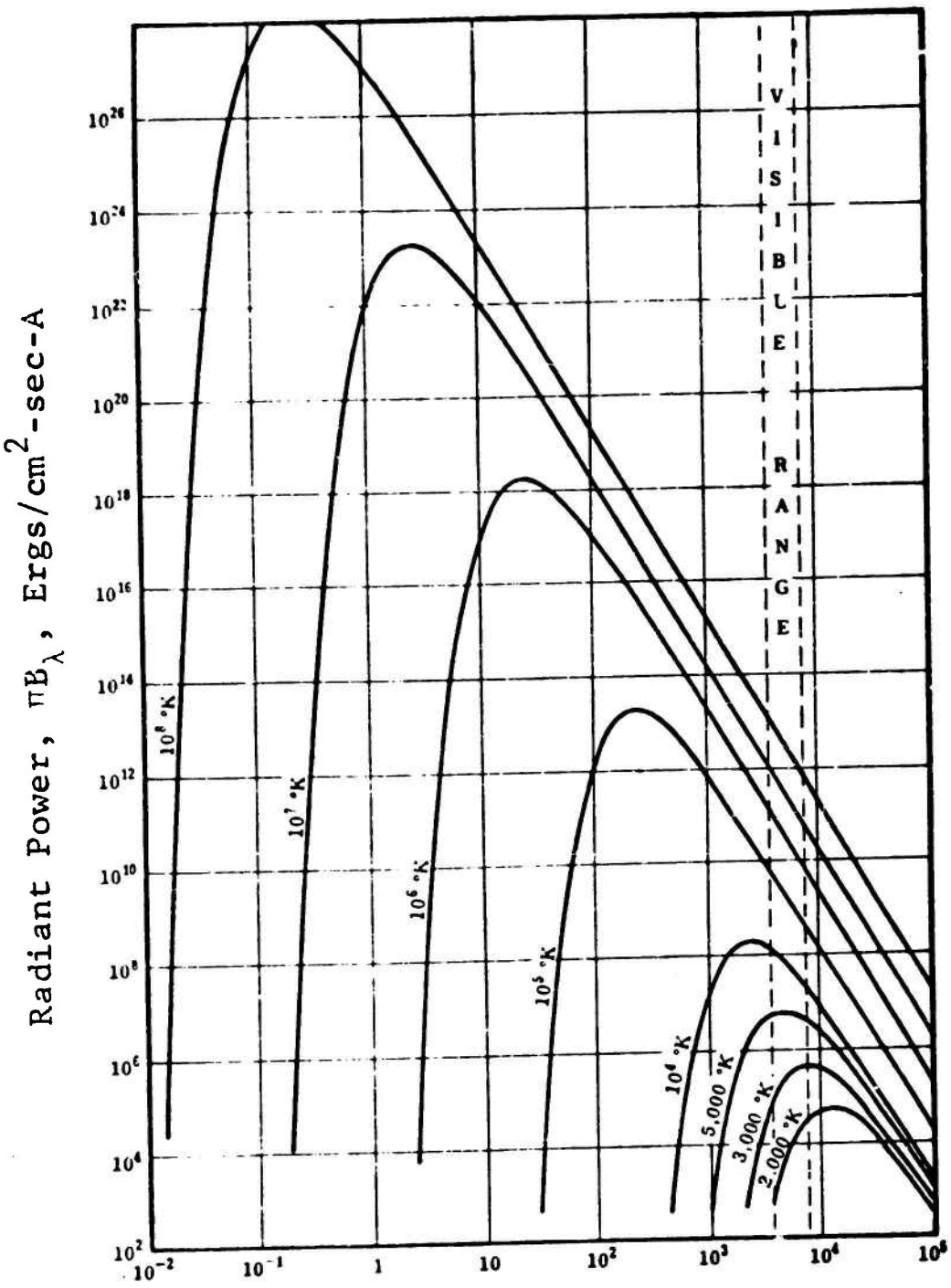

Figure 6.1 Radiant Power of a Black Body as a Function of Wavelength at Various Temperatures

This maximum is for the second thermal pulse; the first pulse is of such brief duration that its thermal contribution is neglected.

The approximate scaled emission as a function of scaled time is shown in Figure 6.2.

Some absorption occurs in the atmosphere, so the radiant intensity is attenuated by the factor

$$\tau_a = \exp(-\kappa D), \tag{6.7}$$

where τ_a is the atmospheric transmittance and κ is an absorption coefficient averaged over the wavelength spectrum and the slant range D. Typical values of transmittance as a function of slant range are shown in Figure 6.3 (Glasstone[6.1]). The height of burst is $H_B = D \cos \theta$, so that

$$\tau_a = \exp(-\kappa H_B \sec \theta). \tag{6.8}$$

Gibbons[6.2] tabulates the values of κH_B (which he calls the optical thickness) as a function of H_B for radiation of wavelength 0.65 micron.

6.3 Soil Temperature

6.3.1 General

The thermal energy which is incident upon the soil surface will be absorbed at the surface and will propagate downward by the process of thermal conduction. Furthermore, if the surface temperature becomes quite hot it will re-radiate energy back up into space. This energy deposition will manifest itself as a temperature variation in the soil near the surface of the soil. When the shock wave sweeps past the soil, the soil will be eroded by the blast winds, and soil particles of various temperatures will enter the dust

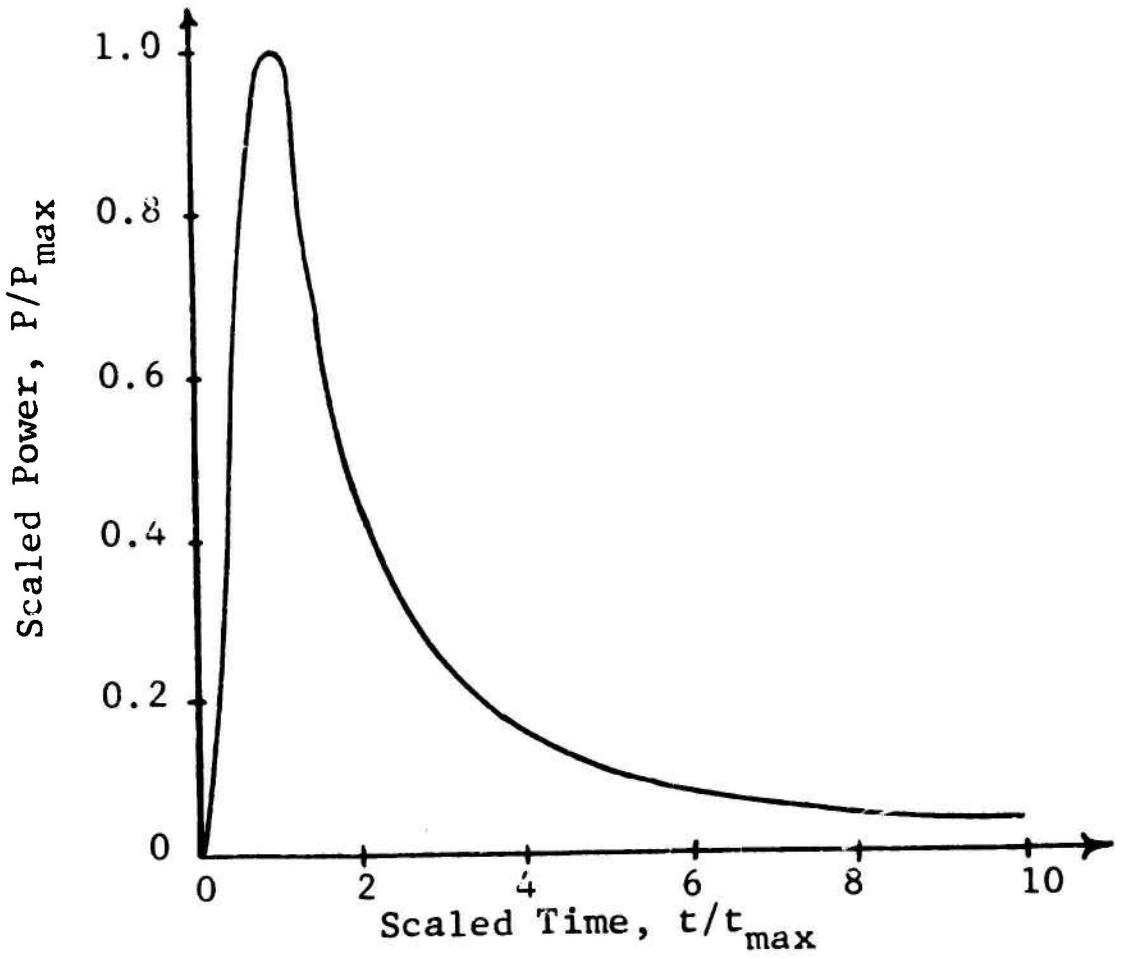

Figure 6.2 Scaled Fireball Power

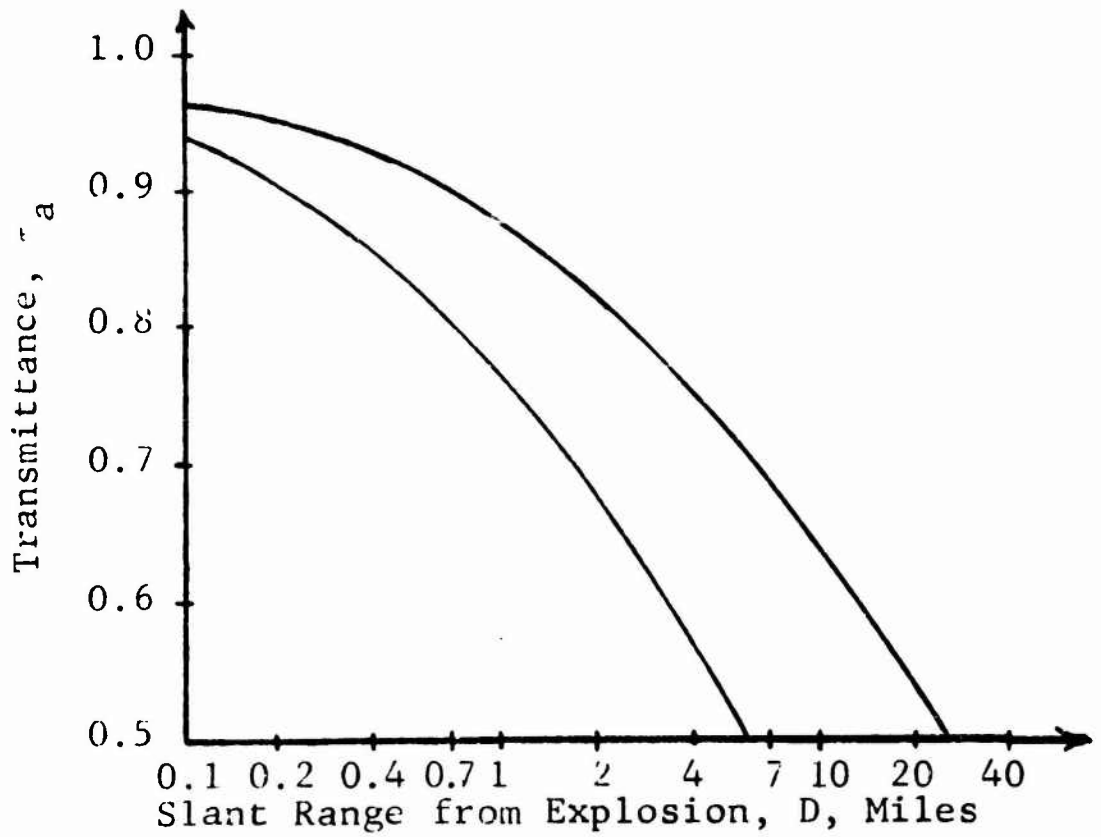

Figure 6.3 Atmospheric Transmittance

cloud at various times. Thus, it is necessary to determine the vertical temperature distribution in the soil at the time of arrival of the shock wave at the site.

The deposition of the thermal energy in the soil represents a mechanism for concentrating, locally, a significant portion of the energy (per unit area) released by the weapon. This concentration of energy can be maximized by neglecting any mechanisms which might tend to distribute the energy more uniformly. Therefore, any mechanical response that the soil might experience will be neglected. Also, any changes of phase of the soil or its constituents (such as water) will be neglected.

The soil temperature distribution at the time of arrival of the shock wave is determined by the solution of a nonsteady one-dimensional heat conduction problem subject to the thermal flux from the weapon, including any re-radiation which might occur.

6.3.2 Conduction Solution

The thermal energy release of a nuclear weapon creates a temperature distribution $T(x,t)$ in the soil according to

$$\left.\begin{aligned} &\frac{\partial T}{\partial t} - \alpha \frac{\partial^2 T}{\partial x^2} = 0, \\ &T(x,0) = T_o, \\ \text{and} \\ &\left.\frac{\partial T}{\partial x}\right|_{x=0} = f(t) = -\frac{1}{k}\left[\dot{Q}_i(t) - \dot{Q}_r(t)\right] ; \end{aligned}\right\} \qquad (6.9)$$

where

x = distance below the surface of the soil,

t = time,

k = thermal conductivity of the soil, and

α = thermal diffusivity of the soil.

The incident thermal power density is

$$\dot{Q}_i(t) = 3.994467(10^{10}) \frac{\tau_a \sqrt{W} \cos \theta}{D^2} P_e(t) \quad , \quad (6.10)$$

and the re-radiated thermal power density is

$$\dot{Q}_r(t) = \sigma \left[T^4(0,t) - T_o^4 \right] \quad (6.11)$$

where σ = Stefan's constant. The quantities τ_a, W, θ, and D are computed as weapons effects variables; $P_e(t)$ is the scaled fireball thermal power provided in tabular form as a function of time; and T(0,t) is the time varying (absolute) surface temperature which is, itself, the solution to Equation 6.9. τ_a was defined previously as the atmospheric attenuation factor, W is the weapon yield in kilotons, θ is the angle of incidence of the radiation upon the soil surface, and D is the slant range from the burst point of the weapon. T_o is the initial temperature of the soil.

The general solution to Equation 6.11 is

$$\Delta T(x,t) = T(x,t) - T_o = -\sqrt{\frac{\alpha}{\pi}} \int_0^t \frac{f(\tau)}{\sqrt{t-\tau}} \exp -\left[\frac{x^2}{4\alpha(t-\tau)} \right] d\tau \quad . (6.12)$$

Letting $g(\tau) = -\sqrt{\frac{\alpha}{\pi}} f(\tau) = C_1 P_e(\tau) - C_2 \left[T^4(0,\tau) - T_o^4 \right]$, Equation 6.12 is, at the surface (x=0),

$$\Delta T(0,t) = \int_0^t \frac{g(\tau)}{\sqrt{t-\tau}} d\tau \quad , \quad (6.13)$$

and below the surface (x > 0),

$$\Delta T(x,t) = \int_0^t \frac{g(\tau)}{\sqrt{t-\tau}} \exp\left[- \frac{x^2}{4\alpha(t-\tau)} \right] d\tau \quad . \quad (6.14)$$

An iterative solution of Equation 6.13 is necessary, since $g(\tau)$ is a function of $\Delta T(0,t)$, but once its solution is obtained, Equation 6.14 can be solved explicitly for $\Delta T(x,t)$ (i.e., at any depth x) without iteration.

Since the integrand of Equation 6.13 is unbounded as $\tau \longrightarrow t$, and the integrand of Equation 6.14, although everywhere bounded, has a sharp spike for values of τ near t and small x, standard numerical integration schemes would require considerable refinement for accurate solutions. Thus, an analytic method of solution was devised for each of these equations.

Figure 6.4 is a graph of g(t) where it is assumed that $\Delta T(0,t_i)$ and therefore, $g_i = g(t_i)$ is known at all t_i for $i < m$. The $g(\tau)$ curve can be approximated by straight line segments over suitably small increments of time, i.e.,

$$g(\tau) = a_i \tau + b_i, \quad t_i \leq \tau \leq t_{i+1} , \tag{6.15}$$

where

$$\left.\begin{aligned} a_i &= (g_{i+1} - g_i)/(t_{i+1} - t_i), \text{ and} \\ b_i &= g_i - a_i t_i . \end{aligned}\right\} \tag{6.16}$$

Substituting Equation 6.15, the integration of Equation 6.13 can be approximated by

$$\Delta T(0,t_m) = \sum_{i=1}^{m-1} \int_{t_i}^{t_{i+1}} \frac{a_i \tau + b_i}{\sqrt{t_m - \tau}} \, d\tau ,$$

resulting in

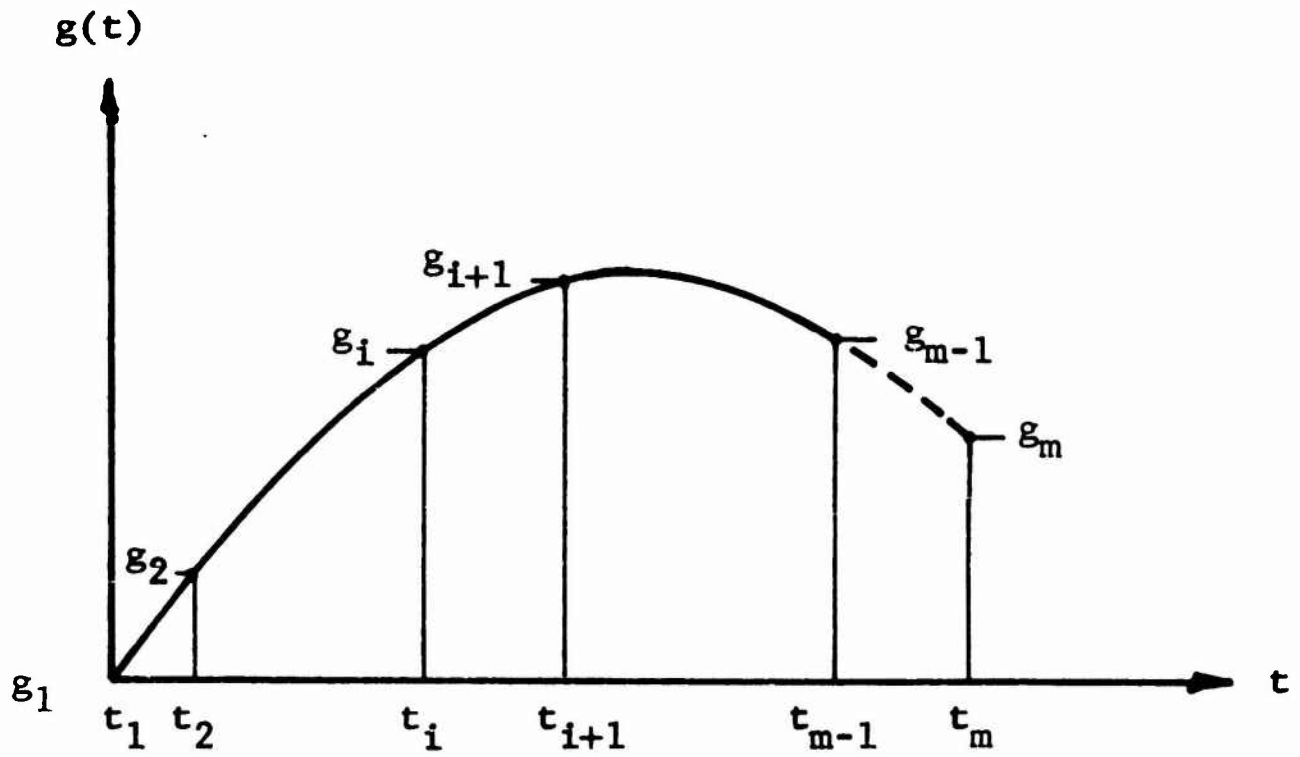

Figure 6.4 Approximation Procedure for g(t)

$$\Delta T(0,t_m) = \frac{2}{3}\left[a_{m-1}(2t_m + t_{m-1}) + 3b_{m-1}\right]\sqrt{t_m - t_{m-1}}$$

$$+ \sum_{i=1}^{m-2} \frac{2}{3}\,(2a_i t_m + a_i t_i + 3b_i)\,\sqrt{t_m - t_i}$$

$$- (2a_i t_m + a_i t_{i+1} + 3b_i)\,\sqrt{t_m - t_{i+1}}\,\Big] \qquad (6.17)$$

where a_{m-1} and b_{m-1} are functions of $T(0,t_m)$. Assuming the solution has previously been obtained at times t_m prior to the current value of t_m, the summation above (to be denoted below by S) is known. Substituting Equations 6.16 and the definition of $g(t_m)$ into Equation 6.17 gives the fourth order algebraic equation

$$T^4(0,t_m) + C_3\,T(0,t_m) - C_4 = 0 \qquad (6.18)$$

where

$$C_3 = 1/\left(\frac{4}{3}\,C_2\,\sqrt{t_m - t_{m-1}}\right) \text{ and}$$

$$C_4 = (T_o + S)\,C_3 + T_o^{\,4} + \frac{g_{m-1}}{2C_2} + \frac{C_1 P_e(t_m)}{C_2}\,.$$

The solution to Equation 6.18 can be found from the simple recursion formula

$$T^{(n+1)}\,(0,t_m) = \frac{3\left[T^{(n)}(0,t_m)\right]^4 + C_4}{4\left[T^{(n)}(0,t_m)\right]^3 + C_3}\,, \qquad (6.19)$$

where the superscript n represents the $n^{\underline{th}}$ iteration, and initially, $T^{(1)}(0,t_m)$ is taken as $T(0,t_{m-1})$.

Equation 6.19 is thus solved at each t_m successively, as time increases, resulting in both $T(0,t)$ and $g(t)$ or, equivalently, the piece-wise linear parameters a_i and b_i.

The subsurface temperatures can now be computed directly by integration of Equation 6.14 according to the approximation

$$\Delta T(x,t_m) = \sum_{i=1}^{m-1} \int_{t_i}^{t_{i+1}} \frac{a_i \tau + b_i}{\sqrt{t-\tau}} \exp -\left[\frac{x^2}{4\alpha(t-\tau)}\right] d\tau$$

where the a_i and b_i are known. Thus,

$$\begin{aligned} T(x,t_m) = T_o &+ \frac{2}{3}\left[a_{m-1}\left(2t_m + t_{m-1} + \frac{x^2}{2\alpha}\right) + 3b_{m-1}\right]\sqrt{t_m - t_{m-1}}\, \exp\left[-\frac{x^2}{4\alpha(t_m - t_{m-1})}\right] \\ &+ \frac{x}{3}\sqrt{\frac{\pi}{\alpha}}\left[a_{m-1}\left(3t_m + \frac{x^2}{2\alpha}\right) + 3b_{m-1}\right]\left[\operatorname{erf}\sqrt{\frac{x^2}{4\alpha(t_m - t_{m-1})}} - 1\right] \\ &+ \frac{1}{3}\sum_{i=1}^{m-2}\left\{2\left[a_i\left(2t_m + t_i + \frac{x^2}{2\alpha}\right) + 3b_i\right]\sqrt{t_m - t_i}\, \exp\left[-\frac{x^2}{4\alpha(t_m - t_i)}\right]\right. \\ &- 2\left[a_i\left(2t_m + t_{i+1} + \frac{x^2}{2\alpha}\right) + 3b_i\right]\sqrt{t_m - t_{i+1}}\, \exp\left[-\frac{x^2}{4\alpha(t_m - t_{i+1})}\right] \\ &+ x\sqrt{\frac{\pi}{\alpha}}\left[a_i\left(3t_m + \frac{x^2}{2\alpha}\right) + 3b_i\right]\left[\operatorname{erf}\sqrt{\frac{x^2}{4\alpha(t_m - t_i)}}\right. \\ &\left.\left. - \operatorname{erf}\sqrt{\frac{x^2}{4\alpha(t_m - t_{i+1})}}\right]\right\} \end{aligned} \qquad (6.20)$$

for the soil temperature at any depth x and time t_m.

6.3.3 Temperature Distribution in Soils

A computer subprogram was written in FORTRAN IV in accordance with the previous analysis to determine the

temperature distribution in the soil at the time of arrival of the shock wave.

Since soils are both varied and complex, it was necessary to investigate the pertinent thermal properties for representative soils and to investigate the influence that any uncertainty of these properties has on both the temperature distributions and the variation which might be introduced into the air-temperature prediction.

Table 6.1 presents a brief summary of the thermal properties[6.3] of soil. The variation is not too large except for a few extreme cases such as mud or very wet soils. A series of temperature distributions were computed for a number of cases for both a small yield and a large yield case. These temperature distributions are presented in Figures 6.5 and 6.6. The temperature distributions for the large yield weapon were used in a series of air-temperature calculations. These results will be discussed in a later section of this chapter.

A low value for the thermal conductivity yields, as is expected, higher surface temperatures. The total energy deposited in the soil increases with both a decreasing value of the thermal conductivity and an increasing value of thermal diffusivity. In the absence of specific site data, a value for the thermal conductivity of 0.10 Btu/hr-ft-°F is recommended for general use. Similarly, a value of 0.007 ft^2/hr for the thermal diffusivity is recommended.

6.4 Radiation Absorption in Dust Cloud

The radiation of energy from the above-ground fireball irradiates the dust cloud generated at the ground surface. The amount of energy radiated is a function of wavelength and fireball temperature. For instance, it is well

Table 6.1 THERMAL PROPERTIES OF SOIL

Soil Description	Density pcf	Conductivity Btu/hr-ft-°F	Specific Heat Btu/16-°F	Diffusivity ft^2/hr
Calcareous earth, 43% water	104	0.41	0.53	0.007
Quartz sand, medium fine, dry	103	0.15	0.19	0.008
Quartz sand, 8.3% moisture	109	0.34	0.24	0.013
Sandy clay, 15% moisture	111	0.53	0.33	0.015
Soil, very dry	---	0.1-0.2	---	0.008-0.012
Some wet soils	---	0.8-2.0	---	0.02-0.04
Wet mud	94	0.50	0.60	0.008
Soil, average	160	0.56	0.20	0.018
Soil, sandy, dry	106	0.15	0.19	0.008
Soil, sandy, moist	112	0.34	0.24	0.013

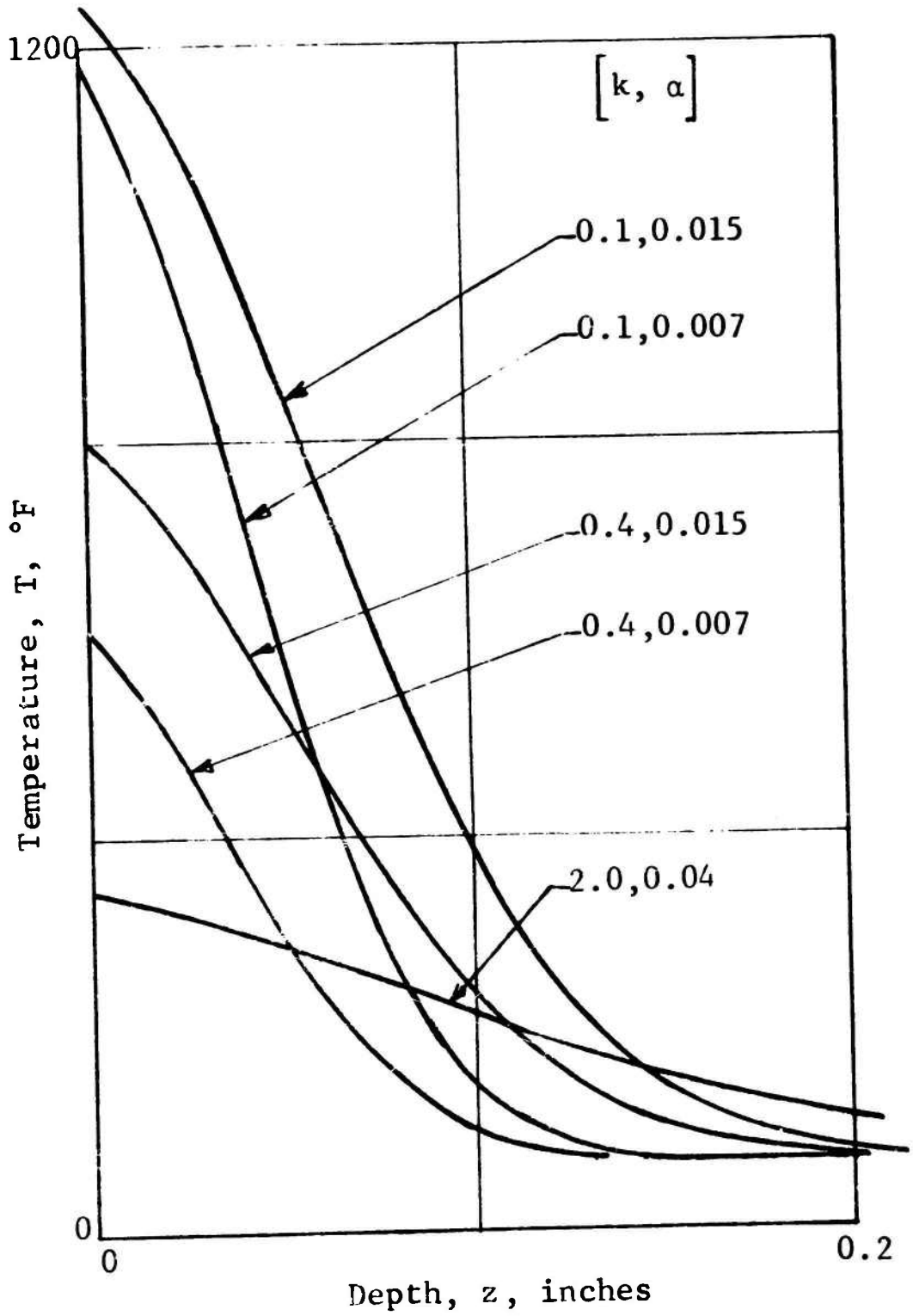

Figure 6.5 Soil Temperature Distribution, Small Yield

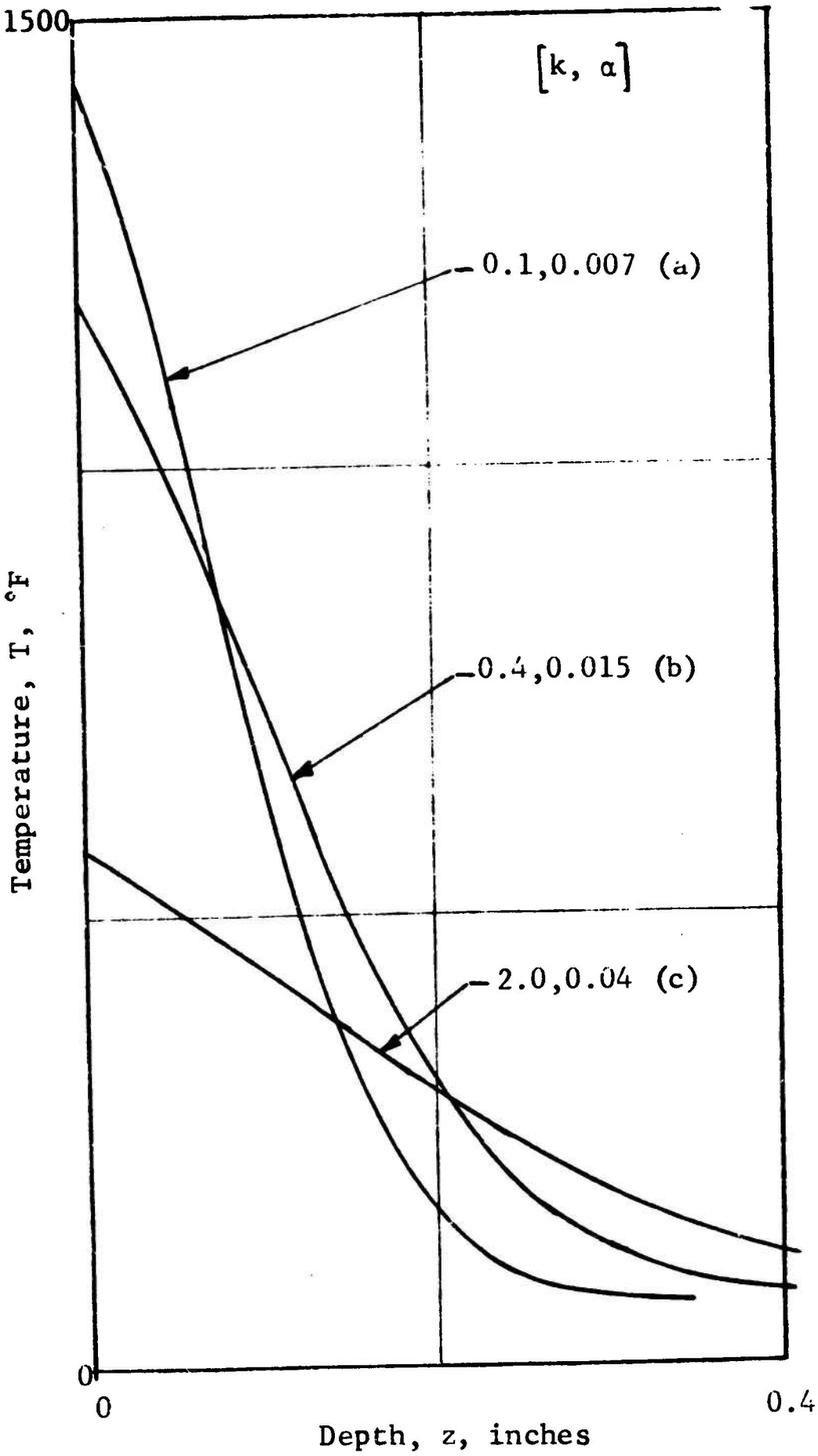

Figure 6.6 Soil Temperature Distributions, Large Yield

known that most of the energy is radiated in the visible range of 0.3 to 0.7 micron wavelengths for a 5000°K fireball. In the infrared range of 0.7 to 15 micron wavelengths, and in the X-ray range of 0.001 to 0.015 micron, there is a two-order magnitude of radiant energy reduction.

The transmission of radiant energy through a cloud of dust particles which are distributed randomly in space and time, and which have a uniform diameter (monodisperse), can be calculated from the formula

$$I = I_o \exp(-\alpha X) \tag{6.21}$$

where I_o is the incident radiation flux at the top of the dust cloud, I is tha radiant flux in the dust cloud at a distance "X" from the top of the dust cloud, and α is the absorption coefficient.

The absorption coefficient can be calculated on the basis of the dust cloud being composed of spherical particles, with an average separation between spherical particles being much greater than the wavelength of the incident radiant energy. Thus, the scattering and absorption properties of the cloud can be determined in terms of the scattering and absorption cross sections of a single spherical particle.

The absorption and scattering of a single spherical particle have been evaluated analytically by Mie. A plane electromagnetic wave, incident upon a spherical particle, excites the various natural electric and magnetic resonance modes in the particle. Thereafter, the particle re-radiates a portion of its energy in all directions and absorbs the other portion of the energy, at the same frequency as the incident energy. Mie's equations have been solved numerically, and the computer results are often presented in terms of a

normalized cross section Q, referring to the spherical particle cross-sectional area πr^2. These cross sections are a function of the size parameter $2\pi r/\lambda$ where r is the radius of the spherical particle, and λ is the wavelength of the incident energy for each value m of complex index of refraction of the particle material.

For very large values of $2\pi r/\lambda$, in the range of $2\pi r/\lambda > 50$, the sum of the normalized absorption (Q_a) and scattering (Q_s) cross sections approaches the value 2.

For very small values of $2\pi r/\lambda$, in the range of $2\pi r/\lambda < 0.1$, the scattering and absorption cross sections are related to $2\pi r/\lambda$, raised to an integral power.

For the range of values of $2\pi r/\lambda$ between 4 and 50, there is a strong oscillatory relation between Q and $2\pi r/a$.

It has become customary to refer to the normalized cross sections Q as efficiencies.[6.4] Also, the sum of the absorption and scattering efficiencies is called the extinction efficiency,

$$Q_{abs} + Q_{sca} = Q_{ext} .$$

Typical results[6.5] of those efficiency (Q)-versus-size parameter ($2\pi r/\lambda$) curves for a particular complex value of index of refraction (m) are shown in Figures 6.7 through 6.10.

Consider that I_o is the intensity (watts/μ^2) of the incident radiation which is not polarized. A spherical particle will intercept $Q_{ext}\pi r^2 I_o$ (watts) from the incident beam, where $Q_{abs}\pi r^2 I_o$ will be the absorbed energy and $Q_{sca}\pi r^2 I_o$ will be the scattered energy of the particle.

The scattered energy has preferred directions depending upon the size parameter and index of refraction,

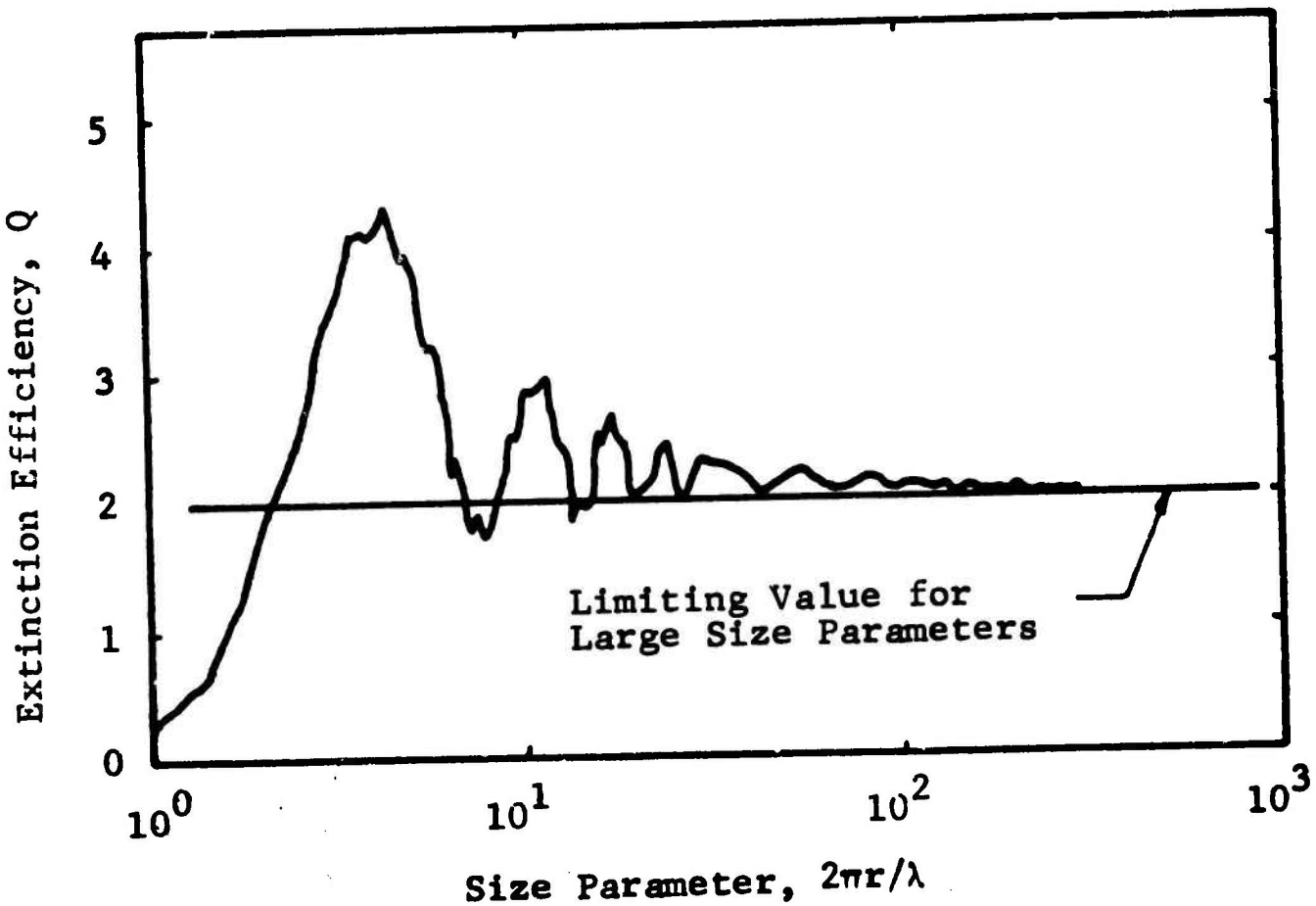

Figure 6.7 Extinction Efficiency for Size Parameters Greater than 1.0:m = 1.50

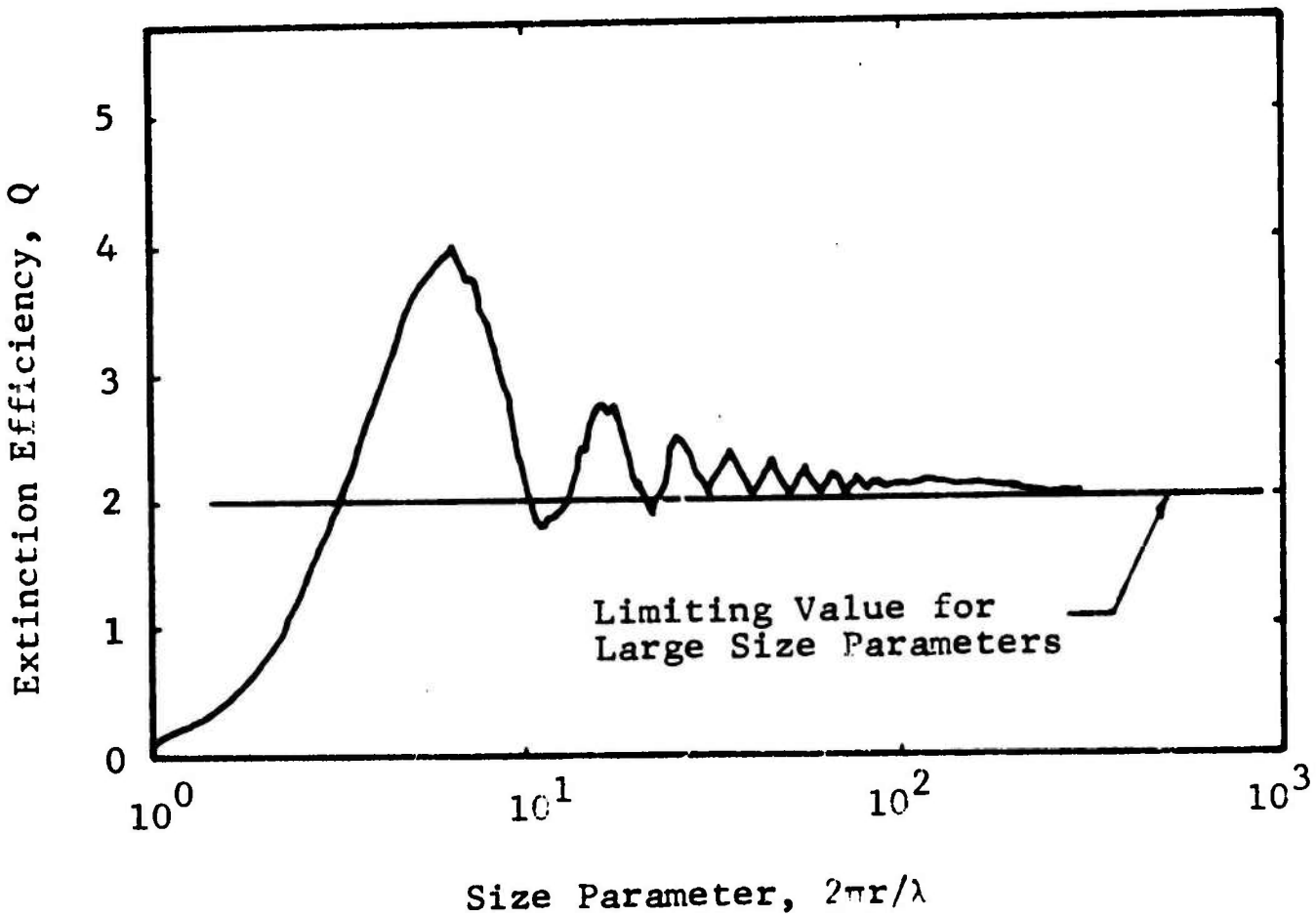

Figure 6.8 Extinction Efficiency for Size Parameters Greater than 1.0:m = 1.33

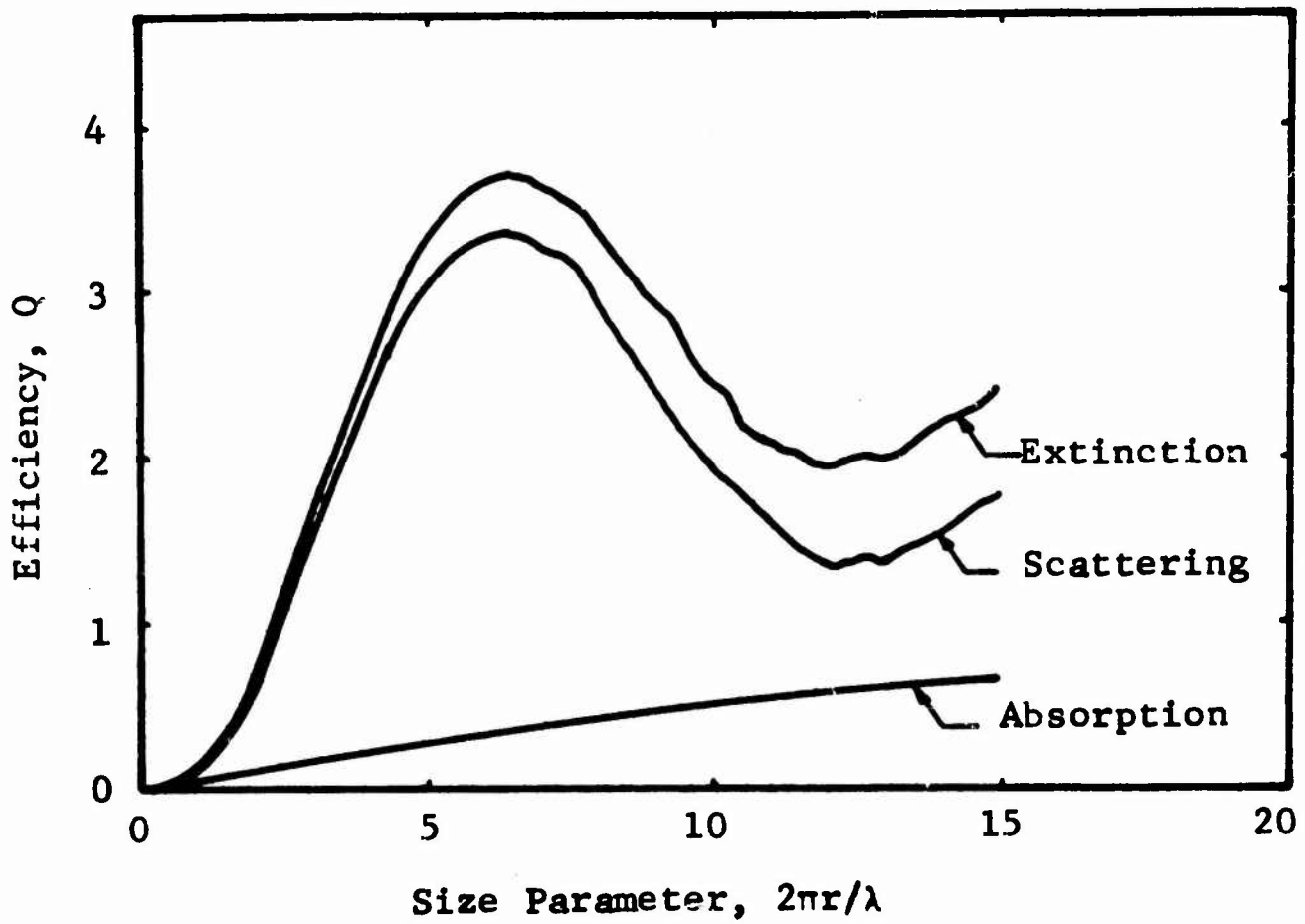

Figure 6.9 Extinction, Scattering, and Absorption Efficiencies vs Size Parameter: m = 1.315-0.0143

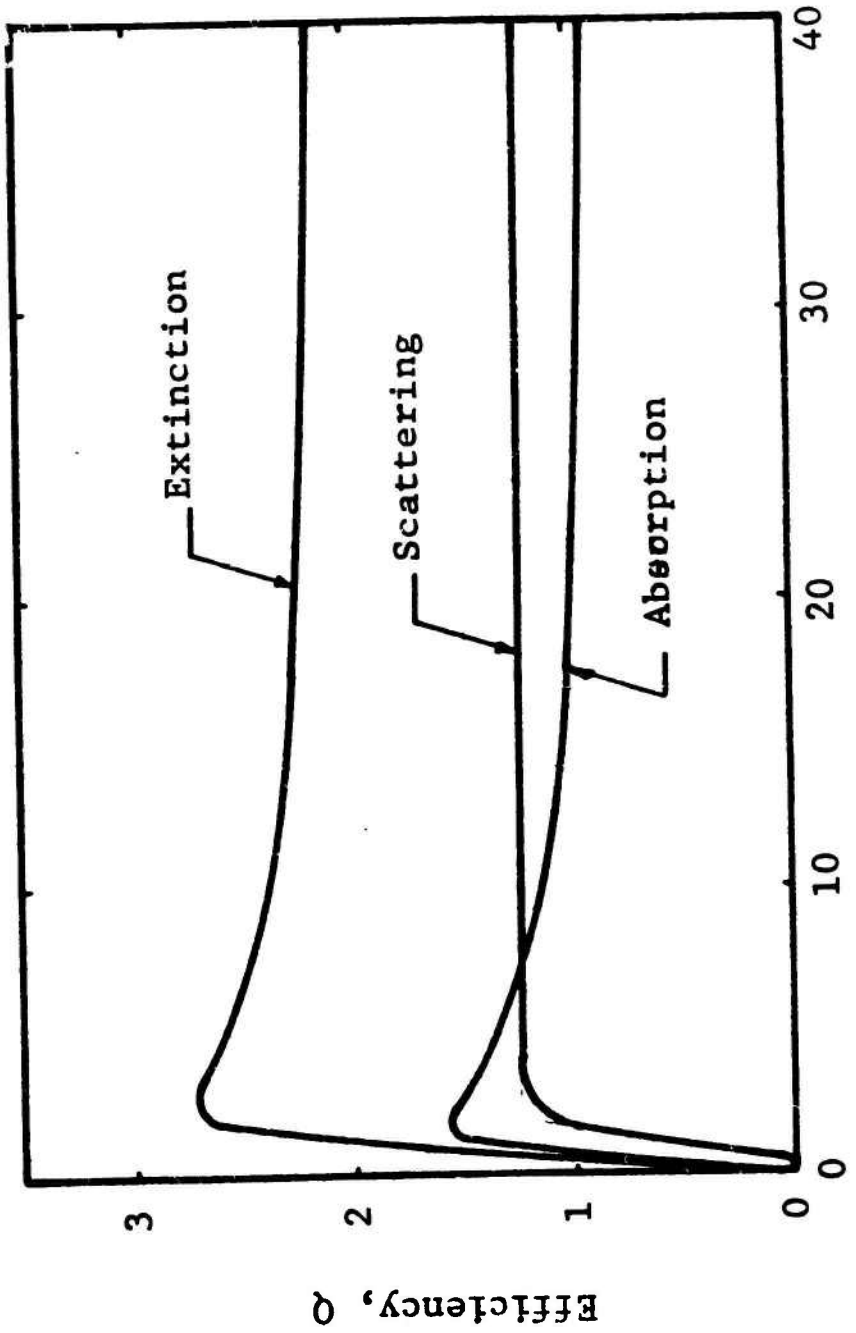

Figure 6.10 Extinction, Scattering, and Absorption Efficiencies vs Size Parameter: m = 1.59-0.66

and has a polarization effect. For instance, when $2\pi r/\lambda << 1$, the well-known Rayleigh Law [6.6] for the scattering of unpolarized radiation is

$$I_o = \frac{\pi^2 V}{2R^2\lambda^4}\left(\frac{m^2-1}{m^2+2}\right)(1 + \cos^2\theta)$$

where I_o is the intensity of the scattered radiation in the direction θ, V is the volume of the particle, and R is the distance between the particle and the observer. The radiation intensity scattered by the particle consists of two incoherent plane-polarized components, i_1 and i_2, whose planes are mutually perpendicular. The factor of unity in the first parenthesis of I_o governs i_1; while the factor $\cos^2\theta$ in the last parenthesis of I_o governs i_2. At $\theta = \pi/2$, the $\cos^2\theta$ factor is zero and the scattered radiation becomes completely plane-polarized, in a plane perpendicular to the plane of observation.

The angular distribution of intensity is symmetrical about a plane normal to the incident light, i.e., as much light is scattered forward as backward when $2\pi r/\lambda < 0.1$. However, about a 1000-fold or more ratio exists favoring the forward over the backward scattering for $2\pi r/\lambda > 1$. Since the average size dust particle is 12.5 microns in radius, and we are concerned with visible light in the range of 0.5 micron, $2\pi r/\lambda > 1$ and there is strong forward scattering. The sensitivity of the scattering to the index of refraction m and size parameter α is shown in the following diagram. Note that the total scattered energy is given by $i_1 + i_2$.

The particles in a dust cloud scatter energy mostly in the forward direction, and weakly to the backward and sideward directions as shown in Figures 6.11 and 6.12. The backward scattered energy will be small and appear as reflected energy from the dust cloud at the top, and the

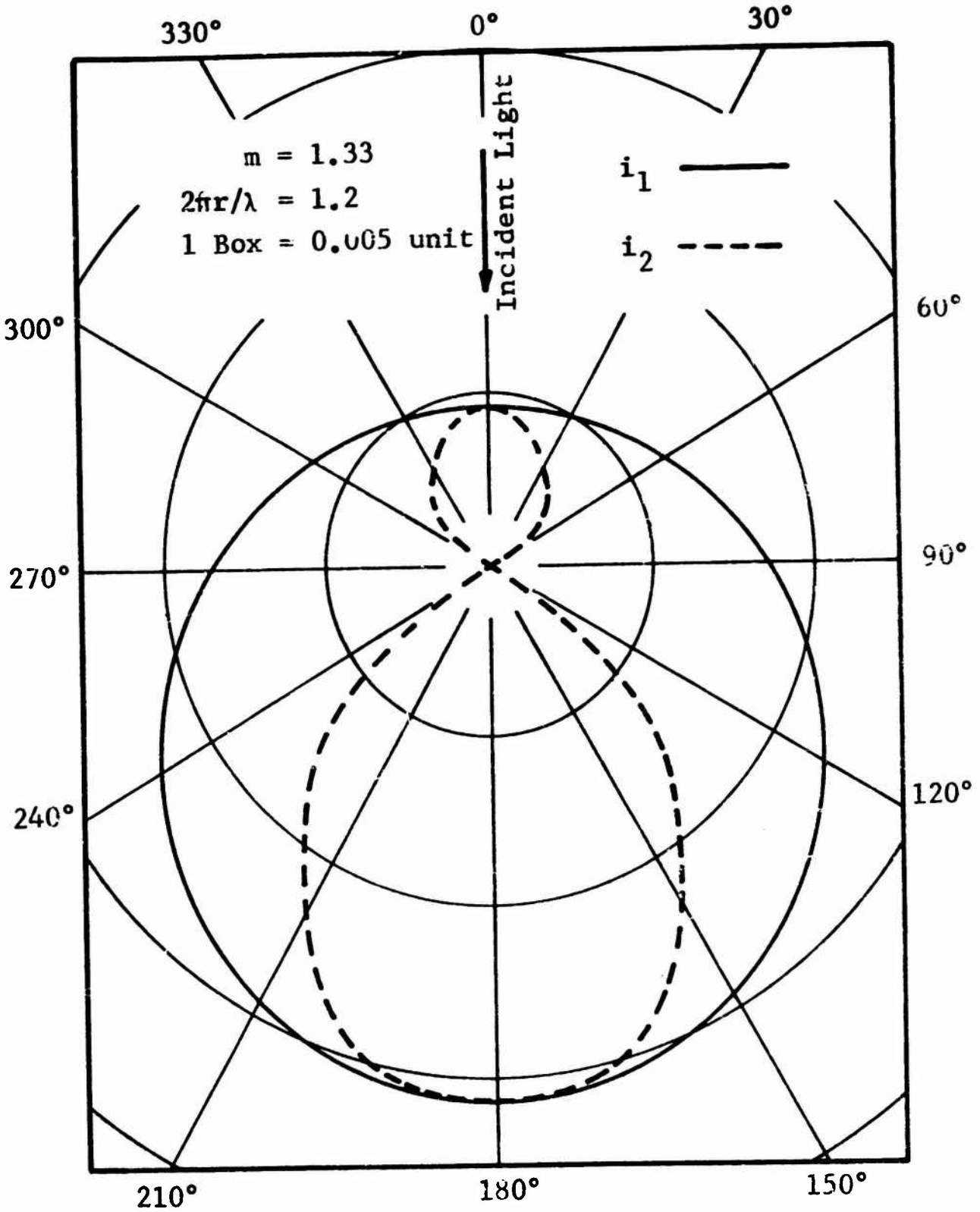

Figure 6.11 Polar Diagram of Scattering for i_1 and i_2 Components for 0.1μ Radius Water Droplet

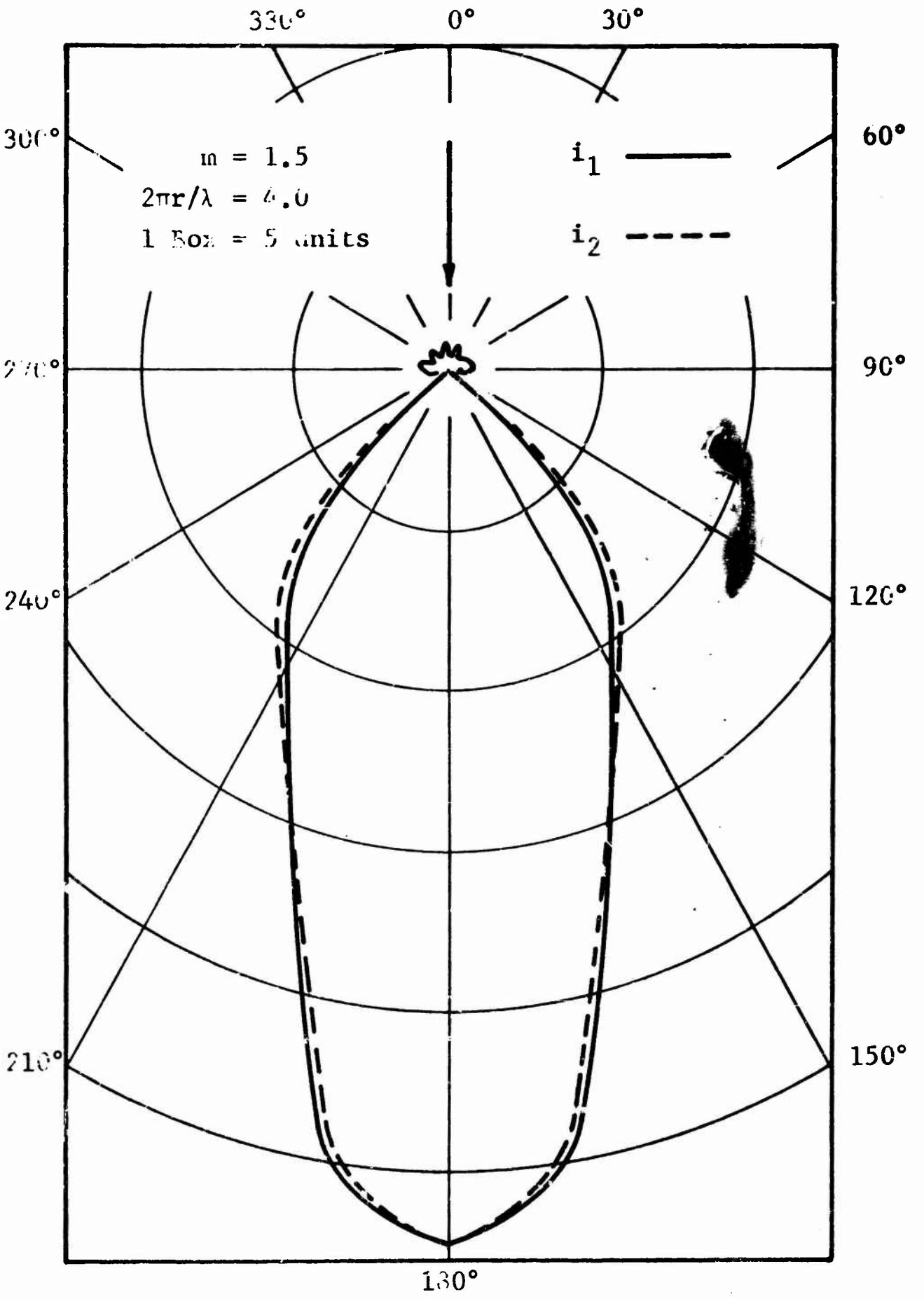

Figure 6.12 Polar Diagram of Scattering for i_1 and i_2 Components for 0.33μ Radius Oil Droplet

forward scattered energy will be large and appear as transmitted energy in the interior of the dust cloud. This is the absorbed energy of the particles that must be used to calculate the temperature changes in the dust cloud.

Kattawar[6.7] calculates Q_{abs}, for several materials m, for size parameters $2\pi r/\lambda = 0.1$, 1.0, and 10. These charts can be used to determine the energy absorbed at various distances into the cloud (X) according to:

$$I = I_o \exp(-NQ_{abs} \pi r^2 X)$$

where N is the number of particles per cubic centimeter, Q_{abs} is the absorption efficiency factor, and r is the radius of the spherical particle. Since the number of particles per cubic centimeter depends upon the density of the dust cloud ρ, the density of the dust particle material ρ_c, and the radius of the particle r, according to

$$N = \frac{\rho}{\rho_c \frac{4}{3} \pi r^3} ,$$

the intensity of the energy in the cloud at a particular depth is

$$I = I_o \exp\left(- \frac{3}{4} Q_{abs} \frac{\rho}{\rho_c} \frac{X}{r}\right) .$$

The absorption efficiency depends upon the wavelength of the incident radiation λ, via the size parameter $2\pi r/\lambda$. The wavelengths of interest are

$\lambda = 0.280 \rightarrow 0.397\,\mu$ (ultraviolet),
$\lambda = 0.397 \rightarrow 0.700\,\mu$ (visible), and
$\lambda = 0.700 \rightarrow 15 \rightarrow 150\,\mu$ (infrared).

Assuming that the average size particle is $r = 12.5$ (microns), then

$$\frac{2\pi r}{\lambda} = \frac{2\pi(15.5\mu)}{(785\mu)} = 0.1 \text{ (electromagnetic)},$$

$$\frac{2\pi r}{\lambda} = \frac{2\ (12.5\mu)}{(78.5\mu)} = 1.0 \text{ (infrared)},$$

$$\frac{2\pi r}{\lambda} = \frac{2\ (12.5\mu)}{(7.85\mu)} = 10.0 \text{ (infrared)},$$

$$\frac{2\pi r}{\lambda} = \frac{2\ (12.5\mu)}{(0.785\mu)} = 100.0 \text{ (visible red), and}$$

$$\frac{2\pi r}{\lambda} = \frac{2\ (12.5\mu)}{(0.393\mu)} = 200.0 \text{ (visible violet).}$$

In the visible region where the fireball emits most of its energy,

$$\frac{2\pi r}{\lambda} > 100$$

and

$$Q_{abs} \cong 1.0 .$$

Thus, the energy absorption in the dust cloud simplifies to

$$I = I_o \exp\left(-\frac{3}{4}\frac{\rho}{\rho_c}\frac{X}{r}\right).$$

In the special case where the dust cloud is $\rho = 0.01$ lb/ft^3, and each dust particle has a specific gravity of 2.65 and a radius of 12.5μ,

$$I = I_o \exp\left(-\frac{X}{10}\right)$$

where X is measured in inches. Thus, the intensity of the radiation is reduced by approximately 2.7 every 10 inches

(25.4 cm). Since there are 7,344 particles/cm^3, there is an average spacing of 0.051 cm between particles. The optical depth is increased beyond 10 in. when ρ_c is increased, ρ is decreased, and r is increased.

In the infrared-to-electromagnetic region where the fireball emits a small fraction of its energy,

$$0.1 < \frac{2\pi r}{\lambda} < 10.0$$

and

$$Q_{abs} < 1.0 \ .$$

Furthermore, Q_{abs} becomes a function of the size parameter $2\pi r/\lambda$ and the complex index of refraction m, as shown in Figures 6.13 through 6.15. Consider the following table.

Table 6.2 ABSORPTION

Type	Index of Refraction $m=n_1-in_2$	$Q_{absorption}$		
		Size Parameter		
		α = 10 Infrared	α = 1.0 for r=25μ	α = 0.1 E.M. for r=25μ
1	1.33-1.000i	0.4500	1.5000	0.2100
2	1.33-0.100i	0.8000	0.2800	0.0210
3	1.33-0.010i	0.3500	0.2800	0.0021
4	1.33-0.001i	0.0410	0.0028	0.0002
5	10-10.000i	0.3000	0.4500	0.03000
6	10-1.000i	0.4500	0.8200	0.00550
7	10-0.100i	0.4500	0.2000	0.00055
8	10-0.010i	0.3000	0.0200	0.0006
9	10-0.001i	0.0500	0.0020	0.00000

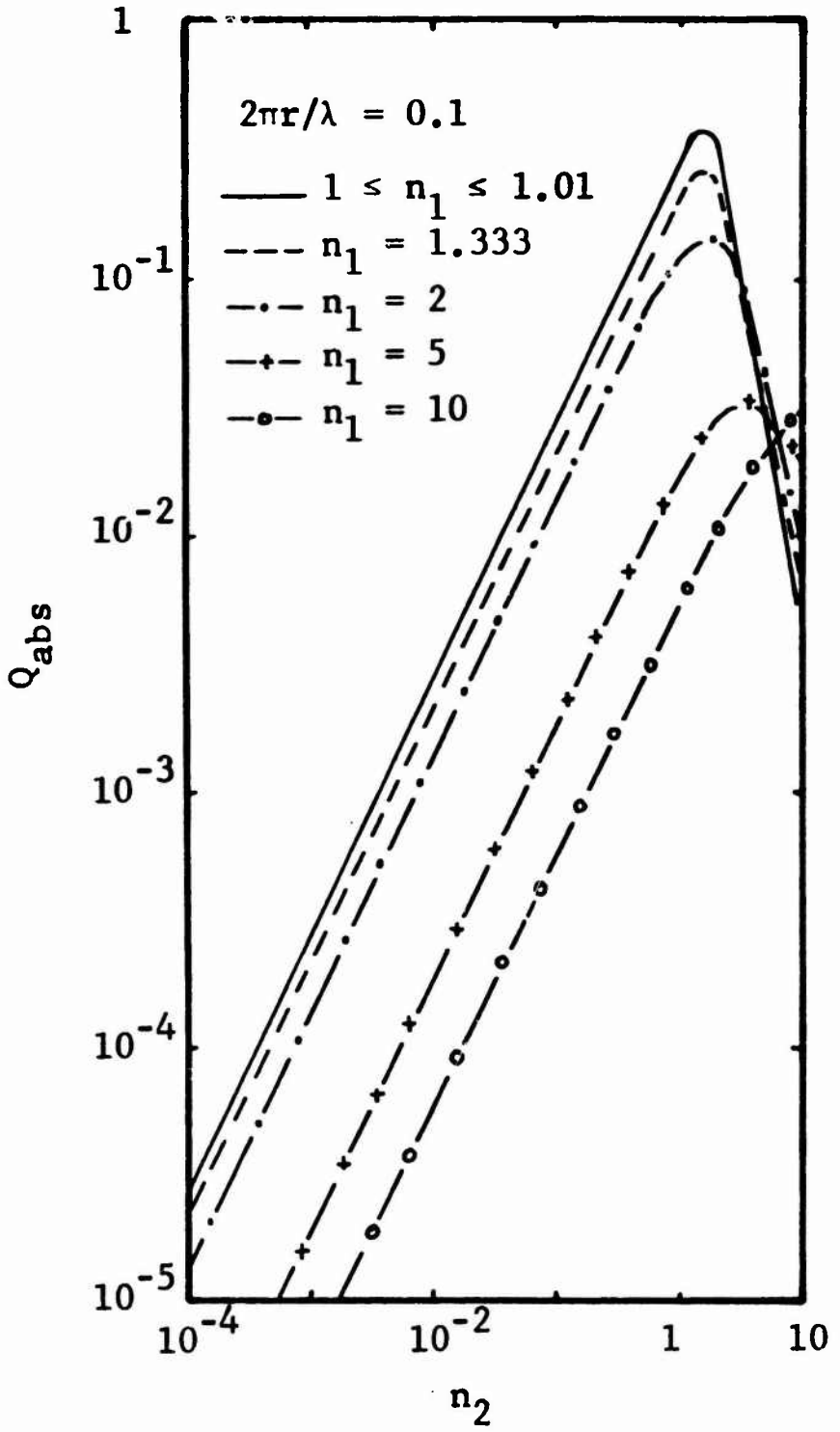

Figure 6.13 Absorption Coefficient Dependence on Index of Refraction, $2\pi r/\lambda = 0.1$

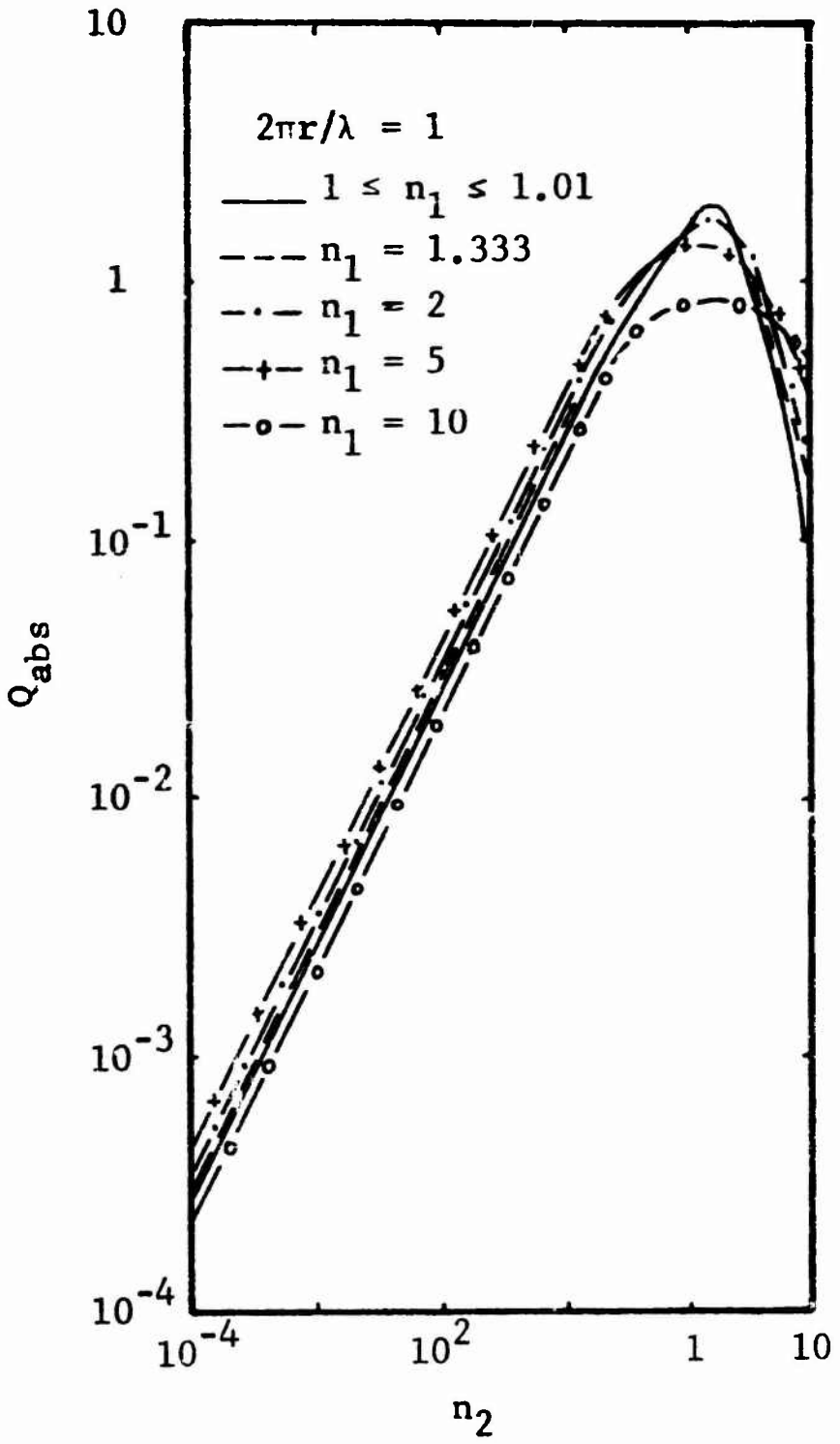

Figure 6.14 Absorption Coefficient Dependence on Index of Refraction, $2\pi r/\lambda = 1$

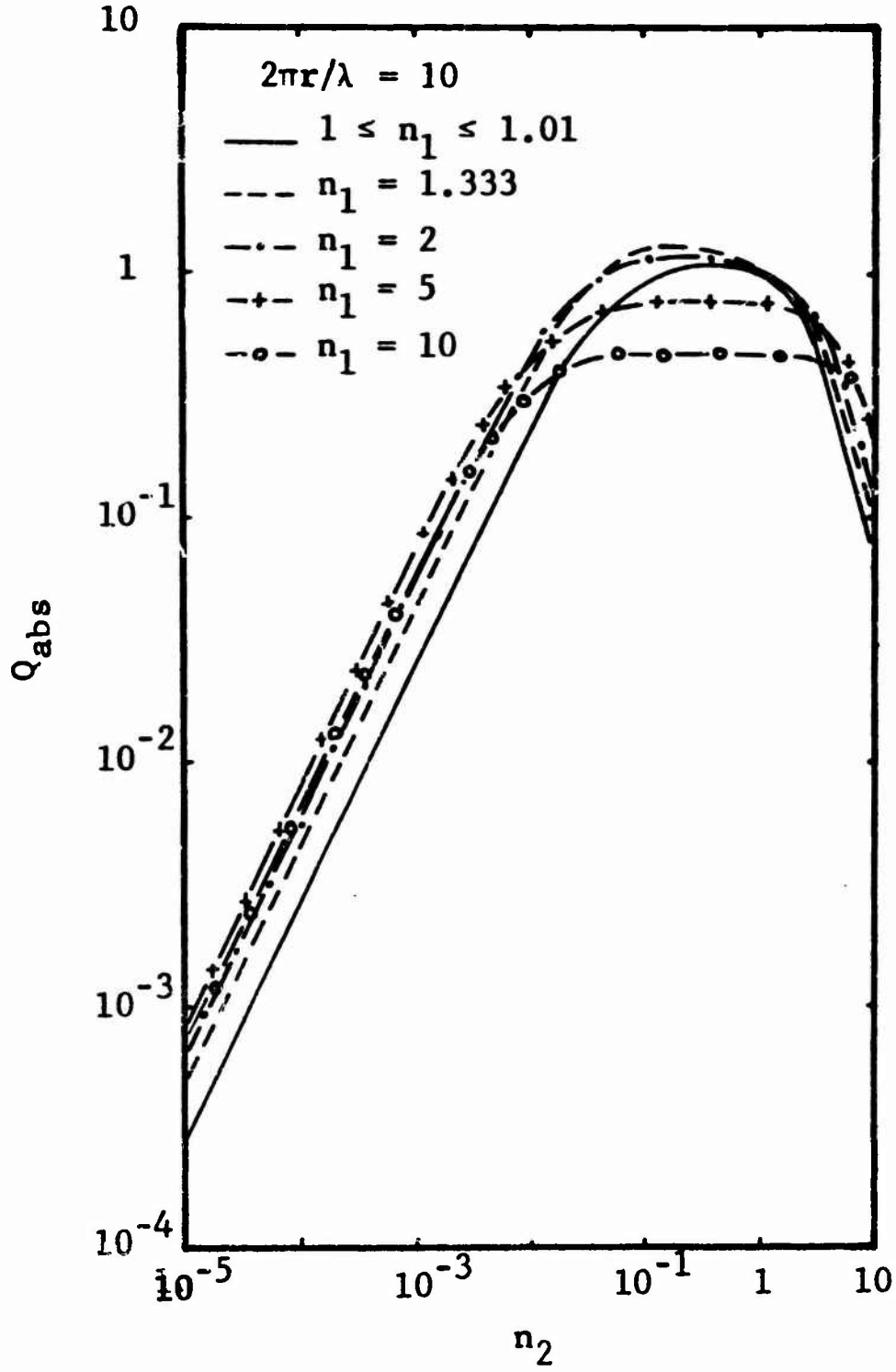

Figure 6.15 Absorption Coefficient Dependence on Index of Refraction, $2\pi r/\lambda = 10$

For types 1, 2, 5, and 6 dust materials, the previous numerical example which resulted in a 10-in. e-folding distance for radiation in the visible region is also applicable to well within an order of magnitude for the visible infrared region, but must be strongly increased for the infrared-to-electromagnetic region.

Material 1 corresponds to water in the optical region, while material 6 corresponds to water in the electromagnetic region. Material 2 corresponds to metals in the optical region, while material 5 corresponds to metals in the infrared region.

Consider a fireball temperature of 5000°K which results in most of the emitted energy being in the visible range of radiation, and an average dust size particle of $r = 12.5\mu$. These combine to yield the simple result that $Q_{absorption} = 1$, regardless of the material properties. The energy intensity e-folding depth is given by

$$\frac{4}{3}\frac{\rho_c}{\rho} r \ .$$

Sinclair's[6.8] handbook of aerosols states that optical interference between particles would be expected if the particles were less than five diameters apart. Since the average spacing between particles is approximately 510 microns and the average size particle is 25 microns in diameter, the particles are spaced about 20 diameters apart. Therefore, it is not necessary to consider interference between particles. The experiments of Churchill, Clark, and Sliepcevich[6.9] enforce this conclusion, since they determined that the upper limit of the ratio of spacing/diameter of the particles in a cloud is more like 1.7, rather than 5, and any ratio above 1.7 indicates that optical interference can be neglected.

The critical dust cloud density for consideration of optical interference is determined by using the criterion

$$\frac{1}{(N)^{1/3}} = \ell_o$$

where N is the concentration of particles per unit volume and ℓ_o is the center-to-center distance between particles. This distance is given by

$$\ell_o = 4r \ .$$

Since

$$N = \frac{\rho}{\frac{4}{3}\pi r^3 \rho_c} \ ,$$

where ρ is the cloud density, ρ_c is the dust particle density, and r is the particle radius,

$$\rho = \frac{\Pi}{32} \rho_c = 0.1 \rho_c \ .$$

In the special case where $\rho_c = 60$ lb/ft^3, the cloud density must be 6 lb/ft^3 for optical interference effects to become significant.

6.5 IITRI Air-Temperature Model

6.5.1 General

The air-temperature model considers the exchange of thermal energy between the dust and the air as the dust is transported vertically through the air. The horizontal and vertical motion of the dust relative to the air has been defined in the previous chapter. In the air-temperature model however, it is important to emphasize the relative aspects of the vertical motion since the air will be permitted to undergo a change in volume and, hence, will experience some gross vertical motion. Results of the dust study,

together with soil surveys at potential sites, indicate (1) that the bulk of the soil mass is composed of fine particles corresponding to the finer three or four size groups, and (2) that the behavior of these fine particles during the positive phase duration portion of the blast wave are essentially the same (see Figure 5.13). The behavior of the particles of these size groups is nearly identical because the influence of gravitational forces (as measured by the magnitude of the terminal velocity) is small. The air-temperature model, therefore, neglects the size effects of the particles as far as the transport aspects of the dust cloud are concerned.

The exchange of energy between a particle of soil and its surroundings, including the air in which it is placed, will be accomplished by the mechanisms of convection and radiation. The transfer of the stored thermal energy in the soil particle will be governed by the mechanism of conduction. An examination of the conduction problems indicates that for the very small particle sizes of interest, the majority of stored energy can be extracted from the interior of the particle in a time of the order of one microsecond. Thus, the conduction process is not a limiting process. An examination of a simple radiation problem indicates that the loss of a significant amount of the stored energy by this mechanism will require approximately 10 sec. The dust will be transported a significant distance through the air in this period of time; hence, a relatively small temperature change will occur in the dust due to thermal radiation.

The dust particles are carried through the air by the local turbulent action of the air; hence, very little relative motion will exist between the air and the dust particles. The convection process will, therefore, be that of natural or free convection. Normally, radiative cooling

represents a significant portion of the energy transport in natural convection heat transfer problems, except for very small objects as is the case herein. Estimates of the heat transfer coefficients for the current problem indicate that the majority of the thermal energy stored in the soil particles will be transferred to the surrounding air in times of the order of several tens of milliseconds. Thus, the controlling heat transfer process is that of natural convection. The air-temperature model is based upon this heat transfer mechanism.

The air-temperature model consists of a simple periodic thermal energy balance for a local mass of air. The dust which mixes with this mass of air approaches thermal equilibrium with the air in some time interval, the time interval being related to the heat transfer coefficient. The dust particles will generally enter the region or cell occupied by the given mass of air at a temperature which differs from the current air temperature. The dust temperature will be determined from the air temperature of the cell from which it just left or, if the air is adjacent to the soil surface, from the temperature of the soil which is currently being eroded by the blast wind. The soil particles in a particular cell will also absorb some incident thermal radiation which is continually being emitted from the fireball. Since the vertical velocity of the dust particles is small when compared to the acoustic velocity of the air, any pressure waves which could be generated would have propagated considerable distances compared to the cell size. Thus, the energy balance occurs at constant pressure, rather than at constant volume. The transient pressure field which exists in the blast wave is assumed to be unaltered by the existence of the dust and thermal energy. The mass of air or the cell will undergo a change in volume due to the changing pressure field and the change in the thermal content of the cell.

The cell will therefore perform work on its surroundings. The initial conditions of the air at the time of arrival of the shock wave will correspond to the shock state at the range of interest.

6.5.2 Description of the Air-Temperature Model

A packet of hot dust, which is eroded at a particular time, enters a given column of air. The horizontal motion of those specific dust particles is identical to that of the air column. The vertical motion is that which is described in the cold dust model. The vertical temperature distribution in the column of air will vary with time as the column sweeps over the ground surface. The vertical temperature distribution at the site is obtained by considering the vertical temperature distribution in the column of air which is currently at the site location. The model, therefore, considers the transient temperature variations of a number of air columns up until the time that they sweep past the site. Time measured along the path of the air column is related to the observation at the site by the equation

$$t = t_{obs} + \frac{R}{U} \tag{6.22}$$

where

t = time following air column,
t = 0 when air column is set into motion,
t_{obs} = time at site location,
t_{obs} = 0 when shock arrives at site,
R = current displacement of air column, and
U = shock velocity.

For a uniform ground condition, all of the air columns experience the same temperature transient except for a time shift. The solution to this simple case is then obtained by considering the temperature variation for a single air column as

it moves across the ground, and then connecting the time scale in accordance with Equation 6.22.

The column of air is divided up into a number of cells whose initial height is δy. The weight of air per unit ground area is

$$\hat{w} = \rho_{sa} \delta y \tag{6.23}$$

where

w = weight of air, and
ρ_{sa} = air density (shock density).

The energy balance for each cell is made periodically at an interval of time needed to approach thermal equilibrium between the dust and the air in the cell. This time, t_e, is determined from the heat transfer coefficient and represents a variable for the current problem.

The maximum vertical velocity of the dust is KV_o where K is the transport coefficient and V_o is the peak air velocity. It will be convenient to select an initial cell size DY such that the dust particles will not move a distance greater than δy during a time step t_e. Furthermore, it will be desirable from a computational point of view to require that all of the cells have the same initial size and, therefore, the same weight of air. Thus,

$$\delta y = t_e \, K \, V_o \, . \tag{6.24}$$

Recalling that, in the absence of gravitational effects, the cloud height H is governed by the differential equation

$$\frac{dH}{dt} = KV \tag{6.25}$$

where

t = time, and

V = horizontal wind velocity,

the current model will be limited to the positive phase duration of the blast-induced winds; hence, the absolute velocity restriction can be dropped from Equation 6.25. It will be convenient to select a somewhat nonuniform time step Δt in order that the change of the height of the cloud during each time step be uniform. During the early portion of the dust cloud growth, when the horizontal wind velocity is changing slowly, the time step will be nearly uniform. The initial time step is equal to t_e; hence, the change in height of the cloud during each time step is equal to the initial cell height δy. It should be noted that these conditions apply in a Lagrangian sense, i.e., in the absence of any vertical dilatation of the air column. The actual height of the dust cloud would depend upon the temperature distribution within the column of air.

A Lagrangian cell configuration can now be established. This configuration is illustrated in Figure 6.16(a). The independent variables are the Lagrangian height y_j and the time t_i, where the indicies i and j refer, respectively, to a specific time and a specific cell. The cell is defined by the coordinate of its upper edge. The top of the cloud is thus given by

$$H_i = (i-1)\,\delta y \tag{6.26}$$

and the time is given by

$$t_i = t_{i-1} + \frac{\delta y}{K\bar{V}_i} \,. \tag{6.27}$$

$\bar{V}_i$ is the average value of the horizontal air velocity during the time step.

The horizontal displacement of the air column during a time step is

$$DR = \bar{V}_i \ (t_i - t_{i-1})$$

and is therefore a constant, equal to

$$DR = \frac{\delta y}{K} \ . \qquad (6.28)$$

Furthermore, the quantity of dust picked up per unit area during a time step is

$$W = Fa\rho_s \bar{V}_i \ (t_i - t_{i-1})$$

where

a = erosion coefficient,
ρ_s = bulk density of soil,
F = land use factor,

and is therefore a constant, equal to

$$W = Fa \frac{\rho_s \delta y}{K} \ . \qquad (6.29)$$

The total horizontal displacement of the air column is

$$R_i = (i-1)\ DR = H_i/K; \qquad (6.30)$$

hence, the observation time $t_{obs,i}$ defined in Equation 6.22 can be rewritten as

$$t_{obs,i} = t_i - \frac{(i-1)DR}{U} \ . \qquad (6.31)$$

A constant-pressure energy balance is made for each cell at each interval of time in accordance with the illustration given in Figure 6.16(b), where w_{ij} is the quantity of dust per unit area in the $j^{\underline{th}}$ cell at the $i^{\underline{th}}$ time. Similarly, w'_{ij} and w''_{ij} are the quantities of dust per unit area which, respectively, leave the j-1 cell and enter the $j^{\underline{th}}$ cell, and which leave the $j^{\underline{th}}$ cell and enter the j+1 cell during the $i^{\underline{th}}$ time interval. Clearly,

$$w''_{ij} = w'_{i,j+1} .$$

Therefore, we need only deal with the quantities w_{ij} and w'_{ij}. A simple formula for w_{ij} can now be developed by considering the contribution of dust in the cell from all of the dust packets. The total quantity of dust in the $k^{\underline{th}}$ packet is w and is distributed to its current height H in a linear manner. This is illustrated in Figure 6.17. The quantity of dust in the $j^{\underline{th}}$ cell is

$$w_{ijk} = \frac{2W}{H}\left[1 - \frac{y}{H}\right]dy .$$

But,

$$H = \delta y\ (i-k),$$
$$y = \delta y\ (j - \tfrac{3}{2}) ,$$

and

$$dy = \delta y\ ;$$

hence,

$$w_{ijk} = \frac{2W}{(i-k)^2}\left[i-k-j + \frac{3}{2}\right] . \qquad (6.32)$$

For a uniform soil condition the total quantity of dust in the cell w_{ij} is given by summing over all of the $k^{\underline{th}}$ dust packets. (It should be noted that dust from packets which

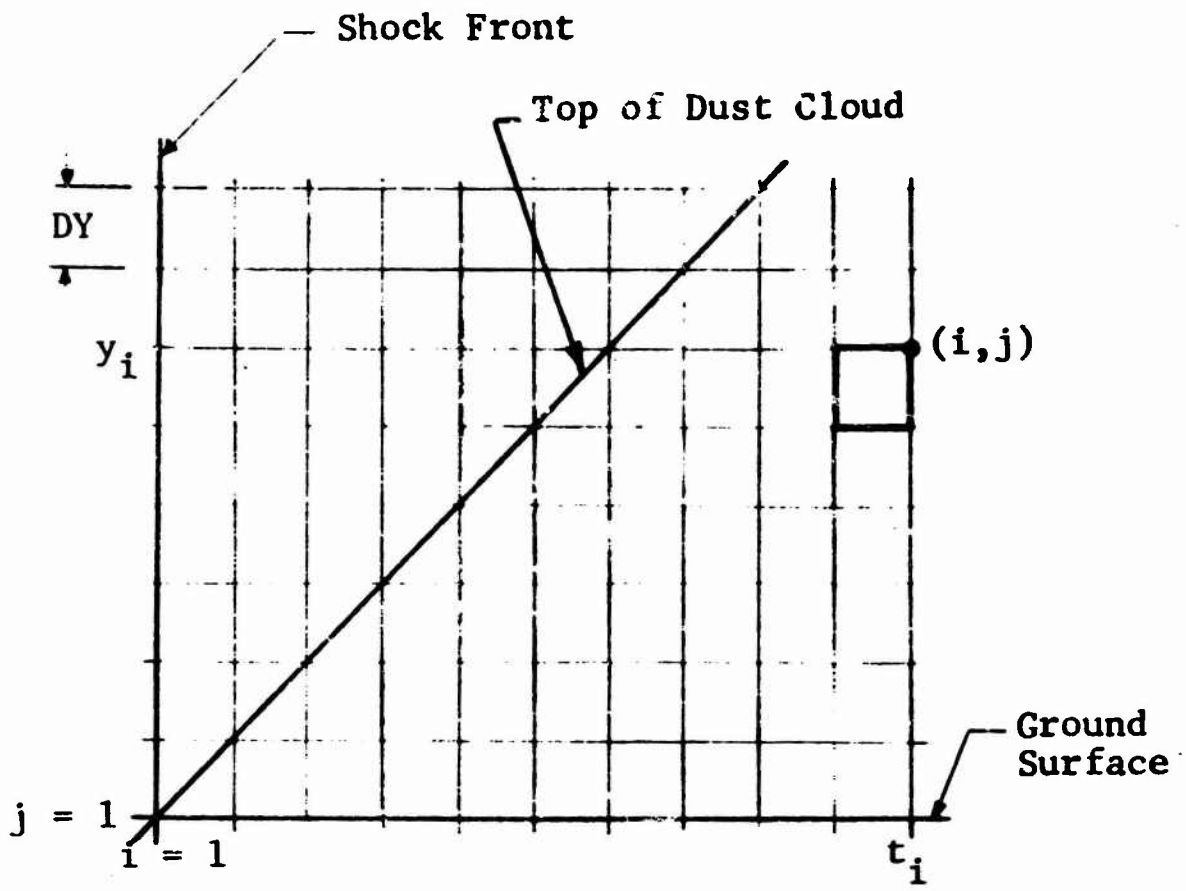

(a) Cell Configuration

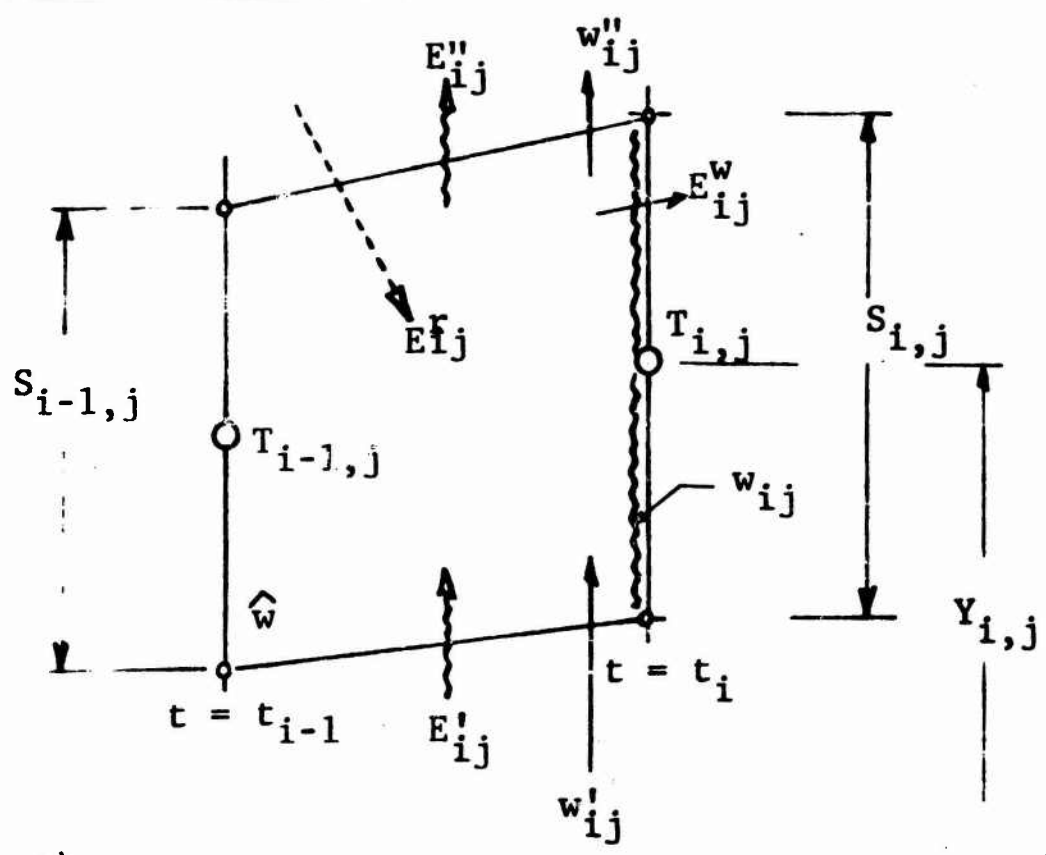

(b) j^{th} Cell

Figure 6.16 Cell Concept - Energy Balance

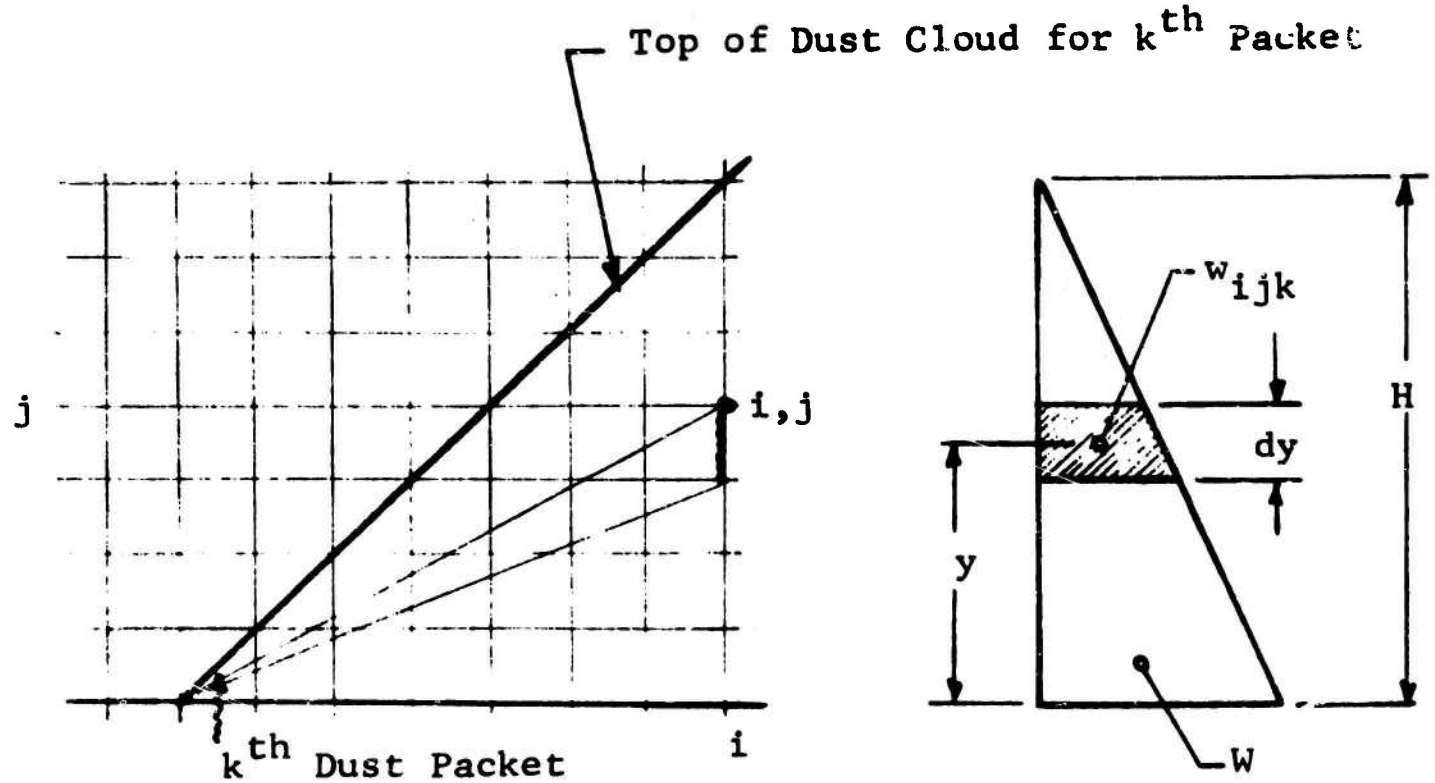

Figure 6.17 Dust in j^{th} Cell Due to k^{th} Dust Packet

have entered the overall cloud, but which cannot reach the $j^{\underline{th}}$ cell at the $i^{\underline{th}}$ time, must be excluded.) Hence,

$$w_{ij} = \sum_{k=1}^{i-j+1} w_{ijk} \tag{6.33}$$

or

$$w_{ij} = w_{i-1,j} + w_{ijl} ,$$

which becomes

$$w_{ij} = w_{i-1,j} + \frac{2W(i-j + 1/2)}{(i-1)^2} . \tag{6.34}$$

The quantity of dust per unit area from the $k^{\underline{th}}$ dust packet which enters the $j^{\underline{th}}$ cell during the $i^{\underline{th}}$ time interval is w_{ijk}. Figure 6.18 illustrates the distribution of the dust from this packet as well as the bounds of the subgroup of particles which enters the $j^{\underline{th}}$ cell. The dust moves in such a manner that the quantity of dust, bounded by any pair of rays passing through the $k^{\underline{th}}$ origin, is constant. Therefore, the dust entering the $j^{\underline{th}}$ cell during the $i^{\underline{th}}$ time is bounded by the ray passing through the point (i-1,j-1) and by the ray passing through the point (i,j-1). The following equations result:

$$w'_{ijk} = \frac{2W}{H} \left[1 - \frac{y}{H}\right] dy ;$$

but

$$H = \delta y \ (i-k) = H_{ik}$$

and

$$y' = y_{j-1} \ B_{ik}$$

where

$$B_{ik} = \frac{H_{ik}}{H_{i-1,k}} ,$$

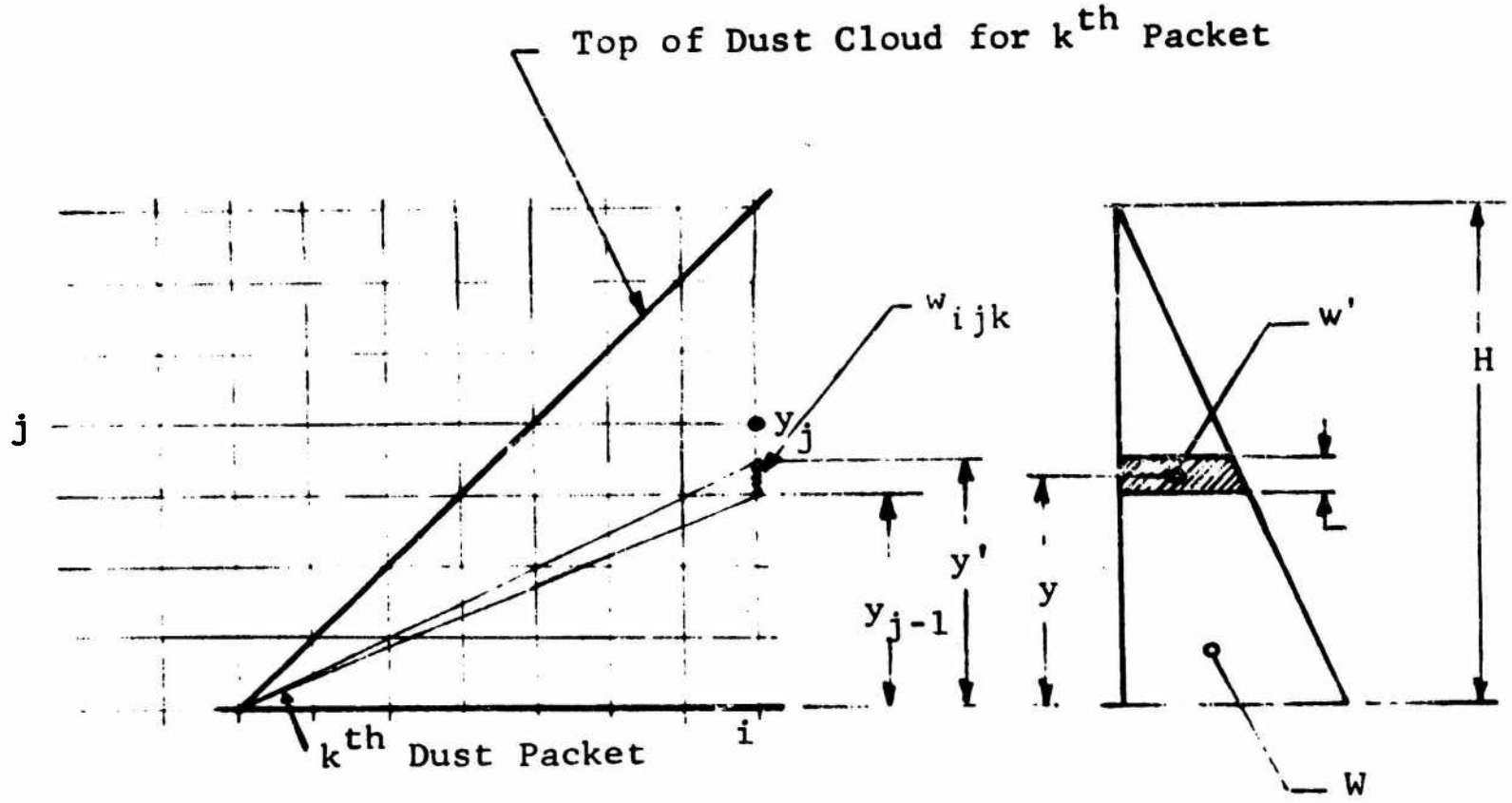

Figure 6.18 Dust Entering j^{th} Cell Due to k^{th} Dust Packet

$$y = \frac{1}{2}\,(y_{i-1} + y') \text{ , and}$$

$$dy = y' - y_{i-1} \text{ ;}$$

hence

$$w'_{ijk} = \frac{2W(j-2)}{(i-k)(i-k-1)} \left\{1 - \frac{(j-2)(i-k-1/2)}{(i-k)(i-k-1)}\right\}. \quad (6.35)$$

For a uniform soil condition the total quantity of dust entering the $j^{\underline{th}}$ cell during the $i^{\underline{th}}$ time interval is given by summing all of the $k^{\underline{th}}$ dust packets, noting again that some packets must be excluded. This quantity, then, is given by

$$w'_{ij} = \sum_{k=1}^{i-j} w'_{ijk} \quad (6.36)$$

or

$$w'_{ij} = w'_{i-1,j} + w'_{ij1} \text{ ,}$$

which becomes

$$w'_{ij} = w'_{i-1,j} + \frac{(2W(j-2)}{(i-1)(i-2)} \left\{1 - \frac{(j-2)(i-3/2)}{(i-1)(i-2)}\right\}. \quad (6.37)$$

It should be further noted that both w_{ij} and w_{ijk} are zero in the region above the dust cloud $(j-i \leq 0)$.

Two types of nonuniform or cutoff ground conditions have also been treated. These are the situations where (1) erosion stops because of an erosion cutoff depth z_c has been reached, or (2) the air column has reached a range where the land use factor has changed. These two problems are similar if we determine two different values for the quantity of soil, W, in a dust packet. Let these be W_1 and W_2, where $W_1 = 0$ for the case of no erosion. The corresponding cell configuration is illustrated in Figure 6.19. Regions 0 and 2 are those treated in the preceding paragraph. Region 1 is the new region introduced by the change in the land use

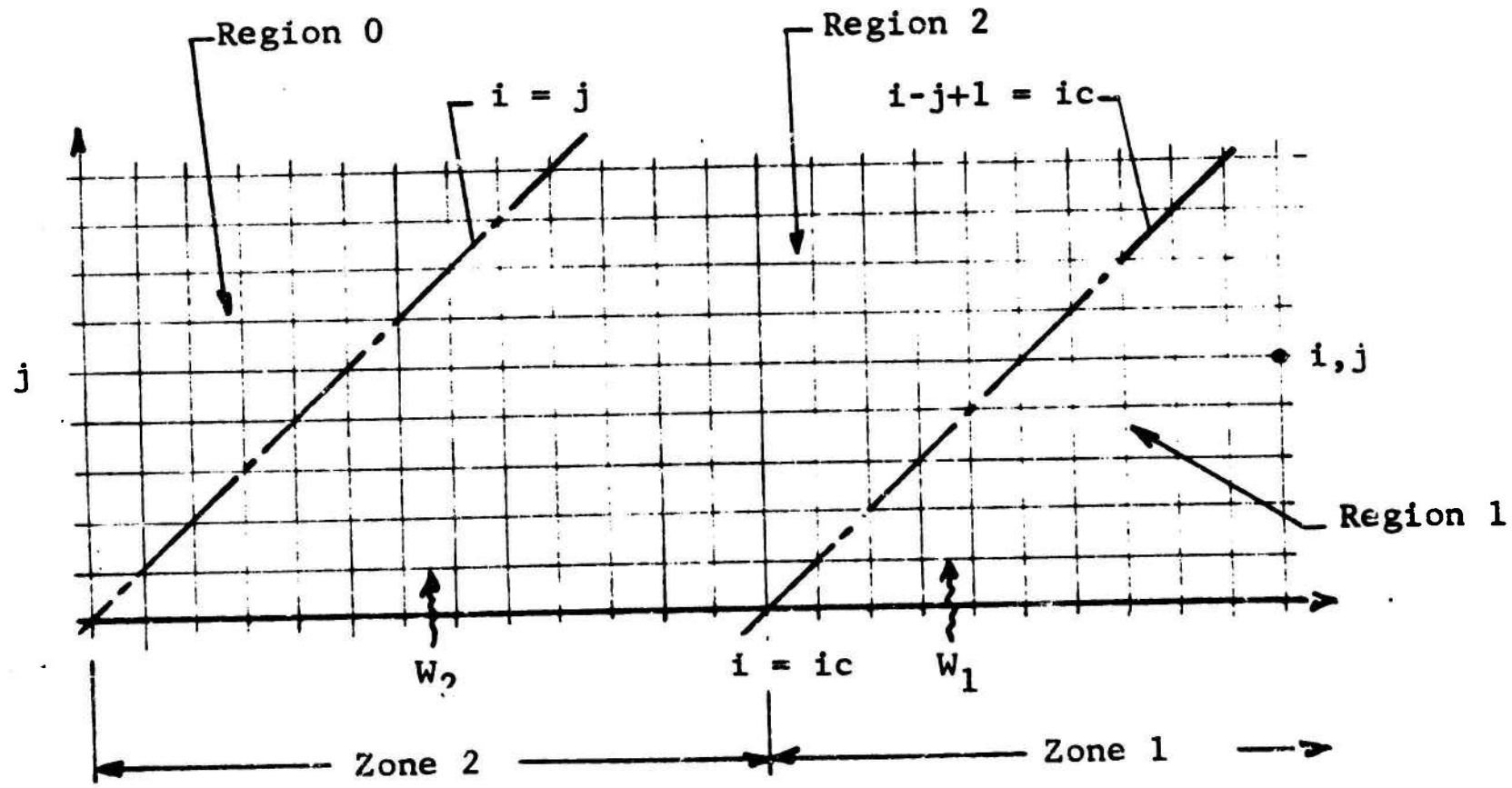

Figure 6.19 Influence of Erosion Cutoff on Dust Transport

factor or by erosion depth cutoff. The boundary between Regions 1 and 2 is defined by the index i = ic. If erosion stops after a depth z_c has been reached, then

$$ic = \frac{z_c \rho_s}{W} \tag{6.38}$$

or the land use factor changes at a range R_c in front of the site. Then,

$$ic = \frac{R_c}{DR} \quad , \tag{6.39}$$

since at the $i^{\underline{th}}$ time, the column is (by definition) at the site.

For cells in Region 1, the quantity of dust w_{ij} in the cell is determined as before; however, the summation is divided into two groups: one involving W_1, and the other involving W_2. The results are

$$w_{ij} = \bar{w}_{ij} + \bar{\bar{w}}_{ij}$$

where $\bar{w}_{ij}$ is the contribution from zone 1 ($W = W_1$) and $\bar{\bar{w}}_{ij}$ is the contribution from zone 2 ($W = W_2$). Therefore,

$$w_{ij} = w_{i-1,j} + \bar{\bar{w}}_{ij1} - \bar{\bar{w}}_{ij,ic} + \bar{w}_{ij,ic} \tag{6.40}$$

or

$$w_{ij} = w_{i-1,j} + \frac{2W_2}{(i-1)^2}(i-j+1/2) - \frac{2(W_2-W_1)}{(i-ic)^2}(i-ic-j+1/2), \tag{6.41}$$

recalling that for the erosion cutoff case, $W_1 = 0$.

A similar treatment for w_{ij} results in

$$w'_{ij} = w'_{i-1,j} + \bar{\bar{w}}'_{ij1} - \bar{\bar{w}}'_{ij,ic} + \bar{w}'_{ij,ic} \quad , \tag{6.42}$$

or

$$w'_{ij} = w'_{i-1,j} + \frac{2W_2(j-2)}{(i-1)(i-2)}\left\{1 - \frac{(j-2)(i-3/2)}{(i-1)(i-2)}\right\}$$

$$- \frac{2(W_2-W_1)}{(i-ic)(i-ic-1)}\left\{1 - \frac{(j-2)(i-ic-1/2)}{(i-ic)(i-ic-1)}\right\}. \qquad (6.43)$$

The energy balance on the cell, as illustrated in Figure 6.16, is

$$E'_{ij} + E^r_{ij} - E''_{ij} - E^w_{ij} = (\hat{cw} + cw_{ij})(T_{ij} - T_{i-1,j}).$$

The left-hand side of the equation represents the net energy flux which consists of the energy convected into the cell by the dust w'_{ij} and is

$$E'_{ij} = w'_{ij}\ c\ T_{i,j-1}$$

where c is the specific heat of the dust, and $T_{i,j-1}$ is the air temperature in the j-1 cell at t_i. The energy deposited in the cell by direct thermal radiation is E^r_{ij}, and is obtained from

$$E^r_{ij} = (Q_{ij} - Q_{i,j-1})(t_i - t_{i-1}) \qquad (6.45)$$

where

$$Q_{ij} = Q_o \exp(- w^*_{ij}/w_o \cos\theta), \qquad (6.46)$$

and

Q_o = thermal flux incident upon the cloud,

w^*_{ij} = quantity of dust above the $j^{\underline{th}}$ cell at time = t_i,

w_o = weight absorption coefficient permit area, and

θ = angle of incidence of radiation.

The energy convected out of the cell by the dust leaving the cell is

$$E''_{ij} = w''_{ij}\ c\ T_{i-1,j+1}$$

or

$$E'_{i,j+1} = w'_{i,j+1}\ c\ T_{i-1,j+1}\ . \qquad (6.47)$$

The expansion work that the cell does upon its surroundings is E^{w}_{ij} and is determined from

$$E^{w}_{ij} = S_{ij}\ (P_i - P_{i-1}) \qquad (6.48)$$

where

P_i = pressure at $t = t_i$, and

S_{ij} = height of $j^{\underline{th}}$ cell at $t - t_i$.

The deviation of S_{ij} will be presented in the following paragraph. The right-hand side of Equation 6.44 is the change in the internal energy of the cell. The mass of air in the cell is w, whereas c is the specific heat of air at constant pressure. $T_{ij} - T_{i-1,j}$ is, of course, the temperature change.

The air cells will undergo a change in volume due to both the thermal input and the changing pressure field. In the absence of dust, the volume change will only be due to the changing pressure field. It is assumed that this volume change will occur in the horizontal direction. The remainder of the volume change will occur in the vertical direction and will transport the air vertically (see Figure 6.20). The volume v of a cell, per unit width, is

$$v = SL$$

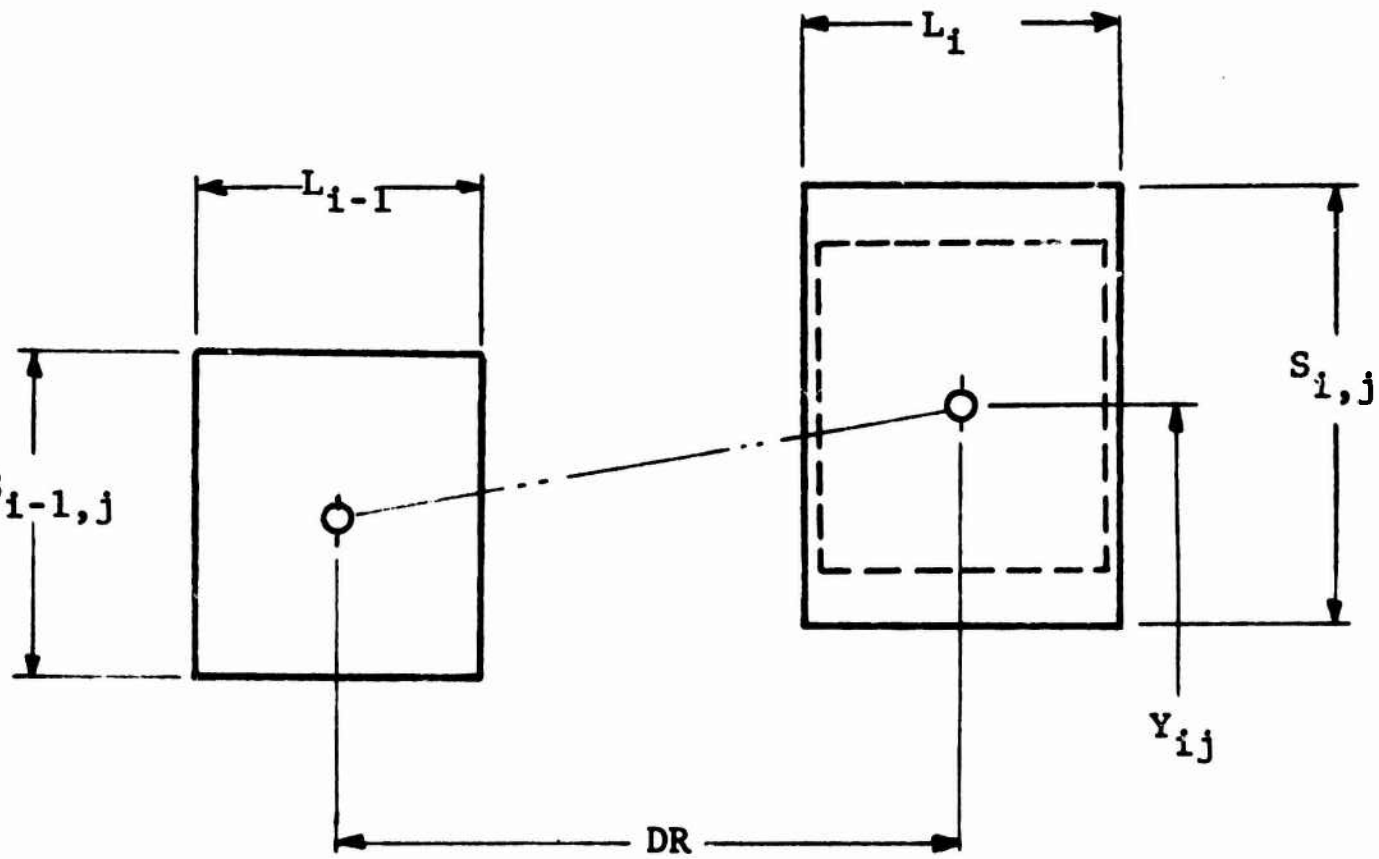

Figure 6.20 Cell Dilation

where

S = cell height and

L = cell length.

Differentiating, we obtain

$$\frac{dv}{v} = \frac{dS}{S} + \frac{dL}{L} .$$

For an isentropic expansion (the cause of the horizontal dilitation),

$$\frac{dL}{L} = - \frac{c_v}{c_p} \frac{dP}{P}$$

where c_v and c_p are the specific heats at constant volume and at constant pressure, respectively, and where P is the pressure. Thus, the vertical dilitation must be

$$\frac{dS}{S} = \frac{dv}{v} - \frac{dL}{L} .$$

But for a perfect gas,

$$\frac{dv}{v} = \frac{dT}{T} - \frac{dP}{P} .$$

Hence,

$$\frac{dS}{S} = \frac{dT}{T} + \left(\frac{c_v}{c_p} - 1 \right) \frac{dP}{P} . \qquad (6.49)$$

Equation 6.49 can now be rewritten as

$$S_i = S_{i-1} \left[1 + \frac{dT}{T} - \left(1 - \frac{c_v}{c_p} \right) \frac{dP}{P} \right] . \qquad (6.50)$$

The center height of the $j^{\underline{th}}$ cell (Y_{ij}) is given by summing over the appropriate cells as

$$Y_{ij} = Y_{i,j-1} + \frac{1}{2} (S_{ij} + S_{i,j-1}) \quad . \qquad (6.51)$$

The energy balance is then performed sequentially on each cell time or ij combination. The number of cells which must be treated depends upon the cell size and the overheight for which information is required. Two specific programs were written in FORTRAN IV based upon the above model.

One program deals with a uniform ground condition and includes erosion cutoff. This program follows a single air column and then adjusts the time scale to the observation time at the site. The temperature is computed at some fixed elevation Y by assuming a linear temperature variation between adjacent cell centers. The dust densities ρ_{ij} are for each cell and also are computed, since both the quantity of the dust in each cell and the volume of each cell is known. For example,

$$\rho_{ij} = \frac{w_{ij}}{S_{ij}} \quad . \qquad (6.52)$$

The dust density at some height Y is obtained by assuming a linear variation between cell centers.

The second program treats a biuniform ground condition, i.e., one in which two uniform ground conditions exist. The boundary between these zones is located a distance RC in front of the site. This code requires a considerably greater computational time since the temperature variation of many air columns must be evaluated. Some savings in computational time can be achieved by noting that (1) during the early portion of the problem the air columns passing the site have only swept past the one zone, hence, the uniform ground approach can be used, and (2) that a first portion of each air column solution in the two zone case is

identical to the preceding air column problem. These programs are presented in Appendix A. Some typical results which illustrate the nature of this phenomenon are presented in Figures 6.21 and 6.22. These figures show the temperature distribution in the air at various times. Initially, all of the air is heated to a uniform temperature by the passage of the shock wave. Then, as the hot soil is eroded and enters the air column, the air temperature over a portion of the column height increases significantly (see t = 0.02 and t = 0.13 sec). However, as the process continues, all of the hot soil has been eroded and the cooler dust begins to lower the temperature of the bottom portion of the air column (see t = 0.27 and 0.38 sec). Finally, at later times, the unheated dust (at the ambient temperature) enters the dust cloud and further cools the air. A very definite cooling or quenching phase does exist. The maximum air temperature at any height decreases with increasing height as indicated in Figure 6.21.

The results illustrated in Figure 6.22 are for the case where cutoff occurs at a time t = 0.39 sec. Once cutoff occurs the temperature at the lower portion of the air column begins to stabilize and the upward motion of the thermal pulse is considerably slowed. A comparison is made with the noncutoff case at t = 135 sec and indicates that a considerable difference occurs. The temperature distribution at t = 4.24 sec indicates that the heated air is undergoing a small change. It is important to note that the air-temperature model used herein assumes that the heated layer of air will not become unstable and break up during the time of interest. Obviously, the time required for the layer to become unstable will depend upon both temperature intensity and the magnitude of the horizontal and vertical temperature gradients in the air.

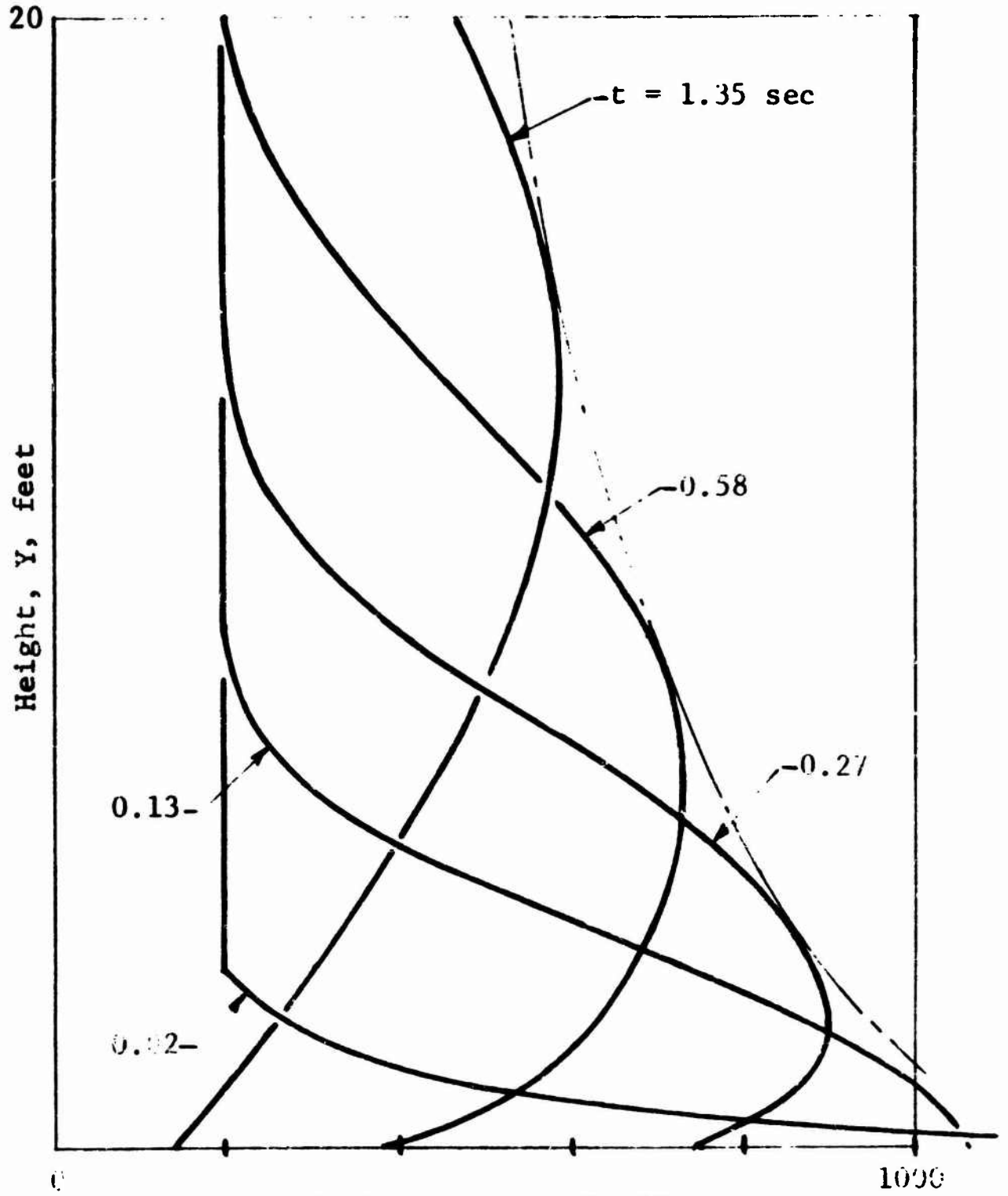

Figure 6.21 Vertical Temperature Distribution in Air Column

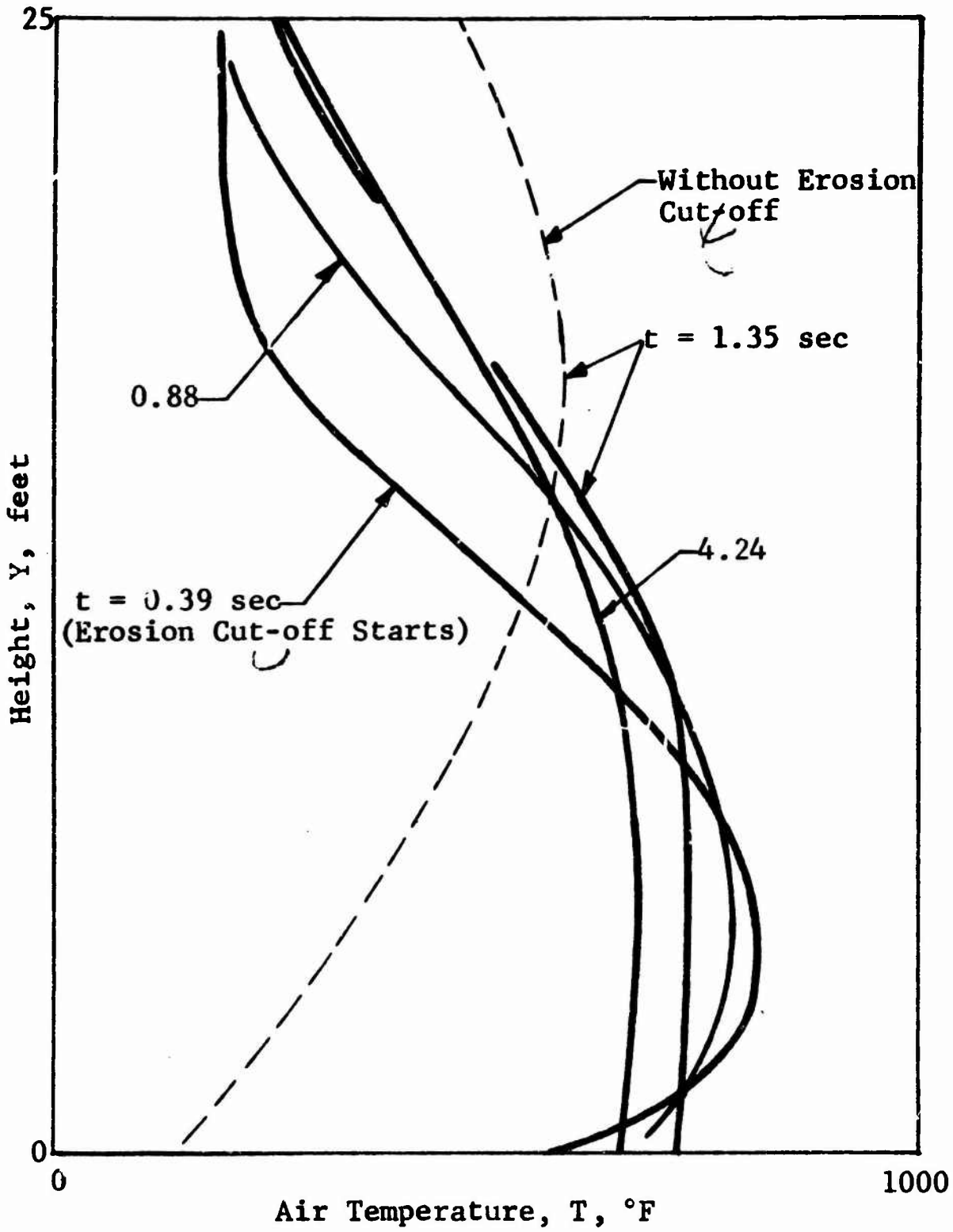

Figure 6.22 Vertical Temperature Distribution in Air Column with Erosion Cut-off

The temperature variation at a specific elevation is presented in Figure 6.23 for a typical problem. This figure presents the results for a variety of all sizes, or what is equivalent to a variety of heat transfer coefficients, as well as the temperature variation for the case of no dust. The air first experiences the shock heating and then the gradual cooling as the pressure field decays. When the dust reaches the elevation of interest the air temperature increases rapidly, reaching a peak, and then decays more gradually. The value of the heat transfer coefficient is not well defined and will be discussed in more detail in a later section of this chapter; however, it should be noted from the results presented in Figure 6.23 that this coefficient is an important variable--one which has a considerable amount of influence upon the peak temperature. In particular, the peak temperature is not approaching a stable value as the cell size is reduced.

6.5.3 Analytic Solution

As a result of the sensitivity of the peak air temperature to the value of the heat transfer coefficient or to the cell size, an investigation was made in an attempt to study the nature of the transport of the energy in the dust cloud. A simple problem was formulated in which all of the secondary effects were omitted. The problem studied was that of an impulsively induced wind eroding a uniform soil. The wind velocity is constant at a value of V_o, the soil temperature is uniform with depth at a value of T_o, and the initial air temperature is zero. Such a simple problem does not involve a characteristic dimension. Hence, it would be reasonable to expect that a similarity solution exists in which the air temperature is a function of a similarity variable, as

$$T(y,t) = T\ (y/t) \tag{6.53}$$

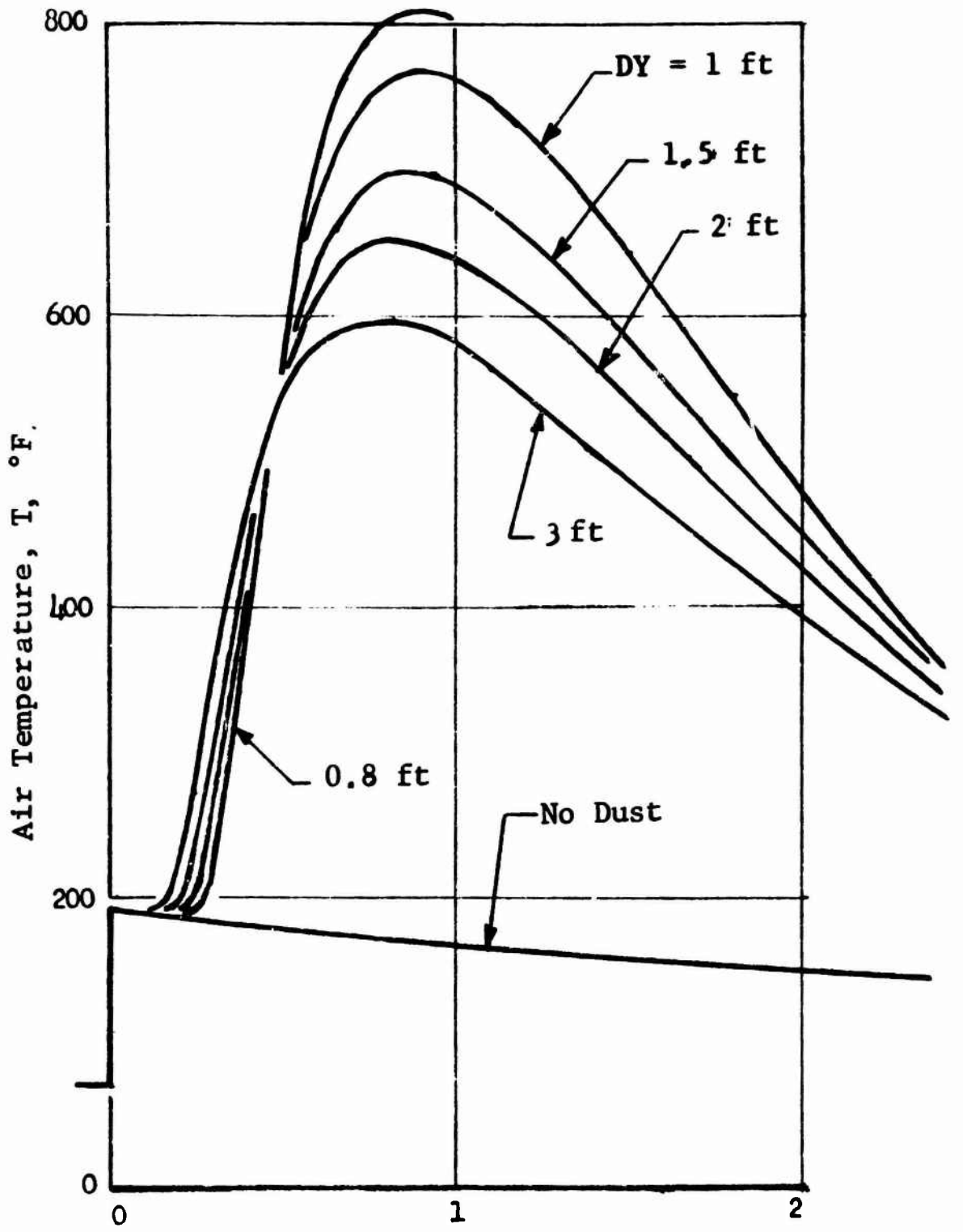

Figure 6.23 Influence of Cell Size

where

y = Lagrangian height above surface and

t = time.

Recall that the dust density is given by the similarity solution

$$\rho(\zeta) = \frac{a\rho_s^2}{K}\left[\zeta - 1 - \ln\zeta\right] \qquad (6.54)$$

where

$$\zeta = y/t \ .$$

Consider the differential element dy (illustrated in Figure 6.24). The net mass flux of dust into the cell equals the rate of increase of dust in the cell; for example,

$$\frac{\partial w'}{\partial y}\, dy = -\frac{\partial w}{\partial t} \qquad (6.55)$$

where

w = weight of dust and

w' = weight flux of dust.

Similarly, an energy balance yields

$$-cw'\frac{\partial T}{\partial y}\, dy - c\frac{\partial w'}{\partial y}\, T\, dy = \frac{\partial E}{\partial t}\ , \qquad (6.56)$$

where

$$E = (wc + \hat{w}\hat{c})\, T, \qquad (6.57)$$

and

$\hat{w}$ = weight of air in differential element, and

$\hat{c}$ = specific heat at constant pressure of air.

Using Equations 6.55 and 6.57, we can rewrite Equation 6.56 as

$$\frac{\partial T}{\partial t} = -\left[\frac{cw'}{cw + cw}\right]\frac{\partial T}{\partial y}\, dy\ ,$$

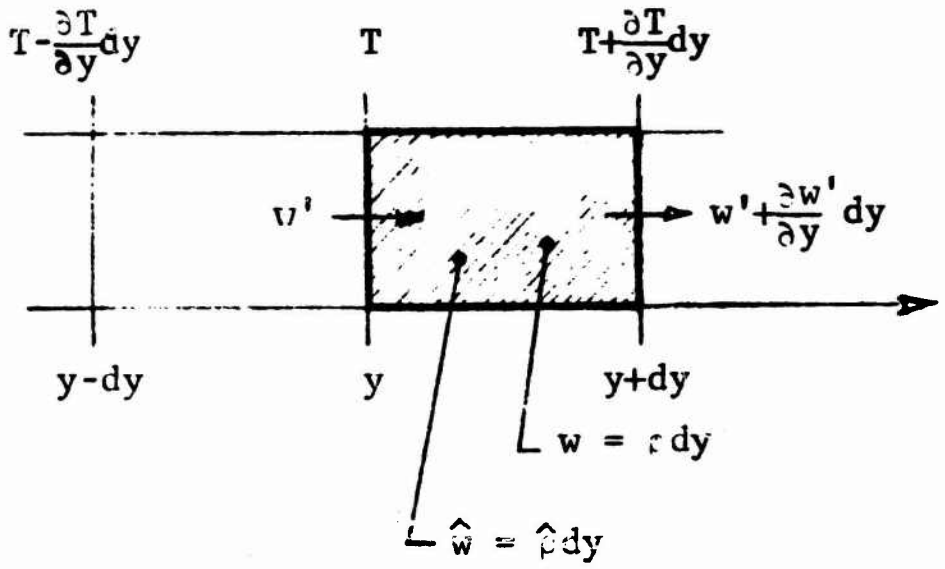

Figure 6.24 Differential Element

since

$w = \rho dy$ and

$w = \rho dy$;

where

ρ = dust density and

ρ_o = air density.

The energy equation then becomes

$$\frac{\partial T}{\partial t} = -\left[\frac{cw'}{\rho c + \rho_o c}\right]\frac{\partial T}{\partial y} \ . \qquad (6.58)$$

The quantity w' can be derived from the dust density distribution illustrated in Figure 6.25. The weight of dust W_1 above a height y_1 is

$$W_1 = \int_{y_1}^{H} \rho dy = H \int_{\zeta_1}^{1} \rho d\zeta \ , \qquad (6.59)$$

which upon integration becomes

$$W_1 = \frac{2H\rho_s a}{K}\left[\frac{1}{2} - \frac{\zeta_1^2}{2} + \zeta_1 \ln \zeta_1\right] \ . \qquad (6.60)$$

The total amount of dust raised W_o is

$$W_o = \frac{H\rho_s a}{K} = V_o t \rho_s a \ . \qquad (6.61)$$

However, since

$$w' = \frac{dW_1}{dt} \ ,$$

we obtain

$$w' = V_o \rho_s a \ (1 - \zeta)^2 \qquad (6.62)$$

where ζ_1 has been set equal to ζ. The differential form of

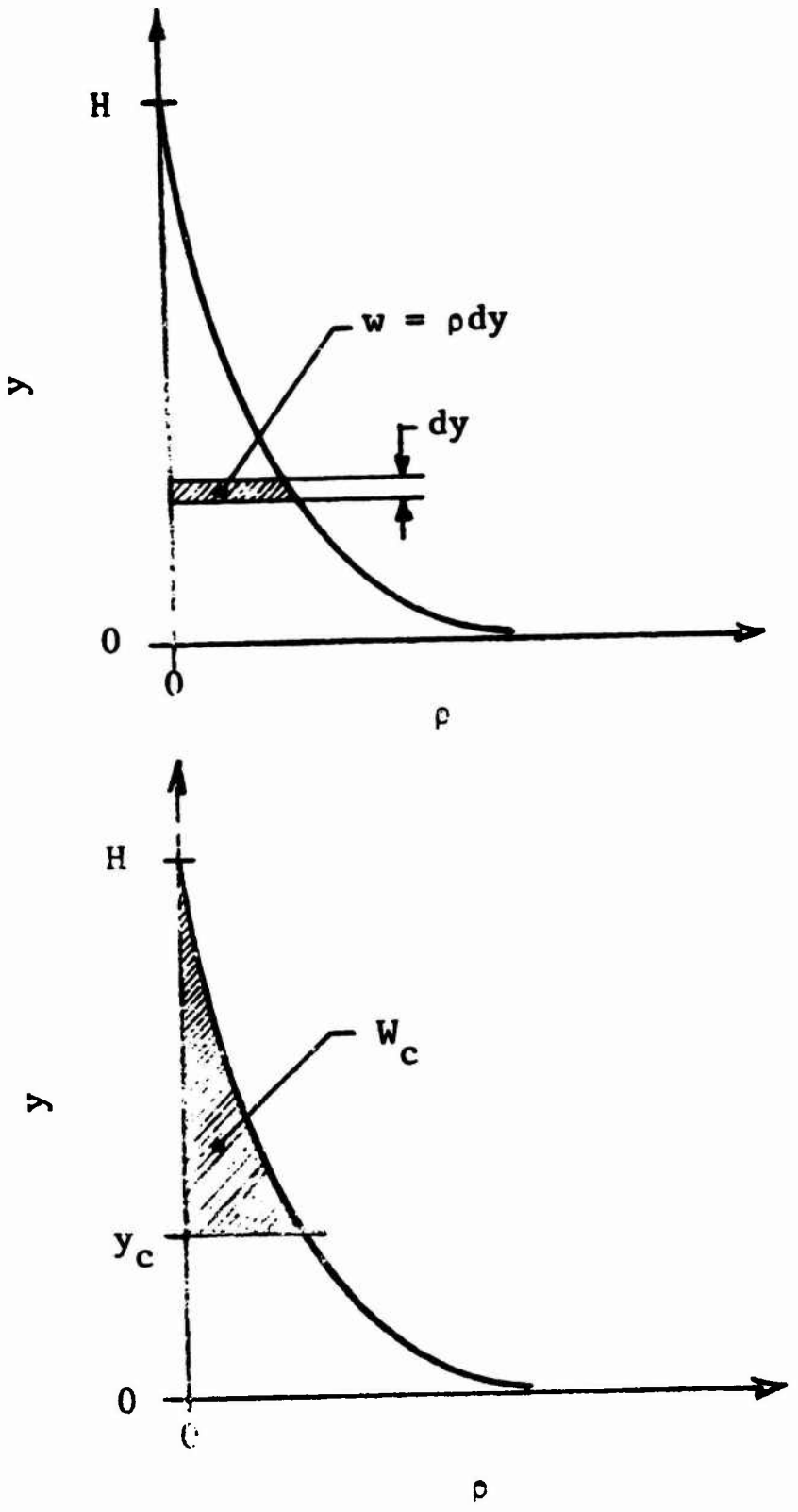

Figure 6.25 Dust Density Distribution

the energy equation (Equation 6.58) can now be rewritten as

$$\frac{\partial T}{\partial t} = - KV_o G(\zeta) \frac{\partial T}{\partial y} \tag{6.63}$$

where

$$G(\zeta) = \frac{(1 - \zeta)^2}{B+2(\zeta - 1 - \ln \zeta)} \tag{6.64a}$$

and

$$B = \frac{\rho cK}{\rho_s ca} . \tag{6.64b}$$

Equation 6.63 does not satisfy the conditions for a similarity solution except in the trivial case where both $\partial T/\partial t$ and $\partial T/\partial y$ vanish. Therefore we must consider the possibility of a discontinuous temperature field. This idealized problem was programmed; however, since the computation starts with a single cell, the temperature distribution is initially uniform. We can only expect that the similarity solution would evolve from this starting procedure. The results of this calculation are presented in Figure 6.26 and clearly demonstrate that, as the number of time steps N becomes large, the temperature distribution approaches a discontinuity at the normalized height $\zeta_1 \cong 0.9$ for this particular example.

If we examine the function $G(\zeta)$ we note that it has a maximum at approximately $\zeta = \zeta_1$ (see Figure 6.28). The function $G(\zeta)$ is the ratio of energy influx to the cell to the thermal capacity of the cell. Differentiating Equation 6.64a results in a relation for the location of the temperature discontinuity $\zeta = \zeta_c$ of

$$1 = B\zeta_c + \zeta_c^2 - 2\zeta_c \ln \zeta_c . \tag{6.65}$$

The similarity solution is illustrated in Figure 6.27.

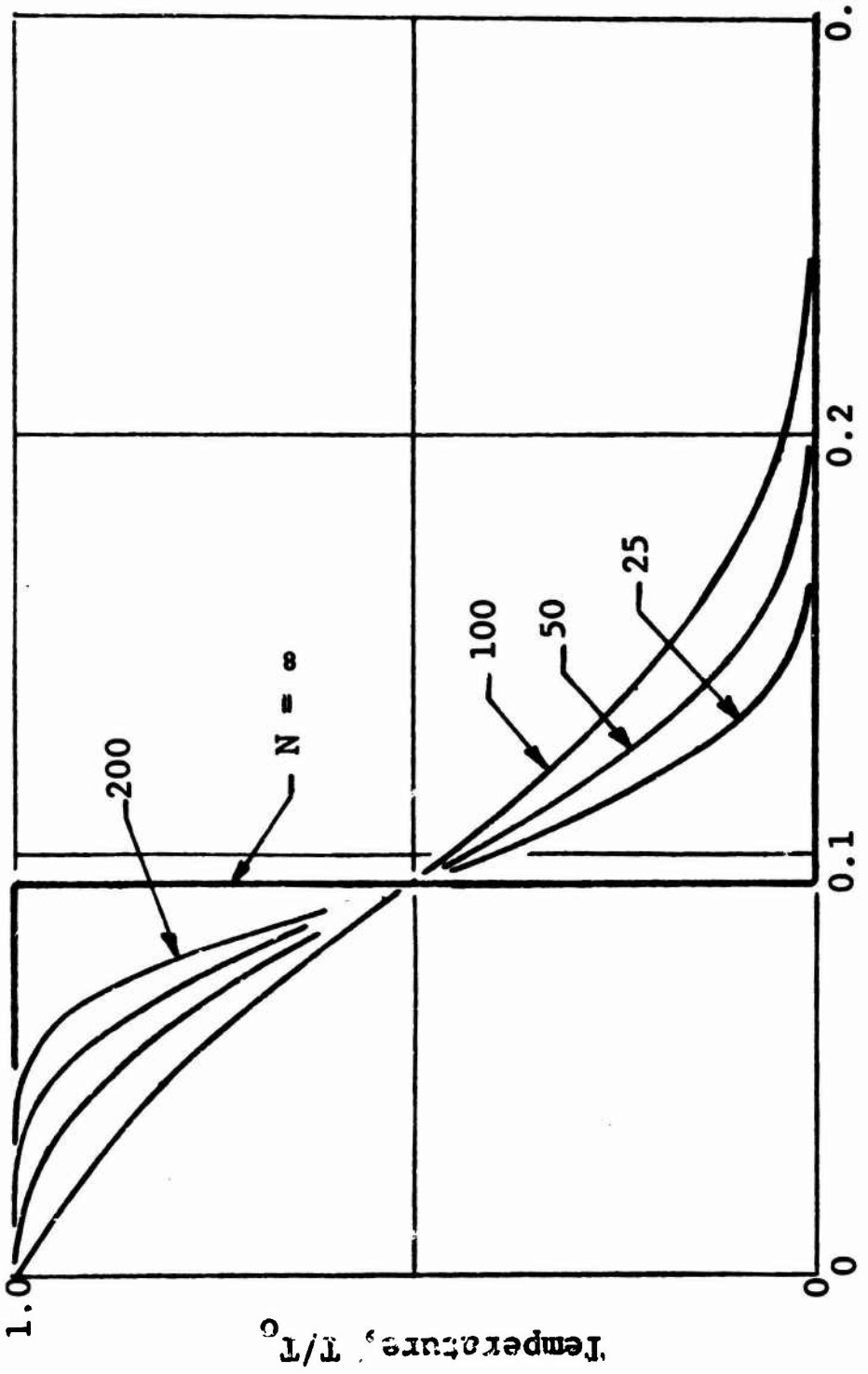

Figure 6.26 Temperature Variation with Computational Increment

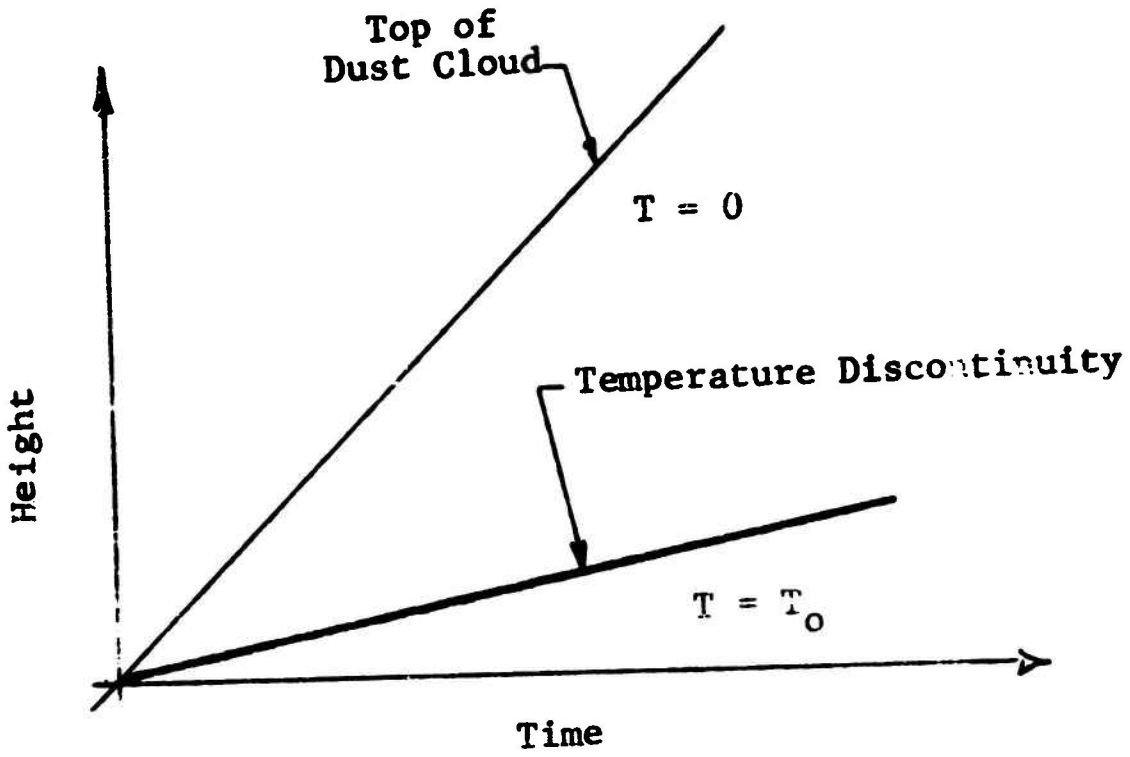

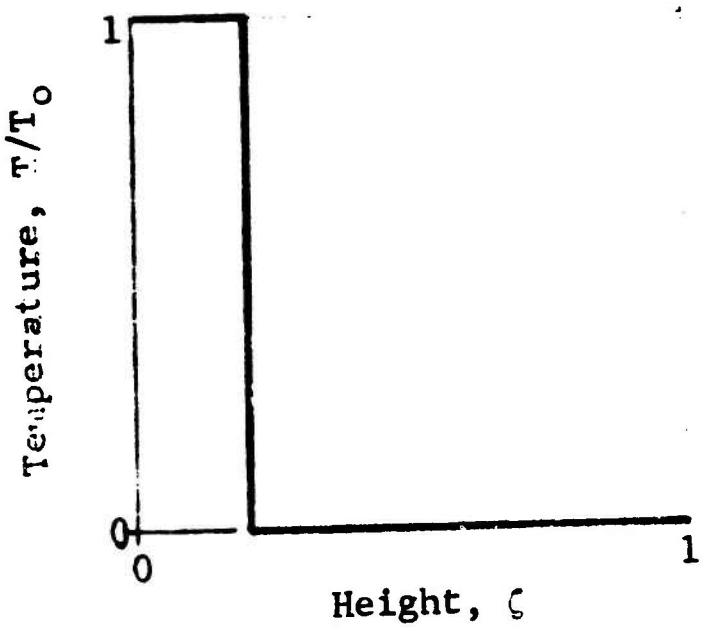

Figure 6.27 Similarity Solution for Temperature Field

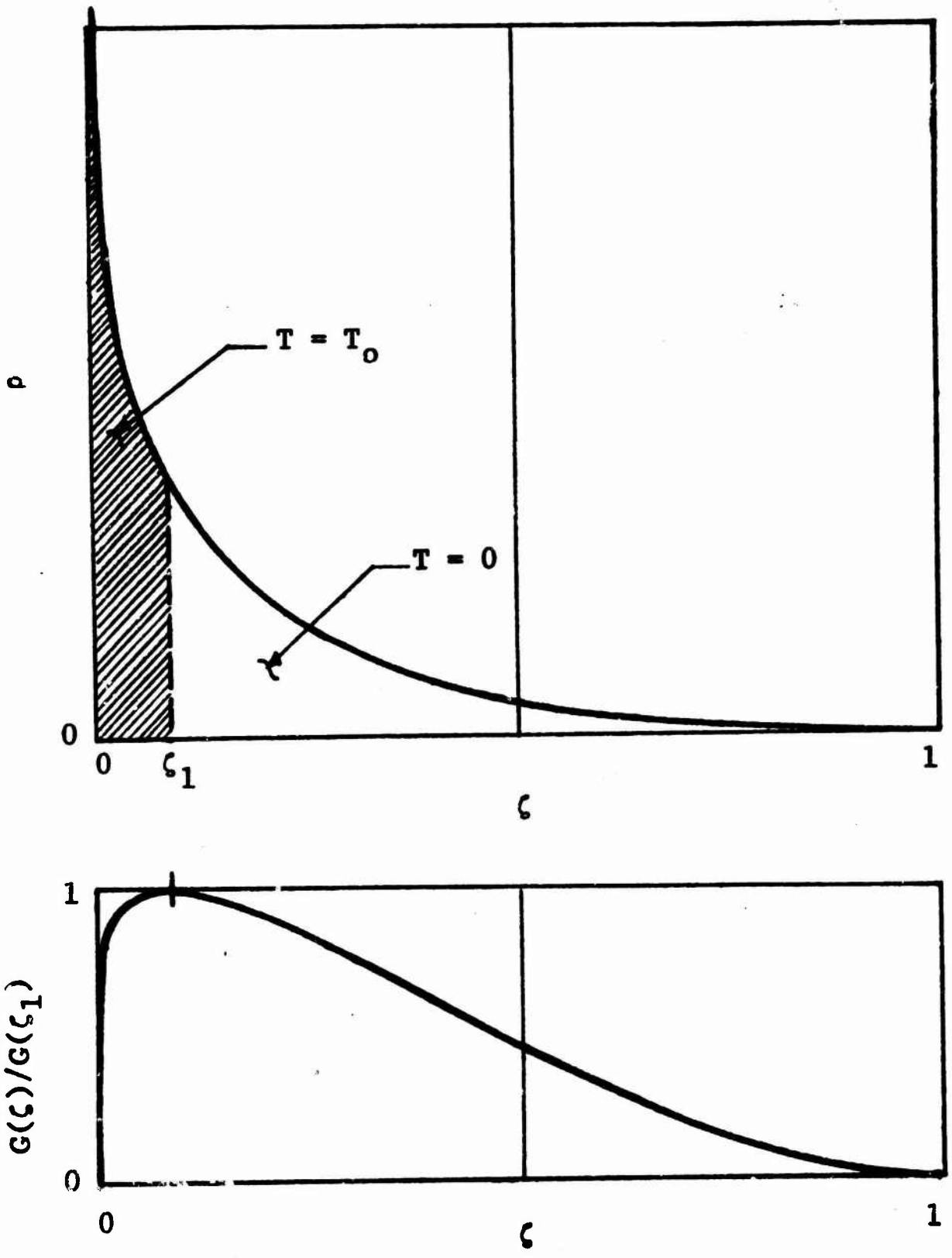

Figure 6.28 Characteristic of G(ζ)

The above solution can be verified by applying the overall energy equation to the system. That is,

$$cT_o W_o = \int_0^1 \left[c\rho(\zeta) + c\dot{\rho} \right] T(\zeta)\, d\zeta \ . \qquad (6.66)$$

By letting

$$T(\zeta) = T_o \qquad 0 \geq \zeta \geq \zeta_c$$

and

$$T(\zeta) = 0 \qquad \zeta_c \geq \zeta \geq 1,$$

Equation 6.65 is confirmed.

The air temperature can be expected to reach or approach the maximum soil temperature if the heat transfer coefficient is very high. Thus, the results illustrated in Figure 6.23 are confirmed and the limits have been established.

6.5.4 Heat Transfer Coefficient

The air temperature model contains only one coefficient which must be evaluated. This is the heat transfer coefficient for natural convection between the small irregularly shaped soil particles and the surrounding air. This coefficient is used to evaluate an energy exchange response time t_e which, in turn, is used to evaluate a cell size. There are other coefficients involved in the overall model. These coefficients have all been discussed and evaluated in the preceding chapter.

Heat transfer data which are pertinent to this problem are both sparse and unreliable. Data exist on simple shapes such as spheres and horizontal cylinders;[6.3] however, these data are generally restricted to objects whose dimensions are of the order of inches in size. There are some data on fine horizontal wires.

The natural convection phenomenon can be analyzed in terms of three dimensionless groups. These are:

Nusselt's Number = hD/k,

Grashof's Number = $D^3\rho^2\beta T/\mu^2$,

and

Prandtl's Number = $c\mu/k$

where

D = diameter,
h = heat transfer coefficient,
k = themal conductivity of air,
ρ = density of air,
μ = viscosity of air,
β = coefficient of thermal expansion for air,
T = temperature difference, and
c = specific heat of air

Experimental data for horizontal cylinders (and wires) have been obtained for a variety of fluids and fluid properties. Thus, the interrelationship between these three dimensionless groups has been established for most engineering applications.

For objects of the order of inches in size, the heat transfer coefficient is proportional to the one-fourth root of the size. As the size decreases, however, the dependence approaches an inverse proportionality. Due to the strong dependence of the Grashof number on the diameter, the current problem falls in a range where little data exist. Because of this lack of pertinent data, an experimental program was designed and conducted to determine the dependence of the heat transfer coefficient for natural convection on the size of typical soil particles. The results of this experiment are reported in Appendix E.

The value of the heat transfer coefficient as a function of particle size is presented in Figure 6.29. The smaller the particle size, the larger the value of the heat

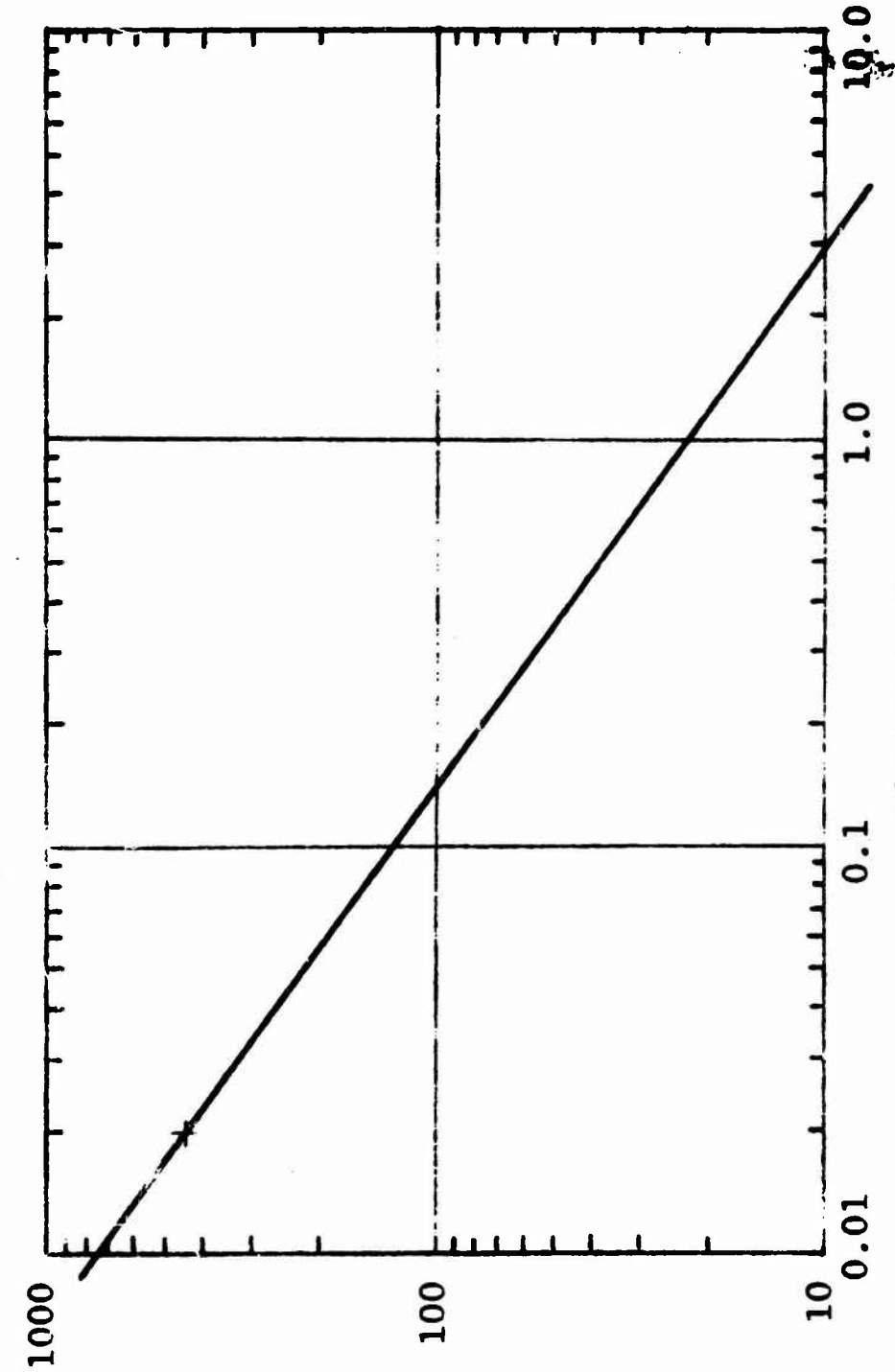

Figure 6.29 Heat Transfer Coefficient for Soil Particles

transfer coefficient. If a mixture of particle sizes was used then the effective value of the heat transfer coefficient appeared to be that associated with the average particle size. Since, in general, soils are composed of a mixture of particle sizes, it was necessary to examine the size distribution curve and select some mean size. For many of the typical soils of interest this mean size is approximately 20 microns in diameter. The value of the heat transfer coefficient for this size is 420 Btu/ft^2-hr-°F.

The energy exchange or heat transfer response time is related to the heat transfer coefficient by the relation:

$$t_e = 3\left[\frac{\rho_c c_p D}{6h}\right] \quad . \tag{6.67}$$

The term enclosed in the brackets is the exponential time constant associated with the transient heat transfer process and the factor 3 is a multiplier that corresponds to the transfer of 95 percent of the thermal energy from the soil particle to the air. The 95 percent criterion is an arbitrary criterion that could be modified if desired. The heat transfer response time corresponding to the 20-micron size particle was approximately 8.5 milliseconds. A nominal value of 10 milliseconds is suggested for the heat transfer response time for those problems where special soil conditions do not exist.

6.5.5 Stability of the Heated Air Layer

The air near the ground surface is heated and then cooled by the passage of dust through this region. In general, the horizontal temperature gradients are small and the transient temperature field is one-dimensional in structure. The heated air near the surface is bounded above and below by cooler air and represents an unstable or metastable configuration. The hot air tends to rise due to local buoyancy

forces, although the migration of dust through this region continuously alters the temperature distribution, hence the buoyancy force distribution. The buoyancy forces are large initially, but decrease rapidly. It is necessary, therefore, to determine whether the predicted temperature fields are stable or whether the buoyancy forces overturn the unstable air locally and grossly change the temperature distribution. This subsection discusses the buoyancy problem and develops and approximate criterion for evaluating the stability of the heated air layer. Suggestions are then made for modifying the temperature distribution when overturning occurs.

The local thermal and displacement field is very complex since it involves not only the exchange of thermal energy between the dust and the air but also the motion of the dust or soil particles. The motion of the dust is postulated to move vertically with respect to the air and the air is restricted to move horizontally. The overturning of the resultant heated air layer necessitates the introduction of simultaneous horizontal and vertical motion of both the dust and the air, and greatly increases the complexity of any analysis that can be used to evaluate the stability problem.

Because similar stability problems occur in the field of meterology, the pertinent literature was reviewed. The convection process involving the two-dimensional nonsteady motion of heated masses of air and the formation or development of water vapor clouds have been reviewed[6.10,6.11] and appear to occur at a variety of size scales and involve a number of discrete phenomena. Numerical methods[6.12] have been developed for computing the motion of the air in some cases. These computational efforts are very large and, therefore, expensive, and are greatly limited by frequent numerical instability problems. These specific methods

are not directly applicable to the dust-ladened heated air problem and a very sizable development effort would be necessary to establish a realistic computer program for the dust problem.

The heated air layers are unquestionably unstable in many situations and a number of local effects will always exist that will result in small pertubations which, in turn, will trigger the overturning process. It is necessary that the time or duration needed for this overturning process be established and then compared with that time interval during which a specific unstable temperature distribution exists. If the overturning duration is greater by some margin, then the preheated air temperature distribution will change to a new distribution in accordance with the air temperature model. On the other hand, if the overturning duration is smaller, then we can expect that the heated air layer will overturn and mix with the surrounding air. The resulting air temperature distribution will be much more uniform and a more stable configuration will result. The scale of mixing cannot be readily established, however engineering estimates that are suitable for this program can be made.

Typically, the vertical air temperature distribution at specific times will be similar to those presented in Figure 6.21 and the temperature variation at a nominal elevation will be similar to that presented in Figure 6.23. If erosion cutoff occurs, then the temperature distribution will be much more uniform over the lower portion of the air region (Figure 6.22). For near-overhead burst situations, the air temperature increases much more slowly than indicated, and high temperatures may persist for periods between five and ten seconds. We might expect that overturning would occur in these cases.

The buoyancy force F_b for a mass of heated air is

$$F_b = \rho\beta\frac{\theta}{2} \tag{6.68}$$

where

ρ = mean air density

β = coefficient of expansion $= \frac{1}{T}$ for perfect gas

T = absolute temperature

θ = temperature difference.

The mass involved will include both the mass of the air and the mass of the airborne dust. The critical acceleration a of this region of heated air will be

$$a = \frac{gF_b}{\rho + \rho_d} = \frac{\rho\beta g\theta}{2(\rho + \rho_d)} . \tag{6.69}$$

The temperature difference θ will exist over some vertical height L and the overturning process will be well developed when the air mass has been displaced this distance. The buoyancy force will decay during the overturning process and the mean acceleration will be somewhat lower than the initial acceleration. A factor of one-half has been introduced as a multiplier of the initial acceleration to compensate approximately for the reduction of the driving force as well as for the increase in mass which will occur due to air entrainment and wake effects. The time t_s required for the mass of air to be displaced distance L is then

$$t_s = \sqrt{\frac{8L(\rho + \rho_d)}{\rho\beta g\theta}} . \tag{6.70}$$

The dust and air density variation as well as the air temperature distribution with vertical height are illustrated in Figure 6.30 for a rather typical situation. The temperature difference is approximately 300°F and occurs over a distance of approximately 20 ft. The dust and air density vary somewhat over this region but the use of average values in Equation (6.70) yields an estimate of the overturning time as

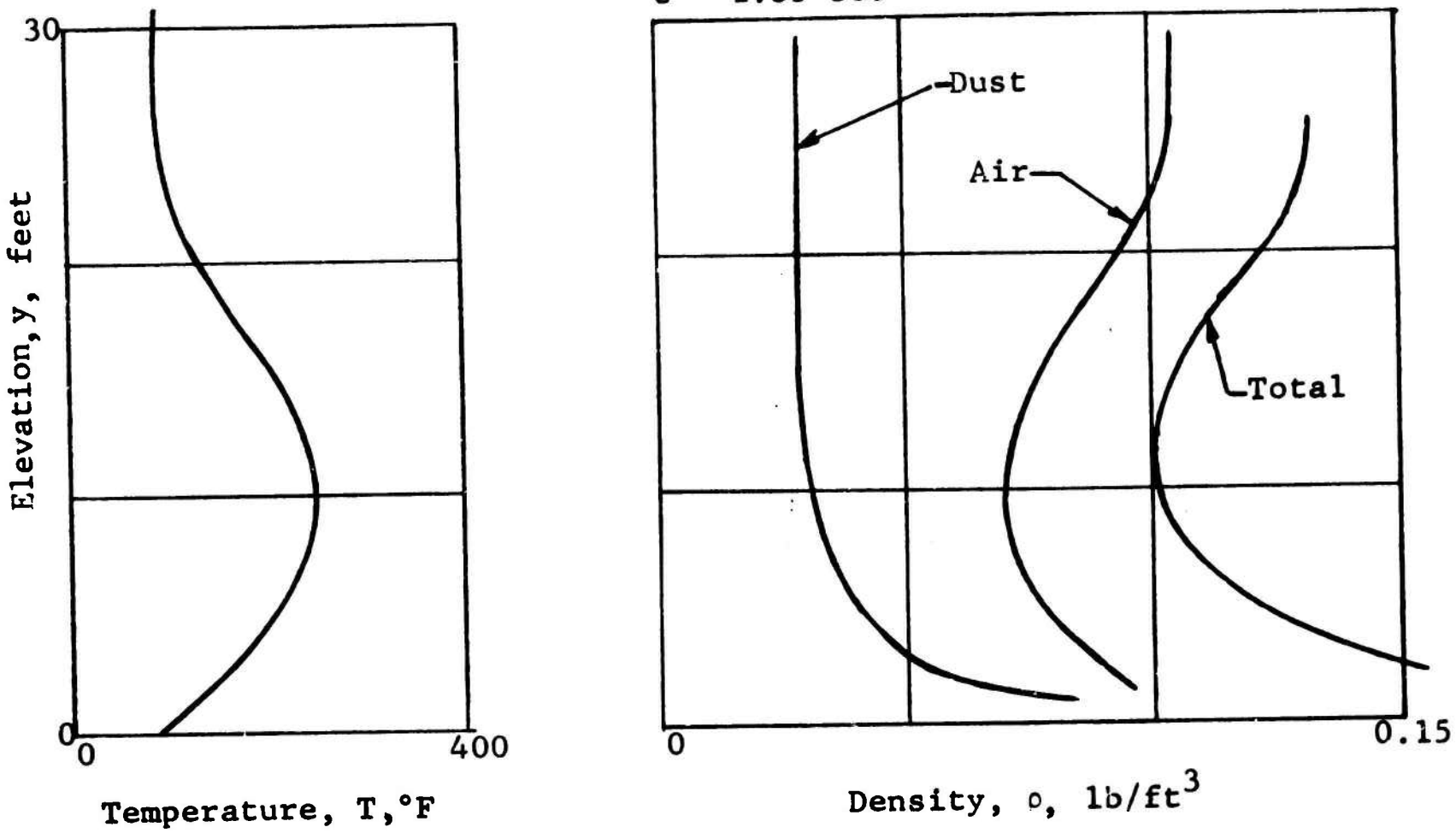

Figure 6.30 Buoyancy Forces in Heated Air Layer

approximately 5 seconds. The temperature transient for this particular case lasts for approximately one second and is, therefore, stable.

In those cases where overturning occurs the heated air has mixed with cooler air, and the region originally filled by the heated air is occupied by air from the surrounding region. The temperature distribution cannot be well established; however, by conserving the overall energy of the system, one can assume that the air temperature in that particular region will be equal to the average temperature over a region two to three times as large as the original region. The following approximate procedure is suggested:

(1) Examine temperature distribution at time t and evaluate overturning time, t_s.

(2) Examine temperature distribution at a time t_s later

if (a) the temperature distribution has changed to a more stable distribution, the process is stable

if (b) the temperature distribution is approximately the same or more unstable, then overturning will occur. If so proceed.

(3) Determine average temperature over a vertical height 3L surround the heated region. This is the adjusted temperature at time $t + t_s$.

If the adjusted temperature is rather high, then the process can be repeated using a large initial region, say 2L, and determining an adjusted temperature at a later time.

6.6 Air-Temperature Environment

A series of calculations was made in order to evaluate the air-temperature environment and to determine the sensitivity of the environment to some of the many variables of the problem. A reference set of variable values was selected as a basis for comparison.

The weapons effect variables were held constant, using a large weapon detonated at an optimum height of burst, for a typical overpressure level. The remaining variables and their reference values are presented in Table 6.3.

The influence of the heat transfer response time is presented in Figure 6.31. It should be noted that as the response time decreases, the peak temperature increases rapidly. This aspect of the problem was discussed in Section 6.5.3. These results demonstrate the importance of using the correct value for this variable. Since value is uncertain, it would appear that some experimental effort should be expended in order to reduce the indicated uncertainty of the peak air temperature.

The influence of a variation in the value of the transport coefficient is presented in Figure 6.32. Clearly the reference value used is adequate for the current design calculations. Figure 6.33 illustrates the influence of the elevation. The value of this design variable will of course be known; however, it should be noted that rather strong vertical gradients do exist in this general height.

The influence of the value of the land use factor is, as expected, important. This is demonstrated in Figure 6.34. Thus, specific site evaluation becomes an important factor if any credit for this effect is to be utilized in the design of the dust and air-temperature conditioning equipment.

Another site variable which has a significant influence on the air temperature is the erosion cutoff depth. Figure 6.35 demonstrates the variations which will occur due to the value of this variable. The worst case calculated is for an erosion cutoff occurring at a depth of 0.5 inch. This depth corresponds approximately to the overall

Table 6.3 REFERENCE VALUES OF AIR-TEMPERATURE VARIABLES

Variable	Reference Values
Heat Transfer Response Time (TM)	15 ms
Transport Coefficient (K)	0.20
Erosion Coefficient (A)	6×10^{-5}
Elevation (Y)	15 ft
Land Use Factor (UF)	0.5
Erosion Depth Cutoff (ZM)	2.0 in.
Bulk Density of Soil (RHOTOT)	100 lb/ft^3
Density of Dust Particles (RHO)	160 lb/ft^3
Particle Specific Heat (C)	0.20 Btu/lb
Soil Conductivity (FK)	0.1 Btu/ft-hr-°F
Soil Diffusivity (ALPHA)	0.007 ft^2/hr
Ambient Air Temperature (TEMPA)	70°F
Ambient Air Pressure (PRESA)	14.7 psia

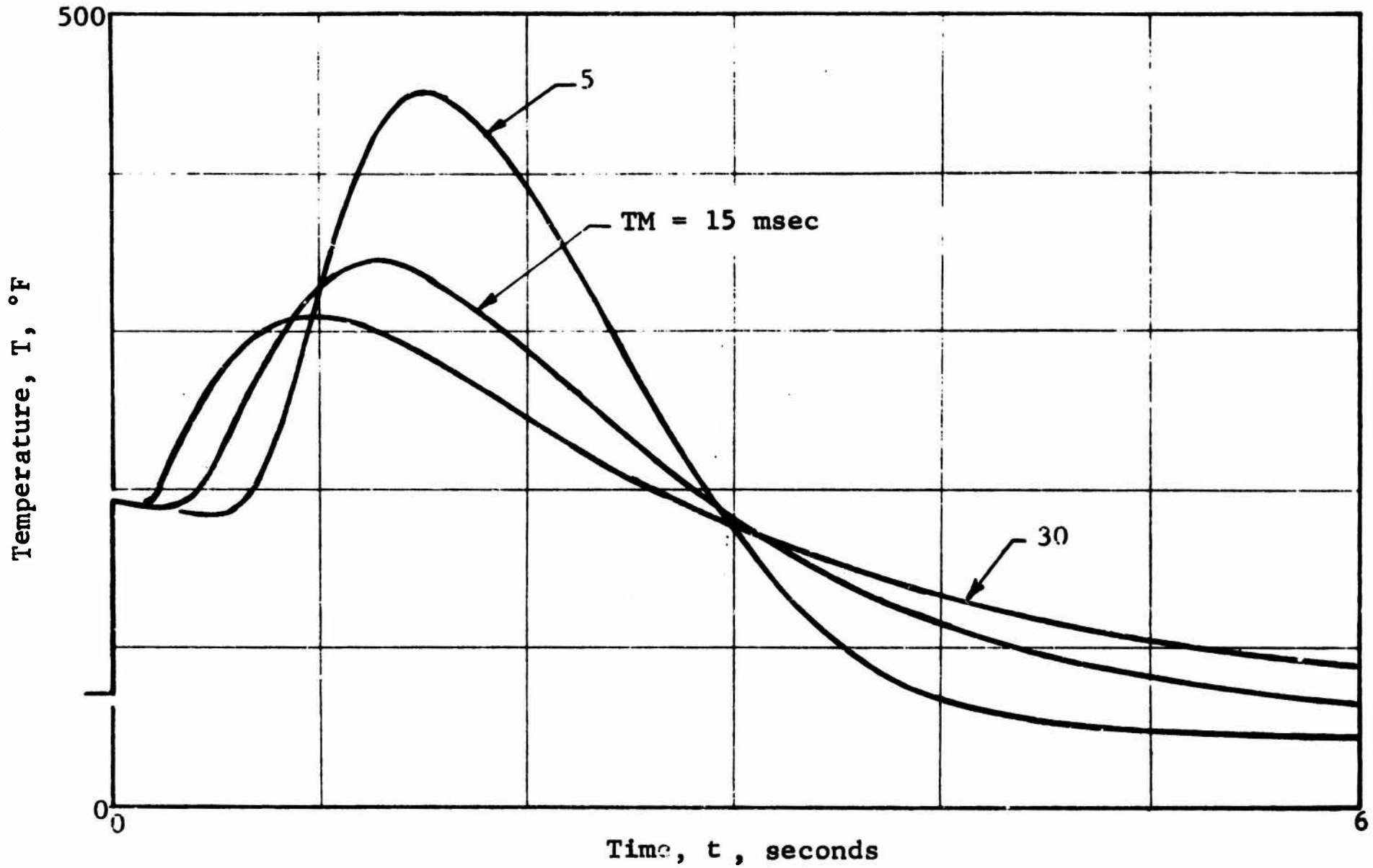

Figure 6.31 Influence of Heat Transfer Response Time

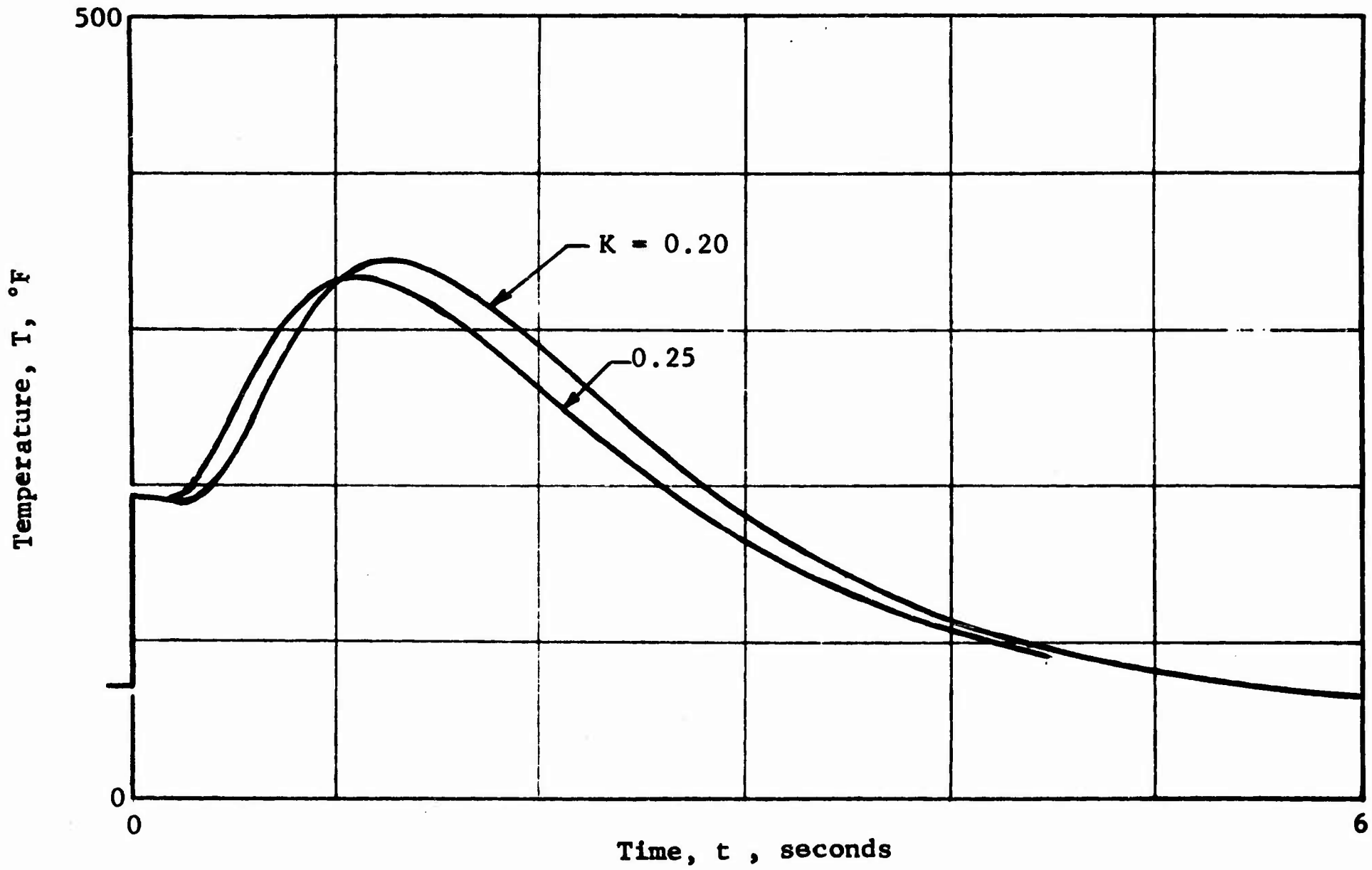

Figure 6.32 Influence of Transport Coefficient

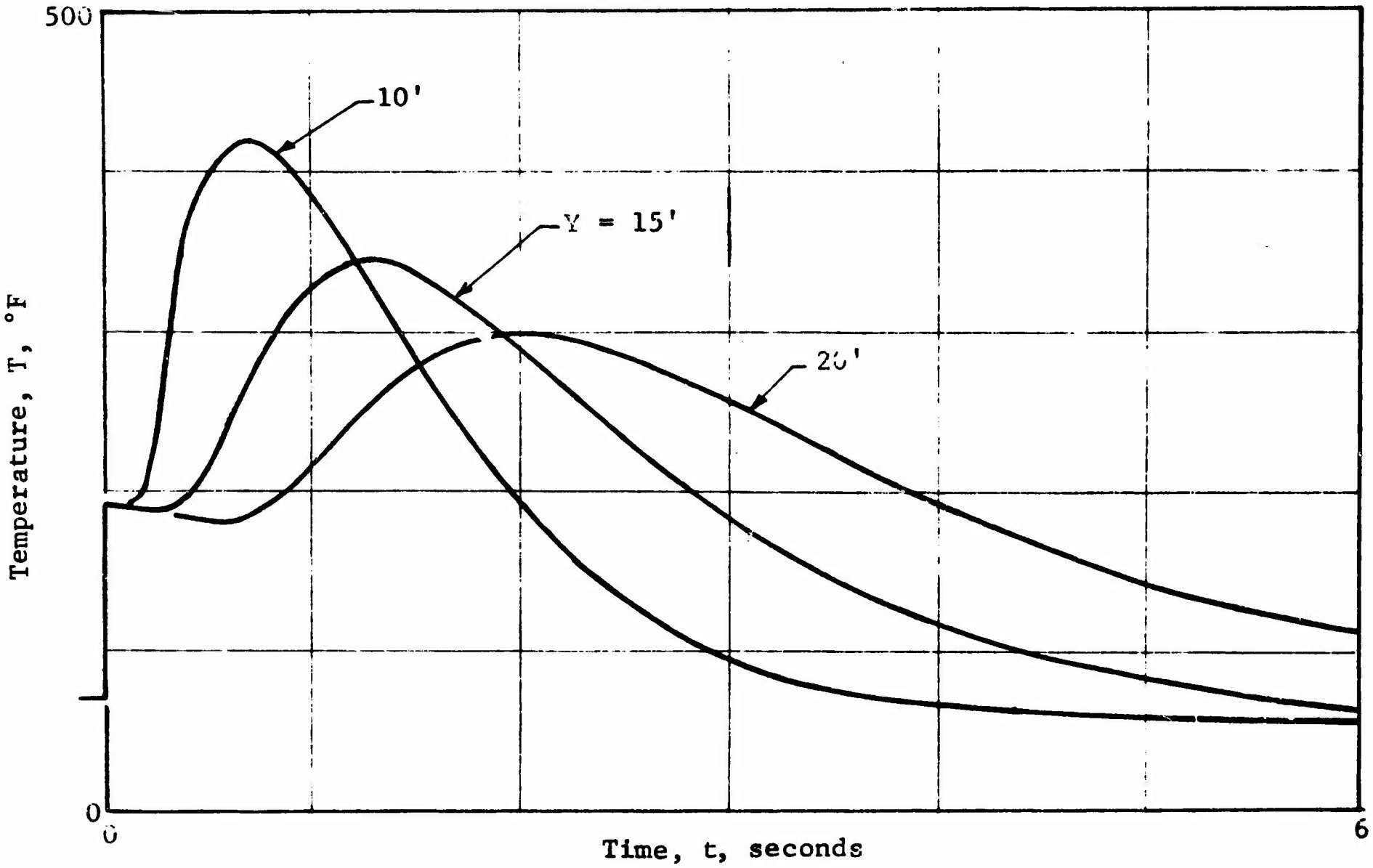

Figure 6.33 Influence of Elevation Above Ground

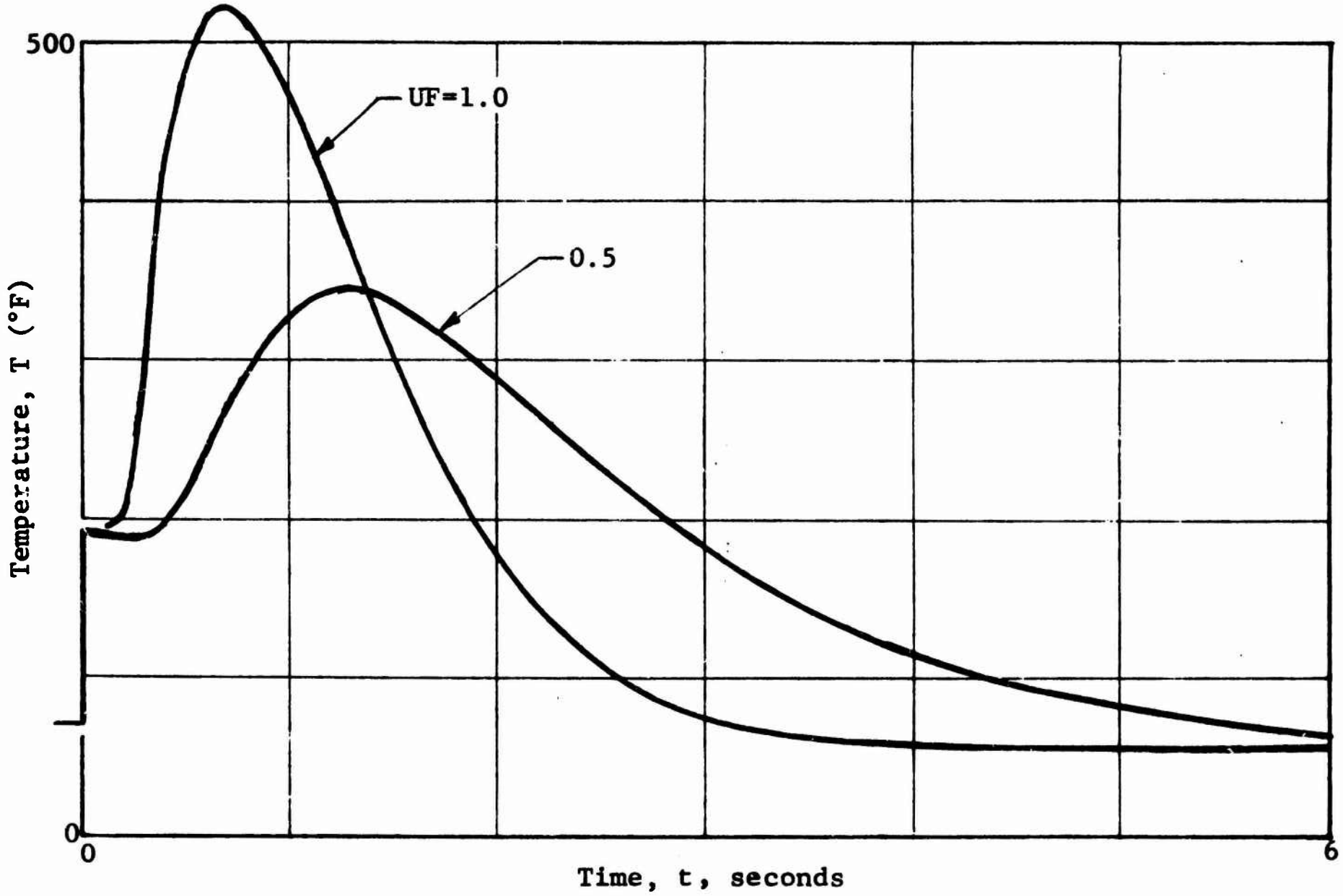

Figure 6.34 Influence of Land Use Factor

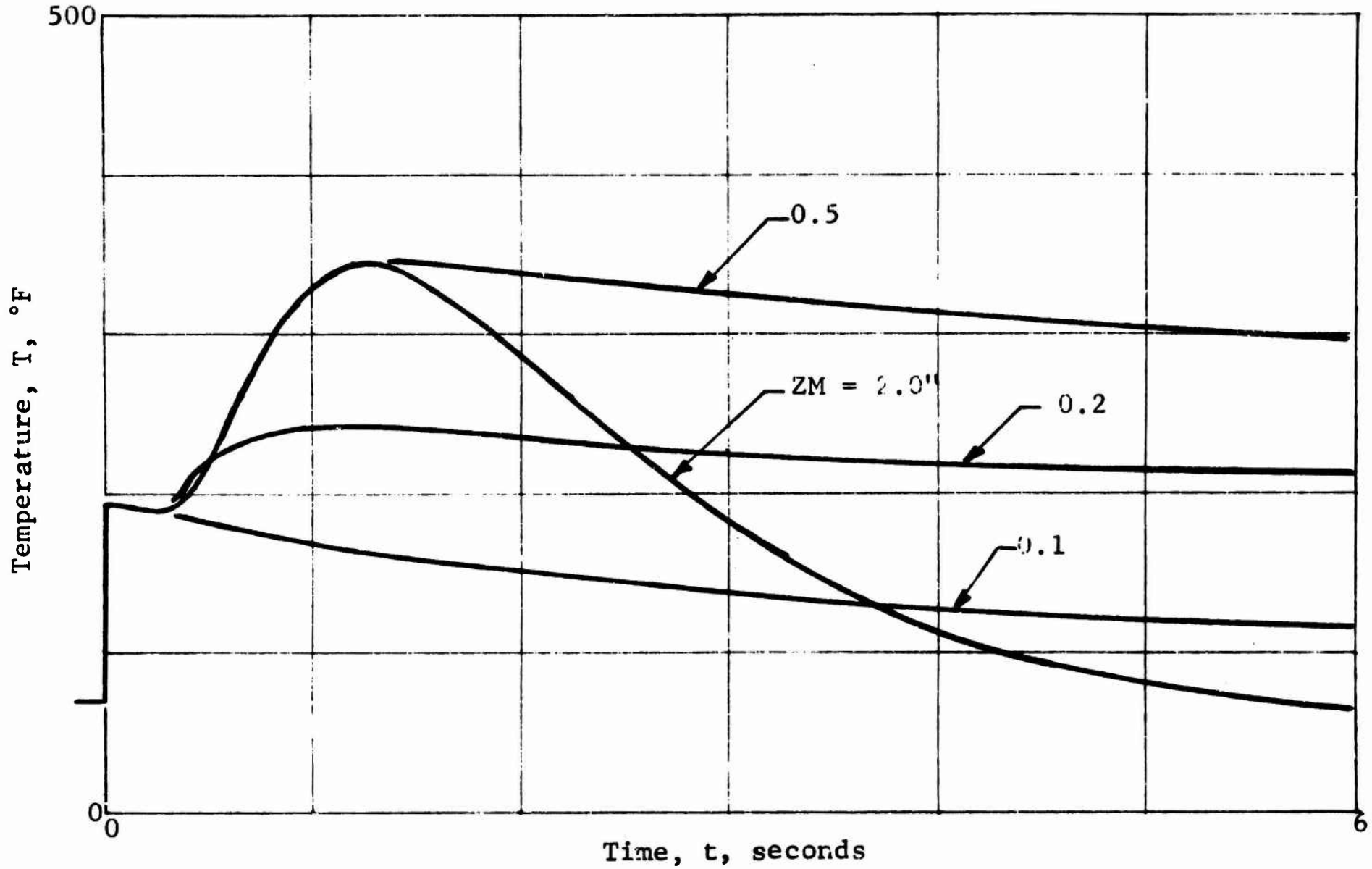

Figure 6.35 Influence of Erosion Cut-off Depth

depth in which the thermal energy absorbed by the soil is distributed. Additional erosion introduces cold dust into the air and a significant amount of cooling occurs. On the other hand, if the cutoff depth is low (say at 0.2 in.), all of the thermal energy is not raised by the dust cloud and a lower peak temperature thus exists. The temperature does, however, remain near its peak value for some time.

A series of calculations was made in which the value of the thermal absorption coefficient was varied. These results are tabulated in Table 6.4 and apply to the case where the dust cloud is (1) very opaque, (2) opaque, and (3) very transparent. A value of 0.01 lb/ft^3 is used for the current model. For a very opaque dust cloud, the thermal energy incident on the cloud is deposited in a narrow zone near the top of the cloud; hence, a small temperature rise occurs early. For a very transparent cloud, the thermal energy is always deposited near the ground surface and the temperature at late times somewhat increases. The intermediate case behaves much like the very opaque case where the late time energy absorbed by the overall cloud is not felt at the lower reaches of the cloud. In each case, the influence of the thermal radiation absorbed by the cloud on the air temperature at the heights of interest is small. This is due to the fact that the rate of the energy being introduced into the cloud by direct thermal radiation is small, compared to the rate at which energy is being introduced by the erosion process. In the case illustrated, the ratio of these energies is approximately 100 to 1.

The influence of the thermal properties of the soil on the air temperature was investigated using the soil property values indicated in Section 6.3. These results are presented in Figure 6.36 and the curves are identified by the letters a, b, and c, as before. The curve identified by

Table 6.4 INFLUENCE OF ABSORPTION COEFFICIENT ON AIR TEMPERATURE

Time, sec	Temperature (°F) at Absorption Coefficient of 0.0004 psf	0.04 psf	4.00 psf
0.000	193.0	193.0	193.0
0.104	193.2	192.4	190.4
0.213	192.2	200.8	197.7
0.329	286.1	288.4	294.1
0.450	439.4	441.4	453.6
0.579	548.4	549.9	564.5

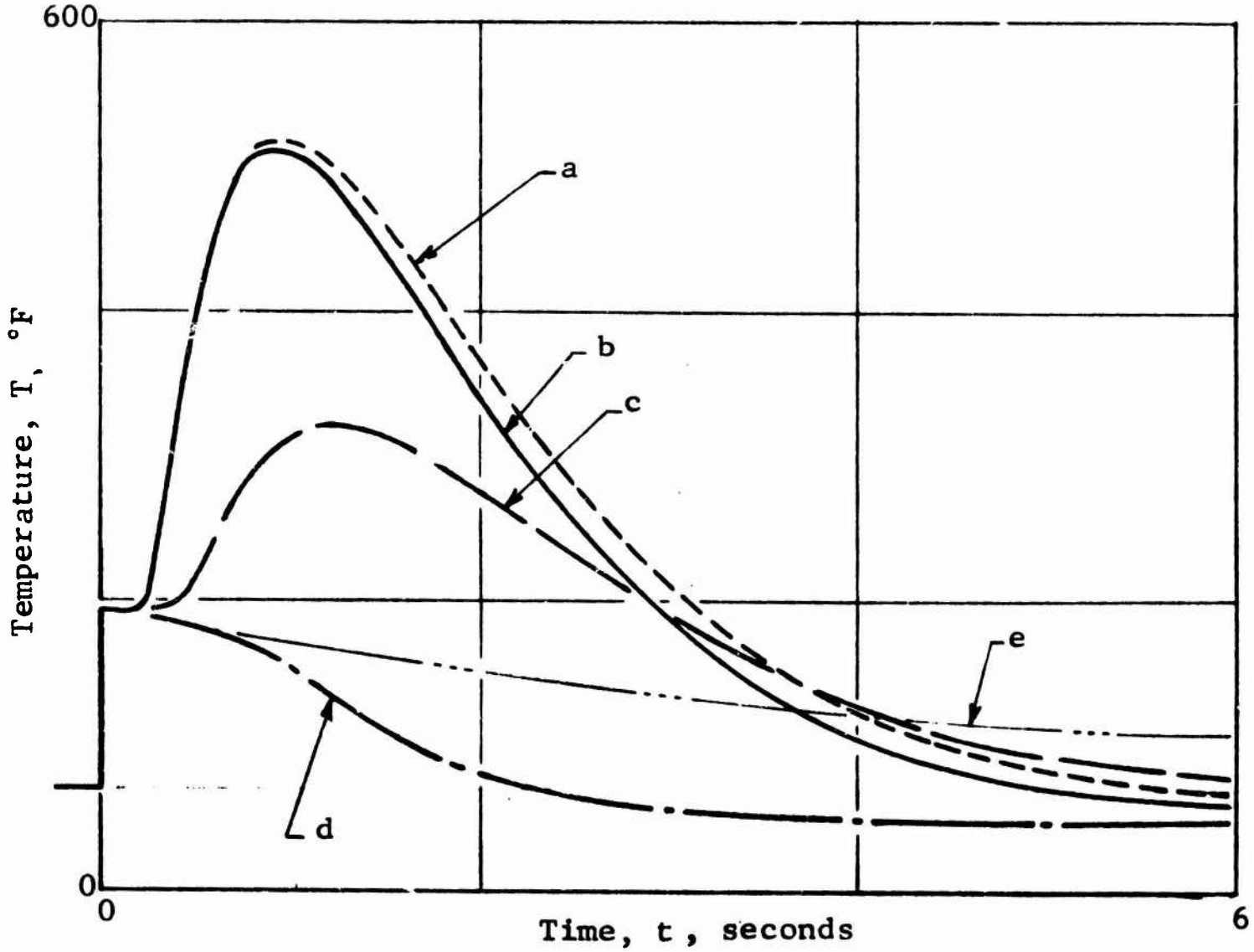

Figure 6.36 Influence of Soil Temperature Distribution

the letter d refers to the cold dust case, whereas the curve identified by the letter e refers to the no dust case. The air temperature does not vary greatly for this normal range of thermal properties of soil. The air temperature can be expected to be considerably lower for the case of very wet soils. The influence of the thermal energy upon the dust density is presented for these cases in Figure 6.37. The curve labeled with the leffer f corresponds to the dust prediction method described in the preceding chapter. The influence of the heated air upon the dust density is manifested in two ways. First, the expansion of the air tends to decrease the actual dust density and secondly, the vertical motion of the air lowers the effective height of interest, thus tending to increase the dust density. Clearly the first process dominates in the current situation. At late times we can expect that the influence of the thermal energy will disappear and all of the curves will approach the "cold" dust curve.

6.7 Multiple Burst Environment

A series of calculations was made for the air-temperature environment resulting for specific two- and three-burst situations. In each case the weapons are of the same size and they are detonated in the same general area. The detonations are separated in time by approximately one positive phase duration. It is implied that the respective fireballs do not interact with each other, and it is assumed that the thermal radiation emitted by the two or three weapons, and incident upon the site, can be added algebraically. The yield of the weapons is relatively large and the site is located at an overpressure range of general interest.

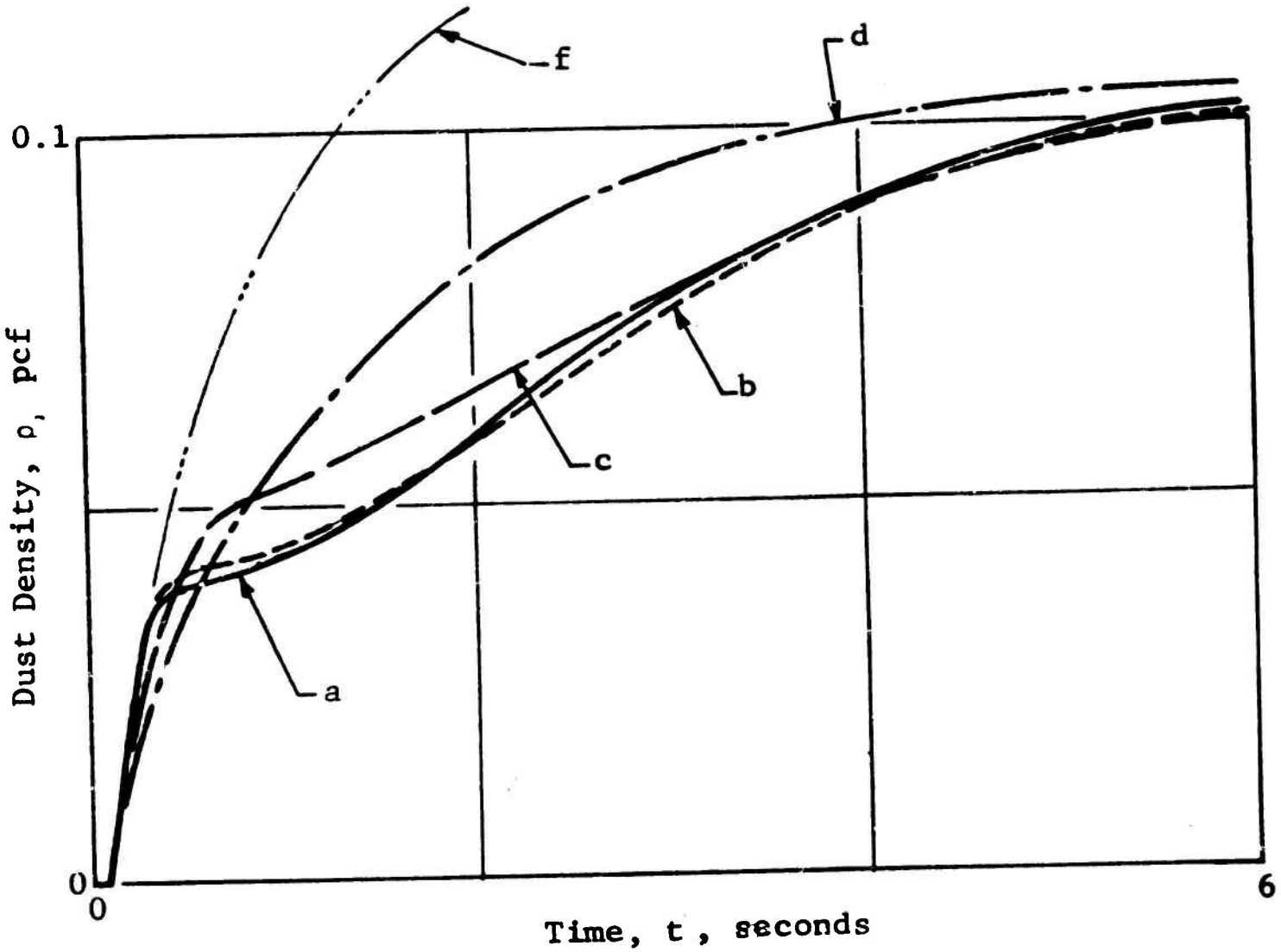

Figure 6.37 Dust Density

The thermal power curve used for these calculations is presented in Figure 6.38. The dashed line indicates the arrival time of the first air shock at the site. The soil temperature distribution resulting from these thermal pulses is shown in Figure 6.39. The quantity of energy absorbed by the soil decreases fro each additional weapon. This is due to the successively high surface temperatures in each case and thus, a greater quantity of energy is reinitiated back into space. The resulting air temperature curves are presented in Figure 6.40 for two different values of the land use factor. The height-peak air temperature for this specific set of input values is a little greater than 900°F.

6.8 List of Symbols

a	erosion coefficient,
B_λ	radiant flux intensity,
c, c_p, c_v	specific heat,
D	slant range distance,
E_{ij}	energy,
F	land use factor,
F_b	buoyancy,
F, F_s	thermal flux,
H, H_B, H_i	height,
g	standard acceleration, 32.2 ft/sec^2,
h	heat transfer coefficient,
I, I_o	radiation flux,
$i_{1,2}$	radiation intensity,
K	transport coefficient,
k	thermal conductivity,
L	distance,
ℓ	distance,
N	number of particles,
P, P_i	pressure,

P, P_e, P_{max}	fireball thermal emission,
Q_o	thermal flux,
O_i, O_r	thermal power density,
$Q, Q_a, Q_{abs}, Q_{ext}, Q_s, Q_{sca}$	efficiencies,
R, R_c, R_i	distance,
S_{ij}	height,
T, T_e, T_o	temperature
$t, t_e, t_i, t_m, t_{max}, t_{obs}, t_s$	time,
U	shock velocity,
V	volume,
V_i, V_o	air velocity
v	volume,
W	weapon yield,
W, W_i, W_o	weight,
w, w_{ij}, w_o	weight,
X	distance,
x	distance below surface,
Y	distance,
y	distance,
z_c	erosion depth,
α	thermal diffusivity, absorption coefficient
β	coefficient of thermal expansion,
ζ	height,
θ	angle, temperature difference,
κ	absorption coefficient,
λ	wavelength,
μ	viscosity,
$\rho, \rho, \rho_c, \rho_{sa}, \rho_d$	density,
σ	Stefan's constant,
τ	time,
τ_a	atmospheric transmittance.

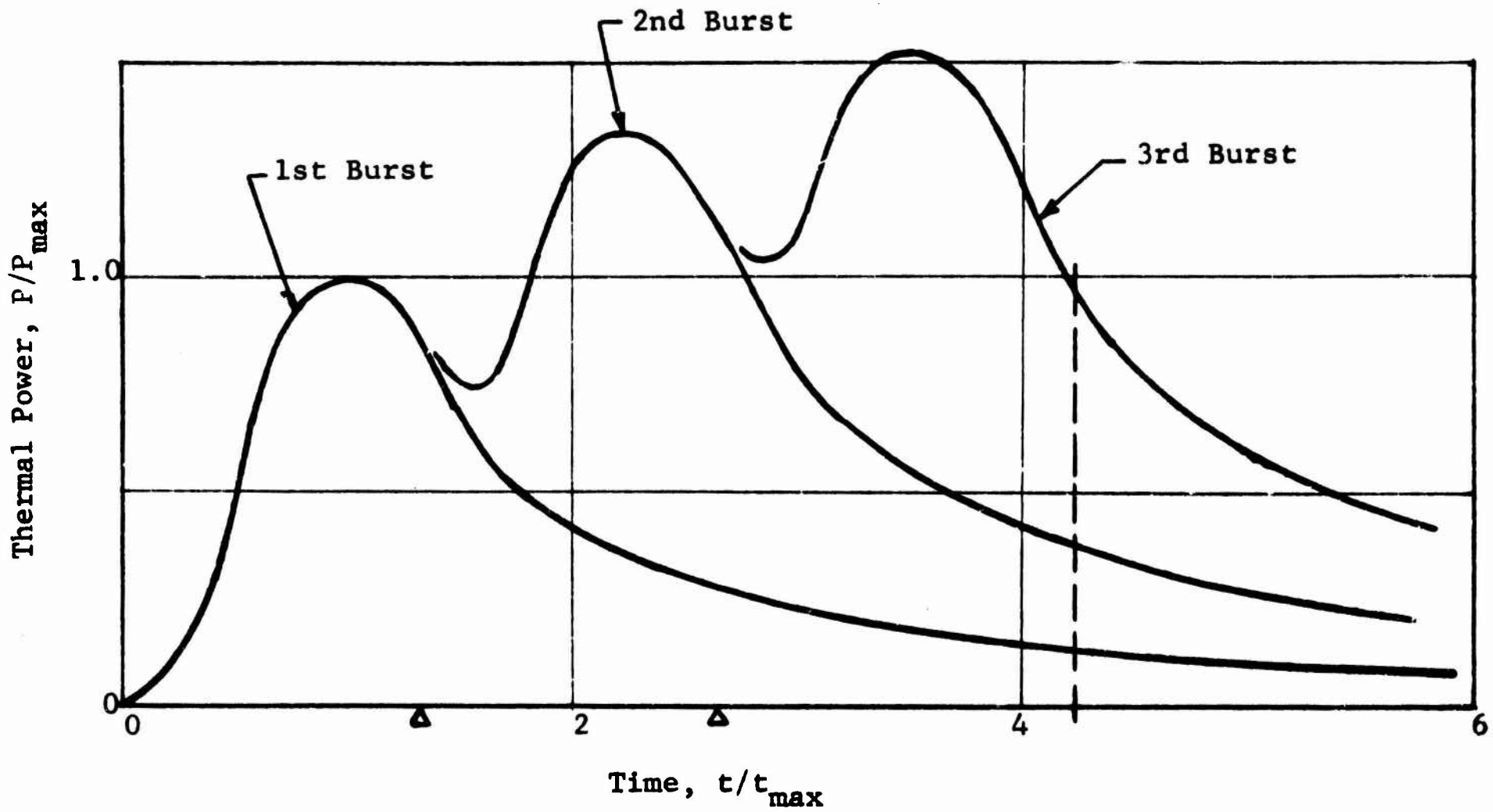

Figure 6.38 Thermal Power for Multiple Bursts

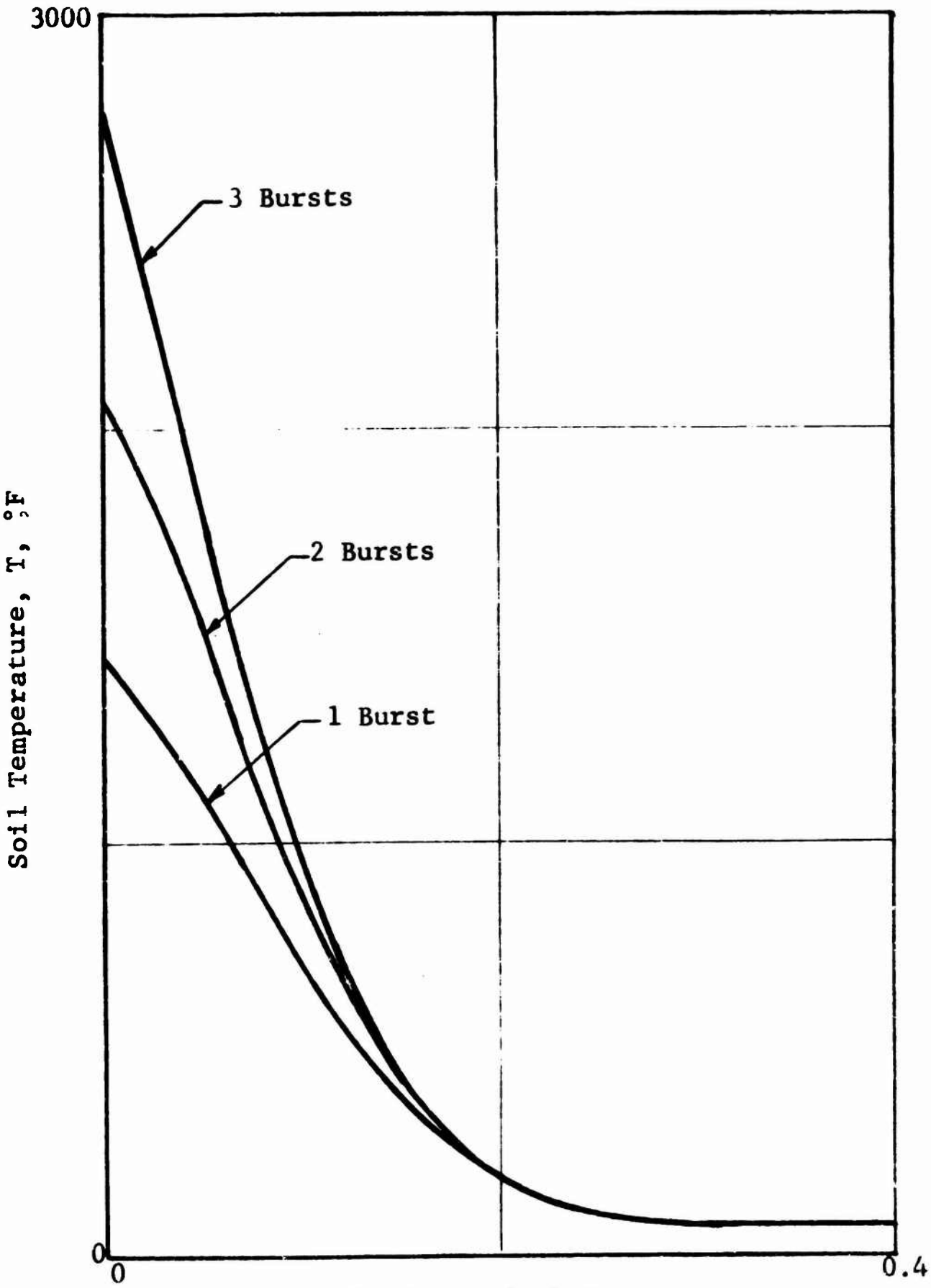

Figure 6.39 Soil Temperature for Multiple Bursts

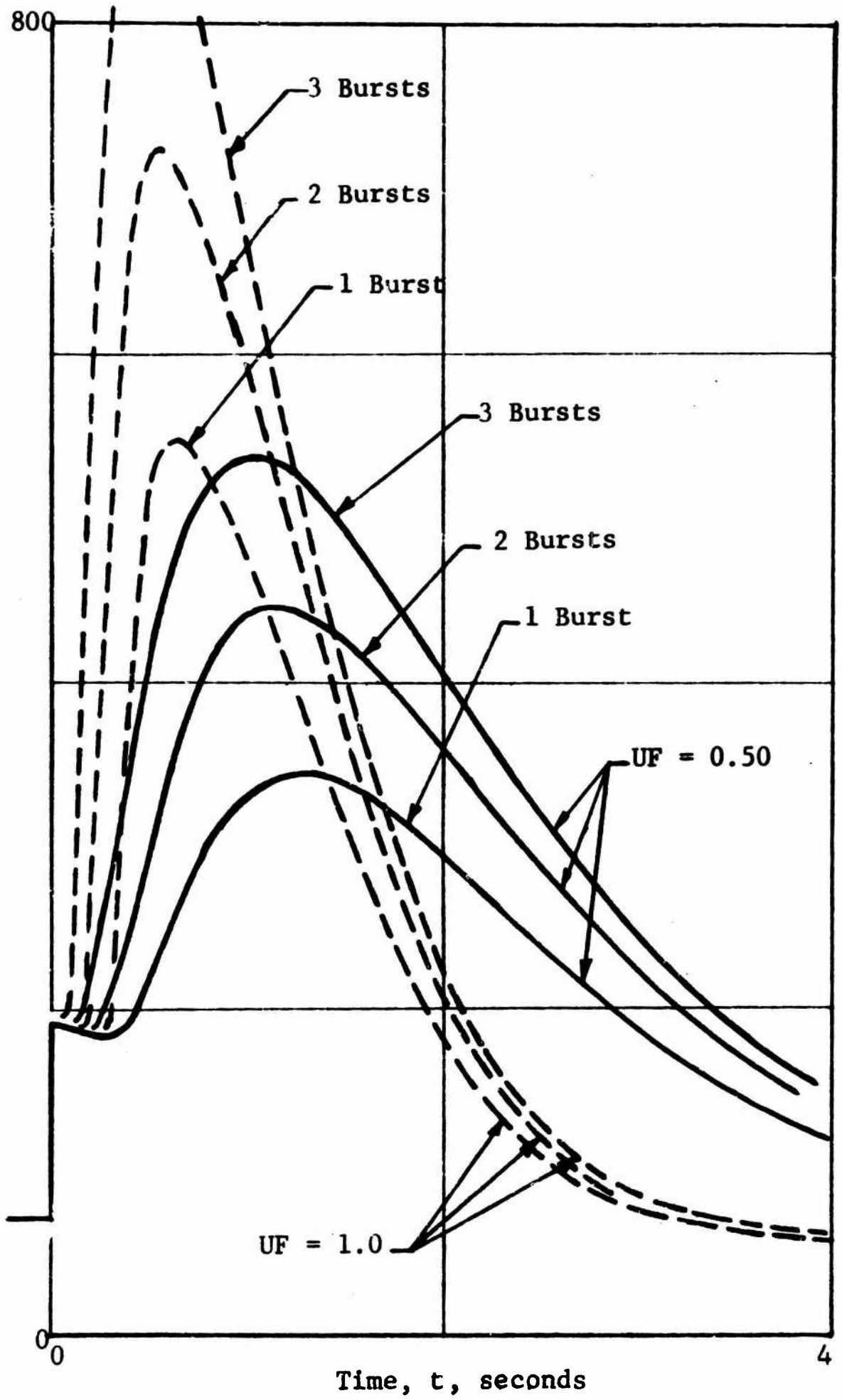

Figure 6.40 Temperature Histories for Multiple Bursts

EXTRACTED

Chapter 7 (U)

REFERENCES

5.1 "Dust Environment Associated with Nuclear Burst," SCR289, United Aircraft Corporate Systems Center.

5.2 Bagnold, R. A., "The Physics of Blown Sand and Desert Dunes," William Morrow, New York, 1946.

5.3 Binder, R. C., "Fluid Mechanics," Prentice-Hall, Inc., New York, 1943.

5.4 Banister, J. R. and Emvich, R. J., "Preliminary Investigation of Dust Raised by Blast Waves (Operation Greasy Stake)," Rept. No. SC-3610, Sandia Corporation, January 1955.

5.6 Ahlers, E. B., "Crater Ejecta Studies - Air Vent Phase I," Final Report, IIT Research Institute, May 1965.

6.1 S. Glasstone Ed., "Effects of Nuclear Weapons," U.S. Dept. of Defense, 1962.

6.2 M. G. Gibbons, "Transmissivity of the Atmosphere for Thermal Radiation from Nuclear Weapons," USNRDL-TR-1060, U.S. Naval Radiological Defense Laboratory, San Francisco, California, August 1966.

6.3 McAdams, W. H., "Heat Transmission," McGraw Hill Book Co., 1942.

6.4 van de Hulst, H. C., "Light Scattering by Small Particles," John Wiley and Sons, Inc., New York, 1962.

6.5 Cunningham, K., Wells, M. B., and D. G. Collins, "Light Transport in the Atmosphere Volume II: Machine Codes for Calculation of Aerosol Scattering and Absorption Coefficients," Radiation Research Associates, Inc., Fort Worth, Texas, U.S. Army Electronics Command Tech. Rept. ECOM-00240-1, Vol. II, September 1966.

6.6 Green, H. L. and H. R. Lane, "Particulate Clouds: Dusts, Smokes, and Mists," D. van Nostrand Co., Inc., New Jersey, 1964.

6.7 Kattawar, G. W., and G. N. Plass, "Electromagnetic Scattering from Absorbing Spheres," Southwest Center for Advanced Studies, Dallas, Texas, Air Force Cambridge Research Laboratories, Rept. No. AFCRL-67-0129, 28 December 1966.

6.8 Sinclair, "Handbook of Aerosols," USAEC, Washington, D.C., 1950.

6.9 Churchill, S. W., Clark, G. C., and C. M. Sliepcevich, "Light Scattering by Very Dense Dispersions of Latex Particles," Discussion of the Faraday Soc., 30, 192-199, 1960.

6.10 Ludlan, F. H., and Scorer, R. S., "Convection in the Atmosphere," Jouranal of the Royal Meteorological Society, Vol. 79, No. 341, July 1953.

6.11 Ogura, Y., and Phillips, N. A., "Scale Analysis of Deep and Shallow Convection in the Atmosphere," Journal of the Atmospheric Sciences, Vol. 19, March 1962.

6.12 Ogura, Y., "A Review of Numerical Modeling Research on Small Scale Convection in the Atmosphere," Meterorological Monographs, Vol. 5, No. 27, September 1963.

EXTRACTED

APPENDIX A (U)

COMPUTER PROGRAM FOR DUST AND AIR-TEMPERATURE PREDICTION

Contract No. DACA 73-67-C-0018

Prepared by:

IIT Research Institute
Chicago, Illinois

for

Directorate of Military Construction
Office of the Chief of Engineers
Department of the Army
Washington, D.C.

R

TABLE OF CONTENTS

TABLE OF CONTENTS (Continued)

Appendix A
COMPUTER PROGRAM FOR DUST AND AIR-TEMPERATURE PREDICTION

A.1 Discussion of the Computer Program

The theoretical models for the dust and thermal environment response to a simulated nuclear attack condition have been coded into a FORTRAN IV compiler language computer program for high-speed numerical prediction calculations. The program contains a total of twelve subprograms:

Subprogram Name	Description
(Main Program)	Executive control of execution, all input statements,
WE(a_1,...,a_{10})	Free-field effects for an air burst,
DUST1	Dust cloud similarity solution, single burst,
DUST2	Dust cloud nonuniform soil solution, single burst,
DUST3	Dust cloud similarity solution, two or three bursts,
DUST4	Late time dust cloud solution,
WE1(a_1,...,a_9)	Overpressure - Range for late time dust cloud,
OUT(a_1)	Output statements for all dust cloud solutions,
AT1(a_1)	Air temperature and dust cloud solution, uniform ground, single burst,
AT2(a_1)	Air temperature and dust cloud solution, biuniform ground, single burst,
ST(a_1,a_2,a_3)	Soil temperature solution, and
PE(a_1,a_2)	Scaled fireball thermal power at any time.

The variables a_1, a_2,...a_{10} are dummy variables, indicating the location and number of subprogram arguments. The four distinct dust cloud subroutines and two distinct air-temperature subroutines were written to achieve the most economical computational method, consistent with the degree

of information required, for specific and general site evaluation. These subprograms will be discussed in detail.

A.1.1 Executive Main Program

The main program is responsible for the primary user-oriented flow of control during execution. It can be regarded as the executive program that interfaces a user's computational objectives with the realization of the appropriate computer results.

All the input statements are included in the main program. A data set contains values of all the input variables necessary for subsequent execution of one of the following basic subroutines: DUST1, DUST2, DUST3, DUST4, AT1, or AT2. Any number of different data sets will be sequentially executed by the computer program.

The first data card of any data set contains the alphanumeric TITLE field, numerical values of RUNTYP and IOUT, and a logical value for TAPSAV which are listed in Table A.1. The value of RUNTYP specifies the type of computation according to

RUNTYP =
1, DUST1 computation,
2, DUST2 computation,
3, DUST3 computation,
4, DUST4 computation
5, AT1 computation, and
6, AT2 computation.

The variable IOUT is used to determine the level of detail of the computed results desired as output. For example, if the dust density is computed internally at one-second intervals, but only the results at five-second intervals are desired on the output listings, then IOUT will be five; for more detailed ouput, the value of IOUT would be suitably decreased. Also, a true or false value is assigned

Table A.1 INPUT VARIABLES I

Description	FORTRAN Symbol
Data set identification (≤ 72 characters)*	TITLE
Type of data set	RUNTYP
Number of observation time increments between entries in output listing	IOUT
Binary save tape option	TAPSAV
Number of observation times	IMAX
Number of observation elevations	NY
Number of bursts*	NB
Number of particle size classes	NCLASS
Number of upstream range zones	NZF
Number of downstream range zones	NZB
Time of second burst (sec)*	TB2
Time of third burst (sec)*	TB3
Observation time increment (sec)	DTOBS
Total observation time (hr)	TMAX
Observation time increment (hr)	DT
Wind speed (mph)*	W
Wind direction (radians)*	ANG

*Included in output.

to TAPSAV to indicate whether or not the computed results are to be written on a binary save tape.

For RUNTYP ≤ 4 (i.e., dust computations only), the second data card contains values of other variables in Table A.1. The number of observation times IMAX must be ≤ 200. The number of elevations NY to be entered as input data must be ≤ 3. The dust density history is computed at each of the specified elevations.

For RUNTYP = 1, 2, or 4 the value of NB must be 1, i.e., single-burst dust computations. In these cases, the time-of-burst variables TB2 and TB3 are superfluous; but, for the purpose of standardized procedure, any such variables that may have assumed arbitrary values will be set equal to zero. For NTYP = 3, NB must be 2 or 3, giving the number of bursts for the multiple-burst dust computation; if NB = 2, then TB2 must be specified and TB3 = 0; and if NB = 3, then both TB2 and TB3 must be specified.

The number of particle classes NCLASS must be ≤ 8. For NTYP = 1, 3, or 4 the range zone numbers NZF and NZB must be zero. For NTYP = 2, the values of NZF and NZB must be specified and less than 21.

The value of the observation time increment DTOBS is arbitrary; the product of IMAX and DTOBS gives the time corresponding to the end of computations.

For RUNTYP = 4, the remaining variables in Table A.1 are provided on the next data card. These are variables that relate only to the late time dust computations and include TMAX, the time corresponding to the end of computations, DT, the time step, W, the wind speed, and ANG, the wind direction. Note that for RUNTYP = 4 the variables IMAX and DTOBS are superfluous.

For RUNTYP = 5 or 6, i.e., air temperature computations, the second data card contains values of the variables given in Table A.2. The variables UF and ZM pertain only to the uniform ground solution and, therefore, have values only if RUNTYP = 5. Similarly, the variables P1, P2, and RC pertain to the biuniform ground solution and have values only if RUNTYP =6.

The next data card of each set contains values for the soil particle density, bulk soil density, ambient air temperature and pressure, and the transport and erosion constants which are given in Table A.3. The other variables in this table are discussed below.

Five variables establish the nuclear attack condition; the weapon yield, the overpressure at the plant site, and three height-of-burst variables that select among optional choices for the height of burst. For RUNTYP $\neq$ 3, the only burst variables entered as input data are YIELD, PRESO, HOB, HOBS, and HOBO. For RUNTYP = 5 or 6, this will be the last data card of the data set. For RUNTYP = 3, the burst variables entered as input data are YIELD1, PRESO1, HOB1, HOBS1, and HOBO1 -- and YIELD2, PRESO2, HOB2, HOBS2, and HOBO2 for NB = 2 or 3, and in addition, YIELD3, PRESO3, HOB3, HOBS3, and HOBO3 for NB = 3.

The data card following the burst variables card(s) contains the one-dimensional array for the particle diameters D(N), N = 1, NCLASS, for RUNTYP $\leq$ 4.

The variable NZR1, which equals the number of upstream zones plus the number of downstream zones plus one (the zone containing the site), is then computed. The next NZR1 data cards contain the two-dimensional array for the adjusted weight fractions, P(N,NN), N = 1,NCLASS, NN = 1,NZR1, where each card contains NCLASS values of P for the respective

Table A.? INPUT VARIABLES II

Description	FORTRAN Symbol
Soil conductivity (Btu/ft-hr-°F)*	FK
Soil diffusivity (ft^2/hr)*	ALPHA
Observation time factor	BETA
Soil particle specific heat (Btu/lb)*	C
Heat transfer response time (msec)*	TM
Observation elevation (ft)*	YC
Uniform ground land use factor*	UF
Uniform ground erosion depth cutoff (in.)*	ZM
Biuniform ground near land use factor*	P1
Biuniform ground far land use factor*	P2
Biuniform ground range boundary (ft)*	RC

*Included in output.

Table A.3 INPUT VARIABLES III

Description	FORTRAN Symbol
Density of soil particles (lb/ft^3)*	RHO
Bulk density of soil (lb/ft^3)*	RHOTOT
Ambient air temperature (°F)*	TEMPA
Ambient air pressure (psia)*	PRESA
Transport constant*	KH
Erosion constant*	A
<u>Single Burst</u>	
Weapon yield (MT)*	YIELD
Overpressure (psig)*	PRESO
Height of burst (ft)*	HOB
Scaled height of burst ($ft/MT^{1/3}$)	HOBS
Optimum height of burst	HOBO
<u>Multiple Bursts</u>	
Weapon yield (MT)*	YIELD1, YIELD2, YIELD3
Overpressures (psi)*	PRESO1, PRESO2, PRESO3
Heights of burst (ft)*	HOB1, HOB2, HOB3
Scaled heights of burst ($ft/MT^{1/3}$)	HOBS1, HOBS2, HOBS3
Optimum heights of burst	HOBO1, HOBO2, HOBO3
Particle diameters (mm)*	D(N), N=1,NCLASS
Adjusted weight fractions*	P(N,NN), N=1,NCLASS, NN=1,NZR1
Observation elevations (ft)*	Y(N), N=1,NY
Forward zone boundaries (ft)	RZF(N), N=1,NZF
Backward zone boundaries (ft)	RZB(N), N=1,NZB

*Included in output.

zone NN. for RUNTYP = 1, 3 or 4, a uniform ground condition is assumed, and therefore NZR1 = 1; for RUNTYP = 2, NZR1 ≤ 41.

For RUNTYP ≤ 4, the specified observation elevations Y(N), N = 1,NY are entered from the next data card that can, at most, specify three elevations. If RUNTYP = 1, 3, or 4, this is the last data card of the data set. If, however, RUNTYP = 2, then the forward and backward zone boundaries RZF(N), N = 1,NZF and RZB(N), N = 1,NZB are entered from the next two and final data cards, respectively. The weight fractions and zone boundaries are introduced in the order of increasing distance in front of, and then in the order of increasing distance behind, the plant location. The plant location is not considered a zone boundary.

Sample problem data sets for a sample site are presented in Section A.2.3 They provide examples of the data card ordering procedure discussed above.

The main program then directs control to the computational subroutines depending on the value of RUNTYP according to

RUNTYP =
- 1, CALL DUST1,
- 2, CALL DUST2,
- 3, CALL DUST3,
- 4, CALL DUST4,
- 5, CALL AT1, and
- 6, CALL AT2

For RUNTYP = 1, 2, or 3, upon return of control from the appropriate subroutine, the output subroutine OUT is called; this provides the off-line listing of computational dust cloud results. The TAPSAV variable is then tested and, if it is true, a binary save tape of these results is generated. For RUNTYP = 4, 5, or 6, the off-line listing is generated in either the DUST4, AT1 or

AT2 subprogram, respectively; the TAPSAV option is similarly tested for binary storage of the temperature computations.

A.1.2 Weapons Effects Subprogram

The dust and thermal environment prediction program requires certain weapons effects variable values as data. These values, in turn, must be determined from a given nuclear attack condition. A weapon effects subroutine was written to provide these variable values over the range of variables of interest.

The many weapon effects variables are interrelated such that the attack situation can be uniquely defined by specifying a limited number of variable values. To limit the complexity of the weapons effects subroutine, the defining weapon effects variables were restricted to weapon yield, YIELD(MT), overpressure, PRESO (psi), and height of burst or equivalent.

The height of burst option permits us to choose (1) the actual height of burst HOB (ft), (2) the scaled height of burst at standard air conditions HOBS ($ft/MT^{1/3}$), (3) the optimum height of burst HOBO, or (4) an overhead burst. The subroutine sequentially examines the value of HOB, HOBS, and HOBO until an acceptable value is indicated. A negative HOB value is not acceptable; hence an input value such as -1 would cause the subroutine to bypass this option. Any positive value, including zero, is an acceptable value. A negative or zero value for HOBS is not acceptable, and a value less than 0.1 is not acceptable for HOBO. If these three input values are not acceptable, then option (4) is automatically selected. The final input data needed to define the attack situation are the ambient pressure PRESA and the temperature TEMPA.

This subroutine is entered through a CALL WE(a_1,...,a_{10}) statement in the main program where a_i represents the arguments

of the subroutine. Execution then proceeds through four parts: (1) an initial computation in which a variety of scale factors and other numbers are generated for subsequent use, (2) the calculation of those weapon effects variables which are not a function of the height of burst, (3) the calculation of those variables which are a function of the height of burst, and (4) the calculation of some thermal data. The first part consists of six steps:

1. Compute absolute ambient temperature, TEMPAS.
2. Compute scale factors for yield, CRY, ambient pressure, PSF, ambient temperature, TSF, and overpressure, SOP.
3. Compute ambient sound velocity, CVELA.
4. Compute shock strength, XI.
5. Compute two height-of-burst scale factors, SRB and SRC.
6. Compute square root of yield, SQRTW.

The second part of the subroutine consists of seven steps:

1. Compute time of maximum thermal emission, TMAX.
2. Compute exponent for velocity pulse, KV. If KV is less than 1, set KV equal to 1.
3. Compute positive phase duration of velocity pulse, TO, using one of two formulas depending upon the value of SOP.
4. Compute the air temperature at the shock front, TES.
5. Compute the air density at the shock front, RHOS, and an average value within the blast wave, RHOF.
6. Compute the positive phase duration of the overpressure, TOP.
7. Compute three coefficients for the overpressure waveform, CP1, CP2, and CP3.

The third part consists of four main steps which are subdivided as follows:

1. This step examines the height-of-burst input information and determines whether the height of burst is such that the following shock regimes exist:
   a. Mach reflection,
   b. regular reflection,
   c. overhead burst.

It also computes the actual height of burst, HOB, or the scaled height of burst, SHOB, whichever is not given as input.

2. This step computes the weapons effects variables if the Mach reflection regime applies. The variables which are evaluated are:

   a. shock velocity, U,
   b. peak air velocity, VO,
   c. time of arrival of shock at site, TASITE,
   d. scaled range, SRA, and
   e. angle of incidence, THETA (if theta is very small, set theta equal to $\pi/2$.

3. This step computes the weapons effects variables if the regular reflection regime applies. The following calculation or tests are made:

   a. compute maximum permissible height of burst, SRD,
   b. compare SHOB with SRD; if SHOB is greater than or equal to SRD, transfer to overhead burst calculations (this automatically sets SHOB to a permissible value),
   c. compute factor, CF, for velocity calculations,
   d. compute angle of incidence, THETA,
   e. compute shock velocity, U,
   f. compute peak air velocity, VO,
   g. compute scaled height of burst, SRE,
   h. compare SHOB with SRE; use one of two equations to compute time of arrival, TASITE.

4. This step computes the weapons effects variables for an overhead burst: shock velocity, U, peak air velocity, VO, angle of incidence, THETA, height of burst, HOB, and time of arrival, TASITE.

5. The last step:

   a. computes cosine of theta, COSTH,
   b. computes slant range, SRANGE,
   c. examines magnitude of HOB (if HOB is small, computes slant range from a second equation),
   d. computes an exponential factor, OPT, from tabular data after first determining the height-of-burst interval applying to the current case,
   e. computes thermal attenuation factor, TAU, and
   f. computes peak radiant power incident at site, CONSW1.

Control is then returned to the main program for subsequent execution.

A.1.3 Uniform Ground Dust Subprogram

This single-burst uniform-ground-condition subroutine makes use of the similarity solution as well as the analytical

expression for cloud height. Thus, the coding reduces to a simple evaluation of these equations for a set of transport times. The dust densities for various particle size classes and for various elevations are computed at uniform time intervals measured at a fixed range (the plant location) to which the corresponding transport times are related.

This subroutine is entered through the CALL DUST1 statement in the main program, the calling program. Execution then proceeds through two main computational parts of this subroutine: (1) an initial computation phase in which a variety of numbers is generated for subsequent use, and (2) an evaluation of the cloud height and the computation of the dust density from the similarity solution. The first part consists of four steps:

1. Computation of the maximum air displacement RO and the related time factors, transit time TAO, modified positive-phase duration TOM, and the exponential factor TAU.
2. Computation of terminal velocities for each particle size class VT(N).
3. If VO is less than 10 fps, CUTOFF is set equal to false and control returns to the main program, thereby eliminating any further computation of the specific problem.
4. Evaluation of a number of constants.

The second part consists of eight steps:

1. Initialization of all dust density storage locations to zero.
2. Computation of observation times TOBS(I).
3. Computation by iteration, of the air displacement R corresponding to TOBS(I). Evaluate the corresponding transit time T.
4. Computation of the height of the cloud HST in the absence of gravity.
5. Computation of the height of the cloud H for each particle class (and for each time).
6. Computation of the value of the similarity variable X for each elevation Y(L) and for each particle size class and for each time.

7. Evaluation of the dust density contribution DYC(I,N,L) from the similarity solution.
8. Summation over all particle size classes to obtain the total dust density D(I,L) at each elevation for each TOBS(I).

Control is then returned to the main program for subsequent output of the computed variables and execution of the remaining problem data sets.

A.1.4 Variable Ground-Dust Subprogram

The single-burst variable-ground codition subroutine computes the dust density variation at various height and times in accordance with the basic IITRI dust model. Equation 5.13 is used to integrate all of the elemental dust contributions picked up along that particular air column which arrives at the site location at the time of interest. The total dust density DY and the dust density for each particle size class DYC are computed and printed out for each elevation Y.

This subroutine is entered through the CALL DUST2 statement in the main program. Execution then proceeds through two main computational parts: (1) an initial computation in which a variety of numbers are generated for subsequent use, (2) the integration or summation in which the elementary dust density contributions are accumulated for each increment of time and along each integration path, and for each particle size class. The initial part consists of 12 steps:

1. Computation of the maximum air displacement RO and the related time factors, transit time TAO, the modified positive-phase duration TOM, and the exponential factor TAU.
2. Computation of terminal velocities for each particle size class VT(N).
3. If VO is less than 10 fps, CUTOFF is set equal to false and control returns to the main program, thereby eliminating any further computation of the specific problem.

4. Computation of the time increment DT for integration along each particle path.
5. Evalutation of constants.
6. Conversion of range boundaries RZF and RZB into an ordered set of range constants R2(I) measured from R = 0 (the site is located at R = RO).
7. Computation of the observation time TOBS(I) and a corresponding constant CONS.
8. Computation, by iteration, of the range R1(I) from which the air column started and just reached the site at the corresponding observation time.
9. Computation of the shock arrival time at R1(I), the total transit time DT1(I), and an exponential factor TAU1.
10. Computation from one of two equations, of the height of the dust cloud H1(I) in the absence of gravity at the corresponding observation time.
11. Computation, for each of 500 integration intervals, of the transit time TI(J); evaluate two corresponding constants; and then computation of the velocity VEL(J) and the air displacement DIS(J).
12. Computation, from one of two equations, of the height of the cloud HSTAR(J) for each integration element.

The second part of the program consists of four steps:

1. Initialization of all dust density storage locations to zero.
2. For each integration path (I=1,IMAX), for each particle size class (M=1,NCLASS) and for each element (J=1,JMAX) along the Ith integration path, computation of
   a. the erosion factor FACT: compare with zero, and set equal to zero or unity;
   b. the range R of Jth element; compare with range constants R2(K), determine ordered zone number K and convert to zone number L, which corresponds to order of input data P(M,L);
   c. the increment of mass of the dust packet DM;
   d. the time increment after dust pickup DELT; and
   e. the height of the dust cloud H, corresponding to the given packet of dust.
3. For each elevation Y(L), computation of the incremental dust contributions and integration over all J elements to obtain DYC(I,M,L).
4. Summation of the dust contribution from each particle size class to obtain the total dust density DY(I,L) at each elevation Y(L) and for each observation time TOBS(I).

The range boundaries are then recomputed and the adjusted weight fractions reindexed for output format purposes. Control is then returned to the main program.

A.1.5 DUST3 Multiple Burst-Dust Subprogram

The multiburst subroutine was written for a uniform ground condition and represents a first estimate of the influence that a multiweapon attack has upon the dust environment, which is created by the resulting airblast winds. The multiweapon attack problem introduces a large number of additional weapon, timing, and geometrical variables into an already complex problem. To make the problem manageable at this stage of development of the dust-environment predictions, a number of simplifying assumptions were made. The assumption or use of a uniform ground condition represents one such simplification. This assumption enables us to disregard the settling or fallout of the dust from the first burst and its special redistribution over the general area of the site. It is also consistent with the basic assumption that there is no interaction between particles of different size classes and their respective availability. Thus, the layering of soil of one distribution on the soil of another distribution need not be considered.

The interaction of one air blast field with another represents a very complex nonlinear interaction problem, except when the intensity of one of the fields (the first one) has decayed somewhat. Thus, it is essential to require that the time interval at the site location between the arrival of the respective shock parts be long enough to allow the air to approach a near-quiescent state. Such a state first occurs at the time of the positive-phase duration of the overpressure and exists thereafter for that particular burst.

Under this condition, the velocity fields generated by the various bursts can be added vectorially. To simplify the computational procedure further, it was assumed that the various bursts occur in the same general direction from the site. Hence, the velocity fields can be now treated as scalar quantities and added algebraically. It is obvious that the addition of the positive phase of the second burst to the negative phase of the first burst will reduce the air velocity and, hence, reduce the dust density. This degradation in air velocity should be small relative to the primary effect of the second burst. If the two weapons are detonated in opposite directions relative to the site, the velocity would be somewhat enhanced; however, such an attack environment is not considered very probable.

The multiburst subroutine for uniform soil conditions is very similar to the corresponding single-burst subroutine in that use is made of the similarity solution. However, the cloud height in the absence of gravity effect is computed by direct numerical integration of the controlling differential equation, the first term of Equation 5.4. A classical three-point integration formula was used within a given time interval. The multiburst subroutine treats either two or three bursts. The shock velocities U for the various bursts are averaged for computational purposes as are the air densities RHOF. This subroutine is entered through the CALL DUST3 statement in the main program. Execution then proceeds through two computational parts, the first dealing with the evaluation of a variety of numbers, and the second dealing with the density computation from the similarity solution. A series of logical constants is used to determine which of three possible equations will be used to compute the cloud height. This is necessary to avoid the effect of negative cloud heights. The first part consists of 13 steps:

1. Definition of arithmetic statement functions for the velocity and displacement contribution from the various bursts.
2. Computation of average values of U and RHOF.
3. Computation of terminal velocity for each particle size class VT(N).
4. Computation of the maximum air displacements RO1 and RO2 for the first two bursts.
5. Computation of the corresponding time factors TOM1, TOM2, and a number of constants FK11 to FK42.
6. Computation of constant CONS1, accuracy criteria CRIT1, and maximum observation time TMAX.
7. Computation of the observation times TOBS(I).
8. Computation, by iteration, of the transit time TC1 between the start of the flow and the time the second shock point reaches the air column.
9. If TC1 > TMAX, CUTOFF is set equal to false, and control returns to the main program, thereby terminating this problem.
10. Evaluation of critical values of I, IB2, IB21, and IB22, separating the first and second bursts.
11. When three bursts are used, computation of
    a. RO3, TOM3, FK13, FK23, and FK43,
    b. the time of maximum displacement for the second burst by iteration,
    c. the transit time TC2 by iteration, and
    d. if TC2 > TMAX, CUTOFF is set equal to false and control returns to the main program, and
    e. critical values of I(IB3, IB31, and IB32).
12. Computation of transit times TA(I) from one of three equations, depending upon the burst interval. When only two bursts occur, IB3 is set equal to IMAX.
13. Computation of the height of the cloud HSTAR(I) in the absence of gravity for each transit time TA(I). This is done over six regions for I=1, I=2, to IB2, I=IB2, I=IB21 to IB3, I=IB31, and I=IB32 to IMAX. Critical values of H, (HC1 and HC2) are also computed, corresponding to TC1 and TC2.

The second portion of the program consists of four steps:

1. Initialization of all dust-density storage locations to zero.
2. Initialization of logical constants Q1, Q2, and Q3 to TRUE.

3. For each particle size class,

   a. compute the cloud height H for each time TOBS(I).
   b. compare H with zero.
   c. if H is greater than zero, compute value of similarity variable and then compute density contribution DCY(I,N,L) for each elevation.
   d. if H ≤ 0, set Q1 = FALSE, set I to IB21.
   e. compute the cloud height H for each time TOBS(I), I=IB21 to IB3 from one of two equations, depending upon logical constant Q1.
   f. compare H with zero.
   g. if H is greater than zero, compute value of similarity variable and then compute the density contribution DCY(I,N,L) for each elevation.
   h. if H ≤ o, set Q2 = FALSE, set I to IB31 (or stops for two bursts).
   i. compute the cloud height H for each time TOBS(I), I=IB31 to IMAX from one of three equations, depending upon the logical constants Q1 and Q2.
   j. compare H with zero.
   k. if H is greater than zero, compute value of similarity variable, then compute the density contribution DCY(I,N,L) for each elevation.
   l. if H ≤ 0, set Q3 = FALSE. This terminates the calculations for the N^{th} particle size class.

4. Summation of the dust contribution for each particle size class to obtain the total density DY(J,L) at each elevation Y(L) and for each observation time TOBS(I).

Control is then returned to the main program.

A.1.6 Late Time Dust Subprogram

This single-burst uniform-ground-condition subroutine makes use of two modified forms of the simulation solution to compute the dust density at late times. One solution relates to the growth phase of cloud development whereas the other solution relates to the settling phase. The coding consists of determining the apparent location of the site within the overall dust cloud formation at uniform time intervals and then evaluating the corresponding overpressure levels, the blast wave variables, and finally, the maximum cloud height at these locations. The dust densities for various particle size classes are then

evaluated by determining which cloud development phase applies and using the appropriate modified simularity solution. Due to limitations of the weaponseffects equations the dust densities at locations for which the overpressure exceeds 60 psig are set equal to a very large number and therefore printed out as "******".

The subroutine is entered through a CALL DUST4 statement in the main program. A series of four function statements is defined in this subroutine which relate to the coordinates of constant overpressure lines in the height of burst-range space. Execution then proceeds through four main computational parts: (1) a preliminary calculation part in which certain numbers are generated for subsequent use, (2) an initialization part in which the individual dust density contributions are set equal to zero, (3) an iteration procedure in which a critical range is evaluated, and (4) the basic dust density evaluations which are made for each time step. The initial part consists of the following steps:

1. Set the value of IC and Q, both of which are used to control the computational flow when the excessive overpressure override is needed.
2. Compute the number of computational or time steps IM. Compare with the allowable dimension size and limit to 201 if exceeded.
3. Compute the fluid density RHOF and the terminal velocity VT(N) for each of the particle size classes.
4. Evaluate a series of constants, CRY, PSF, and TSF. Compute the scaled overpressure S.
5. Compare HOB or other height of burst input data with appropriate criteria to determine which reflection region is applicable for the starting calculation. Then compute the range of the site, RS.
6. Compute a series of constants, CONS1 and RR. Set the value of the overpressure PR equal to PRESO.

The second part consists of equating the total dust densities DY(I,L) and the particle class contribution DYC(I,N,6)

to zero for each height, L, of interest and each time, I.

The third part consists of the following steps:

1. Set the scaled overpressure SP equal to 15.
2. Using a Newton-Ralphson iteration procedure solve for which the actual height of burst is the optimum height of burst. An accuracy criteria of 0.05 psi is used on the convergence interval.
3. Compare SP with 0.1 and if larger use function RCF(SP) to evaluate critical range RCRIT. Otherwise set RCRIT = 1000000.

The final part consists of the following steps:

1. Compute the observation time TOBS(I), the travel distance RR and the range R from the dust cloud origin. Compute the initial value of the scaled overpressure S based upon the last overpressure evaluation.
2. Test IC and Q to determine if overpressure override applies.
3. Compare R with RCRIT and select one of two overpressure functions with which to use with a Newton-Ralphson iteration procedure. An accuracy criterion of 0.1 psi is used on the convergence interval. Evaluate the overpressure PR.
4. Compare PR with 60 psi to determine if the overpressure override should be activated. If so go to statement 121.
5. CALL weapons effects subprogram WE1(PR) to evaluate maximum cloud height HST.
6. Compute change in cloud height DH.
7. Compare DH with 0 to determine which of two modified simularity solutions are to be used to evaluate the dust density contributions. Compare height of cloud with elevation Y(L). If elevation is larger than bypass calculation, otherwise evaluate similarity variable X. Compute dust density contribution DYC(I,N,L).
8. Statement 121 activates the overpressure override by setting Q = FALSE and evaluating the critical index IC where the override is to be removed.
9. This group of statements are used to evaluate the dust density contribution DYC(I,N,L) where the overpressure override condition is active.
10. The total dust densities DY(I,L) are obtained by summing over the particle size classes for each elevation Y(L) and observation time TOBS(I).

Control is then returned to the main program.

A.1.7 WEI (Late Time Dust Weapons Effects) Subprogram

The late time dust subprogram require that certain blast wave variable be evaluated so that the maximum cloud height can be established for each time step. The variables are all functions of the overpressure level which is evaluated in the subprogram. This subroutine is, therefore, entered through a CALL WEI (a_1,...a_9) statement in the Late Time Dust Subprogram. It consists of the following steps:

1. Compute the scaled overpressure SO and shock strength XI.
2. Compute the exponential coefficient KV. Compare with 1 and if less set KV = 1.
3. Compute positive phase duration TO from one of two equations selected on the basis of the scaled overpressure level.
4. Compute optimum height of burst RB, the reciprocal of the shock velocity UR and the peak wind velocity VO, the latter two using the Mach reflection region equations.
5. Compare the height of burst HOB with RB to determine reflection region. If the regular reflection region applies then compute height of burst coordinates RC and RO, a correction factor CF and the incidence angle THETA. Recompute the reciprocal of the shock velocity UR and the peak wind velocity VO.
6. Compute the critical air displacement values RO and ROO. Compute the maximum height of the dust cloud, HST.

Control is then returned to the subprogram DUST4.

A.1.8 Output Subprogram

This subroutine contains the output statements for the off-line listing of the variables computed by DUST1, DUST2 or DUST3 subroutines. The values of RUNTYP, the type of dust computation, and NB, the number of bursts are used to select the appropriate output statements. In addition, an execution terminated message is listed if the value of CUTOFF is false as provided for in each of the dust subroutines.

The output provides the spectral dust density variation as well as the total dust density as functions

of time for each elevation selected. The major computed output variables are the observation times, TOBS(I), the total dust density, DY(I,L), and the dust densities per particle size class, DYC(I,N,L), for N=1 to NCLASS, L=1 to NY, and I=1 to IMAX in steps IOUT.

A.1.9 Uniform Ground Air Temperature Subprogram

An air temperature subroutine was written to compute the air temperature and dust density at the elevation of interest for a site which is surrounded by a uniform ground condition. This subroutine is entered through a CALL AT1 statement in the main program. Execution then proceeds through three parts: (1) an initial computation in which a variety of numbers are generated for subsequent use, (2) initialization of dimensional statements, and (3) the main calculation loops. The first part consists of the following steps:

1. Compute initial cell size, DY.
2. Compute the number of cells needed, JMAX.
3. Compare JMAX with storage allotment for J (if exceeded exit from subroutine).
4. Compute depth, ZA(M), in soil where soil temperature is to be evaluated. Set ZM(10) = 5.
5. Call the soil temperature subroutine, ST(ALPHA, FK, TEMPA).
6. Compute air column motion parameters, RO and TOM.
7. Compute weight of air in cell, WAA.
8. Compute depth of soil eroded per time step, DZ, after evaluating TP and VP.
9. Compute weight of soil eroded per time step, W.
10. Compute critical index for erosion cutoff, IC and FLOAT (IC-1).

The second part consists of the following initialization:

1. The observation time, TOBS(1).
2. The dust density, DDY(1).
3. The conditions for the ground level variables, TEY(1), YY(1), S(1), Q(1).

4. The soil depth index, M.
5. The values of T, TT, P1.
6. The air temperature variable adjacent to the ground, TE(1).
7. The cell variables at the shock front, SUMW(J), SUMWP(J), TE(J), and S(J).

The third part consists of the following calculations:

1. Compute the value of constants T1 and G. Compute maximum time of interest, TOUT.
2. DO loop on I, the time variable,
   a. transfer cell temperatures TEJ(J),
   b. compute FI and FI1,
   c. compute height of cloud, H. Compare with cloud height at end of positive phase duration. If H is greater, set T=T1,
   d. using the above cloud height test, select one of two equations with which to evaluate the total elapsed time, T. A Newton-Ralphson iteration procedure is used and an accuracy test, based upon 0.0001*TM, is made on the convergence step,
   e. again using the above cloud height test select one of two equations with which to evaluate the observation time, TOBS(I),
   f. compute absolute pressure, P2, pressure change, DP, and a related quantity, TERM2,
   g. compute depth of erosion, Z. Compare Z with current temperature depth interval. If exceeded index M or otherwise, compute current value of soil temperature TE(I),
   h. compute total quantity of dust in air column, WA(I).
3. DO loop on J, the height variable (this is a nested DO loop),
   a. compute FJ,
   b. determine which cloud region is applicable, then proceed to one of two groups of statements to evaluate quantity of dust in cell, SUMW(J),
   c. compare J with 2 to determine if cell is adjacent to soil, then use one of two equations to compute the quantity of dust entering the cell, SUMWP(J),
   d. compute the quantity of dust in air column above cell. Evaluate thermal radiation flux incident on cell, Q(J), and then compute the associated energy deposited in cell,
   e. compute new air temperature in cell, TE(J), after evaluating quantities DTN and DTE. Also evaluate TERM1.

f. compute cell size, S(J), and cell center height, YY(J).
g. Compute dust density in cell, DD(J). (End of J DO loop).

4. Continue in I DO loop to:

a. reinitialize T1 and P1,
b. evaluate temperature TEY(I) and dust density DDY(I) at the height YC by linear interpolation. This is done after YC is sequentially compared with the cell height YY(J). A quantity DYY is then computed. (End of I DO loop).

Control is then returned to the main program for subsequent execution.

The major computed output variables are the observation times, TOBS(I), the air temperatures, TEY(I), and the dust densities, DDY(I), for I=1 to IMAX in steps IOUT.

A.1.10 Bi-Uniform Ground Air Temperature Subprogram

An air temperature subroutine was written to compute the air temperature and dust density at the elevation of interest for a site which consists of two uniform-ground-condition regions in front of the site. This subroutine is entered through a CALL AT2 statement in the main program. Execution then proceeds through three parts: (1) an initial computation in which a variety of numbers are generated for subsequent use, (2) initializing of dimensioned statements, and (3) the main calculation loops. The first part consists of the following steps:

1. Compute initial cell size, DY.
2. Compute the number of cells needed, JMAX.
3. Compare JMAX with storage allotment for J (if exceeded, exit from subroutine).
4. Compute depth, ZA(M), in soil where soil temperature is to be evaluated. Set ZM(10) = 0.
5. Call the soil temperature subroutine ST(ALPHA, FK, TEMPA).
6. Compute air column motion parameters, RO and TOM.
7. Compute weight of air in cell, WAA.

8. Compute depth of soil eroded per time step, DZ, after evaluating TP and VP.
9. Compute weights of soil eroded per time step for each zone, W1 and W2.
10. Compute critical index for range cutoff, ISTAR.

The second part consists of the following initializations:

1. Air temperature at ground level, TEY(1).
2. Observation time, TOBS(1).
3. Conditions for the ground level variables DDY(1), YY(1), S(1), and Q(1).
4. Logical value, QQ.
5. The values of T1, V, and PR1.
6. The air temperature variable adjacent to the ground, TE(1).
7. The cell variables at the shock front, SUMW(J), SUMWP(J), TE(J), and S(J).

The third part consists of the following calculations:

1. Compute the number of integration paths to be taken, NMAX. Compare this with storage allotment for N. If exceeded, set NMAX equal to maximum permissible value.
2. DO loop on N, the observation time variable,
   a. evaluate in which zone integration starts. If integration starts in zone 1, evaluate critical indices IS, IM, IC and proceed. If integration starts in zone 2 and if this is not the firt time this occurs, evaluate critical index IS and update M, T1, V, PR1, TE(1), SUMW(J), SUMWP(J), TE(J), and S(J). If integration starts in zone 2 for the first time, change logical value QQ and initialize M, T1, V, PR1, TE(1), SUMW(J), SUMWP(J), TE(J), and S(J). If integration starts in zone 2, evaluate IC and IM,
   b. evaluate FC.
3. DO loop on I, the transit time variable (this is a nested DO loop).
   a. transfer cell temperatures TEJ(J),
   b. compute FI and FI1,
   c. compute velocity correction VC, new time T2, and velocity V.
   d. compute observation time, TOB,
   e. compute absolute pressure, PRZ, pressure change, DP, and a related quantity, TERM2.

f. compute depth of erosion Z. Compare Z with current temperature depth interval. If exceeded, index M and/or otherwise compute current value of soil temperature TE(I).
g. compute total quantity of dust in air column, WA(I), from one of two formulas depending upon starting zone,
h. if WA(1) is very small, set Q1 = 0: otherwise set Q1 = Q0.

4. DO loop on J, the height variable (this is a double nested DO loop).

a. compute FJ,
b. determine which cloud region is applicable, then proceed to one of two groups of statements to evaluate quantity of dust in cell, SUMW(J),
c. compare J with 2 to determine if cell is adjacent to soil, then use one of two equations to compute the quantity of dust entering the cell, SUMWP(J),
d. compute the quantity of dust in air column above cell. Evaluate thermal radiation flux incident on cell, Q(J), and then compute the associated energy deposited in cell,
e. Compute new air temperature in cell, TE(J), after evaluating quantities DTN and DTE. Also estimate TERM1,
f. compute cell size, S(J), and cell center height, YY(J),
g. compute dust density in cell, DD(J). (End of J DO loop).

5. Continue in I DO loop to:

a. reinitialize T1 and P1,
b. evaluate temperature TEY(1) and dust density DDY(I) at the height YC by linear interpolation. This is done after a YC is sequentially compared with the cell height YY(J). A quantity DYY is then computed. (End of I DO loop).

Control is then returned to the main program for subsequent execution.

The major computed output variables are the observation times, TOBS(I), the air temperatures, TEY(I), and the dust densities, DDY(I), for I=1 to IMAX in steps IOUT.

A.1.11 SOTEMP Subprogram

This subroutine was written to compute the temperature distribution in the soil at the time of shock

arrival resulting from the thermal radiation flux of the fireball of a nuclear burst. Reradiation at the surface is also included in the computations. This subroutine is entered through a CALL ST(ALPHA, FK, TEMPA) statement in either of the air temperature subroutines. Execution then proceeds through three basic parts: (1) an initial computation in which a variety of numbers are generated for subsequent use, (2) computation of the temperature and and reradiation at the soil surface, and (3) computation of the temperature distribution and gradient below the surface. The first part consists of the following steps:

1. Compute the values of TEMPAS, TEMPA4, GAMMA, CONS1, CONS2.
2. Compute the time step size, DELT.
3. Compute the values of CONS3 and CONS4.
4. Compute the times, T(M).
5. Compute the incident thermal radiation flux rate, QI(M).

The second part consists of the following surface-condition steps:

1. DO loop on M, the time variable: at each time compute reradiation flux rate, QR(M), the net radiation flux rate, G(M), and the piece-wise linear G(M) curve parameters, A(M1) and B(M1).
2. Inner DO loop on I, the dummy time integration variable,
   a. sum the terms corresponding to time steps prior to M-1 that contribute to the temperature at M; compute SUM,
   b. compute by iteration the temperature at the surface corresponding to M; compute TEMP.

The third part consists of the following temperature distribution steps:

1. Set TS(1) equal to the last computed value of TEMP from the second part.
2. DO loop on N, the soil depth variable: compute the values of C1, C2, C3, C4, E1, and EF1.
3. Inner DO loop on I, the dummy time integration variable,
   a. compute the values of C5, C6, C7, I1, E2, and E3,
   b. compute the temperatures, TS(N).

Control is then returned to the calling subroutine for subsequent execution.

A.1.12 FIRBAL Subprogram

This is a function subprogram named FUNCTION PE(TMAX,T) where the argument T provides the current time at which a value is to be assigned to PE. The scaled fireball thermal power is compiled directly into the subprogram by a table of values of scaled time and scaled power listed in data statement format. The scaled time corresponding to T is computed, and then the value of PE is evaluated by a standard linear interpolation formula.

This subprogram is entered when its name is referenced in an arithmetic statement of the calling subprogram, i.e., SOTEIMP. Control and the value of PE are then returned to said arithmetic statement.

A.2 Sample Problem

Sample computer prediction results were obtained for the dust density and air-temperature environment at a sample site. The computer job consisted of three data sets to illustrate the computer program operation and provide

- uniform ground, single-burst (DUST1) dust computations,
- nonuniform ground, single-burst (DUST2) dust computations,
- uniform ground, single-burst (ATI) air-temperature computations.

The nuclear attack condition assumed was one 20-MT weapon, detonated at optimum height of burst, with a site peak overpressure of 10 psig.

The sample site was located on a quadrangle map; an overlay map was made of the area in and around the site location. The overlay map features distinctive characteristics of the locale that would be influential to the dust

and air-temperature environments at the site. Locations of the site installations, radar, missiles, and so forth, were also drawn on the overlay map. The overlay map for this sample problem is illustrated in Figure A.1.

The numbers shown on the overlay map correspond to the condition of the soil surface in that area. One might expect that different land usages would have varying effects on the soil particles that are able to rise. Each of IITRI's dust models include weight fraction terms for the erodible soils. Under varying land conditions, all of the soil may not be erodible and assumptions have to be made as to the fraction of the soil that is erodible. Table A.4 is a legend of the land usage factors used for various land usages. Table A.5 describes the particle size distribution and atmospheric variables of the sample site. The soil class numbers correspond to the soil classifications as tabulated on Table A.6.

A.2.1 Nonuniform Ground Dust Model Variables

Site input variables were determined for the dust computations for the sample site in the following manner. It was assumed that the attack azimuth is the same as the primary orientation of the radar. A line was drawn parallel to the radar orientation and through the location of the intake and exhaust ports (+). The land over which this line crosses within the 3000-ft radius is the soil surface that will contribute to the dust loading at the intake and exhaust ports. The land along this line was divided into land usage classifications. In front of the intake and exhaust ports, the land usage is:

0 to 200 ft -- Nonerodible land (1), zero soil particle contribution to the dust cloud.

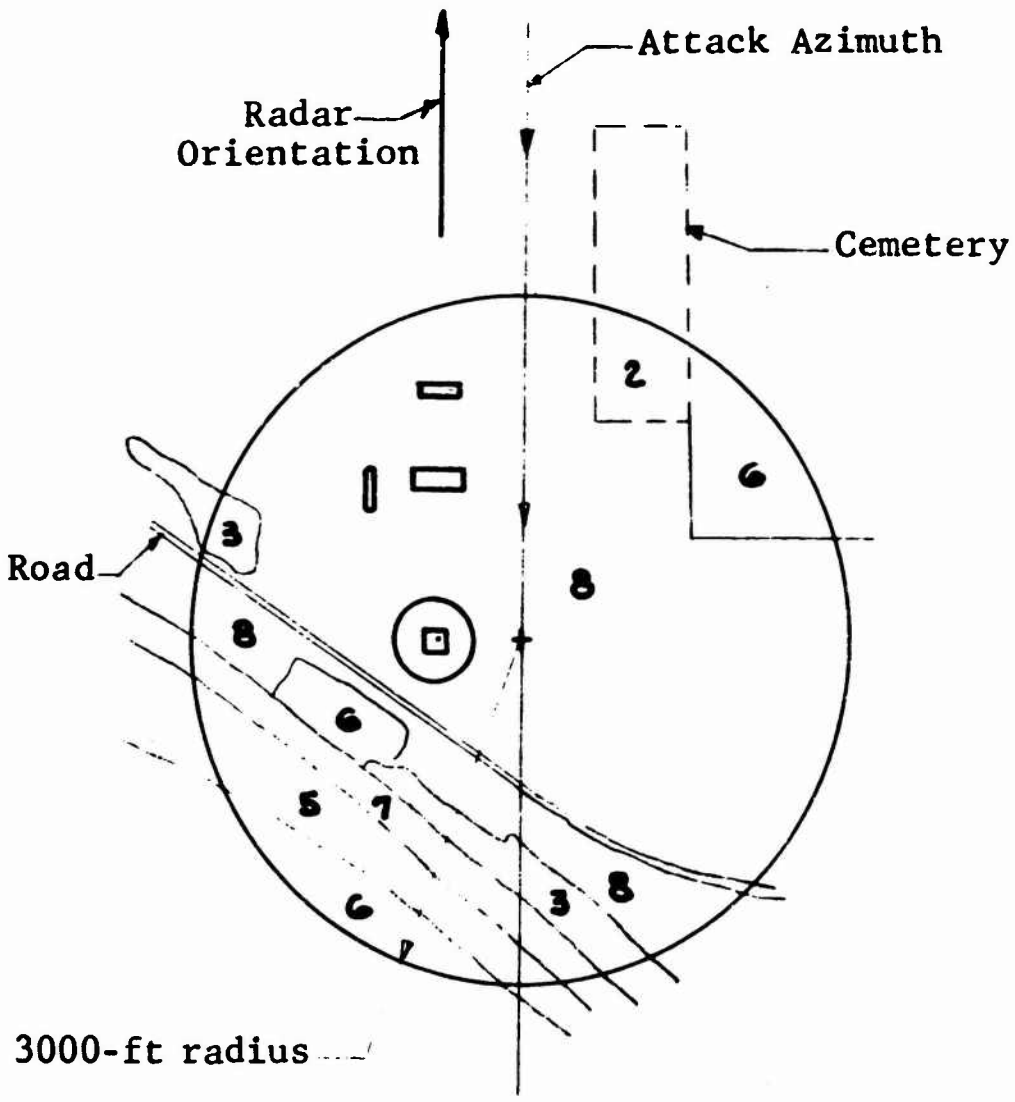

Figure A.1 Site Evaluation Sample

Table A.4 LEGEND OF LAND USAGE FACTORS

Land Classification	Land Description	Land Usage Factors
1	Launch areas, concrete roads, radiation perimeter, barren rock, 200-ft diameter around intake and exhaust ports, etc.	0 erodible soil
2	Thick grassland	0.20 of soil classes 1 and 2
3	Scrubland and woodland areas.	0.50 of all soil classes
4	Farmland, cultivated areas, orchards, beaches, etc.	1.0 of all soil classes
5	Railroads, gravel pits, etc.	1.0 of all soil classes
6	Residential and industrial areas.	0.10 of all soil classes
7	Water.	0 erodible soil
8	Undeveloped land as not classified above.	0.75 of all soil classes

Table A.5 SAMPLE SITE VARIABLES

County: Typical

Temperature:

ave. max.	74°F
yearly ave.	50°F
ave. min.	25°F

Site Elevation: 600 feet

Ave. Barometric Pressure: 14.4 psia

Mechanical Soil Analysis:

Soil Class	8	7	6	5	4	3	2	1
Particle Size (mm)	5.0	1.5	0.7	0.4	0.15	0.07	0.02	.005
Percent	0	0	1	9	53	17	16	4

Table A.6 SOIL CLASSIFICATION

Class	Classification	Size Range (mm)	Mean Diameter (mm)	Terminal Velocity (fps)
1	Clay	< 0.005	0.005	0.01
2	Silt	0.005 - 0.05	0.020	0.09
3	Very fine sand	0.05 - 0.10	0.070	1.09
4	Fine sand	0.10 - 0.25	0.150	3.99
5	Medium sand	0.25 - 0.50	0.400	11.27
6	Coarse sand	0.50 - 1.00	0.700	16.52
7	Very coarse sand	1.00 - 2.00	1.500	25.51
8	Fine gravel	2.00 - 10.00	5.00	47.56

200 to 3000 ft -- Undeveloped land (8), 0.75 of the soil particles of all class sizes will be contributed to the dust cloud.

To the rear of the intake and exhaust ports the land usage is:

0 to 200 ft -- Nonerodible land (1), zero soil particle contribution to the dust cloud.

200 to 1250 ft -- Undeveloped land (8), 0.75 of soil particles of all class sizes will be contributed to the dust cloud.

1250 to 1350 ft -- Nonerodible (1), toll road, zero soil particle contribution to dust cloud.

1350 to 1800 ft -- Undeveloped land (8), 0.75 of the soil particles of all class sizes will be contributed to the dust cloud.

1800 to 2300 ft -- Woodland (3), 0.50 of the soil particles of all class sizes will be contributed to the dust cloud.

2300 to 2700 ft -- Water (7), zero soil particle contribution to the dust cloud.

2700 to 3000 ft -- Railroad (5), 1.00 of soil class size (8) will be contributed to the dust cloud.

The particle size distribution for the site is multiplied by these land usage factors. The product is an adjusted weight fraction of the soil available for erosion in each range area.

A.2.2 Uniform Ground Dust Model Variables

Site input variables are determined for the IITRI uniform soil condition dust model in the following manner. First, no attack azimuth need be chosen as the soil conditions over the entire 3000-ft radius will be averaged; consequently, soil availability is the same for all attack azimuths. The ground conditions are averaged by determining the percent of land area that is within the 3000-ft radius, that is, in each of the land usage classifications as

defined in Table A.4. For the site example chosen (Figure A.1), the ratio of a particular land usage area to the total area within the 3000-ft radius is shown in Table A.7. For example, approximately 0.04 (4 percent) of the land is woodland area (land usage classification 3). The land usage factor for woodland is 0.50, from Table A.4. This factor multiplied by the area ratio gives 0.04 x 0.50 = 0.020, the soil multiplier. The particle size distribution for each particle size is then multiplied by the soil multiplier to obtain a weight fraction for each particle size within the land classification. The soil distribution at the sample site for particle size 4 is 0.53. Multiplying the soil distribution by the soil multiplier gives 0.53 x 0.02 = 0.0106. This number represents the weight fraction of class 4 particles contributed by the woodland areas. The weight fraction for each particle size is totaled over all land classifications. The numbers shown at the bottom of Table A.7 are the adjusted weight fractions for each particle size for the sample site.

A.2.3 Sample Site Data Input

The data input is provided according to the discussion in Section A.1.1. There are three data sets corresponding to the three types of computations performed for the sample site. Table A.8 lists the values of the variables required as input by the computer program. The FORTRAN names of all the variables are given in parentheses where they first appear in the table.

Table A.7 AVERAGE SOIL PROPERTIES FOR SAMPLE SITE

Land Usage		Area Ratio	Land Usage Factor	Soil Multi.	Soil Size Distribution							
					Cl.8	7	6	5	4	3	2	1
No	Description				0	0	.01	.09	.53	.17	.16	.04
1	Nonerodible	.03	0	0	0	0	0	0	0	0	0	0
2	Grassland	.03	.20	.006	0	0	0	0	0	0	.0010	.0002
3	Woodland	.04	.50	.020	0	0	.0002	.0018	.0106	.0034	.0032	.0008
5	Railroads	.03	1.00	.030	.0300	0	0	0	0	0	0	0
6	Residential	.05	.10	.005	0	0	.0001	.0005	.0027	.0009	.0009	.0002
7	Water	.02	0	0	0	0	0	0	0	0	0	0
8	Undeveloped	.80	.75	.600	0	0	.0060	.0540	.3180	.1020	.0900	.0240
Adjusted Weight Fraction					.0300	0	.006	.056	.331	.105	.095	.025

Table A.8 SAMPLE SITE DATA INPUT

First Data Set (DUST1 Computation)

1. SAMPLE CALCULATION 1 1 F
(TITLE) (IOUT) (RUNTYP) (TAPSAV)

2. 50 1 1 7 0 0 0.00 0.00 2.00
(IMAX) (NY) (NB) (NCLASS) (NZF) (NZB) (TB2) (TB3) (DTOBS)

3. 160.0 100.0 50.0 14.40 0.20 0.00006
(RHO) (RHOTOT) (TEMPA) (PRESA) (KM) (A)

4. 20.000 10.000 -1.0 0.0 1.0
(YIELD) (PRESO) (HOB) (HOBS) (HOBO)

5. 0.005 0.020 0.070 0.150 0.400 0.700 5.000
(D(N),N=1,...,NCLASS)

6. 0.025 0.095 0.106 0.331 0.056 0.006 0.000
(P(N,NN),N=1,...,NCLASS,NN=1,...,NZF+NZB+1)

7. 10.000
(Y(N),N=1,...,NY)

Second Data Set (DUST2 Computation)

1. SAMPLE COMPUTATION 2 1 F

2. 50 1 1 7 1 6 0.00 0.00 2.00

3. 160.0 100.0 50.0 14.40 0.20 0.00006

4. 20.000 10.000 -1.0 0.0 1.0

5. 0.005 0.020 0.070 0.150 0.400 0.700 5.000

Table A.8 (continued)

6.	0.000	0.000	0.000	0.000	0.000	0.000	0.000
7.	0.030	0.120	0.130	0.400	0.070	0.010	0.000
8.	0.030	0.120	0.130	0.400	0.070	0.010	0.000
9.	0.000	0.000	0.000	0.000	0.000	0.000	0.000
10.	0.030	0.120	0.130	0.400	0.070	0.010	0.000
11.	0.020	0.080	0.090	0.270	0.050	0.010	0.000
12.	0.000	0.000	0.000	0.000	0.000	0.000	0.000
13.	0.000	0.000	0.000	0.000	0.000	0.000	1.000
14.	10.000						
15.	200.00 (RZF(N),N=1,...,NZF)						
16.	200.00 (RZB(N),N=1,...,NZB)	1250.00	1350.00	1800.00	2300.00	2700.00	

Third Data Set (AT1 Computation)

1.	SAMPLE COMPUTATION				5	8	F				
2.	0.100 (FK)	0.007 (ALPHA)	2.000 (BETA)	0.200 (C)	10.00 (TM)	10.00 (YC)	0.661 (UF)	0.600 (ZM)	0.000 (P1)	0.000 (P2)	0.0 (RC)
3.	160.0	100.0		50.0		14.40	0.20	0.00006			
4.	20.000	10.000		-1.0		0.0	1.0				

B.2.4 Sample Site Computer Output

1-D COMPUTATION OF THE DUST CLOUD ENVIRONMENT GENERATED BY EXPLOSION INDUCED WIND - 1 BURST(S)

(SAMPLE COMPUTATION)

AMBIENT PRESSURE	(PSIA)	= 14.40	PARTICLE DENSITY	(LB/CU-FT)	= 150.0	TRANSPORT COEFFICIENT		= 0.20
AMBIENT TEMPERATURE	(DEGF)	= 50.0	BULK SOIL DENSITY	(LB/CU-FT)	= 100.0	EROSION COEFFICIENT		= 0.00006
WEAPON YIELD	(MT)	= 20.00	PEAK WIND VELOCITY	(FPS)	= 435.4	SHOCK VELOCITY	(FPS)	= 1400.2
SITE OVERPRESSURE	(PSIG)	= 10.00	POSITIVE PHASE DURATION	(SEC)	= 9.69	AIR DENSITY	(LB/CU-FT)	= 0.09346
HEIGHT-OF-BURST	(FT)	= 21391.9	WIND DECAY EXPONENT		= 1.000			

PARTICLE CLASS	SIZE (MM)	TERMINAL VELOCITY (FPS)	ADJUSTED WEIGHT FRACTION
1	0.005	0.006	0.025
2	0.020	0.093	0.095
3	0.070	1.094	0.106
4	0.150	4.035	0.331
5	0.400	11.523	0.056
6	0.700	16.940	0.006
7	5.000	48.874	0.000

TIME VARIATION OF ACCUMULATED DUST CLOUD DENSITY AT AN ELEVATION OF 10.0 FT

TIME (SEC)	TOTAL DENSITY (LB/CU-FT)	DENSITY (LB/CU-FT) PER PARTICLE SIZE CLASS						
CLASS /		1	2	3	4	5	6	7
2.00	0.07053	0.0029	0.0111	0.0123	0.0376	0.0060	0.0006	0.0000
4.00	0.08496	0.0035	0.0134	0.0148	0.0452	0.0071	0.0007	0.0000
6.00	0.09012	0.0036	0.0143	0.0158	0.0480	0.0075	0.0007	0.0000
8.00	0.09173	0.0039	0.0146	0.0162	0.0489	0.0074	0.0007	0.0000
10.00	0.09136	0.0039	0.0147	0.0162	0.0487	0.0072	0.0007	0.0000
12.00	0.09117	0.0039	0.0148	0.0163	0.0485	0.0069	0.0006	0.0000
14.00	0.09181	0.0040	0.0150	0.0165	0.0490	0.0068	0.0005	0.0000
16.00	0.09295	0.0040	0.0153	0.0168	0.0496	0.0067	0.0005	0.0000
18.00	0.09433	0.0041	0.0156	0.0171	0.0504	0.0067	0.0005	0.0000
20.00	0.09580	0.0042	0.0159	0.0174	0.0512	0.0067	0.0004	0.0000
22.00	0.09723	0.0043	0.0162	0.0177	0.0520	0.0067	0.0004	0.0000
24.00	0.09857	0.0043	0.0164	0.0180	0.0528	0.0067	0.0003	0.0000
26.00	0.09976	0.0044	0.0167	0.0183	0.0534	0.0067	0.0003	0.0000
28.00	0.10079	0.0045	0.0169	0.0185	0.0541	0.0067	0.0002	0.0000
30.00	0.10163	0.0045	0.0171	0.0187	0.0546	0.0066	0.0001	0.0000
32.00	0.10235	0.0046	0.0173	0.0189	0.0551	0.0066	0.0000	0.0000
34.00	0.10300	0.0046	0.0174	0.0191	0.0554	0.0065	0.0000	0.0000
36.00	0.10350	0.0046	0.0176	0.0192	0.0558	0.0063	0.0000	0.0000
38.00	0.10386	0.0047	0.0177	0.0193	0.0560	0.0061	0.0000	0.0000
40.00	0.10409	0.0047	0.0178	0.0195	0.0562	0.0059	0.0000	0.0000
42.00	0.10417	0.0047	0.0179	0.0195	0.0563	0.0057	0.0000	0.0000
44.00	0.10413	0.0047	0.0180	0.0196	0.0564	0.0054	0.0000	0.0000
46.00	0.10395	0.0048	0.0181	0.0197	0.0560	0.0050	0.0000	0.0000
48.00	0.10363	0.0048	0.0181	0.0198	0.0564	0.0045	0.0000	0.0000
50.00	0.10314	0.0048	0.0182	0.0198	0.0564	0.0040	0.0000	0.0000
52.00	0.10245	0.0048	0.0182	0.0198	0.0563	0.0033	0.0000	0.0000
54.00	0.10150	0.0048	0.0183	0.0199	0.0561	0.0024	0.0000	0.0000
56.00	0.10015	0.0048	0.0183	0.0199	0.0560	0.0011	0.0000	0.0000
58.00	0.09893	0.0048	0.0184	0.0199	0.0558	0.0000	0.0000	0.0000
60.00	0.09877	0.0048	0.0184	0.0199	0.0556	0.0000	0.0000	0.0000
62.00	0.09859	0.0049	0.0184	0.0199	0.0554	0.0000	0.0000	0.0000
64.00	0.09837	0.0049	0.0184	0.0199	0.0551	0.0000	0.0000	0.0000
66.00	0.09813	0.0049	0.0184	0.0199	0.0549	0.0000	0.0000	0.0000
68.00	0.09786	0.0049	0.0185	0.0199	0.0546	0.0000	0.0000	0.0000
70.00	0.09757	0.0049	0.0185	0.0199	0.0543	0.0000	0.0000	0.0000
72.00	0.09726	0.0049	0.0185	0.0199	0.0540	0.0000	0.0000	0.0000
74.00	0.09693	0.0049	0.0185	0.0199	0.0536	0.0000	0.0000	0.0000
76.00	0.09659	0.0049	0.0185	0.0199	0.0533	0.0000	0.0000	0.0000
78.00	0.09622	0.0049	0.0185	0.0199	0.0529	0.0000	0.0000	0.0000
80.00	0.09584	0.0049	0.0185	0.0199	0.0526	0.0000	0.0000	0.0000
82.00	0.09544	0.0049	0.0185	0.0199	0.0522	0.0000	0.0000	0.0000
84.00	0.09503	0.0049	0.0185	0.0198	0.0518	0.0000	0.0000	0.0000
86.00	0.09461	0.0049	0.0185	0.0198	0.0514	0.0000	0.0000	0.0000
88.00	0.09417	0.0049	0.0185	0.0198	0.0509	0.0000	0.0000	0.0000
90.00	0.09371	0.0049	0.0185	0.0198	0.0505	0.0000	0.0000	0.0000
92.00	0.09325	0.0049	0.0185	0.0198	0.0501	0.0000	0.0000	0.0000
94.00	0.09276	0.0049	0.0185	0.0198	0.0496	0.0000	0.0000	0.0000
96.00	0.09227	0.0049	0.0185	0.0197	0.0491	0.0000	0.0000	0.0000
98.00	0.09176	0.0049	0.0185	0.0197	0.0486	0.0000	0.0000	0.0000
100.00	0.09123	0.0049	0.0185	0.0197	0.0481	0.0000	0.0000	0.0000

2-D COMPUTATION OF THE DUST CLOUD ENVIRONMENT GENERATED BY EXPLOSION INDUCED WIND - 1 BURST(S)

(SAMPLE COMPUTATION)

AMBIENT PRESSURE (PSIA) = 14.40
AMBIENT TEMPERATURE (DEGF) = 50.0

WEAPON YIELD (MT) = 20.00
SITE OVERPRESSURE (PSIG) = 10.00
HEIGHT-OF-BURST (FT) = 21391.8

PARTICLE DENSITY (LB/CU-FT) = 160.0
BULK SOIL DENSITY (LB/CU-FT) = 100.0

PEAK WIND VELOCITY (FPS) = 435.4
POSITIVE PHASE DURATION (SEC) = 9.69
WIND DECAY EXPONENT = 1.000

TRANSPORT COEFFICIENT = 0.26
EROSION COEFFICIENT = 0.00006

SHOCK VELOCITY (FPS) = 1400.2
AIR DENSITY (LB/CU-FT) = 0.09346

PARTICLE CLASS /		1	2	3	4	5	6	7
SIZE (MM) /		0.005	0.020	0.070	0.150	0.400	0.700	5.000
TERMINAL VELOCITY (FPS) /		0.006	0.093	1.094	4.035	11.523	16.940	48.679
ZONE BOUNDARY (FT)	ZONE	ADJUSTED WEIGHT FRACTION						
1752.49	1	0.030	0.120	0.130	0.400	0.070	0.010	0.000
200.00	2	0.000	0.000	0.000	0.000	0.000	0.000	0.000
-200.00	3	0.030	0.120	0.130	0.400	0.070	0.010	0.000
-1250.00	4	0.000	0.000	0.000	0.000	0.000	0.000	0.000
-1350.00	5	0.030	0.120	0.130	0.400	0.070	0.010	0.000
-1800.00	6	0.020	0.080	0.090	0.270	0.050	0.010	0.000
-2300.00	7	0.000	0.000	0.000	0.000	0.000	0.000	0.000
-2700.00	8	0.000	0.000	0.000	0.000	0.000	0.000	1.000

TIME VARIATION OF ACCUMULATED DUST CLOUD DENSITY AT AN ELEVATION OF 10.0 FT

TIME (SEC)	TOTAL DENSITY (LB/CU-FT)	DENSITY (LB/CU-FT) PER PARTICLE SIZE CLASS CLASS / 1	2	3	4	5	6	7
2.00	0.06338	0.0025	0.0100	0.0109	0.0334	0.0058	0.0008	0.0000
4.00	0.07780	0.0030	0.0122	0.0132	0.0410	0.0073	0.0011	0.0000
6.00	0.08593	0.0033	0.0132	0.0144	0.0453	0.0085	0.0012	0.0000
8.00	0.09376	0.0035	0.0140	0.0155	0.0503	0.0093	0.0012	0.0000
10.00	0.09725	0.0035	0.0141	0.0157	0.0539	0.0090	0.0011	0.0000
12.00	0.08972	0.0031	0.0124	0.0140	0.0505	0.0087	0.0010	0.0000
14.00	0.07836	0.0026	0.0105	0.0119	0.0439	0.0085	0.0009	0.0000
16.00	0.06244	0.0020	0.0081	0.0092	0.0338	0.0084	0.0008	0.0000
18.00	0.06842	0.0026	0.0104	0.0113	0.0351	0.0083	0.0007	0.0000
20.00	0.07646	0.0030	0.0119	0.0128	0.0398	0.0083	0.0007	0.0000
22.00	0.08304	0.0033	0.0131	0.0142	0.0443	0.0076	0.0006	0.0000
24.00	0.08781	0.0035	0.0142	0.0154	0.0480	0.0062	0.0006	0.0000
26.00	0.08790	0.0036	0.0145	0.0157	0.0491	0.0044	0.0005	0.0000
28.00	0.09121	0.0038	0.0151	0.0164	0.0516	0.0040	0.0003	0.0000
30.00	0.09366	0.0039	0.0155	0.0168	0.0532	0.0041	0.0002	0.0000
32.00	0.09641	0.0040	0.0159	0.0174	0.0550	0.0041	0.0000	0.0000
34.00	0.10004	0.0041	0.0163	0.0179	0.0571	0.0046	0.0000	0.0000
36.00	0.10183	0.0041	0.0166	0.0182	0.0585	0.0044	0.0000	0.0000
38.00	0.10272	0.0042	0.0166	0.0183	0.0595	0.0042	0.0000	0.0000
40.00	0.10225	0.0041	0.0163	0.0180	0.0601	0.0038	0.0000	0.0000
42.00	0.10036	0.0040	0.0160	0.0178	0.0596	0.0029	0.0000	0.0000
44.00	0.10215	0.0041	0.0162	0.0181	0.0607	0.0031	0.0000	0.0000
46.00	0.10288	0.0041	0.0165	0.0185	0.0612	0.0025	0.0000	0.0000
48.00	0.10058	0.0041	0.0166	0.0186	0.0606	0.0006	0.0000	0.0000
50.00	0.09964	0.0041	0.0166	0.0188	0.0601	0.0000	0.0000	0.0000
52.00	0.09968	0.0042	0.0167	0.0190	0.0599	0.0000	0.0000	0.0000
54.00	0.10053	0.0042	0.0169	0.0193	0.0601	0.0000	0.0000	0.0000
56.00	0.10257	0.0043	0.0173	0.0199	0.0611	0.0000	0.0000	0.0000
58.00	0.10106	0.0043	0.0171	0.0199	0.0598	0.0000	0.0000	0.0000
60.00	0.10071	0.0043	0.0172	0.0202	0.0591	0.0000	0.0000	0.0000
62.00	0.10117	0.0043	0.0172	0.0205	0.0592	0.0000	0.0000	0.0000
64.00	0.10142	0.0043	0.0174	0.0209	0.0587	0.0000	0.0000	0.0000
66.00	0.10201	0.0044	0.0176	0.0214	0.0587	0.0000	0.0000	0.0000
68.00	0.10145	0.0043	0.0176	0.0216	0.0560	0.0000	0.0000	0.0000
70.00	0.10177	0.0044	0.0177	0.0220	0.0576	0.0000	0.0000	0.0000
72.00	0.10002	0.0044	0.0176	0.0222	0.0558	0.0000	0.0000	0.0000
74.00	0.09936	0.0044	0.0176	0.0224	0.0550	0.0000	0.0000	0.0000
76.00	0.09922	0.0044	0.0178	0.0227	0.0544	0.0000	0.0000	0.0000
78.00	0.09804	0.0044	0.0178	0.0227	0.0532	0.0000	0.0000	0.0000
80.00	0.09590	0.0044	0.0178	0.0226	0.0511	0.0000	0.0000	0.0000
82.00	0.09820	0.0044	0.0179	0.0227	0.0533	0.0000	0.0000	0.0000
84.00	0.10194	0.0044	0.0179	0.0226	0.0570	0.0000	0.0000	0.0000
86.00	0.10217	0.0044	0.0178	0.0225	0.0575	0.0000	0.0000	0.0000
88.00	0.10166	0.0044	0.0178	0.0225	0.0570	0.0000	0.0000	0.0000
90.00	0.10120	0.0044	0.0179	0.0224	0.0565	0.0000	0.0000	0.0000
92.00	0.10050	0.0044	0.0179	0.0224	0.0558	0.0000	0.0000	0.0000
94.00	0.10060	0.0044	0.0182	0.0227	0.0553	0.0000	0.0000	0.0000
96.00	0.09683	0.0044	0.0182	0.0226	0.0516	0.0000	0.0000	0.0000
98.00	0.09554	0.0044	0.0182	0.0226	0.0503	0.0000	0.0000	0.0000
100.00	0.09428	0.0044	0.0183	0.0225	0.0490	0.0000	0.0000	0.0000

AIR TEMPERATURE AND DUST DENSITY IN A BLAST INDUCED DUST CLOUD
UNIFORM GROUND CONDITIONS WITH EROSION DEPTH CUT-OFF
SINGLE BURST

WEAPON YIELD	20.00	(MT)
OVERPRESSURE	10.00	(PSIG)
AMBIENT PRESSURE	14.40	(PSIA)
AMBIENT TEMPERATURE	50.00	(DEGF)
HEIGHT-OF-BURST	21391.8	(FT)
DUST PARTICLE DENSITY	160.0	(LB/CU FT)
BULK DENSITY OF SOIL	100.0	(LB/CU FT)
LAND USE FACTOR	0.661	-
EROSION DEPTH CUT-OFF	0.60	(IN)
PARTICLE SPECIFIC HEAT	0.200	(BTU/LB)
SOIL CONDUCTIVITY	0.100	(BTU/FT-HR-DEGF)
SOIL DIFFUSIVITY	0.007	(SQ FT/HR)
EROSION COEFFICIENT	0.00006	-
TRANSPORT COEFFICIENT	0.20	-
HEAT TRANSFER RESPONSE TIME	10.0	(MSEC)

AIR TEMPERATURE AND DUST DENSITY AT AN ELEVATION OF 10.00 FEET

TIME (SEC)	TEMPERATURE (DEGREES F)	DUST DENSITY (LB/CU FT)
C.C	135.5	0.0
C.056	133.9	0.0
C.113	133.5	0.0047
C.171	132.4	0.0146
C.23C	131.6	0.0241
C.291	137.5	0.0322
C.353	16C.6	0.0377
C.417	205.C	0.0403
C.482	26C.7	0.0409
C.549	313.7	0.0408
C.617	357.4	0.0407
C.687	389.9	0.0407
C.759	413.4	0.0409
C.832	430.8	0.0411
C.908	438.8	0.0416
C.986	439.9	0.0423
1.065	437.9	0.0431
1.147	433.3	0.0440
1.231	42C.1	0.0452
1.318	405.3	0.0466
1.4C7	389.1	0.0480
1.498	371.3	0.0495
1.593	348.8	0.0515
1.691	325.9	0.0535
1.791	302.7	0.0557
1.896	279.C	0.0580
2.CC3	255.9	0.0574
2.115	231.5	0.0542
2.231	223.C	0.0511
2.351	211.3	0.0481
2.476	201.5	0.0455

2.606	193.1	0.0431
2.741	185.8	0.0410
2.883	179.3	0.0390
3.031	173.5	0.0373
3.186	168.1	0.0357
3.350	163.2	0.0342
3.522	158.6	0.0329
3.705	154.3	0.0317
3.899	150.3	0.0305
4.106	146.4	0.0294
4.328	142.7	0.0284
4.567	139.1	0.0275
4.828	135.6	0.0266
5.114	132.2	0.0258
5.434	128.7	0.0250
5.795	125.3	0.0243
6.216	121.9	0.0236
6.727	118.2	0.0230
7.399	114.3	0.0223
8.529	109.4	0.0217
11.630	102.1	0.0211
12.847	100.1	0.0206
13.796	98.8	0.0201
14.625	97.8	0.0196
15.385	97.1	0.0192

A.3 Computer Program

```
      COMPUTATION OF DUST CLOUD AND AIR TEMPERATURE ENVIRONMENT
      CAPABILITY - EXECUTIVE CONTROL OF CODE EXECUTION / INPUT
            COMMON /DUSTAT/ A,HOB,KH,KV,PRESO,RHO,RHOF,RHOTOT,TO,U,VO,YIELD
           1        /DUST/   CUTOFF,D(8),P(8,41),DTOBS,DY(201,3),DYC(201,8,3),
           2                 HSTAR(500),IMAX,NCLASS,NY,TOBS(201),VT(8),Y(3)
           3        /TWODEE/ NZB,NZF,NZR,NZR1,RZB(20),RZF(20),R2(41)
           4        /MULTI/  HOB1,HOB2,HOB3,KV1,KV2,KV3,PRESO1,PRESO2,PRESO3,
           5                 NB,RHOF1,RHOF2,RHOF3,TB2,TB3,TO1,TO2,TO3,U1,U2,U3,
           6                 VO1,VO2,VO3,YIELD1,YIELD2,YIELD3
           7        /ATVAR/  ALPHA,BETA,C,FK,P1,P2,RC,TM,UF,YC,ZM
           8        /WEVAR/  CONSW1,COSTH,CP1,CP2,CP3,RHOS,TASITE,TES,TMAX,TOP
           9        /MISC/   NDIMEN,PRESA,RUNTYP,TAPSAV,TEMPA,TITLE(18)
            INTEGER RUNTYP
            REAL    KH,KV,KV1,KV2,KV3
            LOGICAL CUTOFF,TAPSAV
     1      READ (5,2) TITLE,RUNTYP,IOUT,TAPSAV
     2      FORMAT (18A4,2I2,L2)
            CUTOFF=.TRUE.
            IF (RUNTYP .GE. 5)   GO TO 4
            READ (5,3) IMAX,NY,NB,NCLASS,NZF,NZB,TB2,TB3,DTOBS
     3      FORMAT (6I5,3F7.2)
            IF (RUNTYP .NE. 4)   GO TO 6
            READ (5,12) TMAX,DT,W,ANG
            GO TO 6
     4      READ (5,5) FK,ALPHA,BETA,C,TM,YC,UF,ZM,P1,P2,RC
     5      FORMAT (4F7.3,2F7.2,4F7.3,F7.1)
     6      READ (5,7) RHO,RHOTOT,TEMPA,PRESA,KH,A
     7      FORMAT (2F7.1,F5.1,F6.2,F5.2,F8.5)
            IF (RUNTYP .EQ. 3)   GO TO 8
            READ (5,9) YIELD,PRESO,HOB,HOBS,HOBO
            IF (RUNTYP .EQ. 4)   GO TO 10
            CALL WE (YIELD,PRESO,HOB,HOBS,HOBO,RHOF,TO,VO,U,KV)
            GO TO 10
     8      READ (5,9) YIELD1,PRESO1,HOB1,HOBS1,HOBO1
            CALL WE (YIELD1,PRESO1,HOB1,HOBS1,HOBO1,RHOF1,TO1,VO1,U1,KV1)
```

```
      READ (5,9) YIELD2,PRESD2,HOB2,HOBS2,HOBD2
      CALL WE (YIELD2,PRESD2,HOB2,HOBS2,HOBD2,RHOF2,T02,V02,U2,KV2)
      RHOF3=0.
      U3=0.
      IF (NB .LT. 3)   GO TO 10
      READ (5,9) YIELD3,PRESD3,HOB3,HOBS3,HOBD3
      CALL WE (YIELD3,PRESD3,HOB3,HOBS3,HOBD3,RHOF3,T03,V03,U3,KV3)
9     FORMAT (2F7.3,2F8.1,F4.1)
10    IF (RUNTYP .GE. 5)   GO TO 13
      READ (5,12) (D(N),N=1,NCLASS)
      NZR=NZF+NZB
      NZR1=NZR+1
      DO 11   NN=1,NZR1
11    READ (5,12) (F(N,NN),N=1,NCLASS)
      READ (5,12) (Y(N),N=1,NY)
      IF (RUNTYP .NE. 2)   GO TO 13
      READ (5,12) (RZF(N),N=1,NZF)
      READ (5,12) (RZB(N),N=1,NZB)
12    FORMAT (9F8.3)
13    GO TO (14,15,16,17,18,19),RUNTYP
14    CALL DUST1
      NDIMEN=1
      GO TO 20
15    CALL DUST2
      NDIMEN=2
      GO TO 20
16    CALL DUST3
      NDIMEN=1
      GO TO 20
17    CALL DUST4 (PRESA,TEMPA,HOBS,HOBO,TMAX,DT,W,ANG)
      GO TO 1
18    CALL AT1 (IOUT)
      GO TO 1
19    CALL AT2 (IOUT)
      GO TO 1
```

```
20    CALL OUT (ICUT)
      GO TO 1
      END
```

```
      SUBROUTINE WE (YIELD,PRESC,HOB,HOBS,HOBO,RHOF,TO,VO,U,KV)
      COMMON /WEVAR/  CONSW1,COSTH,CP1,CP2,CP3,RHOS,TASITE,TES,TMAX,TOP
     1       /MISC/   NDIMEN,PRESA,RUNTYP,TAPSAV,TEMPA,TITLE(18)
      DIMENSION HOBI(14),CPTI(14)
     DATA HOBI/0.,1320.,1848.,2640.,3696.,5280.,7920.,
     110560.,15840.,26400.,52800.,105600.,158400.,1000000./,
     2CPTI/0.0310,0.0310,0.0443,0.0603,0.0777,0.0952,0.1130,
     30.1239,0.1341,0.1426,0.1531,0.1662,0.1680,0.1680/
      INTEGER RUNTYP
      REAL KV
      LOGICAL TAPSAV
      TEMPAS = TEMPA+460.
      CRY = YIELD**.333
      PSF = (PRESA/14.7)**.333
      TSF = SQRT(TEMPAS/530.)
      SOP = 14.7*PRESC/PRESA
      CVELA = SQRT(2410.*TEMPAS)
      XI = 1.+PRESC/PRESA
      SRB = 5800.-30.*SOP+3900./EXP(.05*SOP)
      SRC = 70000./SOP**.68
      SQRTW = SQRT(YIELD)
      KV = .0877*SOP-.3
      IF (KV .LT. 1.)   KV = 1.
      IF (SOP .GE. 30.)   GO TO 201
      TC = (3.59-.0107*SOP)*CRY/TSF/PSF
      GO TO 202
  201 TC = (4.125-.0285*SOP)*CRY/TSF/PSF
  202 RHOF = 9.45*PRESA*(1.+XI)/(6.+XI)/TEMPAS
      IF (HOB .GE. -.1)   GO TO 210
      IF (HOBS .GT. .00001)   GO TO 212
      IF (HOBO .GT. .1)   GO TO 214
  208 SHOB = 32500./SOP**.414
      HOB = SHOB*CRY/PSF
      GO TO 240
  210 SHOB = HOB*PSF/CRY
```

```
      GC TO 216
  212 SHCB = HOBS*PSF
      HOB = HOBS*CRY
      GC TO 216
  214 SHCB = SRB
      HCB = SHOB*CRY/PSF
      GC TO 218
  216 IF (SHOB .GT. SRB)   GC TO 230
  218 U = CVELA*SQRT(.143+.857*XI)
      VC = 1.89*CVELA*(XI-1.)/SQRT(1.+6.*XI)
      TASITE = (79./SCP**.88)*(.4+.6*SHOB/SRB)*CRY/TSF/PSF
      SRA = 34000./SCP**.518
      THETA = ATAN(SRA/SHOB+(SRC-SRA)/SRB)
      IF (SHOB .LT. .CC0001)   THETA = 1.570796
      GC TO 250
  230 SRD = 32500./SCP**.414
      IF (SHOB .GE. SRD)   GC TO 208
      CF = SIN(ATAN(SRC/SRB))
      THETA = ATAN(SRC*(SRD-SHOB)/(SRD-SRB)/SHOB)
      U = CVELA*SQRT(.143+.857*XI)*CF/SIN(THETA)
      VC = 1.89*CVELA*(XI-1.)*SIN(THETA)/(CF*SQRT(1.+6.*XI))
      SRE = .5*(SRD+SRB)
      IF (SHOB .LT. SRE)   GC TO 232
      TASITE = (30./SCP**.672)*CRY/TSF/PSF
      GC TO 250
  232 T1 = 30./SOP**.672
      T2 = 79./SOP**.88
      TASITE = (T1+(T2-T1)*(SRE-SHOB)/(SRE-SRB))*CRY/TSF/PSF
      GC TO 250
  240 U = 10.**20
      VC = 0.
      THETA = 0.
      HCB = (32500./SCP**.414)*CRY/PSF
      TASITE = (30./SCP**.672)*CRY/TSF/PSF
  250 IF (RUNTYP .LT. 5)   RETURN
```

```
      TMAX = 1.01193*SQRTW
      TES = TEMPAS*X1*(6.+XI)/(1.+6.*XI)-460.
      RHOS = 2.7*PRESA*(1.+6.*XI)/(6.+XI)/TEMPAS
      TOP = (2.5-.024*SOP+1.5/EXP(.16*SOP))*CRY/TSF/PSF
      CP1 = .092*SOP**.328
      CP2 = .398*SOP**.318
      CP3 = 3.13*SOP**.262
      COSTH = COS(THETA)
      SRANGE = HOB/COSTH
      IF (HOB .LT. .00001)    SRANGE = SRA*CRY/PSF
      DO 260   N=1,14
      IF (HOBI(N)-HOB)   260,270,280
  260 CONTINUE
  270 OPT = OPTI(N)
      GO TO 290
  280 N1 = N-1
     OOPT = OPTI(N1)+(HOB-HOBI(N1))*(OPTI(N)-OPTI(N1))/
     1(HOBI(N)-HOBI(N1))
  290  TAU = EXP(-OPT/COSTH)
      CONSN1 = 3.994467E10*TAU*SQRTW*COSTH/SRANGE**2
      RETURN
      END
```

```
      SUBROUTINE DUST1
C COMPUTATION OF THE DUST CLOUD FOR A SINGLE BURST
C CONDITIONS - UNIFORM GROUND / EIGHT PARTICLE CLASSES
      COMMON /DUSTAT/ A,HOB,KH,KV,PRESU,RHO,RHOF,RHOTOT,TO,U,VO,YIELD
     1       /DUST/   CUTOFF,D(8),P(8,41),DTOBS,DY(201,3),DYC(201,8,3),
     2                HSTAR(500),IMAX,NCLASS,NY,TOBS(201),VT(8),Y(3)
      REAL     KH,KV
      LOGICAL CUTOFF
      RC=TO/(KV*KV/(VO*(EXP(-KV)+KV-1.))-1./U)
      TAC=RO/U
      TOM=TO+TAO
      TAU=TOM/KV
      DO 101    I=1,NCLASS
      TERM1=.097256/(RHOF*D(I))
  101 VT(I)=SQRT(TERM1*TERM1+.281424*D(I)*RHO/RHOF)-TERM1
      IF (VO .GE. 10.)   GO TO 102
      CUTOFF=.FALSE.
      GO TO 109
  102 I1=TO/DTOBS
      CONS1=2.*A*RHOTOT/KH
      FK1=KV/(VO*TAU)
      FK2=1.-KV
      FK6=1./(TAU*U)
      DO 103    I=1,200
      DO 103    L=1,3
      DY(I,L)=0.
      DO 103    N=1,8
  103 DYC(I,N,L)=0.
      DO 108    I=1,IMAX
      TOBS(I)=DTOBS*FLOAT(I)
      CONS=(KV*(TOBS(I)+TAO))/TOM
      R=RO
  104 FK7=FK6*R-CONS
      FK=(RO-R)*FK1+FK2-EXP(FK7)*(FK2-FK7)
      FKP=-FK1+EXP(FK7)*FK6+FK6*(FK-(RO-R)*FK1+FK2)
```

```
      DR=-FK/FKP
      R=R+DR
      IF (ABS(DR) .GT. 1.)    GO TO 104
      T=TAO+TOBS(I)-R/U
      IF (I .GT. I1)    GO TO 105
      HST=KH*(RO-R)
      GO TO 106
  105 HST=KH*(RO+R)
  106 DO 107    N=1,NCLASS
      H=HST-VT(N)*T
      DO 107    L=1,NY
      IF (H .LE. Y(L))    GO TO 107
      X=Y(L)/H
      DYC(I,N,L)=CONS1*(X-1. ALOG(X))*P(N,1)
  107 CONTINUE
      DO 108    L=1,NY
      DO 108    N=1,NCLASS
  108 DY(I,L)=DY(I,L)+DYC(I,N,L)
  109 RETURN
      END
```

```
      SUBROUTINE DUST2
COMPUTATION OF THE DUST CLOUD FOR A SINGLE BURST
CONDITIONS - VARIABLE GROUND / EIGHT PARTICLE CLASSES
      COMMON /DUSTAT/ A,HOB,KH,KV,PRESO,RHO,RHOF,RHOTOT,TO,U,VO,YIELD
     1       /DUST/   CUTOFF,D(8),P(8,41),DTOBS,DY(201,3),DYC(201,8,3),
     2                HSTAR(500),IMAX,NCLASS,NY,TOBS(201),VT(8),Y(3)
     3       /TWODEE/ NZB,NZF,NZR,NZR1,RZB(20),RZF(20),R2(41)
     DIMENSION DIS(500),DT1(200),H1(200),JMAX(200),R1(200),
     1          TI(500),VEL(500)
      REAL KH,KV
      LOGICAL CUTOFF
      RO=TO/(KV*KV/(VO*(EXP(-KV)+KV-1.))-1./U)
      TAO=RO/U
      TOM=TO+TAO
      TAU=TOM/KV
      DO 201   I=1,NCLASS
      TERM1=.097256/(RHOF*D(I))
  201 VT(I)=SQRT(TERM1*TERM1+.281424*D(I)*RHO/RHOF)-TERM1
      IF (VO .GE. 10.)   GO TO 202
      CUTOFF=.FALSE.
      GO TO 219
  202 DT=DTOBS*FLOAT(IMAX)/500.
      CONS1=A*RHOTOT*DT
      ICRIT=TO/DTOBS
      JCRIT=TOM/DT
      FK1=KV/(VO*TAU)
      FK2=1.-KV
      FK3=1.-1./KV
      FK4=KH*VO*TOM/KV
      FK5=2.*KH*RO
      FK6=1./(TAU*U)
      NZF1=NZF+1
      DO 203   I=1,NZF
      J=NZF1-I
  203 R2(I)=RO-RZF(J)
```

```
      DO 204    I=NZF1,NZR
      J=I-NZF
204   R2(I)=RO+RZB(J)
      R2(NZR1)=10.**2C
      DO 207    I=1,IMAX
      TOBS(I)=DTOBS*FLCAT(I)
      CONS=(KV*(TOBS(I)+TAO))/TOM
      RA=RO
205   FK7=FK6*RA-CONS
      FK=(RO-RA)*FK1+FK2-EXP(FK7)*(FK2-FK7)
      FKP=-FK1+EXP(FK7)*FK6+FK6*(FK-(RO-RA)*FK1+FK2)
      DR=-FK/FKP
      RA=RA+DR
      IF (ABS(DR) .GT. 1.)    GO TO 205
      R1(I)=RA
      DT1(I)=-R1(I)/C+TOBS(I)+TAO
      TAU1=DT1(I)/TAU
      JMAX(I)=DT1(I)/DT
      IF (I .GT. ICRIT)    GO TO 206
      H1(I)=FK4*(FK3+EXP(-TAU1)*(TAU1/KV-FK3))
      GO TO 207
206   H1(I)=FK5-FK4*(FK3+EXP(-TAU1)*(TAU1/KV-FK3))
207   CONTINUE
      DO 209    J=1,5CC
      TI(J)=(FLOAT(J)-.5)*DT
      FK6=TI(J)/TAU
      FK7=EXP(-FK6)
      VEL(J)=VO*(1.-TI(J)/TOM)*FK7
      DIS(J)=FK4*(FK3+FK7*(FK6/KV-FK3))/KH
      IF (J .GT. JCRIT)    GO TO 208
      HSTAR(J)=KH*DIS(J)
      GO TO 209
208   HSTAR(J)=FK5-KH*DIS(J)
209   CONTINUE
      DO 210    I=1,2CC
```

```
      DC 210   L=1,3
      DY(I,L)=0.
      DC 210   N=1,8
210   DYC(I,N,L)=0.
      DC 218   I=1,IMAX
      JM2=JMAX(I)
      DC 218   M=1,NCLASS
      DC 217   J=1,JM2
      FACT=1.-5.*VT(M)/ABS(VEL(J))
      IF (FACT .GE. 0.)   GC TO 211
      F1=0.
      GC TO 212
211   F1=FACT
212   R=R1(I)+DIS(J)
      K=1
213   IF (R .LT. R2(K))   GC TO 214
      K=K+1
      GC TO 213
214   IF (K .GT. NZF1)   GC TO 215
      LL=NZF+2-K
      GC TO 216
215   LL=K
216   DM=CONS1*F1*ABS(VEL(J))*P(M,LL)
      DELT=DT1(I)-TI(J)
      H=H1(I)-HSTAR(J)-VT(M)*DELT
      DC 217   L=1,NY
      IF (H .LT. Y(L))   GO TO 217
      DYC(I,M,L)=DYC(I,M,L)+2.*DM*(1.-Y(L)/H)/H
217   CONTINUE
      DC 218   L=1,NY
218   DY(I,L)=DY(I,L)+DYC(I,M,L)
219   N=NZR1+1
      DC 220   I=1,NZR
      N=N-1
220   R2(N)=RO-R2(N-1)
```

```
      R2(1)=RO
      NFIN=(NZF+1)/2
      NN=NZF+2
      DO 221    N=1,NFIN
      NN=NN-1
      DO 221    I=1,NCLASS
      DUM=P(I,N)
      P(I,N)=P(I,NN)
221   P(I,NN)=DUM
      RETURN
      END
```

```
      SUBROUTINE DUST3
C COMPUTATION OF THE DUST CLOUD FOR MULTIPLE BURSTS
C CONDITIONS - UNIFORM GROUND / EIGHT PARTICLE CLASSES
      COMMON /DUSTAT/ A,HOB,KH,KV,PRESO,RHO,RHOF,RHOTOT,TO,U,VO,YIELD
     1       /DUST/   CUTOFF,D(8),P(8,41),DTOBS,DY(201,3),DYC(201,8,3),
     2                HSTAR(500),IMAX,NCLASS,NY,TOBS(201),VT(8),Y(3)
     3       /MULTI/  HOB1,HOB2,HOB3,KV1,KV2,KV3,PRESO1,PRESO2,PRESO3,
     4                NB,RHOF1,RHOF2,RHOF3,TB2,TB3,TO1,TO2,TO3,U1,U2,U3,
     5                VO1,VO2,VO3,YIELD1,YIELD2,YIELD3
      DIMENSION TA(200),VEL(3)
      REAL KH,KV,KV1,KV2,KV3
      LOGICAL CUTOFF,G1,G2,G3
      V1(TT) = VO1*(1.-TT/TOM1)*EXP(-KV1*TT/TOM1)
      V2(TT) = VO2*(1.-(TT-TC1)/TOM2)*EXP(-KV2*(TT-TC1)/TOM2)
      V3(TT) = VO3*(1.-(TT-TC2)/TOM3)*EXP(-KV3*(TT-TC2)/TOM3)
      V(TT,A,B) = V1(TT)+A*V2(TT)+B*V3(TT)
      D1(TT) = FK11*(-FK21+EXP(-FK41*TT)*(FK41*TT+FK21))
     OD2(TT) = FK12*(-FK22+EXP(-FK42*(TT-TC1))*(FK42*(TT-TC1)
     1+FK22))
     CD3(TT) = FK13*(-FK23+EXP(-FK43*(TT-TC2))*(FK43*(TT-TC2)
     1+FK23))
      U = (U1+U2+U3)/FLOAT(NB)
      RHOF = (RHOF1+RHOF2+RHOF3)/FLOAT(NB)
      DO 301  I=1,NCLASS
      TERM1 = .097256/(RHOF*D(I))
  301 VT(I) = SQRT(TERM1*TERM1+.281424*D(I)*RHO/RHOF)-TERM1
      RC1 = TO1/(KV1*KV1/(VO1*(EXP(-KV1)+KV1-1.))-1./U)
      RC2 = TO2/(KV2*KV2/(VO2*(EXP(-KV2)+KV2-1.))-1./U)
      TOM1 = TO1+RO1/U
      TOM2 = TO2+RO2/U
      FK11 = (VO1*TOM1)/(KV1*KV1)
      FK12 = (VO2*TOM2)/(KV2*KV2)
      FK21 = 1.-KV1
      FK22 = 1.-KV2
      FK41 = KV1/TOM1
```

```
      FK42 = KV2/TOM2
      CONS1 = 2.*A*RHCTOT/KH
      CRIT1 = DTOBS/10.
      TMAX = DTOBS*FLOAT(IMAX)
      DO 302  I=1,IMAX
  302 TOBS(I) = DTOBS*FLOAT(I)
      TC1 = TB2+R01/U
  303 F1 = D1(TC1)+U*(TB2-TC1)
      F1P = V1(TC1)-U
      DCT1 = -F1/F1P
      TC1 = TC1+DTC1
      IF (ABS(DTC1) .GT. CRIT1)  GO TO 303
      IF (TC1 .LE. TMAX)  GO TO 304
      CUTOFF=.FALSE.
      GO TO 333
  304 IB2 = TB2/DTOBS
      IB21 = IB2+1
      IB22 = IB2+2
      IF (NB .LT. 3)  GO TO 308
      RO3 = TO3/(KV3*KV3/(VO3*(EXP(-KV3)+KV3-1.))-1./U)
      TOM3 = TO3+RO3/U
      FK13 = (VO3*TOM3)/(KV3*KV3)
      FK23 = 1.-KV3
      FK43 = KV3/TOM3
      TM = TC1+TOM2
  305 F2 = V1(TM)+V2(TM)
      F21P = VO1*(1.+KV1-KV1*TM/TOM1)*EXP(-KV1*TM/TOM1)/TOM1
      RATIO=KV2*(TM-TC1)/TOM2
      F23P = (1.+KV2-RATIO)*EXP(-RATIO)
      F22P = VO2*F23P/TOM2
      F2P = F21P+F22P
      DTM = F2/F2P
      TM = TM+DTM
      IF (ABS(DTM) .GT. CRIT1)  GO TO 305
      TC2 = TB3+(D1(TM)+D2(TM))/U
```

```
306   F3 = D1(TC2)+D2(TC2)-U*(TC2-TB3)
      F3P = V1(TC2)+V2(TC2)-L
      DTC2 = -F3/F3P
      TC2 = TC2+DTC2
      IF (ABS(DTC2) .GT. CRIT1)  GO TO 306
      IF (TC2 .LE. IMAX)  GO TO 307
      CUTOFF=.FALSE.
      GO TO 333
307   IB3 = TB3/DTOBS
      IB31 = IB3+1
      IB32 = IB3+2
308   DO 310  I=1,IB2
      TT = TOBS(I)
309   F4 = D1(TT)+U*(TOBS(I)-TT)
      F4P = V1(TT)-L
      DT = -F4/F4P
      TT = TT+DT
      IF (ABS(DT) .GT. CRIT1)  GO TO 309
310   TA(I) = TT
      IF (NB .GT. 2)  GO TO 311
      IB3 = IMAX
311   DO 313  I=IB21,IB3
      TT = TOBS(I)
312   F5 = D1(TT)+D2(TT)+L*(TOBS(I)-TT)
      F5P = V(TT,1.,0.)-U
      DT = -F5/F5P
      TT = TT+DT
      IF (ABS(DT) .GT. CRIT1)  GO TO 312
313   TA(I) = TT
      IF (NB .LT. 3)  GO TO 316
      DO 315  I=IB31,IMAX
      TT = TOBS(I)
314   F6 = D1(TT)+D2(TT)+D3(TT)+L*(TOBS(I)-TT)
      F6P = V(TT,1.,1.)-L
      DT = -F6/F6P
```

```
      TT = TT+DT
      IF (ABS(DT) .GT. CRIT1)  GO TO 314
  315 TA(I) = TT
  316 T2 = TA(1)/2.
      T3 = TA(1)
      VEL(3) = V1(T3)
      HSTAR(1) = KH*T3*(VC1+4.*V1(T2)+VEL(3))/6.
      DO 317  I=2,IB2
      VEL(1) = VEL(3)
      T1 = T3
      T2 = (TA(I)+T1)/2.
      T3 = TA(I)
      VEL(3) = V1(T3)
      DHST = KH*(T3-T1)*(ABS(VEL(1)+4.*V1(T2)+VEL(3)))/6.
  317 HSTAR(I) = HSTAR(I-1)+DHST
      T1 = T3
      VEL(1) = VEL(3)
      T2= (TC1+T1)/2.
      VEL(3) = V1(TC1)
      DHST = KH*(TC1-T1)*(ABS(VEL(1)+4.*V1(T2)+VEL(3)))/6.
      HC1 = HSTAR(IB2)+DHST
      VEL(1) = VEL(3)
      T3 = TA(IB21)
      T2 = (TC1+T3)/2.
      VEL(3) = V(T3,1.,0.)
      DHST=KH*(T3-TC1)*(ABS(VEL(1)+4.*V(T2,1.,0.)+VEL(3)))/6.
      HSTAR(IB21) = HC1+DHST
      DO 318  I=IB22,IB3
      VEL(1) = VEL(3)
      T1 = T3
      T2 = (TA(I)+T1)/2.
      T3 = TA(I)
      VEL(3) = V(T3,1.,0.)
      DHST=KH*(T3-T1)*(ABS(VEL(1)+4.*V(T2,1.,0.)+VEL(3)))/6.
  318 HSTAR(I) = HSTAR(I-1)+DHST
```

```
      IF (NB .LT. 3)  GO TO 320
      T1 = T3
      VEL(1) = VEL(3)
      T2 = (TC2+T1)/2.
      VEL(3) = V(TC2,1.,0.)
      DHST=KH*(TC2-T1)*(ABS(VEL(1)+4.*V(T2,1.,0.)+VEL(3)))/6.
      HC2 = HSTAR(IB3)+DHST
      VEL(1) = VEL(3)
      T3 = TA(IB31)
      T2 = (TC2+T3)/2.
      VEL(3) = V(T3,1.,1.)
      DHST=KH*(T3-TC2)*(ABS(VEL(1)+4.*V(T2,1.,1.)+VEL(3)))/6.
      HSTAR(IB31) = HC2+DHST
      DO 319  I=IB32,IMAX
      VEL(1) = VEL(3)
      T1 = T3
      T2 = (TA(I)+T1)/2.
      T3 = TA(I)
      VEL(3) = V(T3,1.,1.)
      DHST=KH*(T3-T1)*(ABS(VEL(1)+4.*V(T2,1.,1.)+VEL(3)))/6.
  319 HSTAR(I) = HSTAR(I-1)+DHST
  320 DO 321  I=1,200
      DO 321  L=1,3
      DY(I,L) = 0.
      DO 321  N=1,8
  321 DYC(I,N,L) = 0.
      DO 331  N=1,NCLASS
      Q1 = .TRUE.
      Q2 = .TRUE.
      Q3 = .TRUE.
      DO 331  I=1,IMAX
      IF (I .GT. IB2)  GO TO 322
      IF (.NOT. Q1)  GO TO 331
      H = HSTAR(I)-VT(N)*TA(I)
      IF (H .GT. 0.)  GO TO 329
```

```
      C1 = .FALSE.
      GO TO 331
  322 IF (I .GT. IB3)  GO TO 325
      IF (.NOT. Q2)  GO TO 331
      IF (Q1)  GO TO 323
      H = HSTAR(I)-HC1-VT(N)*(TA(I)-TC1)
      GO TO 324
  323 H = HSTAR(I)-VT(N)*TA(I)
  324 IF (H .GT. 0.)  GO TO 329
      Q2 = .FALSE.
      GO TO 331
  325 IF (.NOT. Q3)  GO TO 331
      IF (Q1 .AND. Q2)  GO TO 327
      IF (Q2)  GO TO 326
      H = HSTAR(I)-HC2-VT(N)*(TA(I)-TC2)
      GO TO 328
  326 H = HSTAR(I)-HC1-VT(N)*(TA(I)-TC1)
      GO TO 328
  327 H = HSTAR(I)-VT(N)*TA(I)
  328 IF(H .GT. 0.)  GO TO 329
      Q3 = .FALSE.
      GO TO 331
  329 DO 330  L=1,NY
      IF (H .LT. Y(L))  GO TO 330
      X = Y(L)/H
      DYC(I,N,L) = CONS1*(X-1.-ALOG(X))*P(N,1)
  330 CONTINUE
  331 CONTINUE
      DO 332  I=1,IMAX
      DO 332  L=1,NY
      DO 332  N=1,NCLASS
  332 DY(I,L) = DY(I,L)+DYC(I,N,L)
  333 RETURN
      END
```

```
      SUBROUTINE DUST4 (PRESA,TEMPA,HOBS,HOBC,TMAX,DT,W,ANG)
C COMPUTATION OF THE LATE TIME DUST HISTORY FOR A SINGLE BURST
C CONDITIONS - UNIFORM GROUND / EIGHT PARTICLE CLASSES
      COMMON /DUSTAT/ A,HOB,KH,KV,PRESO,RHO,RHOF,RHOTOT,TO,U,VO,YIELD
     1       /DUST/   CUTOFF,D(8),P(8,41),DTOBS,DY(201,3),DYC(201,8,3),
     2                HSTAR(500),IMAX,NCLASS,NY,TOBS(201),VT(8),Y(3)
      LOGICAL G,CUTOFF
      REAL KH,KV
      RAF(S) = (34000./S**.518)*CRY/PSF
      RBF(S) = (5800.-30.*S+3900./EXP(.05*S))*CRY/PSF
      RCF(S) = (70000./S**.68)*CRY/PSF
      RDF(S) = (32500./S**.414)*CRY/PSF
      IC = 202
      G = .TRUE.
      IM = TMAX/DT+1.5
      IF (IM .GT. 201)   IM = 201
      RHOF = 2.7*PRESA/(TEMPA+460.)
      DO 104   N=1,NCLASS
      TERM1 = .0973/RHOF/D(N)
104   VT(N) = SQRT(TERM1*TERM1+.2814*D(N)*RHO/RHOF)-TERM1
      CRY = YIELD**.333
      PSF = (PRESA/14.7)**.333
      TSF = SQRT((TEMPA+460.)/530.)
      CVELA = SQRT(2410.*(TEMPA+460.))
      S = 14.7*PRESO/PRESA
      IF (HOB .GE. -.1)   GO TO 107
      IF (HOBS .GT. .00001)   GO TO 106
      IF (HOBC .GT. .1)   GO TO 105
      HOB = RDF(S)
      RS = 0.
      GO TO 109
105   HOB = RBF(S)
      RS = RCF(S)
      GO TO 109
106   HOB = HOBS*CRY
```

```
107   RB = RBF(S)
      IF (HOB .GT. RB)    GO TO 108
      RS = RAF(S)+(RCF(S)-RAF(S))*HOB/RB
      GO TO 109
108   RC = RDF(S)
      IF (HOB .GT. RC)    HOB = RC
      RS = RCF(S)*(RC-HOB)/(RC-RB)
109   CONS1 = 2.*A*RFCTOT/KH
      RR = -DT*W*5280.
      PR = PRESO
      DO 110    I=1,IM
      DO 110    L=1,NY
      DY(I,L) = 0.
      DO 110    N=1,NCLASS
110   DYC(I,N,L) = C.
      SP = 15.
111   FS = HOB-RBF(SP)
      DFS = (30.+195./EXP(.05*SP))*CRY/PSF
      SP = SP-FS/DFS
      IF (ABS(FS/DFS) .GT. .05)    GO TO 111
      IF (SP .LT. .1)    GO TO 112
      RCRIT = RCF(SP)
      GO TO 113
112   RCRIT = 10000000.
113   DO 400    I=1,IM
      TOBS(I) = DT*FLOAT(I-1)
      RR = RR+DT*W*5280.
      R = SQRT(RR*RR+RS*RS-2.*RR*RS*COS(ANG))
      S = 14.7*PR/PRESA
      IF (I .LT. IC .AND. .NOT. C)    GO TO 124
114   IF (R .LT. RCRIT)    GO TO 115
      RA = RAF(S)
      RB = RBF(S)
      G = RB*(R-RA)+HOB*(RA-RCF(S))
      DG = ((30.+195./EXP(.05*S))*(RA-R)+HOB*47600./S**1.68
```

```
     1+(RB-HOB)*17612./S**1.518)*CRY/PSF
      GC TO 116
115   RC = RCF(S)
      RC = RDF(S)
      G = R*(RD-RBF(S))+RC*(HOB-RD)
      DG = ((RD-HOB)*47600./S**1.68+R*(30.+195./EXP(.J5*S))
     1+(RC-R)*13455./S**1.414)*CRY/PSF
116   S = S-G/DG
      IF (ABS(G/DG) .GT. .1)   GO TO 114
      PR = PRESA*S/14.7
      IF (PR .GT. 6C.)   GC TO 121
      CALL WEI (PR,PRESA,CRY,TSF,PSF,HOB,CVELA,KH,HST)
      DC 119   N=1,NCLASS
      CH = TOBS(I)*(5280.*KH*W-3600.*VT(N))
      IF (CH .LE. 0.)   GO TC 118
      DC 117   L=1,NY
      IF (HST+DH .LE. Y(L))   GO TO 117
      X = Y(L)/(HST+CH)
      DYC(I,N,L) = CCNS1*HST*(X-1.-ALOG(X))*P(N,1)/(HST+DH)
117   CCNTINUE
      GC TO 119
118   DC 119   L=1,NY
      IF (HST+DH .LE. Y(L))   GO TO 119
      X = (Y(L)-DH)/HST
      DYC(I,N,L) = CCNS1*P(N,1)*(X-1.-ALCG(X))
119   CCNTINUE
      GC TO 123
121   C = .FALSE.
      RI = RS*COS(ANG)+SQRT((RS*COS(ANG))**2-RS*RS+R*R)
      IC = RI/(W*DT*5280.)+3
124   DC 122   N=1,NCLASS
      DC 122   L=1,NY
122   DYC(I,N,L) = 1CC000.
123   DC 120   L=1,NY
      DC 120   N=1,NCLASS
```

```
120   DY(I,L) = DY(I,L)+DYC(I,N,L)
400   CONTINUE
      WRITE (6,300) YIELD,PRESO,PRESA,TEMPA,HOB,W,ANG,A,KH,RHC,RHOTOT,RS
300   FORMAT (1H1,49X22HLATE TIME DUST HISTORY////
     135X29HWEAPON YIELD                    F10.2,2X19H(MT)                /
     235X29HOVERPRESSURE                    F10.2,2X19H(PSIG)              /
     335X29HAMBIENT PRESSURE                F10.2,2X19H(PSIA)              /
     435X29HAMBIENT TEMPERATURE             F10.2,2X19H(DEGF)              /
     535X29HHEIGHT-OF-BURST                 F10.1,2X19H(FT)                /
     635X29HWIND SPEED                      F10.2,2X19H(MPH)               /
     735X29HWIND DIRECTION                  F10.2,2X19H(RAD)               /
     835X29HEROSION COEFFICIENT             F10.5,2X19H -                  /
     935X29HTRANSPORT COEFFICIENT           F10.2,2X19H -                  /
     135X29HDUST PARTICLE DENSITY           F10.1,2X19H(LB/CU FT)          /
     235X29HBULK DENSITY OF SOIL            F10.1,2X19H(LB/CU FT)          /
     335X29HRANGE OF SITE                   F10.1,2X19H(FT)                )
      WRITE (6,301) (N,D(N),VT(N),P(N,1),N=1,NCLASS)
301   FORMAT (1HO,///34X51H DUST PARTICLE PARAMETERS AND INITIAL DISTRIB
     1UTIONS ///45X29H NCLASS      D         VT        P//(I50,F10.3,F8.3,
     2F8.3))
      IF (Q)   GO TO 402
      WRITE (6,401)
401   FORMAT(1HO,10X55HWARNING - OVERPRESSURE HAS EXCEEDED ALLOWABLE VAL
     1UE FOR/21X46HTHOSE TIMES WHERE DENSITY IS INDICATED BY ****)
402   DO 304   L=1,NY
      WRITE (6,302) Y(L)
302   FORMAT (1H1,11X85H COMPUTATION OF ACCUMULATED DUST CLOUD DENSITY P
     1ER PARTICLE SIZE CLASS AT A HEIGHT OF F6.1,5H  FT.///55X19H DUST C
     2LOUD DENSITY//13X94H I     T-OBS     TOTAL     CLASS 1  CLASS 2  CLAS
     3S 3  CLASS 4  CLASS 5  CLASS 6  CLASS 7  CLASS 8)
      WRITE (6,303)
303   FORMAT (1HO)
      DO 304   I=1,IM
304   WRITE (6,305) I,TOBS(I),DY(I,L),(DYC(I,N,L),N=1,NCLASS)
305   FORMAT (I15,F9.3,F10.5,F10.4,7F9.4)
```

RETURN
END

```
      SUBROUTINE  WEI (P1,PRESA,CRY,TSF,PSF,HOB,CVELA,KH,HST)
      REAL KH,KV
      SC = 14.7*P1/PRESA
      XI = 1.+P1/PRESA
      KV = .0877*SC-.3
      IF (KV .LT. 1.)   KV = 1.
      IF (SC .GE. 30.)   GO TO 201
      TC = (3.59-.0107*SC)*CRY/TSF/PSF
      GO TO 202
  201 TC = (4.125-.0285*SC)*CRY/TSF/PSF
  202 RB = (5800.-30.*SC+3900./EXP(.05*SC))*CRY/PSF
      UR = 1./(CVELA*SQRT(.143+.857*XI))
      VC = 1.89*CVELA*(XI-1.)/SQRT(1.+6.*XI)
      IF (HOB .LE. RB)   GO TO 204
      RC = (70000./SC**.68)*CRY/PSF
      RO = (32500./SC**.414)*CRY/PSF
      CF = SIN(ATAN(RC/RB))
      THETA = ABS(ATAN(RC*(RC-HOB)/(RC-RB)/HOB))
      UR = SIN(THETA)*UR/CF
      VC = SIN(THETA)*VO/CF
  204 RC = TC/(KV*KV/(VC*(EXP(-KV)+KV-1.))-UR)
      RCO = (KV-1.)*VC*(TC+RC*UR)/(KV*KV)
      HST = KH*(2.*RC-RCO)
      RETURN
      END
```

```
      SUBROUTINE CUT (ICUT)
C CAPABILITY - OUTPUT FOR SUBROUTINES DUST1, DUST2, DUST3
      COMMON /DUSTAT/ A,HOB,KH,KV,PRESO,RHO,RHOF,RHOTOT,TO,U,VO,YIELD
     1       /DUST/   CUTOFF,D(8),P(8,41),DTORS,DY(201,3),DYC(201,8,3),
     2                HSTAR(500),IMAX,NCLASS,NY,TOBS(201),VT(8),Y(3)
     3       /TWODEE/ NZB,NZF,NZR,NZR1,RZB(20),RZF(20),R2(41)
     4       /MULTI/  HOB1,HOB2,HOB3,KV1,KV2,KV3,PRESO1,PRESO2,PRESO3,
     5                NB,RHOF1,RHOF2,RHOF3,TB2,TB3,TO1,TO2,TO3,U1,U2,U3,
     6                VO1,VO2,VO3,YIELD1,YIELD2,YIELD3
     7       /MISC/   NDIMEN,PRESA,RUNTYP,TAPSAV,TEMPA,TITLE(18)
      INTEGER RUNTYP
      REAL    KH,KV,KV1,KV2,KV3
      LOGICAL CUTOFF,TAPSAV
      WRITE (6,700) NDIMEN,NB,TITLE
  700 OFORMAT (1H1,17X12,82H-D COMPUTATION OF THE DUST CLOUD ENVIRONMENT
     1GENERATED BY EXPLOSION INDUCED WIND -I2,9H BURST(S)///30X18A4)
      WRITE (6,701) PRESA,RHO,KH,TEMPA,RHOTOT,A
  701 FORMAT (1HO/31H   AMBIENT PRESSURE    (PSIA) =F8.2,7X32H PARTICLE
     1DENSITY   (LB/CU-FT) =F7.1,7X28H TRANSPORT COEFFICIENT     =F8.2/
     231H   AMBIENT TEMPERATURE (DEGF) =F8.1,7X32H BULK SOIL DENSITY  (L
     3B/CU-FT) =F7.1,7X28H EROSION COEFFICIENT       =F8.5)
      IF (NB .GT. 1)   GO TO 702
      WRITE (6,706) YIELD,VO,U,PRESO,TO,RHOF
      WRITE (6,707) HOB,KV
      GO TO 709
  702 WRITE (6,703)
  703 FORMAT (12HOFIRST BURST)
      WRITE (6,706) YIELD1,VO1,U1,PRESO1,TO1,RHOF1
      WRITE (6,707) HOB1,KV1
      WRITE (6,704)
  704 FORMAT (13HOSECOND BURST)
      WRITE (6,706) YIELD2,VO2,U2,PRESO2,TO2,RHOF2
      WRITE (6,708) HOB2,KV2,TB2
      IF (NB .NE. 3)   GO TO 709
      WRITE (6,705)
```

```
705  FORMAT (12H0THIRD BURST)
     WRITE (6,706) YIELD3,VC3,U3,PRESC3,TO3,RHOF3
     WRITE (6,708) HCB3,KV3,TB3
706  FORMAT (31H0  WEAPON YIELD          (MT) =F8.2,7X32H PEAK WIND VEL
    1OCITY      (FPS) =F7.1,7X28H SHOCK VELOCITY      (FPS) =F8.1/31H
    2 SITE OVERPRESSURE   (PSIG) =F8.2,7X32H POSITIVE PHASE DURATION (S
    3EC) =F7.2,7X28H AIR DENSITY    (LB/CU-FT) =F8.5)
707  FORMAT (31H   HEIGHT-OF-BURST       (FT) =F8.1,7X32H WIND DECAY EX
    1PONENT           =F7.3)
708  FORMAT (31H   HEIGHT-OF-BURST       (FT) =F8.1,7X32H WIND DECAY EX
    1PONENT           =F7.3,7X28H TIME OF BURST       (SEC) =F8.2)
709  IF (RUNTYP .EQ. 2)   GO TO 711
     WRITE (6,710) (N,D(N),VT(N),P(N,1),N=1,NCLASS)
710 OFORMAT (1HO///25X80H PARTICLE CLASS   SIZE (MM)   TERMINAL VELOCIT
    1Y (FPS)   ADJUSTED WEIGHT FRACTION //(I34,F16.3,F19.3,F27.3))
     GO TO 718
711  WRITE (6,712) (N,N=1,NCLASS)
712  FORMAT (1HO///23X17H PARTICLE CLASS /I8,7I10)
     WRITE (6,713) (D(N),N=1,NCLASS)
713  FORMAT (1HO,27X12H SIZE (MM) /8F10.3)
     WRITE (6,714) (VT(N),N=1,NCLASS)
714  FORMAT (14X26H TERMINAL VELOCITY (FPS) /8F10.3)
     WRITE (6,715)
715 OFORMAT (1HO,10X27H ZONE BOUNDARY (FT)    ZONE,6X25H ADJUSTED WEIGH
    1T FRACTION/1X)
     DO 716   I=1,NZR1
716  WRITE (6,717) R2(I),I,(P(N,I),N=1,NCLASS)
717  FORMAT (F25.2/I37,F13.3,7F10.3)
718  IF (CUTOFF)   GO TO 722
     IF (RUNTYP .EQ. 3)   GO TO 720
     WRITE (6,719)
719 OFORMAT (1HO////60H EXECUTION TERMINATED DUE TO SHOCK STRENGTH CUTO
    1FF CRITERION)
     GO TO 727
720  WRITE (6,721)
```

```
721 CFCRMAT (1HO////36H EXECUTION TERMINATED DUE TO TIME SCALE CUTOFF C
    1RITERION)
     GC TO 727
722  DC 725   L=1,NY
     WRITE (6,723) Y(L),(N,N=1,NCLASS)
723  FCRMAT (1H1,9X68H TIME VARIATION OF ACCUMLLATED DUST CLOUD DENSITY
    1 AT AN ELEVATION OF F5.1,3H FT///12X5H TIME,5X14H TOTAL DENSITY,9X
    243H DENSITY (LB/CU-FT) PER PARTICLE SIZE CLASS/11X6H (SEC),7X11H (
    3LB/CU-FT),4X8H CLASS /I3,7I10)
     WRITE (6,724)
724  FCRMAT (1H )
     DC 725   I=1,IMAX,IOUT
725  WRITE (6,726) TCBS(I),CY(I,L),(CYC(I,N,L),N=1,NCLASS)
726  FORMAT (F17.2,F16.5,F19.4,7F10.4)
     IF (TAPSAV)   WRITE (10) TITLE,IMAX,NCLASS,NY,Y,TOBS,DYC,DY
727  RETURN
     END
```

```
      SUBROUTINE ATI (ICUT)
C ALCULATION OF AIR TEMPERATURE AND DUST DENSITY IN BLAST INDUCED DUST CLOUD
C  UNIFORM GROUND CONDITIONS WITH EROSION DEPTH CUT-OFF
C  SINGLE BURST
      COMMON /DUSTAT/ A,HOB,KH,KV,PRESO,RHO,RHOF,RHOTCT,TO,U,VO,YIELD
     1       /ATVAR/  ALPHA,BETA,C,FK,P1,P2,RC,TM,UF,YC,ZM
     2       /WEVAR/  CONSW1,COSTH,CP1,CP2,CP3,RHOS,TASITE,TES,TMAX,TOP
     3       /MISC/   NDIMEN,PRESA,RUNTYP,TAPSAV,TEMPA,TITLE(18)
     4       /STVAR/  B(9),QC,TS(10),ZS(10)
     5       /ARRAYS/ CC(51),CDY(1001),Q(51),TE(51),TEJ(51),TEY(1001),
     6                TCBS(1001),S(51),SUMW(51),SUMWP(51),WA(51),YY(51)
      INTEGER RUNTYP
      REAL KH,KV
      LOGICAL TAPSAV
      DY = .001*KH*VC*TM
      JMAX = YC*(TES+460.)/(TEMPA+460.)/DY+3.
      I = 1
      IF (JMAX .GE. 52)   GO TO 599
      DO 502   M=1,9
  502 ZS(M) = .031*FLOAT(M-1)*YIELD**.15
      ZS(10) = 5.
      CALL ST (ALPHA,FK,TEMPA)
      RC = TO/(KV*KV/(VO*(EXP(-KV)+KV-1.))-1./U)
      TOM = TO+RC/U
      WAA = DY*RHOS
      TP = DY/(KH*VC-.5*DY*(1.+KV)/TOM)
      VP = VO*(1.-TP/TOM)*EXP(-KV*TP/TOM)
      DZ = 6.*A*(VP+VC)*TP
      W = UF*DZ*RHOTCT/12.
      IC = ZM/DZ+.5
      FC = FLOAT(IC-1)
      TCBS(1) = 0.
      DDY(1) = 0.
      TEY(1) = TES
      YY(1) = 0.
```

```
      S(1) = 0.
      Q(1) = 0.
      M = 1
      T = 0.
      TT = 0.
      P1 = PRESO+PRESA
      TE(1) = TS(1)
      DO 504    J=2,JMAX
      SUMW(J) = 0.
      SUMWP(J) = 0.
      TE(J) = TES
  504 S(J) = DY
      T1 = TOM*(1.+1./KV)
      G = KH*VO*TOM/KV
      TCUT = BETA*TC
      DO 590    I=2,ICC1
      DO 506    J=1,JMAX
  506 TEJ(J) = TE(J)
      FI = FLOAT(I-2)
      FI1 = FLOAT(I-1)
      H = DY*FI1
      IF (H .GT. KH*RC)    T = T1
  100 CONTINUE
      IF (H .GT. KH*RC)    GO TO 101
      F = H/G-1.+1./KV+EXP(-KV*T/TOM)*(1.-T/TOM-1./KV)
      GO TO 102
  101 F = 2.*KH*RO/G-H/G-1.+1./KV+EXP(-KV*T/TOM)*(1.-T/TOM-1./KV)
  102 FP = KV*EXP(-KV*T/TOM)*(T/TOM-1.)/TOM
      T = T-F/FP
      IF (ABS(F/FP) .GT. .0001*TM)    GO TO 100
      IF (H .GT. KH*RC)    GO TO 103
      TOBS(I) = T-H/(U*KH)
      GO TO 104
  103 TOBS(I) = T-2.*RO/U+H/(U*KH)
  104 CONTINUE
```

```
      IF (TCUT .GE. TOBS(I))   GO TO 105
      IMAX=I-1
      GO TO 600
  105 P2 = PRESA+PRESC*(1.-TOBS(I)/TOP)*((1.-CP1)*EXP(-CP2*TOBS(I)/TOP)+
     1CP1*EXP(-CP3*TOBS(I)/TOP))
      DP = P2-P1
      TERM2 = .583*DP/(P1+P2)
      Z = DZ*(FI1-.5)
      IF (Z .LT. ZS(M+1))   GO TO 508
      M = M+1
  508 TE(1) = TS(M)+B(M)*(ZS(M)-Z)
      WA(1) = W*FI1
      DO 518   J=2,JMAX
      FJ = FLOAT(J-2)
      IF (I-J .LT. 0)   GO TO 516
      IF (I-J+1 .GE. IC)   GO TO 512
      SUMW(J) = SUMW(J)+2.*W*(FI-FJ+.5)/(FI1**2)
      IF (J .GT. 2)   GO TO 510
      SUMWP(J) = W
      GO TO 516
  510 SUMWP(J) = SUMWP(J)+2.*W*FJ*(1.-FJ*(FI1-.5)/(FI*FI1))/(FI*FI1)
      GO TO 516
  512 DSW1 = (FI-FJ+.5)/(FI1**2)
      DSW2 = (FI-FJ-FC+.5)/((FI1-FC)**2)
      SUMW(J) = SUMW(J)+2.*W*(DSW1-DSW2)
      IF (J .GT. 2)   GO TO 514
      SUMWP(J) = 0.
      GO TO 516
  514 DS1 = (1.-FJ*(FI1-.5)/(FI*FI1))/(FI*FI1)
      DS2 = (1.-FJ*(FI1-FC-.5)/((FI-FC)*(FI1-FC)))/((FI-FC)*(FI1-FC))
      SUMWP(J) = SUMWP(J)+2.*W*FJ*(DS1-DS2)
  516 WA(J) = WA(J-1)-SUMW(J)
      Q(J) = QO*EXP(-WA(J)/(.01*COSTH))
      ER = (Q(J)-Q(J-1))*(T-TT)
      DTN = ER+.185*S(J)*DP-C*SUMWP(J)*(TE(J)-TEJ(J-1))
```

```
      DTE = DTN/(.24*WAA+C*SUMW(J))
      TE(J) = TE(J)+DTE
      TERM1 = DTE/(TE(J)+460.-.5*DTE)
      S(J) = S(J)*(1.+TERM1-TERM2)
      YY(J) = YY(J-1)+.5*(S(J)+S(J-1))
  518 DD(J) = SUMW(J)/S(J)
      P1 = P2
      TT = T
      DO 520   J=2,JMAX
      IF (YC .GT. YY(J))   GO TO 520
      DYY = (YY(J)-YC)/(YY(J)-YY(J-1))
      TEY(I) = TE(J)+(TE(J-1)-TE(J))*DYY
      DDY(I) = DD(J)+(DD(J-1)-DD(J))*DYY
      GO TO 590
  520 CONTINUE
  590 CONTINUE
  599 IMAX = I
  600 WRITE (6,602) TITLE,YIELD,PRESO,PRESA,TEMPA,HOB,RHO,RHOTOT,UF,ZM,
     1C,FK,ALPHA,A,KH,TM
  602 FORMAT (1H1,28X62HAIR TEMPERATURE AND DUST DENSITY IN A BLAST INDU
     1CED DUST CLOUD/34X52HUNIFORM GROUND CONDITIONS WITH EROSION DEPTH
     2CUT-OFF/54X12HSINGLE BURST//24X18A4                              ////
     335X29HWEAPON YIELD                    F10.2,2X19H(MT)             /
     435X29HOVERPRESSURE                    F10.2,2X19H(PSIG)           /
     535X29HAMBIENT PRESSURE                F10.2,2X19H(PSIA)           /
     635X29HAMBIENT TEMPERATURE             F10.2,2X19H(DEGF)           /
     735X29HHEIGHT-OF-BURST                 F10.1,2X18H(FT)            //
     835X29HDUST PARTICLE DENSITY           F10.1,2X19H(LB/CU FT)       /
     935X29HBULK DENSITY OF SOIL            F10.1,2X19H(LB/CU FT)       /
     135X29HLAND USE FACTOR                 F10.3,2X19H  -              /
     235X29HEROSION DEPTH CUT-OFF           F10.2,2X19H(IN)             /
     335X29HPARTICLE SPECIFIC HEAT          F10.3,2X19H(BTU/LB)         /
     435X29HSOIL CONDUCTIVITY               F10.3,2X19H(BTU/FT-HR-DEGF) /
     535X29HSOIL DIFFUSIVITY                F10.3,2X18H(SQ FT/HR)      //
     635X29HEROSION COEFFICIENT             F10.5,2X18H  -              /
```

```
     735X29HTRANSPORT COEFFICIENT          F10.2,2X19H  -                  /
     835X29HHEAT TRANSFER RESPONSE TIME    F10.1,2X19H(MSEC)                )
      WRITE (6,604) YC
604   FORMAT (1H1,11X52H AIR TEMPERATURE AND DUST DENSITY AT AN ELEVATIO
     1N OF F6.2,1X4HFEET///8X10HTIME (SEC),16X23HTEMPERATURE (DEGREES F),
     29X23HDUST DENSITY (LB/CU FT)/1X)
      DO 606    I=1,IMAX,ICUT
606   WRITE (6,608) TOBS(I),TEY(I),DDY( )
608   FORMAT (F16.3,F32.1,F32.4)
      IF (TAPSAV)    WRITE (10) TITLE,IMAX,YC,TOBS,TEY,DDY
      RETURN
      END
```

```
      SUBROUTINE AT2 (NOUT)
CALCULATION OF AIR TEMPERATURE AND DUST DENSITY IN BLAST INDUCED DUST CLOUD
C   BI-UNIFORM GROUND CONDITIONS
C   SINGLE BURST
      COMMON /DUSTAT/ A,HOB,KH,KV,PRESO,RHO,RHOF,RHOTOT,TO,U,VO,YIELD
     1       /ATVAR/  ALPHA,BETA,C,FK,P1,P2,RC,TM,UF,YC,ZM
     2       /WEVAR/  CONSW1,COSTH,CP1,CP2,CP3,RHOS,TASITE,TES,TMAX,TOP
     3       /MISC/   NDIMEN,PRESA,RUNTYP,TAPSAV,TEMPA,TITLE(18)
     4       /STVAR/  B(9),CO,TS(10),ZS(10)
     5       /ARRAYS/ CD(51),CDY(1001),Q(51),TE(51),TEJ(51),TEY(1001),
     6                TOBS(1001),S(51),SUMW(51),SUMWP(51),WA(51),YY(51)
      DIMENSION SWJ(51),SWPJ(51),TEJJ(51),SJ(51)
      INTEGER RUNTYP
      REAL KH,KV
      LOGICAL QQ,TAPSAV
      DY = .001*KH*VO*TM
      JMAX = YC*(TES+460.)/(TEMPA+460.  DY+3.
      IF (JMAX .GE. 52)   GO TO 599
      DO 502   M=1,9
  502 ZS(M) = .031*FLOAT(M-1)*YIELD**.1.
      ZS(10) = 5.
      CALL ST (ALPHA,FK,TEMPA)
      RO = TO/(KV*KV/(VO*(EXP(-KV)+KV-1.))-1./U)
      TOM = TO+RC/U
      WAA = DY*RHOS
      TP = DY/(KH*VC-.5*DY*(1.+KV)/TOM)
      VP = VO*(1.-TP/TOM)*EXP(-KV*TP/TOM)
      DZ = 6.*A*(VP+VC)*TP
      W1 = P1*DZ*RHOTOT/12.
      W2 = P2*DZ*RHOTOT/12.
      ISTAR = RC*KH/DY+.5
      TEY(1) = TES
      TOBS(1) = 0.
      CDY(1) = 0.
      YY(1) = 0.
```

```
      S(1) = 0.
      Q(1) = 0.
      CC = .TRUE.
      M = 1
      T1 = 0.
      V = V0
      PR1 = PRESA+PRESC
      TE(1) = TS(1)
      DO 504   J=2,JMAX
      SUMW(J) = 0.
      SUMWP(J) = 0.
      TE(J) = TES
  504 S(J) = DY
      NMAX = .5*(KH*(RO+RC)/DY+1.)
      IF (NMAX .GT. 1001)   NMAX = 1001
      DO 552   N=2,NMAX
      IF (N .GE. ISTAR+2)   GO TO 506
      IS = N
      IM = N
      IC = 1
      GO TO 516
  506 IF (CC)   GO TO 510
      IS = IS+2
      M = MJ
      T1 = T1J
      V = VJ
      PR1 = P1J
      TE(1) = TE1J
      DO 508   J=2,JMAX
      SUMW(J) = SWJ(J)
      SUMWP(J) = SWPJ(J)
      TE(J) = TEJJ(J)
  508 S(J) = SJ(J)
      GO TO 514
  510 IS = 2
```

```
      QC = .FALSE.
      M = 1
      T1 = 0.
      V = VC
      PR1 = PRESA+PRESO
      TE(1) = TS(1)
      DO 512   J=2,JMAX
      SUMW(J) = 0.
      SUMWP(J) = 0.
      TE(J) = TES
  512 S(J) = DY
  514 IC = IS+1
      IM = IC+ISTAR
  516 FC = FLOAT(IC-1)
      DO 548   I=IS,IM
      DO 518   J=1,JMAX
  518 TEJ(J) = TE(J)
      FI = FLOAT(I-2)
      FI1 = FLOAT(I-1)
      VC = DY*(1.+KV-KV*T1/TOM)/(2.*TOM*KH*(1.-T1/TOM))
      T2 = T1+DY/((V-VC)*KH)
      V = VO*(1.-T2/TOM)*EXP(-KV*T2/TOM)
      TOB = T2-DY*FI1/(U*KH)
      PR2 = PRESA+PRESO*(1.-TOB/TOP)*((1.-CP1)*EXP(-CP2*TOB/TOP)+
     1CP1*EXP(-CP3*TOB/TOP))
      DP = PR2-PR1
      TERM2 = .583*DP/(PR1+PR2)
      Z = DZ*(FI1-.5)
      IF (Z .LT. ZS(M+1))   GO TO 520
      M = M+1
  520 TE(1) = TS(M)+B(M)*(ZS(M)-Z)
      IF (I .LE. IC)   GO TO 522
      WA(1) = (W2-W1)*FC+W1*FI1
      GO TO 524
  522 WA(1) = W2*FI1
```

```
524   IF (WA(1) .GT. .00001)   GO TO 526
      Q1 = 0.
      GO TO 528
526   Q1 = Q0
528   CONTINUE
      DO 542   J=2,JMAX
      FJ = FLOAT(J-2)
      IF (I-J .LT. 0)   GO TO 540
      IF (IC .EQ. 1)   GO TO 536
      IF (I-J+1 .GE. IC)   GO TO 532
      SUMW(J) = SUMW(J)+2.*W2*(FI-FJ+.5)/(FI1**2)
      IF (J .GT. 2)   GO TO 530
      SUMWP(J) = W2
      GO TO 540
530   SUMWP(J) = SUMWP(J)+2.*W2*FJ*(1.-FJ*(FI1-.5)/(FI*FI1))/(FI*FI1)
      GO TO 540
532   DSW1 = (FI-FJ+.5)/(FI1**2)
      DSW2 = (FI-FJ-FC+.5)/((FI1-FC)**2)
      SUMW(J) = SUMW(J)+2.*W2*DSW1-2.*(W2-W1)*DSW2
      IF (J .GT. 2)   GO TO 534
      SUMWP(J) = W1
      GO TO 540
534   DS1 = (1.-FJ*(FI1-.5)/(FI*FI1))/(FI*FI1)
      DS2 = (1.-FJ*(FI1-FC-.5)/((FI1-FC)*(FI-FC)))/((FI1-FC)*(FI-FC))
      SUMWP(J) = SUMWP(J)+2.*W2*FJ*DS1-2.*(W2-W1)*FJ*DS2
      GO TO 540
536   SUMW(J) = SUMW(J)+2.*W1*(FI-FJ+.5)/(FI1**2)
      IF (J .GT. 2)   GO TO 538
      SUMWP(J)   W1
      GO TO 540
538   SUMWP(J) = SUMWP(J)+2.*W1*FJ*(1.-FJ*(FI1-.5)/(FI*FI1))/(FI*FI1)
540   WA(J) = WA(J-1)-SUMW(
      Q(J) = Q1*EXP(-WA(J)/(.01*COSTH))
      ER = (Q(J)-Q(J-1))*(T2-T1)
      DTN = ER+.185*S(J)*DP-C*SUMWP(J)*(TE(J)-TEJ(J-1))
```

```
      DTE = DTN/(.24*WAA+C*SUMW(J))
      TE(J) = TE(J)+DTE
      TERM1 = DTE/(TE(J)+460.-.5*DTE)
      S(J) = S(J)*(1.+TERM1-TERM2)
      YY(J) = YY(J-1)+.5*(S(J)+S(J-1))
  542 DD(J) = SUMW(J)/S(J)
      IF (I .NE. IC)   GO TO 546
      MJ = M
      T1J = T2
      VJ = V
      P1J = PR2
      TE1J = TE(1)
      DO 544   J=2,JMAX
      SWJ(J) = SUMW(J)
      SWPJ(J) = SUMWP(J)
      TEJJ(J) = TE(J)
  544 SJ(J) = S(J)
  546 T1 = T2
  548 PR1 = PR2
      TOBS(N) = TOB
      DO 550   J=2,JMAX
      IF (YC .GT. YY(J))   GO TO 550
      DYY = (YY(J)-YC)/(YY(J)-YY(J-1))
      TEY(N) = TE(J)+(TE(J-1)-TE(J))*DYY
      DDY(N) = DD(J)+(DD(J-1)-DD(J))*DYY
      GO TO 552
  550 CONTINUE
  552 CONTINUE
      GO TO 600
  599 NMAX = 1
  600 WRITE (6,602) TITLE,YIELD,PRESO,PRESA,TEMPA,HOB,RHO,RHOTOT,C,FK,
     1ALPHA,RC,P1,P2,A,KH,TM
  602 FORMAT (1H1,28X62HAIR TEMPERATURE AND DUST DENSITY IN A BLAST INDU
     1CED DUST CLOUD/46X44HBI-UNIFORM GROUND CONDITIONS                 /
     254X12HSINGLE BURST//24X18A4                                       ////
```

```
335X29HWEAPON YIELD                F10.2,2X19H(MT)                  /
435X29HOVERPRESSURE                F10.2,2X19H(PSIG)                /
535X29HAMBIENT PRESSURE            F10.2,2X19H(PSIA)                /
635X29HAMBIENT TEMPERATURE         F10.2,2X19H(DEGF)                /
735X29HHEIGHT-OF-BURST             F10.1,2X18H(FT)                 //
835X29HDUST PARTICLE DENSITY       F10.1,2X19H(LB/CU FT)            /
935X29HBULK DENSITY OF SOIL        F10.1,2X19H(LB/CU FT)            /
135X29HPARTICLE SPECIFIC HEAT      F10.3,2X19H(BTU/LB)              /
235X29HSOIL CONDUCTIVITY           F10.3,2X19H(BTU/FT-HR-DEGF)      /
335X29HSOIL DIFFUSIVITY            F10.3,2X18H(SQ FT/HR)           //
435X29HRANGE BOUNDARY              F10.1,2X19H(FT)                  /
535X29HNEAR LAND USE FACTOR        F10.3,2X19H  -                   /
635X29HFAR LAND USE FACTOR         F10.3,2X18H  -                  //
735X29HEROSION COEFFICIENT         F10.5,2X18H  -                   /
835X29HTRANSPORT COEFFICIENT       F10.2,2X19H  -                   /
935X29HHEAT TRANSFER RESPONSE TIME F10.1,2X19H(MSEC)                )
 WRITE (6,604) YC
604  FORMAT (1H1,16X52H AIR TEMPERATURE AND DUST DENSITY AT AN ELEVATIO
    1N OF F5.1,3H FT///24X4HTIME,12X11HTEMPERATURE,9X12HDUST DENSITY/23X
    25H(SEC),12X11H(DEGREES-F),10X10H(LB/CU-FT)/1X)
 DO 606   N=1,NMAX,NOUT
606  WRITE (6,608) TOBS(N),TEY(N),DDY(N)
608  FORMAT (F28.3,F20.1,F21.4)
 IF (TAPSAV)   WRITE (10) TITLE,NMAX,YC,TOBS,TEY,DDY
 RETURN
 END
```

```
      SUBROUTINE ST (ALPHA,FK,TEMPA)
      COMMON /DUSTAT/ EC,HOB,KH,KV,PRESO,RHC,RHOF,RHOTOT,TO,U,VO,YIELD
     1       /WEVAR/  CONSW1,COSTH,CP1,CP2,CP3,RHOS,TASITE,TES,TMAX,TOP
     2       /STVAR/  B(9),QC,TS(10),ZS(10)
      DIMENSION A(21),B3(21),G(21),QI(21),QR(21),T(21)
      REAL KH,KV
      TEMPAS = TEMPA+460.
      TEMPA4 = TEMPAS**4
      ALPHA = ALPHA/3600.
      FK = FK/3600.
      GAMMA = SQRT(ALPHA/3.14159)/FK
      CONS1 = CONSW1*GAMMA
      CONS2 = GAMMA*4.79E-13
      DELT = .05*TASITE
      CONS3 = SQRT(DELT)/1.5
      CONS4 = 1./(2.*CONS2*CONS3)
      DO 100   M=1,21
      T(M) = FLOAT(M-1)*DELT
  100 QI(M) = CONS1*PE(TMAX,T(M))
      TEMP = TEMPAS
      QR(1) = 0.
      G(1) = 0.
      DO 104   M=2,21
      M1 = M-1
      SUM = TEMPAS
      DO 104   I=1,M1
      IF (I .EQ. M1)   GO TO 101
      I1 = I+1
      C1 = 2.*A(I)*T(M)+B3(I)
     QSUM = SUM+2.*(SQRT(T(M)-T(I))*(C1+A(I)*T(I))-SQRT(T(M)-T(I1))*(C1+
     1A(I)*T(I1)))/3.
      GO TO 104
  101 CONS5 = CONS4*SUM+(QI(M)+.5*G(M1))/CONS2+TEMPA4
  102 TEMPO = TEMP
      TEMP = (3.*TEMPO**4+CONS5)/(4.*TEMPO**3+CONS4)
```

```
      IF (ABS(TEMP-TEMPC) .GE. 0.1)   GO TO 102
103   GR(M) = CONS2*(TEMP**4-TEMPA4)
      G(M) = GI(M)-GR(M)
      A(M1) = (G(M)-G(M1))/DELT
      B3(M1) = 3.*(G(M1)-A(M1)*T(M1))
104   CONTINUE
      TS(1) = TEMP
      DO 106   N=2,10
      TS(N) = TEMPAS
      C1 = ZS(N)*SQRT(3.14159/ALPHA)/36.
      C2 = ZS(N)**2/(288.*ALPHA)
      C3 = C2/2.
      C4 = SQRT(C3)
      E1 = C3/DELT
      IF (E1 .GT. 88.)   E1 = 88.
      EF1 = C4/SQRT(DELT)
      DO 106   I=1,20
      I1 = I+1
      C5 = A(I)*(2.*T(21)+C2)+B3(I)
      IF (I .EQ. 20)   GO TO 105
      C6 = SQRT(T(21)-T(I))
      E2 = C3/C6**2
      IF (E2 .GT. 88.)   E2 = 88.
      C7 = SQRT(T(21)-T(I1))
      E3 = C3/C7**2
      IF (E3 .GT. 88.)   E3 = 88.
      TS(N) = TS(N)+((C5+A(I)*T(I))*C6/EXP(E2)-(C5+A(I)*T(I1))*C7/
     1EXP(E3))/1.5+C1*(A(I)*(3.*T(21)+C2)+B3(I))*(ERF(C4/C6)-ERF(C4/C7))
      GO TO 106
105   TS(N) = TS(N)+CONS3*(C5+A(I)*T(I))/EXP(E1)+C1*(A(I)*(3.*T(21)+C2)+
     1B3(I))*(ERF(EF1)-1.)
106   CONTINUE
      DO 107   N=1,10
107   TS(N) = TS(N)-460.
      DO 108   M=1,9
```

```
108   B(M) = (TS(M+1)-TS(M))/(ZS(M)-ZS(M+1))
      QC = QI(21)/GAMMA
      ALPHA = 3600.*ALPHA
      FK = 3600.*FK
      RETURN
      END
```

```
      FUNCTION PE(TMAX,T)
C COMPUTATION OF SCALED FIREBALL THERMAL POWER AT TIME T
      DIMENSION TRI(40),PRI(40)
      DATA TRI/0.0,0.1,0.2,0.3,0.4,0.5,0.6,0.7,0.8,0.9,1.0,
     1 1.1,1.2,1.3,1.4,1.5,1.6,1.7,1.8,1.9,2.0,2.2,2.4,2.6,
     2 2.8,3.0,3.2,3.4,3.6,3.8,4.0,4.5,5.0,5.5,6.0,6.5,7.0,
     3 8.0,9.0,10.0/, PRI/0.0,0.04,0.09,0.16,0.3,0.55,0.71,
     4 0.84,0.92,0.975,1.0,0.985,0.95,0.89,0.78,0.67,0.59,
     5 0.53,0.485,0.45,0.42,0.365,0.32,0.285,0.255,0.23,0.21,
     6 0.19,0.17,0.155,0.145,0.12,0.1,0.085,0.075,0.065,
     7 0.055,0.045,0.04,0.04/
      TR = T/TMAX
      IF (TR .LT. 1.)   GO TO 301
      PE = 0.04
      GO TO 303
  301 J = 0
  302 J = J+1
      IF (TR .GE. TRI(J))   GO TO 302
      J1 = J-1
      PE = PRI(J1)+(PRI(J)-PRI(J1))*(TR-TRI(J1))/(TRI(J)-TRI(J1))
  303 RETURN
      END
```

EXTRACTED

APPENDIX C (U)

WEAPONS EFFECTS VARIABLES

Contract No. DACA 73-67-C-0018

Prepared by:

IIT Research Institute
Chicago, Illinois

for

Directorate of Military Construction
Office of the Chief of Engineers
Department of the Army
Washington, D.C.

R

Appendix C

WEAPONS EFFECTS VARIABLES

The dust and air-temperature prediction models depend upon certain weapons effects variables. This appendix briefly summarizes the variables of interest and the empirical equations which were developed for computer application. The attack situation is defined in terms of the weapon yield, the overpressure, and the height of burst or its equivalent (i.e., scaled height of burst, optimum height of burst, or overhead burst are the equivalents considered). The ambient air pressure and temperature are also used to define the weapons effects environment. The general range of overpressures considered herein is from approximately 5 psi to 50 psi. The accuracy level to which the pertinent variables are determined, by the simplified equations, is approximately 10 percent.

The weapons effects variables that must be evaluated are:

- peak air velocity, V_o, fps,
- positive phase duration of wind, t_o, sec,
- exponential constant for air velocity, k,
- shock velocity, U, fps,
- shock air density, ρ_s, lb/ft^3,
- shock air temperature, T_s, °F,
- average air density, ρ_a, lb/ft^3,
- positive phase duration of overpressure, t_o', sec,
- overpressure waveform parameter A, α, and β,
- time of arrival at site t_a, sec,

- time of maximum thermal power, t_{max}, sec,
- maximum thermal power, P_{max}, Btu/ft^2 sec,
- atmospheric attenuation, τ, and
- the angle of incidence, θ.

The weapons effects data were, for the most part, obtained from Gladstone.[C.1]

The scaled height-of-burst for overpressure were fitted with two straight line segments: one line connecting the overhead burst point with the optimum height-of-burst point, and the second line connecting the optimum height-of-burst point with the surface burst point. These two straight line segments are defined by four scaled quantities: H_{sd} is the scaled overhead burst height, H_{sb} is the scaled optimum height of burst, R_{sc} is the scaled range for optimum height of burst, and R_{sa} is the scaled range for a surface burst.

The scaled overpressure p_{ss} is defined as

$$p_{ss} = \frac{p_s}{P_o} - P_{so} \quad , \tag{C.1}$$

where

p_s = actual overpressure,
P_{so} = standard ambient pressure, 14.7 psia, and
P_o = actual ambient pressure.

This approximate scaling law is used because it is expected that P_o will deviate only slightly from P_{so}. The scaled height of burst and ranges are defined as

$$H_s = \frac{H}{W^{1/3}} \left(\frac{P_o}{P_{so}} \right)^{1/3} \quad , \tag{C.2}$$

where

H_s = the scaled height or range, $ft/MT^{1/3}$,

H = the corresponding actual height or range, ft, and

W = weapon yield, MT.

The four scaled quantities defining the height-of-burst approximations are:

$$H_{sd} = 32{,}500\ p_{ss}^{-0.414}, \tag{C.3}$$

$$H_{sb} = 5{,}800 - 30\ p_{ss} + 3{,}900\ e^{-.05\ p_{ss}}, \tag{C.4}$$

$$R_{sc} = 70{,}000\ p_{ss}^{-0.68}, \text{ and} \tag{C.5}$$

$$R_{sa} = 34{,}000\ p_{ss}^{-0.518}. \tag{C.6}$$

Another scaled height-of-burst factor will be needed for the time-of-arrival calculation. This scaled quantity is

$$H_{se} = \frac{1}{2}\ (H_{sd} + H_{sb}). \tag{C.7}$$

A number of the weapons effects variables depend only upon the scaled overpressure p_{ss}. These relate primarily to the wind and overpressure waveforms. The exponential coefficient k used in the velocity waveform has been approximated as

$$k = 0.877\ p_{ss} - 0.3, \tag{C.8}$$

with a minimum value of k=1 for the lower overpressure range. The overpressure waveform parameters were obtained from Brode.[C.2] A double exponential waveform is used for the overpressure range of interest; that is

$$p_s(t) = p_{ss}\left(1 - \frac{t}{t'_o}\right)\left[(1-B)\ e^{-\alpha(t/t'_o)} + B\ e^{-\beta(t/t'_o)}\right] \tag{C.9}$$

where

t = time,

t'_o = positive phase duration, and

B, α, and β are the waveform parameters. The following empirical equations were developed for these parameters:

$$B = 0.092\ p_{ss}^{0.328}\ , \tag{C.10}$$

$$\alpha = 0.398\ p_{ss}^{0.318}\ , \text{ and} \tag{C.11}$$

$$\beta = 3.13\ p_{ss}^{0.262}\ . \tag{C.12}$$

The positive phase duration of the wind and the overpressure are both relatively independent of the height of burst and can therefore be formulated in terms of the overpressure alone. The time variables scale in the following manner:

$$t = t_s\ W^{1/3} \left(\frac{T_{os}}{T_o}\right)^{1/2} \left(\frac{P_{os}}{P_o}\right)^{1/3} \tag{C.13}$$

where

t = actual time variable,
t_s = scaled time variable,
T_{os} = standard ambient temperature, 70°F, and
T_o = actual ambient temperature.

Temperature must be specified by its absolute value.

The following empirical equations were developed:

$$t_{os} = 3.59 - 0.107\ p_{ss} \qquad p_{ss} \leq 30 \text{ psi} \tag{C.14}$$

or

$$t_{os} = 4.125 - 0.0285\ p_{ss} \qquad p_{ss} \geq 30 \text{ psi} \tag{C.15}$$

where t_{os} is the positive phase duration of the velocity.

$$t'_{os} = 2.5 - 0.024\ p_{ss} + 1.5\ e^{-0.16\ p_{ss}} \tag{C.16}$$

where t'_{os} is the positive phase duration of the overpressure.

The value of some of the weapons effects variables depend upon both the strength of the incident wave and the nature of the shock reflection process. For the range of overpressures of interest and the accuracy requirements, the influence of the shock reflection process can be eliminated for some of the variables. Thus, the temperature and density of the air at the shock front can be determined from the conventional Rankine-Hugoniot equation. The average air density has been determined as a simple arithmetic mean between the values at the shock front and the ambient density.

The apparent shock velocity (i.e., the velocity at which initial pressure disturbances sweep over the ground surface) and the horizontal component of the air velocity at the shock front are strongly dependent upon the shock configuration. The shock configuration can be divided into two regions: (1) the Mach reflection region, and (2) the regular reflection region. These shock reflection configurations are illustrated in Figure C.1.

The Mach reflection process will exist for all heights of burst below the optimum; that is, the optimum height of burst is the approximate transition point between the two reflection regions. The shock velocity and the peak air velocity are both given by classical Rankine-Hugoniot relations. The time of arrival of the shock wave does, however, vary with the hieght of burst within this region. The following empirical equation was developed for the scaled time of arrival.

$$t_{as} = 79.0\ p_{ss}^{-0.88}\ (0.4 + 0.6\ H_s) \qquad (C.17)$$

The reflection process in the regular reflection region has been idealized as simple linear process such that the angle of incidence α is equal to the angle of shock

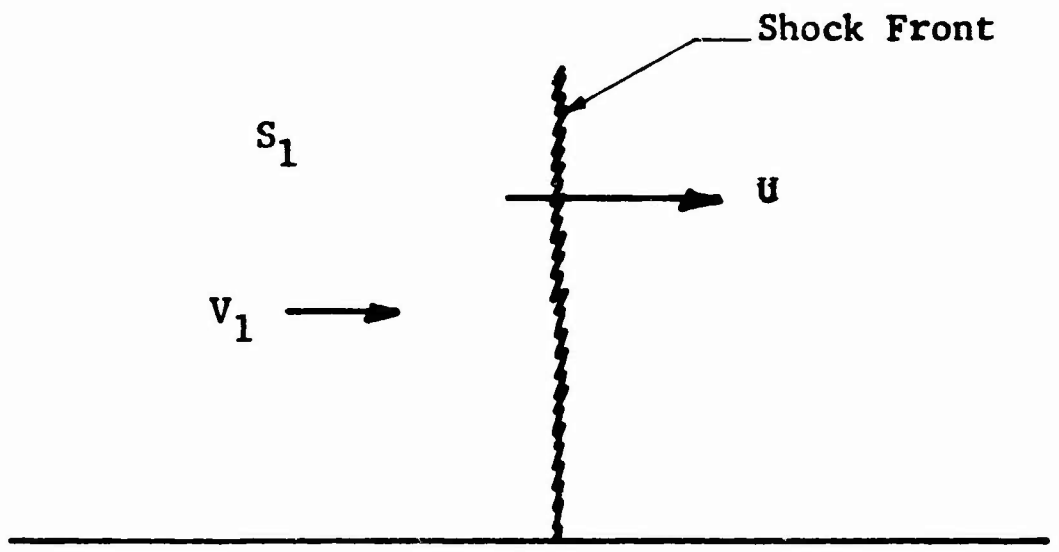

(a) Mach Reflection Region

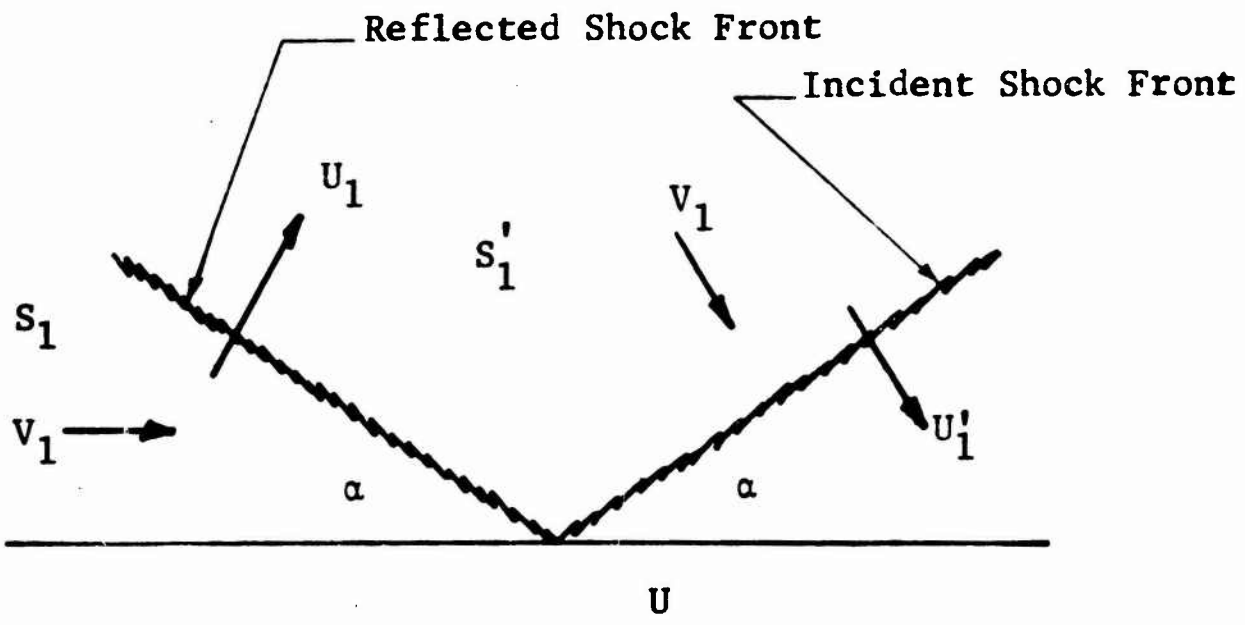

(b) Regular Reflection Region

Figure C.1 Shock Configuration at Ground Surface

reflection and that the strength of the two waves are equal. The pressure is known in the reflection region (State S_1). These assumptions permit us to compute the pressure behind the incident wave (State S_1'). Thus, the shock velocity U_1' and the particle velocity V_1' associated with the incident wave are known. The following approximate relations were thus obtained:

$$U_1' = c_o \sqrt{0.572 + .428\ \xi} \qquad \text{(C.18)}$$

and

$$V_1' = \frac{0.945(\xi-1)c_o}{\sqrt{4 + 3\ \xi}} \qquad \text{(C.19)}$$

where

ξ = overall pressure ratio = p_s/P_o, and
c_o = ambient sound velocity.

The apparent shock velocity U is given as

$$U = \frac{U_1'}{\sin \alpha} \qquad \text{(C.20)}$$

where α is the angle of incidence. Also, the horizontal component V_1 of the air velocity is

$$V_1 = ? V_1' . \qquad \text{(C.21)}$$

The use of the above approximate regular reflection equations results in values of both shock velocity and particle velocity, at the optimum height of burst point, which differ slightly from the values obtained from the corresponding Mach reflection equations. This discrepancy is of the order of two to four percent and is a function of the strength of

the shock wave. In order to eliminate this discrepancy the following equations were developed and used.

$$U = U_r \cdot f/\sin \alpha \tag{C.22}$$

$$V_1 = V_r \sin \alpha/f \tag{C.23}$$

where

$$f = \sin (\arctan (R_{sc}/H_{sb})), \tag{C.24}$$

U_r = Rankine-Hugoniot shock velocity, and

V_r = Rankine-Hugoniot particle velocity.

The scaled time of arrival in the regular reflection region is calculated from the following empirical equations:

$$t_{as} = t_1 + \frac{(t_2-t_1)(H_{se}-H_s)}{(H_{se}-H_{sb})} , \quad H_s \geq H_{se} , \tag{C.25}$$

$$t_1 = 30\ p_{ss}^{-0.672} , \tag{C.26}$$

$$t_2 = 79\ p_{ss}^{-0.88} , \tag{C.27}$$

and

$$t_{as} = 30\ p_{ss}^{-0.672} \tag{C.28}$$

REFERENCES

C.1 Glasstone, S., Ed., "Effects of Nuclear Weapons," U.S. Department of Defense, 1962.

C.2 Brode, H. J., "A Review of Nuclear Explosion Phenomena Pertinent to Protective Construction," Rand Corp., Report 425, May 1964.